

UC Berkeley

UC Berkeley Electronic Theses and Dissertations

Title

Chemical glycoproteomics for identification and discovery of glycoprotein alterations in human cancer

Permalink

<https://escholarship.org/uc/item/0t47b9ws>

Author

Spiciarich, David

Publication Date

2017

Peer reviewed|Thesis/dissertation

Chemical glycoproteomics for identification and discovery of
glycoprotein alterations in human cancer

by David Spiciarich

A dissertation submitted in partial satisfaction of the requirements for the degree

Doctor of Philosophy

in

Chemistry

in the

Graduate Division

of the

University of California, Berkeley

Committee in charge:

Professor Carolyn R. Bertozzi, Co-Chair

Professor David E. Wemmer, Co-Chair

Professor Matthew B. Francis

Professor Amy E. Herr

Fall 2017

Chemical glycoproteomics for identification and discovery of
glycoprotein alterations in human cancer

© 2017

by David Spiciarich

Abstract

Chemical glycoproteomics for identification and discovery of glycoprotein alterations in human cancer

by

David Spiciarich

Doctor of Philosophy in Chemistry

University of California, Berkeley

Professor Carolyn R. Bertozzi, Co-Chair

Professor David E. Wemmer, Co-Chair

Changes in glycosylation have long been appreciated to be part of the cancer phenotype; sialylated glycans are found at elevated levels on many types of cancer and have been implicated in disease progression. However, the specific glycoproteins that contribute to cell surface sialylation are not well characterized, specifically in *bona fide* human cancer. Metabolic and bioorthogonal labeling methods have previously enabled enrichment and identification of sialoglycoproteins from cultured cells and model organisms. The goal of this work was to develop technologies that can be used for detecting changes in glycoproteins in clinical models of human cancer.

In Chapter 1 of this dissertation, I present an overview of the structures and functions of glycans and their relationship to cancer progression. I also discuss applications of *in vivo* bioorthogonal labeling in model organisms and how in humans, the significant regulatory and ethical barriers associated with introducing chemically altered sugars into people have hindered it. Finally, I review mass spectrometry-based proteomics and how it can be applied to clinical glycoproteomics.

In Chapter 2, I demonstrate the first application of this bioorthogonal labeling in a glycoproteomics platform applied to human tissues cultured *ex vivo*. Both normal and cancerous prostate tissues were sliced and cultured in the presence of functionalized derivatives of N-acetyl mannosamine, the sialic acid biosynthetic precursor. Chemical biotinylation followed by enrichment and mass spectrometry led to the identification of glycoproteins that were found at elevated levels or uniquely in cancerous prostate tissue. This work therefore extends the use of bioorthogonal labeling strategies to problems of human clinical relevance.

Secretome proteins play important roles in regulation of many physiological processes and show utility as potential biomarkers and for noninvasive diagnostics and treatment monitoring. In Chapter 3, I discuss a platform for identifying sialoglycoproteins that were secreted in the conditioned media from bioorthogonally labeled human prostate tissue

slice cultures. This platform could be used to identify disease biomarkers in a faithful clinical model of human disease.

Mutations in granulocyte colony-stimulating factor 3 receptor (CSF3R), also known as G-CSFR, occur in the majority of patients with chronic neutrophilic leukemia (CNL) and are more rarely present in other kinds of leukemia. In Chapter 4, I discuss novel variants in CSF3R at asparagine residue N610, one of which was germline. Interestingly, these N610 substitutions are potentially oncogenic and result in ligand-independent receptor activation. They confer activation of the JAK-STAT signaling pathway and concurrent sensitivity to JAK kinase inhibitors. The N610 residue is part of a consensus N-linked glycosylation motif in the receptor. Detailed mass spectrometry analysis demonstrates that this site is occupied by both complex and complex bisecting glycans. Further analysis demonstrates that N610 is the primary site of sialylation of the receptor. This study demonstrates that membrane-proximal N-linked glycosylation is critical for maintaining the ligand dependence of the receptor. Furthermore, it expands the repertoire of potentially oncogenic mutations in CSF3R that are therapeutically targetable

This dissertation is dedicated to my family and friends for all their support.

With great appreciation to my mom, sister, and Giorgio.

Chemical glycoproteomics for identification and discovery of glycoprotein alterations in human cancer

Table of Contents

List of Figures	iv
List of Tables	vi
List of Abbreviations	vii
Acknowledgments	ix
Chapter 1. Glycoproteomics and unnatural sugars to study protein glycosylation.....	1
1.1 Introduction	1
1.2 Glycosylation is part of the cancer phenotype	4
1.3 Mass spectrometry-based glycoproteomics	6
1.4 Unnatural sugars for bioorthogonal enrichment of glycans	9
1.5 Conclusion	12
1.6 References	13
Chapter 2. Bioorthogonal labeling of human prostate cancer tissue slice cultures for glycoproteomics	22
2.1 Introduction	22
2.2 Results	24
2.3 Discussion	34
2.4 Methods and Materials	37
2.5 Code	40
2.6 References	43

Chapter 3. Enrichment of sialoglycoproteins from human prostate tissue slice culture conditioned media.....	49
3.1 Introduction	49
3.2 Results	52
3.3 Conclusion	60
3.4 Tables	61
3.5 Methods and Materials	63
3.6 References	68
Chapter 4. A novel germline variant in CSF3R reveals a N-glycosylation site that is important in receptor regulation	73
4.1 Introduction	73
4.2 Results	74
4.3 Conclusion	81
4.4 Tables	85
4.5 Methods and Materials	88
4.6 References	93
Appendices	96
Appendix Table 1. Proteomic dataset of proteins found in normal prostate tissue slice cultures (TSCs)	97
Appendix Table 1. Proteomic dataset of proteins found in cancer prostate tissue slice cultures (TSCs)	117
Appendix Table 2. Proteomic dataset of proteins found in benign prostate hyperplasia prostatic tissue slice cultures (TSCs)	142

List of Figures

Figure 1-1.	Common monosaccharides found invertebrate glycans along with standard graphical representation	2
Figure 1-2.	Examples of some classes of N-linked glycans covalently attached to protein at asparagine (Asn) residues by an N-glycosidic bond	3
Figure 1-3.	Examples of protein O-glycosylation	4
Figure 1-4.	Extracellular types of tumor-associated glycans	5
Figure 1-5.	A schematic of a typical bottom-up or shotgun proteomic experiment	8
Figure 1-6.	Metabolic bioorthogonal engineering	10
Figure 1-7.	Bioorthogonal reactions with azides and terminal alkynes	11
Figure 2-1.	Workflow for preparation and bioorthogonal labeling of human prostate tissues slice cultures (TSCs)	23
Figure 2-2.	Structure of azide-functionalized unnatural sialic acid precursor monosacchride (Ac ₄ ManNAz) used for metabolic labeling of sialoglycoproteins	24
Figure 2-3.	Histology of prostate tissue slice cultures (TSCs) by hematoxylin and eosin (H&E) staining	25
Figure 2-4.	Western blot analysis of human prostate TSCs lysate administered azide- and alkyne- functionalized sugars and reacted with corresponding biotin probe under copper-catalyzed azide-alkyne [3+2] cycloaddition (CuAAC) conditions	26
Figure 2-5.	Labeling and imaging of cell surface sialoglycoproteins in human prostate tissue slice cultures (TSCs)	27
Figure 2-6.	Efficient biotinylation of sialoglycoproteins using Ac ₄ ManNAz	28
Figure 2-7.	Distribution of identified proteins after enrichment	29
Figure 2-8.	Voltage-dependent anion-selective channel 1 (encoded by the gene VDAC1) is overexpressed in human prostate cancer tissue	31
Figure 2-9.	Legumain is over-expressed and glycosylated in human prostate cancer tissue	34
Figure 2-10.	Comparative analysis of differentially regulated glycoproteins between normal and cancer TSCs	36

Figure 3-1.	Dynamic range of proteins present in serum	50
Figure 3-2.	Schematic for acquisition of conditioned media (CM) from prostate tissue slice cultures (TSCs)	51
Figure 3-3.	Western blot analysis of conditioned media (CM) collected from PC-3 cells incubated with Ac ₄ ManNAc (-) or Ac ₄ ManNAz (+) and subsequently reacted with biotin-functionalized reagents	52
Figure 3-4.	Time independence of alkyne-biotin labeling on CM collected from PC-3 cells	54
Figure 3-5.	Concentration dependence of biotin-alkyne reaction on CM derived from human TSC CM	56
Figure 3-6.	Labeling of CM harvested from human prostate TSCs varies by collection time	58
Figure 3-7.	Labeled glycoproteins from conditioned media administered Ac ₄ ManNAz or Ac ₄ ManNAc.....	59
Figure 3-8.	Optimized enrichment of labeled glycoproteins from conditioned media administered Ac ₄ ManNAz or Ac ₄ ManNAc	59
Figure 4-1.	A novel germline mutation in CSF3R	75
Figure 4-2.	The CSF3R N610H mutation is transforming and activates the JAK-STAT pathway in a ligand-independent manner	76
Figure 4-3.	Annotated MALDI-TOF MS spectra of permethylated N-glycans from CSF3R WT.....	77
Figure 4-4.	Identification of sialic acid glycosylation on N610. Schematic of labeling of sialic acid glycoproteins with an azide-functionalized sugar	79
Figure 4-5.	General scheme for stable isotope labeling by amino acids in cell culture (SILAC) analysis of cellular proteome dynamics	80
Figure 4-6.	A somatic N610S mutation identified in a patient with CNL is transforming and therapeutically targetable.....	83

List of Tables

Table 1-1.	Listing of glycosylated US Food and Drug Administration (FDA) approved cancer biomarkers	6
Table 2-1.	Proteins identified from enriched in cancer (n=8) versus normal (n=8) prostate tissue datasets	30
Table 2-2.	Proteins identified in prostate cancer proteomic dataset that were absent in normal dataset. All proteins were identified in at least 4 out of 8 cancer patients	32
Table 3-1.	Concentration of CuAAC reagents tested for covalently conjugating biotin to azide-labeled glycoproteins	56
Table 3-2.	Proteins identified in Normal Ac ₄ ManNAz-incubated CM dataset that were absent in Normal Ac ₄ ManNAc dataset	62
Table 4-2.	Compositional assignments of mono charged molecular ions observed in MALDI-TOF spectrum of permethylated N-glycans from CSF3R WT ...	85

List of Abbreviations

Ac₄ManNAc	peracetylated <i>N</i> -acetylmannosamine
Ac₄ManNAI	peracetylated <i>N</i> -pentynoylmannosamine
Ac₄ManNAz	peracetylated <i>N</i> -azidoacetylmannosamine
ACN	acetonitrile
AML	acute myeloid leukemia
BCA	bicinchoninic acid
BPH	benign prostate hyperplasia
BTAA	2-(4-((bis((1-tert-butyl-1H-1,2,3-triazol-4-yl)methyl)amino)methyl)-1H-1,2,3-triazol-1-yl) acetic acid
BTPS	3-(4-((bis((1-tert-butyl-1H-1,2,3-triazol-4-yl)methyl)amino)methyl)-1H-1,2,3-triazol-1-yl)propyl hydrogen sulfate
CEA	carcinoembryonic antigen
CID	collision-induced dissociation
CUAAC	copper-catalyzed azide-alkyne [3+2] cycloaddition
CM	conditioned media
CNL	chronic neutrophilic leukemia
CSF3R	colony-stimulating factor 3 receptor
DBCO	dibenzoazacyclooctyne
DIBAC	dibenzoazacyclooctyne
DDA-MS	data-dependent acquisition tandem mass spectrometry
DDT	dithiothreitol
ECD	electron capture dissociation
EPS	expressed prostatic secretion
ER	endoplasmic reticulum
ETD	electron transfer dissociation
EndoH	endoglycosidase H
EDTA	ethylenediaminetetraacetic acid
ESI	electrospray ionization
ETD	electron transfer dissociation
FA	formic acid
FDR	false discovery rate
FFPE	formalin-fixed, paraffin-embedded
Fruc	fructose
Her2	herceptin-2
Gal	galactose
GalN	galactosamine
GalNAc	<i>N</i> -acetylgalactosamine
GalNAc-1-P	<i>N</i> -acetylgalactosamine-1-phosphate
GalNAz	<i>N</i> -azidoacetylgalactosamine
GC	gas chromatography
Glc	glucose

Glc-6-P	glucose-6-phosphate
GlcN	glucosamine
H&E	hematoxylin and eosin
HexNAc	<i>N</i> -acetylhexosamine
IAM	iodoacetamide
HPLC	high performance liquid chromatography
LC-MS	liquid chromatography and mass spectrometry
m/z	m/z mass-to-charge ratio
MALDI	matrix-assisted laser desorption ionization mass spectrometry
Man	mannose
Man-6-P	mannose-6-phosphate
ManN	mannosamine
ManNAc	<i>N</i> -acetylmannosamine
ManNAz	<i>N</i> -azidoacetylmannosamine
MS	mass spectrometry
MUDPIT	multidimensional protein identification technology
MVP	multivesicular bodies
PBS	phosphate buffered saline
PCA	principal component analysis
PFA	paraformaldehyde
PNGase	peptide <i>N</i> -glycosidase <i>N</i> -glycanase
PTM	post-translational modification
SDS-PAGE	sodium dodecyl sulfate polyacrylamide gel electrophoresis
SILAC	stable isotope labeling by amino acids in cell culture
SPAAC	strain-promoted-azide-alkyne-cycloaddition
SPCA	supervised principal component analysis
TBTA	tris-(benzyltriazolylmethyl)amine
TCA	trichloroacetic acid
TCEP	tris-(2-carboxyethyl)phosphine
TSC	tissue slice culture
VDAC1	voltage-dependent anion-selective channel 1

Acknowledgments

“If you ask young people today what the rewards are of being a scientist, you'll find that many people think the rewards are to win a lot of prizes and get a lot of money. Perhaps have a piece of a company, and get promoted, and have grants, and have a big group and have all the material things. Some people want to have publications and have them in proper journals... But really, the great thing about science is that you can take something which is confused, a mess, and not only find a solution but prove it's the right one. That to me is really what should drive us. And the other things ought to be dismissed.

-Sydney Brenner (*My Life in Science*)

I would like to thank everyone in the Bertozzi lab for their knowledge, support and tutelage over these years. Every lab member, as well as many collaborators, made a difficult trek more successful and enjoyable.

I would like to thank Carolyn Bertozzi for orchestrating an environment that fosters creativity and congeniality. I enjoyed an independence rarely seen in graduate programs and appreciated that she neither demanded positive results nor entertained modest ambitions for any of my projects. In my third year, I was a graduate student instructor for the graduate chemical biology course that Carolyn taught. During that course, I learned how to design and instruct a curriculum. I remain thankful that Carolyn shared her presentation and communication skills. I am also appreciative that she has always been supportive and encouraging of my conference attendance, which honed my presentation and analytic skills.

Early in graduate school, I was informally mentored by Lauren Wagner and Lissette Andres. I appreciate both for their knowledge and for their assistance in planning experiments, they possess the kind of intellect you always want in your corner. Lauren is exceptionally kind and I can't imagine grad school without her friendship. Lissette was generous with her time and answered every question with more questions. I sat next to Brian Belardi, Peyton Shieh and Christina Woo for the majority of grad school, and I appreciate the many thoughtful suggestions and wonderful laughs. Brian is a modern renaissance man and taught me the importance of being well-read on diverse subjects. He exposed me to confocal microscopy and, in collaboration; we were able to image prostate tissue slice cultures. Peyton is brilliant and taught me to always be scientifically curious, I appreciate that he helped me become a well-rounded scientist. I've rarely met someone with less risk-aversion than Christina and she taught me the importance of being critical of your results and, I will always remember working with her on IsoTag.

Donna Peehl provided more than just the prostate tissue (Chapter 2) but also guidance, experimental design and training in cancer biology. I appreciated attending and presenting at her group meetings. I also acknowledge Sophia Maund and Rosie Nolley who made the collaboration successful. Collaborators Matteo Metruccio and Amber Jolly from Suzie Fleiszig's lab (UC Berkeley, School of Optometry), allowed me to study mucin glycosylation in a murine model. (As a vegetarian, I never thought I would participate in animal research but I appreciated the opportunity.) Julia Maxson and I began collaborating while she was a postdoc at the Fred Hutchinson, a collaboration that carried on to her independent lab at OHSU where we studied the glycosylation in neutrophil proliferation (leukemia). This collaboration exposed me to quantitative

Acknowledgments

proteomics and glycan analysis, and reunited me with molecular biology (Chapter 4). Julia and I could bounce ideas off of each other for hours; I appreciate her mentorship, positivity and hope there is an opportunity to work with each other again. I'm very happy that Michael Hollander, a talented bioengineering student who recently joined the lab, will continue this collaboration.

The mass spectrometry proteomic subgroup of the lab has always been a small but dedicated band of miscreants. Kanna Palaniappan, Neil Rumachik, Christina Woo and recent additions Stacy Malaker and Marc Driessen have shared in the frustration but also the hope/dream that proteomics can one day give biologists the precision that NMR has given chemists. When I joined the lab, proteomics was entirely in Kanna's very precise hands. His meticulous organization and notes allowed me to thrive in the early years. I appreciated long conversations about science with Neil and his contrarian questions. I wish him the greatest success as he finishes graduate school. Stacy has been a great addition to the team, bringing spectrum assignment that aided my later experiments. Mark has also been a great addition and I'm eager to see what he achieves with IsoTag.

I have a special appreciation for Anthony Iavarone, a well-read and rigorous researcher who generously taught me all aspects of mass spectrometry and liquid chromatography. None of these projects would have been successful without his technical assistance. More importantly, I count Tony a friend.

I worked with a talented undergrad at UC Berkeley, Sean Purcell, who took on the conditioned media project and mastered chemical biology techniques. Sean made major progress with labeling secreted proteins (Chapter 3), and from mentoring him I developed real confidence in my ability to design experiments. Working with Sean was a highlight of my PhD and I look forward to seeing what he produces in his own graduate research at UC San Diego.

I would like to thank Sam Keyser who touched every aspect of this dissertation. Literally. She edited almost every word and her grammarian skills helped to make this a more cogent document that no doubt saved you, the reader, considerable confusion. Any mistakes that remain are entirely my own; I couldn't have asked for a better editor and friend. I wish Sam the greatest success as she finishes her research.

I acknowledge my classmates Mason Appel, Ioannis Mountziaris, Frances Rodriguez-Rivera and Nathan Yee who became close friends and loyal cheerleaders throughout this journey. I enjoyed our qual practices together, our early fumbling with mini-meetings at Café Strada, our birthday celebrations and many other enjoyable grad school experiences we shared. Nathan taught me zebrafish and why this is a faithful model of cancer, and Frances the importance of lipid labeling in mycobacteria. Mason taught me how to design an enzymology experiment, and top-down proteomics. Yiannis knows everything about synthesis, his depth and breadth are inspiring. I am very grateful for their uncompromising encouragement and friendship during this journey.

One of the things that broadened my perspective in graduate school was Journal Club, spearheaded by Peyton and including Brian, Christina, Frances, and later CJ Cambier, Rachel Willand-Charnley and Ben Schumann. The only rule for JC was that it couldn't be something you would ever read for your own research; this led us on many amazing adventures.

Acknowledgments

A postdoc in the lab, Marjoke Debets, inventor of DIBAC, gave me technical advice and was a good sounding board for the conditioned media experiments. Jessica Kramer taught me how to have a life-work balance and about designing efficient experiments that play to your strengths. Both Marjoke and Jessica were wonderfully helpful as I thought about life after graduate school. For a period in the lab, every dissertation thanked Mike Boyce and I am grateful that I also had the opportunity to overlap with him. His mental adroitness shaped early experiments and helped me design proper controls. I would also be remiss if I did not thank Shana Topp, who kindly introduced me to the prostate tissue cultures. I also acknowledge Ben Schumann who is always full of ideas; I appreciate all of his advice and assistance with experiments and publications.

I enjoyed lunching with Mireille Kamariza and talking science; I appreciate that she shares my love of international conferences. I've enjoyed our late night excursions in SF and look forward to great things from her as she finishes her PhD. Doug Fox has always been generous with his time and a source of great ideas, whether he knows it or not he has touched many of my projects. I know he will do amazing things. I also appreciated scientific conversations with fellow podmate, Yi-Chang Liu. I appreciated Peter Robinson and Matt Zhou for their organization of Friday minimeetings and I've enjoyed conversations with Ian Blong and Fred Tomlin. I would also like to acknowledge Ioana Aanei and Kanwal Palla (both from Matt Francis's lab) who, along with my classmates, helped form a cohort of support from the first days of grad school and throughout. I would also like to express my sincere gratitude to Asia Avelino, Karen Carkhuff, Maryann Koopman, Sia Kruschke, Meridee Mannino, Olga Martinez and Cheryl McVaugh for keeping the lab running, bending rules to advance my projects and for their kindness. Asia has been especially encouraging and has put graduate school into context many times; I thank her for her counsel and friendship.

Many friends outside of lab were incredibly supportive of my decision to go back to school. I am indebted to Eme' O. Akpabio and appreciate her silver tongue and logic. I thank her for always being there for me. Amy Dietz is an amazing cheerleader who I could count on to provide perspective and support (and a superb voice). Steven Dudek, whose constant "roar" is infectious, trailblazed this path before and I appreciate his grad school mentorship, counsel and our Sunday runs through Golden Gate park. They, along with many friends, were on speed dial and I couldn't have done it without them.

I would like to express my sincere gratitude to my mom, Flora, who has been a constant source of support. I would also like to acknowledge my wonderful sister, Rachel, her husband, Zaza Atanelov, and their fabulous son, Ezra Atanelov, for being supportive throughout. I would like to thank the Spiciarich family – Robert, Andrew, Abra, Davida Rosenbaum and Joseph – who have been encouraging throughout this process, thank you for rooting for me. I'm very proud of the insights Abra Spiciarich is revealing in archeology. This dissertation is in loving memory of my grandparents Irene and Joseph.

I'm incredibly thankful to Giorgio Molinario for his constant support throughout this entire journey. Early in graduate school when data tables were starting to become unmanageable, he taught me pivot tables, one of the most powerful features in Excel. All of the appendices in this dissertation were easily made from this early help. I also appreciate that he took many of the challenges I faced in grad school on himself. The move from Berkeley to Stanford was not an insignificant challenge and he was supportive. Thank you for always keeping me at my very best.

Glycoproteomics and unnatural sugars to study protein glycosylation

1.1 Introduction

Since Mark Wilkins coined the term “proteomics” in his 1994 graduate dissertation, there has been a proliferation of other “omics” sciences. Proteomics is named after the well-known field of genomics, which refers to the study of DNA that make up an organism’s genome. In the post-genomic era, there has been a growing appreciation of proteins as the biological workhorses of the cell. As seen through numerous accounts, this appreciation is beginning to extend to protein conjugation such post-translational modifications (PTM) such as glycosylation.¹⁻³ Glycans, the monosaccharide and oligosaccharide components of glycoproteins, adorn eukaryotic cell surfaces and secreted proteins, where they mediate a variety of molecular recognition events. All cells are adorned with glycans, which are essential mediators of the interactions that take place between cells and their environments.⁴ For example, in embryonic development, the proper spatial and temporal expression of cell-surface glycans is essential for cell-cell adhesion and signaling events.⁵

Like nucleic acids and proteins, glycans come in a diversity of structures that underlie a vast array of biological functions. However, in contrast to DNA transcription and RNA translation, glycosylation is not template-driven. Instead, glycoproteins are generated through enzymatic addition of monosaccharides and complex oligosaccharides onto protein scaffolds producing significant diversity and complexity.

The structural diversity of glycans is derived from the attachment site and the configuration of the constituent monosaccharides. In eukaryotes, there are nine common monosaccharide building blocks that are incorporated into glycans (**Figure 1-1**). These monosaccharides (and their abbreviations) are: D-glucose (Glc), *N*-acetyl-D-glucosamine (GlcNAc), D-glucuronic acid (GlcA), D-galactose (Gal), *N*-acetyl-D-galactosamine (GalNAc), D-mannose (Man), D-xylose (Xyl), L-fucose (Fuc), and sialic acid (Sia), primarily *N*-acetylneuraminic acid (Neu5Ac). Glycan diversity arises from differences in monosaccharide composition (for example, Gal or GalNAc) in linkage between monosaccharides (for example, between carbons 1 and 3 or carbons 1 and 4), in anomeric state, in branching structures, in other substitutions (such as sulfation state) and in linkage to their aglycone part (protein or lipid).⁴

On the cell surface, glycans are crucial to physiological processes, such as vertebrate immune response and organ development.⁶ Inside the cell, glycans modulate protein trafficking and have been proposed to modulate signaling pathways.⁵ Glycosylation has also been shown to play integral roles in cellular homeostasis,⁷ protein quality control,⁸ nutrient sensing⁹ and development of eukaryotic organisms.¹⁰

Chapter 1: Glycoproteomics and unnatural sugars to study protein glycosylation

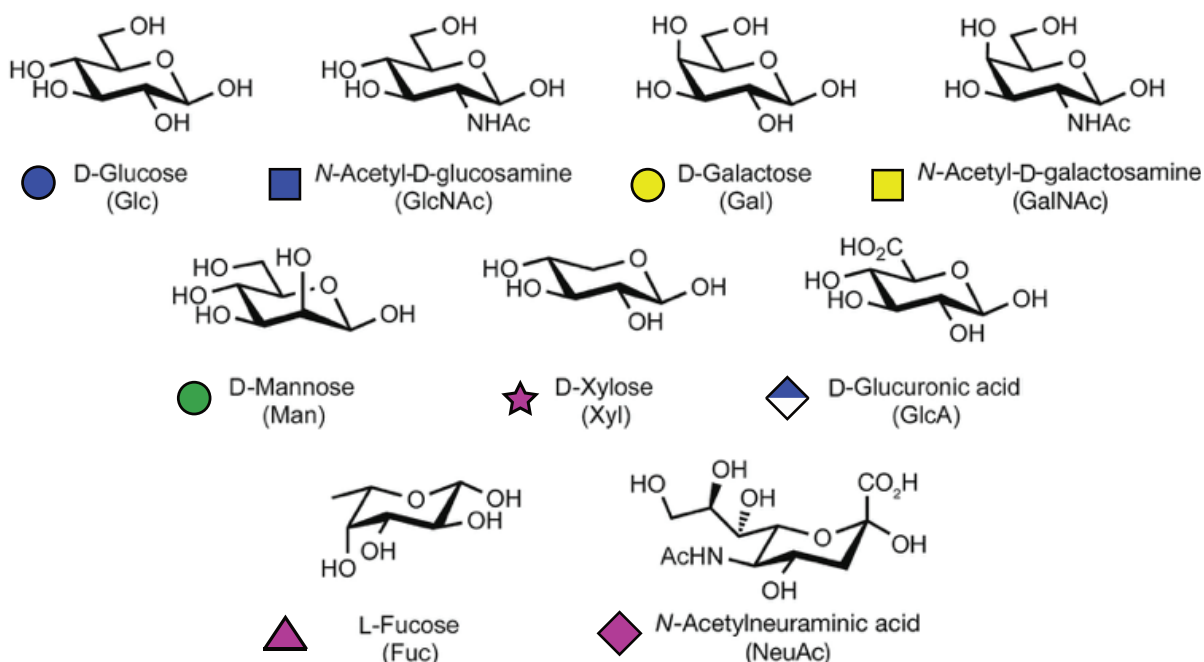


Figure 1-1: Common monosaccharides found invertebrate glycans along with standard graphical representation. Figure adapted from Varki *et al.*¹¹

The term “glycoproteome” then refers to the repertoire of glycoproteins produced by cells under specific conditions of time, space and environment. An intriguing feature of the glycoproteome is that changes in protein glycosylation have been found to accompany cancer progression, suggesting that specific glycoform patterns may serve as biomarkers of disease.⁶ Bioinformatics analyses of eukaryotic genomes have suggested that over 50% of predicted proteins are likely glycosylated.¹² Yet, the vast majority of these glycoproteins have not been characterized at a molecular level, and the functions of their glycans, even when identified, remain mostly unknown.¹³

Protein glycosylation occurs on specific amino acid side-chains, and these modifications are designated as C, N- and O-glycosylation. C-glycosylation features an α -mannopyranosyl group on the indole side-chain of a tryptophan residue. A consensus sequence for this modification, Trp-X-X-Trp has been reported, in which the first Trp residue will be modified.¹⁴ N-glycosylation occurs on Asn residues that reside within a consensus sequence for N-glycosylation: Asn-X-Ser/ Thr/Cys,^{15,16} where X is any amino acid except proline. N-linked oligosaccharides share a common core structure of GlcNAc₂Man₃ and occur on many secreted and membrane-bound glycoproteins (**Figure 1-2**).

O-glycosylation occurs at serine or threonine residues, usually in sequences rich in hydroxy amino acids, but there has been no consensus sequence determined for this modification. Mucin-type O-glycans are frequently found in secreted or membrane-associated glycoproteins and are initiated by N-acetylgalactosamine (GalNAc) O-linked to Ser/Thr. O-glycans can be extended, producing various 'cores' and different terminal

Chapter 1: Glycoproteomics and unnatural sugars to study protein glycosylation

structures: mammalian proteins have been reported to bear O-linked *N*-acetylgalactosamine,^{17,18} glucose,¹⁹ as well as *N*-acetylglucosamine²⁰ and sialic acid.²¹

The characterization of *N*- and *O*-glycosylation is complicated by the fact that the same amino acids within a population of protein molecules may be modified with an array of different carbohydrate structures, or remain unoccupied. This site-specific heterogeneity may vary by species and tissue²² and may be affected by physiological changes.²³ Chemical tools for perturbing and profiling glycans can enable studies of biological function, but so far such tools have only been available for *N*-glycan targets.^{24,25}

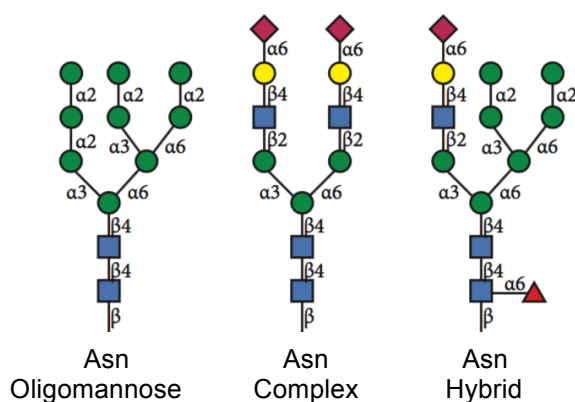


Figure 1-2: Examples of some classes of *N*-linked glycans covalently attached to protein at asparagine (Asn) residues by an *N*-glycosidic bond. The minimal amino acid sequence begins with asparagine followed by any amino acid except proline and it ends with serine or threonine (Asn-X-Ser/Thr). All *N*-glycans share a common core sugar sequence, $\text{Man}\alpha 1\text{--}6(\text{Man}\alpha 1\text{--}3)\text{Man}\beta 1\text{--}4\text{GlcNAc}\beta 1\text{--}4\text{GlcNAc}\beta 1\text{--Asn-X-Ser/Thr}$, and are classified into three types: (1) oligomannose, in which only mannose residues are attached to the core; (2) complex, in which “antennae” initiated by *N*-acetylglucosaminyltransferases (GlcNAcTs) are attached to the core; and (3) hybrid, in which only mannose residues are attached to the $\text{Man}\alpha 1\text{--}6$ arm of the core and one or two antennae are on the $\text{Man}\alpha 1\text{--}3$ arm.

N-Glycosylation can be disrupted globally using the natural product tunicamycin²⁶⁻²⁸ and more subtle perturbations to *N*-glycan peripheral structures can be achieved with the natural products nojirimycin and castanospermine.²⁹⁻³³ In addition, an enzyme, peptide *N*-glycosidase F (PNGase F), removes unaltered most of the common *N*-linked carbohydrates from proteins while hydrolyzing the originally glycosylated Asn residue to Asp. Detection of *N*-glycosylated proteins in a rapid profiling format is also possible. The conserved pentasaccharide core is recognized by the lectins ConA and LPHA. These reagents can be used for enrichment of *N*-glycosylated proteins by affinity chromatography or detection in a Western blot format. Indeed, both lectin chromatography and *N*-glycanase-mediated deglycosylation have been employed in proteomic studies of *N*-glycoproteins from complex biological samples.³⁴⁻³⁶ Collectively, these tools have enabled a number of functional assignments for protein-associated *N*-glycans as well as correlations of their structures with disease states.³⁷⁻⁴⁰

Chapter 1: Glycoproteomics and unnatural sugars to study protein glycosylation

An elaboration of glycosylation from the native “normal state” to aberrant glycosylation as seen in cancer cells likely follows a distinct pathway. Altered expression of glycans can be attributed to under- or overexpression of glycosyltransferases, the enzymes that install and elaborate the carbohydrate moiety, at the transcriptional level,^{57,58} dysregulation of chaperone function⁵⁹ and/or altered glycosidase activity, the enzyme family that removes the glycan.⁶⁰ Alternatively, altered glycan expression can be due to changes in the tertiary conformation of the peptide backbone and that of the nascent glycan chain. Third, the differences can stem from the variability of various acceptor substrates, as well as the availability and abundance of the sugar nucleotide donors and cofactors.⁶¹ Finally, changes in glycan expression can be due to the expression and localization of the relevant glycosyltransferases in the Golgi apparatus.^{62,63}

The most-widely occurring cancer-associated changes in glycosylation are sialylation, fucosylation, O-glycan truncation, and N- and O-linked glycan branching.²³ However, little is known about changes to occupancy and heterogeneity at the site of glycosylation, or glycosite, due to a lack of tools to study both N- and O-linked glycoproteins (Figure 1-4).

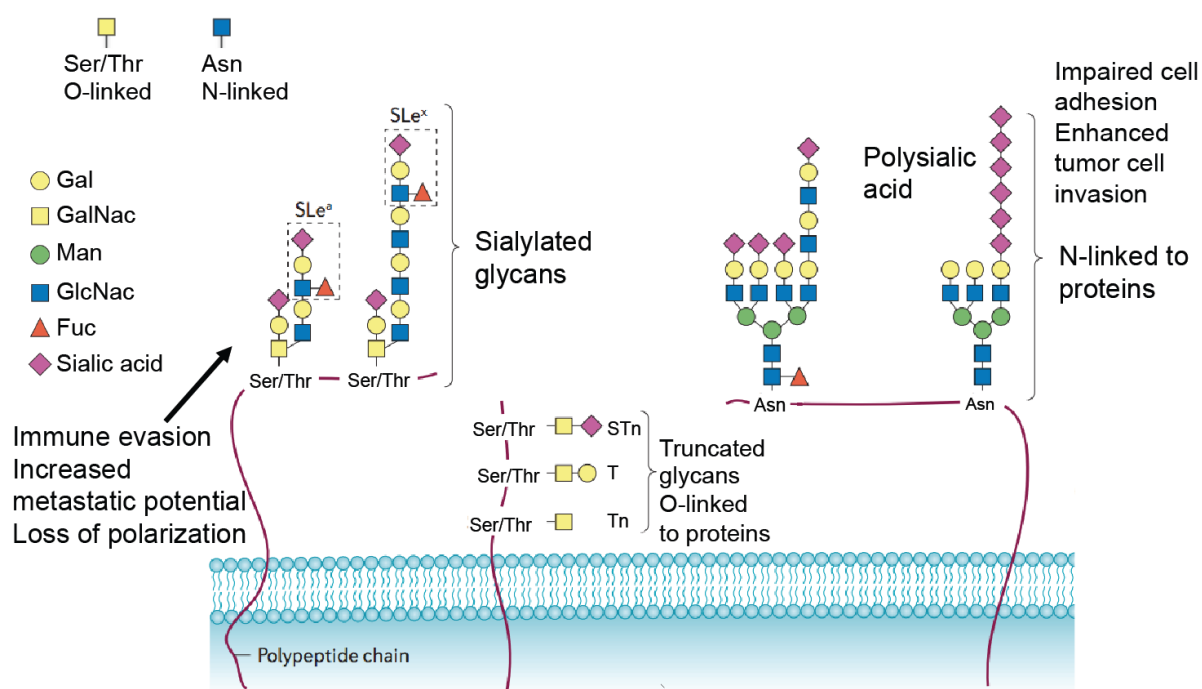


Figure 1-4. Extracellular types of tumor-associated glycans. Tumor cells often display glycans with different structures and levels of expression compared with normal cells. These tumor-specific glycans are part of the cancer phenotype. The most-widely occurring changes in glycosylation in cancer include an increase in overall sialylation. Aberrant glycosylation in cancer frequently involves an increase in sialyl Lewis x (SLe^x) and SLe^a antigens, as well as an increase in terminal α 2,6-sialylated structures, both in truncated O-linked glycans (such as sialyl Tn (STn)) and in N-linked glycans, and an increase in the α 2,8-linked polysialic acid. Overexpression of ‘core’ fucosylation to the innermost GlcNAc of N-glycans) is also considered an important event in

Chapter 1: Glycoproteomics and unnatural sugars to study protein glycosylation

tumor development and progression. Gal, galactose; GalNAc, *N*-acetylgalactosamine; Fuc, fucose; Man, mannose. Figure adapted from Pinho & Reis.²

Table 1-1: Listing of glycosylated US Food and Drug Administration (FDA) approved cancer biomarkers (Glyco denotes glycosylated).

Protein Name	Source	Disease	Glyco
α -Fetoprotein	Serum	Nonseminomatous testicular cancer	Yes
Human chorionic gonadotropin- β	Serum	Testicular cancer	Yes
CA19-9	Serum	Pancreatic cancer	Yes
CA125	Serum	Ovarian cancer	Yes
CEA (carcinoembryonic antigen)	Serum	Colon cancer	Yes
Epidermal growth factor receptor	Tissue	Colon cancer	Yes
KIT	Tissue	Gastrointestinal (GIST) cancer	Yes
Thyroglobulin	Serum	Thyroid cancer	Yes
PSA-prostate-specific antigen	Serum	Prostate cancer	Yes
CA15-3	Serum	Breast cancer	Yes
CA27-29	Serum	Breast cancer	Yes
HER2/NEU	Tissue, Serum	Breast cancer	Yes
Fibrin/FDP-fibrin degradation protein	Urine	Bladder cancer	Yes
BTA-bladder tumor-associated antigen	Urine	Bladder cancer	Yes

1.3 Mass spectrometry-based glycoproteomics

Mass spectrometry (MS) has evolved impressively since it began nearly 100 years ago. Initially, it was not obvious that an instrument developed to identify the intensities of mass-to-charge, m/z , could be used for biological applications. The technique began with organic molecules including amino acids but as high-resolution mass spectrometers with accurate mass analyzers emerged, it became a tool for sequencing small purified peptides.⁶⁴ Innovations in *de novo* peptide sequencing led to the analysis of proteins using enzymatic digestion of the intact protein to produce peptides small enough to be analyzed by the mass spectrometer.⁶⁴ From observing overlapping peptide fragments, the sequence of the proteins could be reconstituted. Additionally, innovations in gas chromatography (GC) provided a means to separate peptides which were then analyzed in-line with the mass spectrometer.

It was Hunt and coworkers who began use of high performance liquid chromatography (HPLC) to separate proteolytically digested proteins off-line and then analyzing peptides by MS.⁶⁵ This fundamental approach comprises of digesting intact proteins, separating peptides by HPLC, and then sequencing the peptides by tandem MS. This workflow developed in the 1980s is essentially the same strategy used today. “Bottom-up proteomics” referring to the identification of proteins following proteolytic digestion.

Early reports of bottom-up proteomics were hindered by the mass accuracy of the instrument employed. At the same time Hunt was developing bottom-up proteomics,

Chapter 1: Glycoproteomics and unnatural sugars to study protein glycosylation

Fenn and coworkers demonstrated the ability to ionize large proteins and measure m/z ratios accurately on proteins, using a novel electrospray ionization (ESI) source.⁶⁶ ESI accuracy on proteins inspired Smith and coworkers to implement ESI to interface with capillary electrophoresis to analyze peptides.⁶⁷

Subsequently, several groups devised a strategy to marry ESI with the microscale packed capillary columns developed by the groups of Novotny and Jorgenson.^{68,69} This led to a novel nanoLC ESI tandem MS method to sequence peptides isolated from MHC proteins based on the previously developed MS-MS strategy.⁷⁰ Early methods required users to manually select ions for MS-MS, necessitating two analyses: one to identify peptide ion m/z values and a second to select ions for MS-MS, which decreased throughput and made mass spectrometry an almost entirely academic pursuit. Furthermore, this approach limited the number of ions that could be selected in a single analysis. To improve on this process, a “peak parking” technique was used that slowed the flow rate of the HPLC effluent to allow more time to collect MS-MS.^{70,71}

In 1990, the NIH and DOE presented a plan to complete mapping and understanding of all the genes of human beings.⁷² Almost immediately, databases started to fill with DNA sequence information, and bioinformatic algorithms for mining the data proliferated. Yates and coworkers developed a method for automated analysis of peptide tandem MS data that involved searching MS-MS data using the sequences being generated by the genome sequencing projects.⁶⁵ This method allowed for rapid interpretation of MS peptide data.

It was John Yates who developed methods for liquid chromatogram (LC) followed by tandem MS analysis (LC/MS-MS) of peptides that began to allow the identification of complex peptide mixtures in a bottom-up approach.^{73,74} The full proteome of an organism was known after genome sequencing, though individual proteins may vary within a species, allowing for the identification and characterization of proteins involved in specific processes. Protein identification with tandem MS facilitated that process and was critical to the creation of “shotgun” proteomics enabling large-scale, high-throughput data analysis (**Figure 1-5**).

Over the past decade, proteomics has emerged as a powerful tool for screening biological samples. The in-depth and quantitative characterization of a number of proteomes has advanced our understanding of cellular processes. For example, we now have an initial framework for the protein content of discrete cell types and subcellular structures, and we are beginning to define the connectivity and dynamics among those components which can enable both basic research and drug discovery and development.⁷⁵

MS-based proteomics has become a robust method with most universities, companies and institutes having an active MS proteomics core facility or in-house program. MS methods for profiling the proteome, have largely been democratized to even non-specialists. However, expansion of MS to study PTMs, specifically glycoproteins, has not advanced as quickly. The molecular complexity and dynamic resolution of cells and tissue lysate renders some biologically interesting peptides and glycopeptides difficult to distinguish from the vast population of more abundant species. For example, in serum, highly abundant proteins function to nonspecifically bind to components, with their

Chapter 1: Glycoproteomics and unnatural sugars to study protein glycosylation

removal resulting in the loss of circulating proteins or peptides secreted from cells.⁷⁶ It is believed that such low abundant proteins and glycoproteins, a potential class of biomarkers, would appear in serum at low microgram to high picogram per milliliter concentrations.⁷⁷

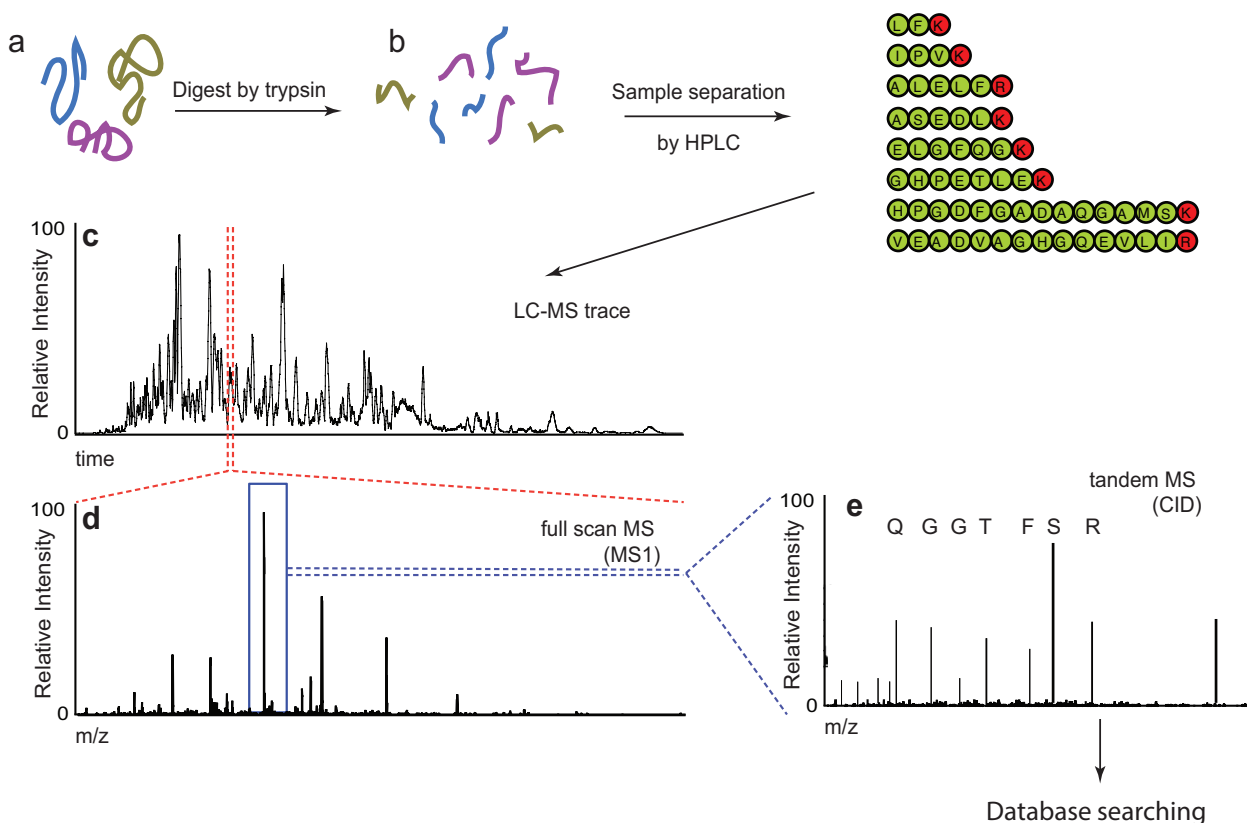


Figure 1-5: A schematic of a typical bottom-up or shotgun proteomic experiment. (a) A biological sample containing proteins is digested with a protease (typically with trypsin which cleaves after lysine and arginine residues) to (b) produce a solution of peptic fragments. (c) These fragments are then separated by on-line high performance liquid chromatography (HPLC). (d) A mass spectrum of the eluting sample is taken at regular intervals (often in the ms). (e) From the full scan mass spectrum, ions are chosen and subjected to secondary fragmentation, (termed tandem MS-MS) in a data-dependent fashion (e.g., based on ion abundance). These fragment mass spectra are subjected to a database search to produce peptide and protein identifications.

Additionally, in contrast to proteomic profiling of uniform PTMs (such as phosphorylation⁷⁸ and acetylation⁷⁹), intact-glycopeptide analysis faces challenges on two fronts: detection by MS and computational identification via database searching. Glycan heterogeneity produces a number of substoichiometric modifications to the glycopeptide that effectively reduce the quantity of any particular glycoform. Because of this, as well as the lower ionization efficiency of glycoconjugates,⁸⁰ the detection of intact glycopeptides often requires increased sample quantities, enrichment or both. Moreover, the heterogeneity and non-template nature of glycopeptides stymie computational analysis. Crucially, most high-throughput proteomic platforms rely on database searches

for peptide identification.⁸¹

As mentioned above, the non-template nature of glycosylation presents significant computational challenges on the proteome level. Whereas a consensus sequence exists for N-glycosylation (N-X-S/T, where X is not proline), there are no defined consensus motifs for the various types of O-glycosylation. Indeed, the sheer number of possible glycoforms associated with the entire proteome yields an unmanageable sum of combinations for database search algorithms to match. To overcome this limitation, often some type of enrichment of low abundant species is performed.

1.4 Unnatural sugars for bioorthogonal enrichment of glycans

Without a universal method to identify glycoforms by database searches, enrichment of specific glycoprotein subtypes and reduction of glycan heterogeneity are presently required for glycoproteomic profiling. Enrichment of specific glycoprotein subtypes has been achieved with chemical tagging,⁸² enzymatic labeling⁸³ and lectin chromatography.^{84,85} However, methods for broadly profiling intact glycopeptides on the whole-proteome scale are still incomplete.

Metabolic labeling methods have been developed to enrich classes of proteins and glycoproteins. Metabolic labeling of glycoproteins with unnatural functionalities is a technique developed for the detection, visualization, and enrichment of cellular and secreted glycoproteins.⁸⁶ This strategy involves incubating cells with an unnatural monosaccharide that is functionalized with a chemical reporter group that can undergo covalent modification with an enrichment probe. Metabolic labeling relies on the ability of the cell's biosynthetic machinery to process and install the unnatural, functionalized, monosaccharide into endogenous glycoproteins (**Figure 1-6**).⁸⁷

The most common method for introducing functionalized monosaccharides into glycans via metabolic labeling was pioneered by Mahal and coworkers with ketone-labeled sialic acid precursors.⁸⁸ This takes advantage of work by Warner Reutter's lab that demonstrated the promiscuous nature of the endogenous neuraminic acid biosynthetic pathways for small chemical modifications.^{89,90} In this approach, cells are typically treated with the cell permeable, per-*O*-acetylated version of a precursor monosaccharide that has been chemically modified with reporter group such as ketone, azide, or alkyne. The per-*O*-acetylation enables the functionalized precursor to passively diffuse through the cellular membrane and access intracellular glycosyltransferase enzymes that install and elaborate the glycan. With small modifications the functionalized monosaccharide will be installed on nascent glycans.

Once labeled with chemical reporter groups, glycans can be labeled via bioorthogonal ligations to appropriately functionalized enrichment molecules. Since Reutter and Mahal first introduced this work, several bioorthogonal reactions have been developed to proceed rapidly under physiological conditions and create covalent ligation products that can be purified.

Saxon and coworkers expanded the bioorthogonal toolbox with the azide, N₃, and a unique reaction with a triaryl phosphine, termed the Staudinger ligation. In this reaction, an ester bond is cleaved and a covalent attachment of the triaryl phosphine moiety to the

glycan is formed (**Figure 1-7A**).⁹¹ The copper(I)-catalyzed azide-alkyne cycloaddition (CuAAC), coined the “click” reaction, developed independently by Sharpless and Meldal, produces triazole products between azides and terminal alkynes reagents (**Figure 1-7B**).⁹² This reaction is very fast and proceeds in water under physiological conditions. Wong and coworkers have shown that some reactions proceed with enhanced kinetics when the azide and alkyne partners are switched (**Figure 1-7C**).^{93,94}

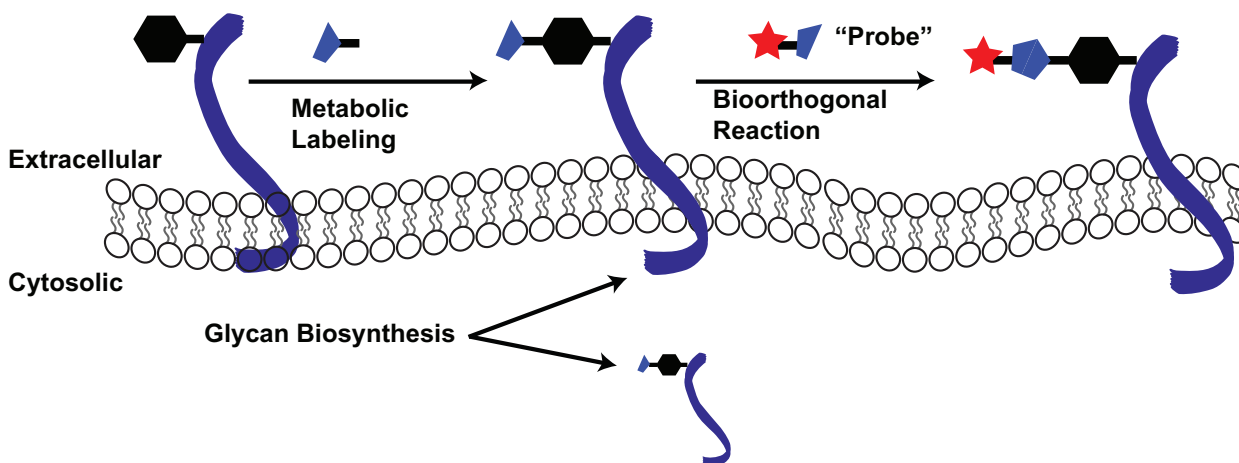


Figure 1-6: Metabolic bioorthogonal engineering. Unnatural sugar building blocks are taken up by cells, processed by cells’ biosynthetic machinery, and ultimately incorporated into the glycoconjugates, including cell surface glycoproteins and cytosolic glycoproteins. After incorporation into glycoproteins of interest, they can then be selectively reacted with a probe to a bioorthogonal probe resulting in a covalent linkage between the biomolecule of interest and the probe.

As an alternative to copper(I) catalysis, the azide-alkyne cycloaddition reaction can be activated by strain promoted azide-alkyne cycloaddition (SPAAC) reaction (**Figure 1-7-d**). When the alkyne is placed in an eight-membered ring, the angles around the triple bond are distorted from the ideal 180° to approximately 160° ,⁹⁵ which contributes to ring strain of ~ 18 kcal/mol.⁹⁶ With such a highly destabilized ground state, the cycloaddition reaction with azide to produce the triazole product proceeds under metal-free and physiological conditions.⁹⁷

A number of methodologies developed over the last decade address bioorthogonal labeling of glycans, proteins, lipids, nucleic acids and other metabolites with functional groups that enable both imaging and enrichment.^{98,99} These techniques began with labeling biomolecules in cultured cells,⁹¹ but there was a motivation to deploy these techniques to systems that more closely mimic human disease. As reflected in reports of bioorthogonal labeling in *Caenorhabditis elegans*,¹⁰⁰ *Drosophila melanogaster*,¹⁰¹ zebrafish¹⁰² and murine models.^{103,104}

The Bertozzi Lab has produced chemical tools for use this bioorthogonal approach to studying mucin-type O-linked glycans by MS. Metabolic labeling with peracetylated *N*-azidoacetyl-galactosamine (Ac₄GalNAz) introduces an azidosugar into the extracellular

Chapter 1: Glycoproteomics and unnatural sugars to study protein glycosylation

O-glycan. Bioorthogonal copper-click chemistry of the azide with an alkyne introduces a handle for affinity enrichment from biological samples.

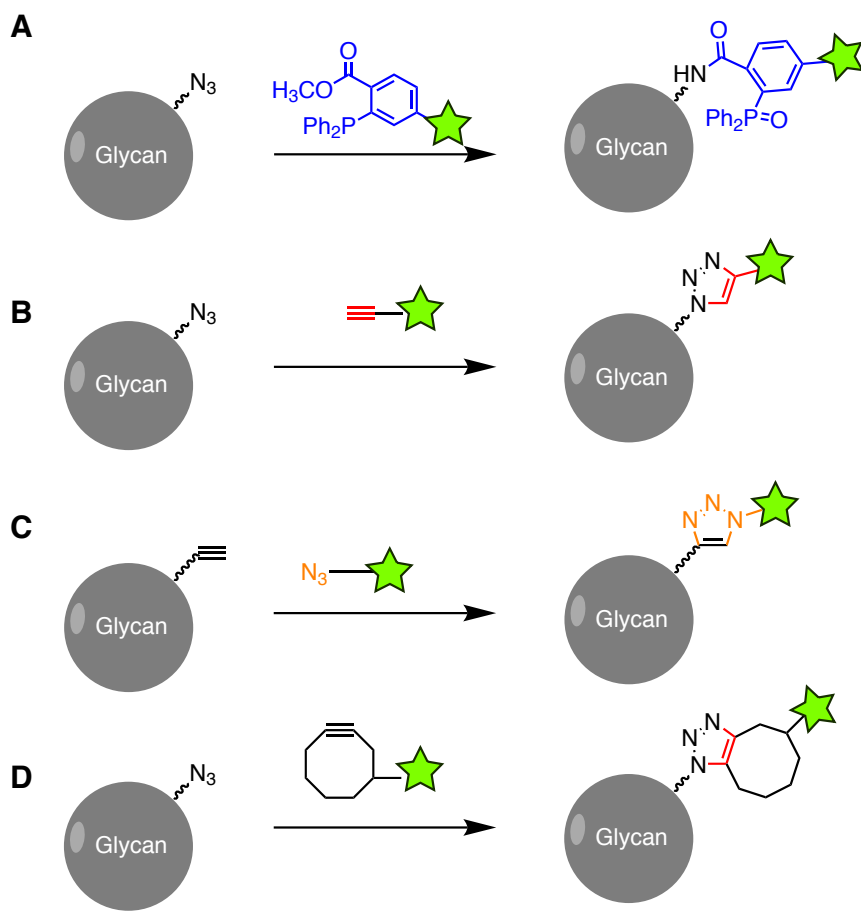


Figure 1-7: Bioorthogonal reactions with azides and terminal alkynes. (A) The Staudinger ligation between azides and triarylphosphine reagents. (B, C) Overview of cycloaddition reaction to produce a triazole-containing product. Either the azide or the alkyne can be incorporated into glycans, then reacted with the appropriate reaction partner in the presence of copper(I) and ligand. (D) Copper-free click reaction between azides and cyclooctyne reagents to produce a triazole product. Green star denotes either a fluorophore for imaging, e.g. fluorogenic azido-coumarin reagent that becomes fluorescent upon reaction with terminal alkynes, or biotin- or FLAG-tagged affinity reagents for enrichment.

Using this approach, PC-3 cells, an androgen-insensitive prostate cell lines were metabolically labeled with $Ac_4GaINaz$. Lysate was covalently reacted with a phosphine-FLAG affinity probe, labeled proteins were captured by immunoprecipitation of the FLAG tag, and followed by SDS-PAGE separation was done. Gel bands were then excised and analyzed by LC-MS/MS. This analysis by MS revealed 71 glycoproteins that change in comparison to a LNCaP a cell line of androgen-sensitive prostate cancer.¹⁰⁵ These results establish cell-surface glycoproteomics as an effective technique for the

bioorthogonal enrichment of cell surface glycoproteins. However, many physiological properties are lost in cell culture and we sought to study glycosylation in faithful models of human disease.

1.5 Conclusion

This dissertation addresses the dearth of tools in the areas of glycoprotein enrichment and glycoproteomic analysis through the application of bioorthogonal labeling and directed mass spectrometry. The unique challenges glycans pose due to their complex structures and biosynthesis, has led to the development of new methods for their labeling and identification. In particular, the chemical reporter method has enabled imaging of several classes of glycans and has also been extended to other classes of biomolecules. Further improvements in these technologies should help to expand the models for studying clinical glycoproteomics in human cancers.

In this dissertation, Chapter 1 describes a broad overview of the relatively intersecting fields of glycobiology and mass spectrometry, underscoring the need to develop new tools in these fields to aid future discovery. Chapter 2 describes the development of a metabolic approach to bioorthogonal labeling of human prostate cancer cell lines and tissues, utilizing cell-surface incorporation and labeling of azidosugars for selective enrichment and identification of sialoglycoproteins. Chapter 3 extends these methods to prostate tissue slice culture conditioned media, a faithful model of the clinical secretome. Finally, in Chapter 4, we describe mutations in granulocyte colony-stimulating factor 3 receptor (CSF3R) in a site of glycosylation that drives neutrophilic production in a rare chronic neutrophilic leukemia (CNL). Detailed mass spectrometry analysis demonstrates that this site is glycosylated with complex bisecting glycans. Interestingly, these mutations substitutions are potently oncogenic and result in ligand-independent receptor activation.

1.6 References

- 1 Fuster, M. M. & Esko, J. D. The sweet and sour of cancer: Glycans as novel therapeutic targets. *Nature Review Cancer* **5**, 526-542 (2005).
- 2 Pinho, S. S. & Reis, C. A. Glycosylation in cancer: mechanisms and clinical implications. *Nature Reviews Cancer* **15**, 540-555 (2015).
- 3 Freeze, H. H. Understanding human glycosylation disorders: biochemistry leads the charge. *Journal of Biological Chemistry* **288**, 6936-6945 (2013).
- 4 Varki, A., Esko, J. D., Colley, K. J., Varki, A., Cummings, R. D., Esko, J. D., Freeze, H. H., Stanley, P., Bertozzi, C. R., Hart, G. W. & Etzler, M. E. *Essentials of Glycobiology*. (2009).
- 5 Ohtsubo, K. & Marth, J. D. Glycosylation in Cellular Mechanisms of Health and Disease. *Cell* **126**, 855 (2006).
- 6 Rudd, P. M., Elliott, T., Cresswell, P., Wilson, I. A. & Dwek, R. A. Glycosylation and the Immune System. *Science* **291**, 2370 (2001).
- 7 Cheung, P., Pawling, J., Partridge, E. A., Sukhu, B., Grynepas, M. & Dennis, J. W. Metabolic homeostasis and tissue renewal are dependent on beta1,6GlcNAc-branched N-glycans. *Glycobiology* **17**, 828-837 (2007).
- 8 Roth, J. Protein N-glycosylation along the secretory pathway: relationship to organelle topography and function, protein quality control, and cell interactions. *Chemical Reviews* **102**, 285-303 (2002).
- 9 Taylor, R. P., Parker, G. J., Hazel, M. W., Soesanto, Y., Fuller, W., Yazzie, M. J. & McClain, D. A. Glucose deprivation stimulates O-GlcNAc modification of proteins through up-regulation of O-linked N-acetylglucosaminyltransferase. *Journal of Biological Chemistry* **283**, 6050-6057 (2008).
- 10 Poirier, F. & Kimber, S. Cell surface carbohydrates and lectins in early development. *Molecular Human Reproduction* **3**, 907-918 (1997).
- 11 Varki, A., Lowe, J. B., Varki, A., Cummings, R. D., Esko, J. D., Freeze, H. H., Stanley, P., Bertozzi, C. R., Hart, G. W. & Etzler, M. E. *Essentials of Glycobiology*. (2009).
- 12 Apweiler, R., Hermjakob, H. & Sharon, N. On the frequency of protein glycosylation, as deduced from analysis of the SWISS-PROT database. *Biochimica Et Biophysica Acta-General Subjects* **1473**, 4-8 (1999).
- 13 Varki, A. Biological roles of glycans. *Glycobiology* **27**, 3-49 (2017).
- 14 Furmanek, A. & Hofsteenge, J. Protein C-mannosylation: facts and questions. *Acta Biochimica Polonica* **47**, 781-789 (2000).

Chapter 1: Glycoproteomics and unnatural sugars to study protein glycosylation

- 15 Pless, D. D. & Lennarz, W. J. Enzymatic conversion of proteins to glycoproteins. *Proceedings of the National Academy of Sciences USA* **74**, 134-138 (1977).
- 16 Satomi, Y., Shimonishi, Y. & Takao, T. N-glycosylation at Asn(491) in the Asn-Xaa-Cys motif of human transferrin. *FEBS Letters* **576**, 51-56 (2004).
- 17 Hanisch, F. G. & Peter-Katalinic, J. Structural studies on fetal mucins from human amniotic fluid. Core typing of short-chain O-linked glycans. *European Journal of Biochemistry* **205**, 527-535 (1992).
- 18 Hanisch, F. G., Jovanovic, M. & Peter-Katalinic, J. Glycoprotein Identification and Localization of O-Glycosylation Sites by Mass Spectrometric Analysis of Deglycosylated/Alkylaminylated Peptide Fragments. *Analytical Biochemistry* **290**, 47 (2001).
- 19 Nishimura, H., Kawabata, S., Kisiel, W., Hase, S., Ikenaka, T., Takao, T., Shimonishi, Y. & Iwanaga, S. Identification of a disaccharide (Xyl-Glc) and a trisaccharide (Xyl₂-Glc) O-glycosidically linked to a serine residue in the first epidermal growth factor-like domain of human factors VII and IX and protein Z and bovine protein Z. *Journal of Biological Chemistry* **264**, 20320-20325 (1989).
- 20 Snow, D. M. & Hart, G. W. Nuclear and cytoplasmic glycosylation. *International Review of Cytology* **181**, 43-74 (1998).
- 21 Brockhausen, I., Yang, J., Lehotay, M., Ogata, S. & Itzkowitz, S. Pathways of mucin O-glycosylation in normal and malignant rat colonic epithelial cells reveal a mechanism for cancer-associated Sialyl-Tn antigen expression. *Journal of Biological Chemistry* **382**, 219-232 (2001).
- 22 Hironaka, T., Furukawa, K., Esmo, P. C., Yokota, T., Brown, J. E., Sawada, S., Fournel, M. A., Kato, M., Minaga, T. & Kobata, A. Structural study of the sugar chains of porcine factor VIII--tissue- and species-specific glycosylation of factor VIII. *Arch Biochem Biophys* **307**, 316-330 (1993).
- 23 Hakomori, S. Glycosylation defining cancer malignancy: new wine in an old bottle. *Proceedings of the National Academy of Sciences USA* **99**, 10231-10233 (2002).
- 24 Prescher, J. A. & Bertozzi, C. R. Chemical technologies for probing glycans. *Cell* **126**, 851-854 (2006).
- 25 Hang, H. C. & Bertozzi, C. R. The chemistry and biology of mucin-type O-linked glycosylation. *Bioorganic & Medicinal Chemistry* **13**, 5021-5034 (2005).
- 26 Elbein, A. D. Inhibitors Of The Biosynthesis And Processing Of N-Linked Oligosaccharides. *Crc Critical Reviews In Biochemistry* **16**, 21-49 (1984).
- 27 Takatsuk, A., Arima, K. & Tamura, G. Tunicamycin, A New Antibiotic .1. Isolation And Characterization Of Tunicamycin. *Journal Of Antibiotics* **24**, 215-& (1971).

Chapter 1: Glycoproteomics and unnatural sugars to study protein glycosylation

- 28 Lehle, L. & Tanner, W. Specific Site Of Tunicamycin Inhibition In Formation Of Dolichol-Bound N-Acetylglucosamine Derivatives. *FEBS Letters* **71**, 167-170 (1976).
- 29 Saul, R., Chambers, J. P., Molyneux, R. J. & Elbein, A. D. Castanospermine, A Tetrahydroxylated Alkaloid That Inhibits Beta-Glucosidase And Beta-Glucocerebrosidase. *Archives Of Biochemistry And Biophysics* **221**, 593-597 (1983).
- 30 Hohenschutz, L. D., Bell, E. A., Jewess, P. J., Leworthy, D. P., Pryce, R. J., Arnold, E. & Clardy, J. Castanospermine, A 1,6,7,8-Tetrahydroxyoctahydroindolizine Alkaloid, From Seeds Of *Castanospermum-Australe*. *Phytochemistry* **20**, 811-814 (1981).
- 31 Reese, E. T., Parrish, F. W. & Ettlige, M. Nojirimycin And D-Glucono-1,5-Lactone As Inhibitors Of Carbohydrases. *Carbohydrate Research* **18**, 381-& (1971).
- 32 Inouye, S., Tsuruoka, T., Ito, T. & Niida, T. Structure And Synthesis Of Nojirimycin. *Tetrahedron* **24**, 2125-& (1968).
- 33 Ishida, N., Kumagai, K., Niida, T., Hamamoto, K. & Shomura, T. Nojirimycin A New Antibiotic .I. Taxonomy And Fermentation. *Journal Of Antibiotics* **20**, 62-& (1967).
- 34 Kaji, H., Saito, H., Yamauchi, Y., Shinkawa, T., Taoka, M., Hirabayashi, J., Kasai, K., Takahashi, N. & Isobe, T. Lectin affinity capture, isotope-coded tagging and mass spectrometry to identify N-linked glycoproteins. *Nature Biotechnology* **21**, 667-672 (2003).
- 35 Zhang, H., Li, X. J., Martin, D. B. & Aebersold, R. Identification and quantification of N-linked glycoproteins using hydrazide chemistry, stable isotope labeling and mass spectrometry. *Nature Biotechnology* **21**, 660-666 (2003).
- 36 Zielinska, D. F., Gnad, F., Wisniewski, J. R. & Mann, M. Precision Mapping of an In Vivo N-Glycoproteome Reveals Rigid Topological and Sequence Constraints. *Cell* **141**, 897-907.
- 37 Lau, K. S. & Dennis, J. W. N-Glycans in cancer progression. *Glycobiology* **18**, 750-760 (2008).
- 38 Partridge, E. A., Cheung, P. & Dennis, J. W. in *Functional Glycomics Methods in Enzymology* **417** 3-11 (2006).
- 39 Helenius, A. & Aebi, M. Roles of N-linked glycans in the endoplasmic reticulum. *Annual Review Of Biochemistry* **73**, 1019-1049 (2004).
- 40 Helenius, A. & Aebi, M. Intracellular functions of N-linked glycans. *Science* **291**, 2364-2369 (2001).

Chapter 1: Glycoproteomics and unnatural sugars to study protein glycosylation

- 41 Prescher, J. A. & Bertozzi, C. R. Chemical Technologies for Probing Glycans. *Cell* **126**, 851 (2006).
- 42 Shogren, R., Gerken, T. A. & Jentoft, N. Role of glycosylation on the conformation and chain dimensions of O-linked glycoproteins: light-scattering studies of ovine submaxillary mucin. *Biochemistry* **28**, 5525-5536 (1989).
- 43 Hanisch, F. G. & Muller, S. MUC1: the polymorphic appearance of a human mucin. *Glycobiology* **10**, 439-449 (2000).
- 44 Kramer, J. R., Onoa, B., Bustamante, C. & Bertozzi, C. R. Chemically tunable mucin chimeras assembled on living cells. *Proceedings of the National Academy of Sciences USA* **112**, 12574-12579 (2015).
- 45 Coltart, D. M., Royyuru, A. K., Williams, L. J., Glunz, P. W., Sames, D., Kuduk, S. D., Schwarz, J. B., Chen, X. T., Danishefsky, S. J. & Live, D. H. Principles of mucin architecture: Structural studies on synthetic glycopeptides bearing clustered mono-, di-, tri-, and hexasaccharide glycodomains. *Journal of the American Chemical Society* **124**, 9833-9844 (2002).
- 46 Live, D. H., Williams, L. J., Kuduk, S. D., Schwarz, J. B., Glunz, P. W., Chen, X. T., Sames, D., Kumar, R. A. & Danishefsky, S. J. Probing cell-surface architecture through synthesis: an NMR-determined structural motif for tumor-associated mucins. *Proceedings of the National Academy of Sciences USA* **96**, 3489-3493 (1999).
- 47 Dube, D. H. & Bertozzi, C. R. Glycans in Cancer and Inflammation - Potential for Therapeutics and Diagnostics. *Nature Review Drug Discovery* **4**, 477-488 (2005).
- 48 Meezan, E., Wu, H. C., Black, P. H. & Robbins, P. W. Comparative Studies on the Carbohydrate-Containing Membrane Components of Normal and Virus-Transformed Mouse Fibroblasts. II. Separation of Glycoproteins and Glycopeptides by Sephadex Chromatography. *Biochemistry* **8**, 2518-2524 (1969).
- 49 Hakomori, S. I. & Murakami, W. T. Glycolipids of hamster fibroblasts and derived malignant-transformed cell lines. *Proceedings of the National Academy of Sciences USA* **59**, 254-261 (1968).
- 50 Nath, S. & Mukherjee, P. MUC1: a multifaceted oncoprotein with a key role in cancer progression. *Trends in Molecular Medicine* **20**, 332-342 (2014).
- 51 Shukla, H. D., Paulius, V. & Cotter, R. J. Advances in membrane proteomics and cancer biomarker discovery: Current status and future perspective. *Proteomics* **12**, 3085-3104 (2012).
- 52 Hollingsworth, M. A. & Swanson, B. J. Mucins in Cancer: Protection and Control of the Cell Surface. *Nature Review Cancer* **4**, 45-60 (2004).

Chapter 1: Glycoproteomics and unnatural sugars to study protein glycosylation

- 53 Wong, N. K., Easton, R. L., Panico, M., Sutton-Smith, M., Morrison, J. C., Lattanzio, F. A., Morris, H. R., Clark, G. F., Dell, A. & Patankar, M. S. Characterization of the Oligosaccharides Associated with the Human Ovarian Tumor Marker CA125. *Journal of Biological Chemistry* **278**, 28619-28634 (2003).
- 54 Song, E., Hu, Y., Hussein, A., Yu, C. Y., Tang, H. & Mechref, Y. Characterization of the Glycosylation Site of Human PSA Prompted by Missense Mutation using LC-MS/MS. *Journal of Proteome Research* **14**, 2872-2883 (2015).
- 55 Tajiri, M., Ohyama, C. & Wada, Y. Oligosaccharide profiles of the prostate specific antigen in free and complexed forms from the prostate cancer patient serum and in seminal plasma: a glycopeptide approach. *Glycobiology* **18**, 2-8 (2008).
- 56 Tabares, G., Jung, K., Reiche, J., Stephan, C., Lein, M., Peracaula, R., de Llorens, R. & Hoesel, W. Free PSA forms in prostatic tissue and sera of prostate cancer patients: analysis by 2-DE and western blotting of immunopurified samples. *Clinical Biochemistry* **40**, 343-350 (2007).
- 57 Kannagi, R., Sakuma, K., Miyazaki, K., Lim, K. T., Yusa, A., Yin, J. & Izawa, M. Altered expression of glycan genes in cancers induced by epigenetic silencing and tumor hypoxia: clues in the ongoing search for new tumor markers. *Cancer Science* **101**, 586-593 (2010).
- 58 Buckhaults, P., Chen, L., Fregien, N. & Pierce, M. Transcriptional regulation of N-acetylglucosaminyltransferase V by the src oncogene. *Journal of Biological Chemistry* **272**, 19575-19581 (1997).
- 59 Schietinger, A., Philip, M., Yoshida, B. A., Azadi, P., Liu, H., Meredith, S. C. & Schreiber, H. A mutant chaperone converts a wild-type protein into a tumor-specific antigen. *Science* **314**, 304-308 (2006).
- 60 Kakugawa, Y., Wada, T., Yamaguchi, K., Yamanami, H., Ouchi, K., Sato, I. & Miyagi, T. Up-regulation of plasma membrane-associated ganglioside sialidase (Neu3) in human colon cancer and its involvement in apoptosis suppression. *Proceedings of the National Academy of Sciences USA* **99**, 10718-10723 (2002).
- 61 Kumamoto, K., Goto, Y., Sekikawa, K., Takenoshita, S., Ishida, N., Kawakita, M. & Kannagi, R. Increased expression of UDP-galactose transporter messenger RNA in human colon cancer tissues and its implication in synthesis of Thomsen-Friedenreich antigen and sialyl Lewis A/X determinants. *Cancer Research* **61**, 4620-4627 (2001).
- 62 Gill, D. J., Chia, J., Senewiratne, J. & Bard, F. Regulation of O-glycosylation through Golgi-to-ER relocation of initiation enzymes. *Journal of Cellular Biology* **189**, 843-858 (2010).
- 63 Kellokumpu, S., Sormunen, R. & Kellokumpu, I. Abnormal glycosylation and altered Golgi structure in colorectal cancer: dependence on intra-Golgi pH. *FEBS Letters* **516**, 217-224 (2002).

Chapter 1: Glycoproteomics and unnatural sugars to study protein glycosylation

- 64 Biemann, K., Cone, C., Webster, B. R. & Arsenault, G. P. Determination of the amino acid sequence in oligopeptides by computer interpretation of their high-resolution mass spectra. *Journal of the American Chemical Society* **88**, 5598-5606 (1966).
- 65 Hunt, D. F., Yates, J. R., 3rd, Shabanowitz, J., Winston, S. & Hauer, C. R. Protein sequencing by tandem mass spectrometry. *Proceedings of the National Academy of Sciences USA* **83**, 6233-6237 (1986).
- 66 Fenn, J. B., Mann, M., Meng, C. K., Wong, S. F. & Whitehouse, C. M. Electrospray ionization for mass spectrometry of large biomolecules. *Science* **246**, 64-71 (1989).
- 67 Smith, R. D. & Udseth, H. R. Capillary zone electrophoresis-MS. *Nature* **331**, 639-640 (1988).
- 68 Novotny, M. & Zlatkis, A. Capillary columns and their significance in biochemical research. *Chromatographic Reviews* **14**, 1-44 (1971).
- 69 Kennedy, R. T. & Jorgenson, J. W. Quantitative analysis of individual neurons by open tubular liquid chromatography with voltammetric detection. *Analytical Chemistry* **61**, 436-441 (1989).
- 70 Hunt, D. F., Henderson, R. A., Shabanowitz, J., Sakaguchi, K., Michel, H., Sevilir, N., Cox, A. L., Appella, E. & Engelhard, V. H. Characterization of peptides bound to the class I MHC molecule HLA-A2.1 by mass spectrometry. *Science* **255**, 1261-1263 (1992).
- 71 Davis, M. T., Stahl, D. C., Hefta, S. A. & Lee, T. D. A microscale electrospray interface for on-line, capillary liquid chromatography/tandem mass spectrometry of complex peptide mixtures. *Analytical Chemistry* **67**, 4549-4556 (1995).
- 72 Collins, F. & Galas, D. A new five-year plan for the U.S. Human Genome Project. *Science* **262**, 43-46 (1993).
- 73 McCormack, A. L., Schieltz, D. M., Goode, B., Yang, S., Barnes, G., Drubin, D. & Yates, J. R., 3rd. Direct analysis and identification of proteins in mixtures by LC/MS/MS and database searching at the low-femtomole level. *Analytical Chemistry* **69**, 767-776 (1997).
- 74 Yates, J. R., 3rd, Eng, J. K., McCormack, A. L. & Schieltz, D. Method to correlate tandem mass spectra of modified peptides to amino acid sequences in the protein database. *Analytical Chemistry* **67**, 1426-1436 (1995).
- 75 Cravatt, B. F., Simon, G. M. & Yates, J. R. The Biological Impact of Mass-Spectrometry-Based Proteomics. *Nature* **450**, 991 (2007).
- 76 Raso, C., Cosentino, C., Gaspari, M., Malara, N., Han, X., McClatchy, D., Park, S. K., Renne, M., Vadalà, N., Prati, U., Cuda, G., Mollace, V., Amato, F. & Yates, J. R. Characterization of Breast Cancer Interstitial Fluids by TmT Labeling, LTQ-

Chapter 1: Glycoproteomics and unnatural sugars to study protein glycosylation

- Orbitrap Velos Mass Spectrometry, and Pathway Analysis. *Journal of Proteome Research* (2012).
- 77 Aebersold, R. & Mann, M. Mass Spectrometry-Based Proteomics. *Nature* **422**, 198 (2003).
- 78 Zhou, H., Watts, J. D. & Aebersold, R. A systematic approach to the analysis of protein phosphorylation. *Nature Biotechnology* **19**, 375-378 (2001).
- 79 Choudhary, C., Kumar, C., Gnad, F., Nielsen, M. L., Rehman, M., Walther, T. C., Olsen, J. V. & Mann, M. Lysine acetylation targets protein complexes and co-regulates major cellular functions. *Science* **325**, 834-840 (2009).
- 80 Pouria, S., Corran, P. H., Smith, A. C., Smith, H. W., Hendry, B. M., Challacombe, S. J. & Tarelli, E. Glycoform composition profiling of O-glycopeptides derived from human serum IgA1 by matrix-assisted laser desorption ionization-time of flight-mass spectrometry. *Analytical Biochemistry* **330**, 257-263 (2004).
- 81 Zhang, Y., Fonslow, B. R., Shan, B., Baek, M.-C. & Yates, J. R. Protein Analysis by Shotgun/Bottom-up Proteomics. *Chemical Reviews* **113**, 2343-2394 (2013).
- 82 Zhang, H., Li, X. J., Martin, D. B. & Aebersold, R. Identification and Quantification of N-Linked Glycoproteins Using Hydrazide Chemistry, Stable Isotope Labeling and Mass Spectrometry. *Nature Biotechnology* **21**, 660 (2003).
- 83 Khidekel, N., Ficarro, S. B., Clark, P. M., Bryan, M. C., Swaney, D. L., Rexach, J. E., Sun, Y. E., Coon, J. J., Peters, E. C. & Hsieh-Wilson, L. C. Probing the Dynamics of O-GlcNAc Glycosylation in the Brain Using Quantitative Proteomics. *Nat. Chem. Biol.* **3**, 339 (2007).
- 84 Zielinska, D. F., Gnad, F., Wisniewski, J. R. & Mann, M. Precision Mapping of an in Vivo N-Glycoproteome Reveals Rigid Topological and Sequence Constraints. *Cell* **141**, 897 (2010).
- 85 Chalkley, R. J., Baker, P. R., Huang, L., Hansen, K. C., Allen, N. P., Rexach, M. & Burlingame, A. L. Comprehensive analysis of a multidimensional liquid chromatography mass spectrometry dataset acquired on a quadrupole selecting, quadrupole collision cell, time-of-flight mass spectrometer: II. New developments in Protein Prospector allow for reliable and comprehensive automatic analysis of large datasets. *Molecular Cellular Proteomics* **4**, 1194-1204 (2005).
- 86 Laughlin, S. T. & Bertozzi, C. R. Metabolic labeling of glycans with azido sugars and subsequent glycan-profiling and visualization via Staudinger ligation. *Nature Protocols* **2**, 2930-2944 (2007).
- 87 Boyce, M. & Bertozzi, C. R. Bringing chemistry to life. *Nature Methods* **8**, 638-642 (2011).

Chapter 1: Glycoproteomics and unnatural sugars to study protein glycosylation

- 88 Mahal, L. K., Yarema, K. J. & Bertozzi, C. R. Engineering Chemical Reactivity on Cell Surfaces through Oligosaccharide Biosynthesis. *Science* **276**, 1125 (1997).
- 89 Keppler, O. T., Horstkorte, R., Pawlita, M., Schmidt, C. & Reutter, W. Biochemical Engineering of the N-Acyl Side Chain of Sialic Acid: Biological Implications. *Glycobiology* **11**, 11R (2001).
- 90 Keppler, O. T., Stehling, P., Herrmann, M., Kayser, H., Grunow, D., Reutter, W. & Pawlita, M. Biosynthetic Modulation of Sialic Acid-Dependent Virus-Receptor Interactions of 2 Primate Polyoma Viruses. *Journal of Biological Chemistry* **270**, 1308-1314 (1995).
- 91 Saxon, E. Cell Surface Engineering by a Modified Staudinger Reaction. *Science* **287**, 2007-2010 (2000).
- 92 Rostovtsev, V. V., Green, L. G., Fokin, V. V. & Sharpless, K. B. A Stepwise Huisgen Cycloaddition Process: Copper(I)-Catalyzed Regioselective Ligation of Azides and Terminal Alkynes. *Search Results*
Angewandte Chemie International Edition **41**, 2596 (2002).
- 93 Hsu, T. L., Hanson, S. R., Kishikawa, K., Wang, S. K., Sawa, M. & Wong, C. H. Alkynyl sugar analogs for the labeling and visualization of glycoconjugates in cells. *Proceedings of the National Academy of Sciences* **104**, 2614-2619 (2007).
- 94 Hanson, S. R., Hsu, T. L., Weerapana, E., Kishikawa, K., Simon, G. M., Cravatt, B. F. & Wong, C. H. Tailored Glycoproteomics and Glycan Site Mapping Using Saccharide-Selective Bioorthogonal Probes. *Journal of the American Chemical Society* **129**, 7266 (2007).
- 95 Meier, H., Gerold, J., Kolshorn, H., Baumann, W. & Bletz, M. Oligo(phenylenevinylene)s with terminal donor-acceptor substitution. *Angewandte Chemie International Edition* **41**, 292-295 (2002).
- 96 Turner, R. B., Goebel, P., Mallon, B. J. & Jarrett, A. D. Heats O Hydrogenation .9. Cyclic Acetylenes and Some Miscellaneous Olefins. *Journal of the American Chemical Society* **95**, 790-792 (1973).
- 97 Agard, N. J., Prescher, J. A. & Bertozzi, C. R. A Strain-Promoted [3 + 2] Azide-Alkyne Cycloaddition for Covalent Modification of Biomolecules in Living Systems. *Journal of the American Chemical Society* **126**, 15046 (2004).
- 98 Grammel, M. & Hang, H. C. Chemical reporters for biological discovery. *Nature Chemical Biology* **9**, 475-484 (2013).
- 99 Chuh, K. N. & Pratt, M. R. Chemical Methods for the Proteome-Wide Identification of Posttranslationally Modified Proteins. *Current Opinion in Chemical Biology* **24**, 27 (2015).

Chapter 1: Glycoproteomics and unnatural sugars to study protein glycosylation

- 100 Laughlin, S. T. & Bertozzi, C. R. In vivo imaging of *Caenorhabditis elegans* glycans. *ACS Chemical Biology* **4**, 1068-1072 (2009).
- 101 Bianco, A., Townsley, F. M., Greiss, S., Lang, K. & Chin, J. W. Expanding the genetic code of *Drosophila melanogaster*. *Nature Chemical Biology* **8**, 748-750 (2012).
- 102 Laughlin, S. T., Baskin, J. M., Amacher, S. L. & Bertozzi, C. R. In Vivo Imaging of Membrane-Associated Glycans in Developing Zebrafish. *Science* **320**, 664 (2008).
- 103 Prescher, J. A., Dube, D. H. & Bertozzi, C. R. Chemical remodelling of cell surfaces in living animals *Nature*, **430**, 873-877 (2004).
- 104 Ernst, R. J., Krogager, T. P., Maywood, E. S., Zanchi, R., Beranek, V., Elliott, T. S., Barry, N. P., Hastings, M. H. & Chin, J. W. Genetic code expansion in the mouse brain. *Nature Chemical Biology* **12**, 776-778 (2016).
- 105 Hubbard, S. C., Boyce, M., McVaugh, C. T., Peehl, D. M. & Bertozzi, C. R. Cell surface glycoproteomic analysis of prostate cancer-derived PC-3 cells. *Bioorganic & Medicinal Chemistry Letters* **21**, 4945-4950 (2011).

Bioorthogonal labeling of human prostate cancer tissue slice cultures for glycoproteomics

Rosalie Nolley, Sophia Maund, Jason Herschel, Anthony Iavarone and Donna Peehl contributed to the work presented in this chapter. Portions of the work described in this chapter have been reported in a separate publication.¹

2.1 Introduction

As previously described in Chapter 1, metabolic labeling of glycans, proteins, lipids, nucleic acids and other metabolites with bioorthogonal functional groups is now a widely used platform for studying these biomolecules in living systems.^{2,3} Once functionalized, the target biomolecules are armed for chemical reaction with probes that enable direct visualization or capture and subsequent biochemical analysis. Since its inception, bioorthogonal labeling has been employed in experimental settings of increasingly higher complexity. Early work focused on labeling biomolecules in cultured cells,⁴ but for studies that address questions of biomedical relevance there is motivation to deploy this chemical platform in systems more closely related to human disease. Translation to model organisms has been an important step in this direction, as reflected in reports of bioorthogonal labeling in *mycobacterium*,⁵ *Caenorhabditis elegans*,^{6,7} *Drosophila melanogaster*,^{8,9} *Danio rerio*^{10,11} and murine models.^{12,13} However, the application of metabolic/chemical labeling methods in the most authentic model of human disease, i.e., live human tissues, is appealing to conceptualize but difficult to realize in practice.

Accurate models of human biology are particularly important for research at the intersection of glycoscience and human health. There is a substantive body of literature that correlates changes in glycosylation with cancer progression;^{14,15} several groups have sought to define these changes at a level of molecular detail that would enable new diagnostic or therapeutic interventions.¹⁶ Sialylated glycans and glycoproteins have attracted special attention based on observations that they are upregulated on numerous cancers and, in circulation, have the potential to serve as biomarkers of disease.¹⁷

Motivated by these observations, we¹⁸ and others^{19,20} have applied metabolic and bioorthogonal labeling methods to profile glycoproteins from prostate cancer cell lines using mass spectrometry (MS)-based proteomics.^{21,22} To target sialoglycoproteins specifically, cells are metabolically labeled with a modified peracetylated *N*-acetylmannosamine (Ac₄ManNAc) analog such as peracetylated *N*-azidoacetylmannosamine (Ac₄ManNAz, **1**)⁴ or its alkynyl counterpart, peracetylated *N*-pentynoylmannosamine (Ac₄ManNAI).²³ These compounds are converted by the Roseman-Warren pathway into the corresponding sialic acid derivatives, which are, in turn, incorporated into sialoglycoproteins.²⁴ The functionalized sialoglycoproteins are reacted with a complementary enrichment probe. One might choose among phosphine-

Chapter 2: Bioorthogonal labeling of human prostate cancer tissue slice cultures for glycoproteomics

terminal alkyne- or cyclooctyne-functionalized probes to tag azido sialic acids, or an azide-functionalized probe to tag alkynyl sialic acids.^{25,26} More recently, Chen and coworkers have transitioned such studies to a mouse tumor model.²⁷

While metabolic labeling can be performed in model organisms, in humans, it is hindered by the significant regulatory and ethical barriers associated with introducing chemically altered sugars into people. We were therefore intrigued by the prospect of using live human tumor tissue *ex vivo* in the form of tissue slice cultures (TSCs). TSCs can maintain their native *in vivo* cell-cell and cell-matrix interactions for many days while remaining viable and, importantly, metabolically active.^{28,29}

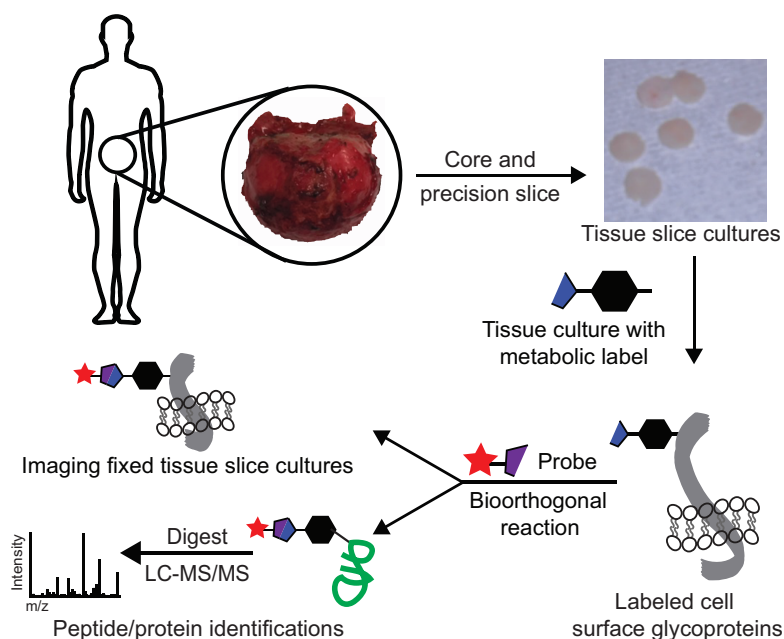


Figure 2-1. Workflow for preparation and bioorthogonal labeling of human prostate tissues slice cultures (TSCs). Radical prostatectomy specimens were cored and precision sliced for *ex vivo* culture. TSCs were incubated with a metabolic reporter (e.g., Ac₄ManNAz, **1**) for specific labeling of sialoglycoproteins. After incubation, slices were either fixed and reacted with a cyclooctyne-functionalized optical probe **3** for imaging, or alternatively, lysed, reacted with an alkyne affinity probe **2** for enrichment, analyzed by mass spectrometry-based proteomics

Prostate TSCs retain physiological properties that are lost in cell culture and also allow direct comparisons of cancerous and normal tissue from the same patient source.³⁰ Here we demonstrate that cultured human prostatic tissue slices can be metabolically labeled with Ac₄ManNAz and subjected to glycoproteomic analysis. MS-based proteomic analysis allowed identification of glycoproteins that were found at elevated levels or unique to prostate cancer TSCs. These data suggest that bioorthogonal labeling methods may be applied to human TSCs to reveal disease biomarkers in a more authentic experimental setting.

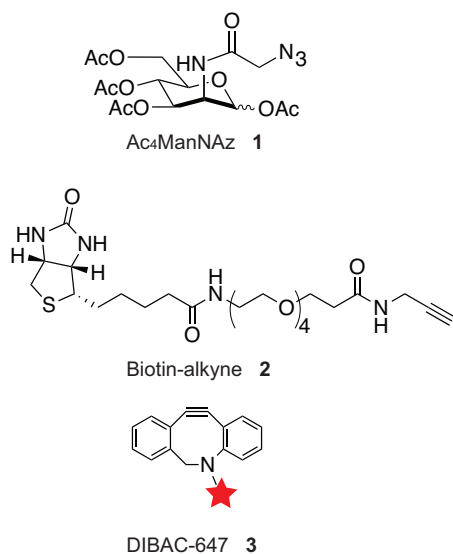


Figure 2-2: Structure of azide-functionalized unnatural sialic acid precursor monosacchride (Ac₄ManNAz) used for metabolic labeling of sialoglycoproteins. Although structure is shown in the peracetylated form, after entering cells by passive diffusion, cytosolic esterases will cleave the acetyl groups. Alkyne-functionalized probes for imaging or capturing azidosialic acid residues.

2.2 Results

Prostate tissue slices were collected as previously reported and subjected to the workflow depicted in **Figure 2-1**, TSCs were derived from an 8 mm in diameter core from a fresh radical prostatectomy specimen, precision-cut into 300- μ m-thick slices and incubated in a rotary culture apparatus. Slices defined as high-quality were round, equally thick at all sides, and with smooth edges. Importantly, structural and functional fidelity of the TSCs could be maintained for at least five days.³¹ The TSCs were labeled by incubating with 50 μ M Ac₄ManNAz, Ac₄ManNAI or Ac₄ManNAc, a control sugar lacking the chemical reporter functionality for subsequent analysis. For imaging, TSCs were fixed and reacted with a suitable conjugated fluorescent probe.³² For proteomic identification, TSCs were homogenized in lysis buffer and covalently reacted with a biotin probe. Proteins were captured with avidin resin, digested on-bead with trypsin and analyzed by LC-MS/MS (**Figure 2-1**).

We first sought to confirm that Ac₄ManNAz (**1**, **Figure 2-2**) metabolism would not grossly perturb the integrity of prostatic TSCs. Histological analysis of TSC by hematoxylin and eosin (H&E) staining showed that Ac₄ManNAz, Ac₄ManNAc, and Ac₄ManNAI treatments had no obvious effect on TSC morphology (**Figure 2-3**).

Prior to proteomic analysis of sialoglycoproteins, we confirmed that Ac₄ManNAz-labeled lysate reacted with biotin-alkyne probe (**2**, **Figure 2-2**) under copper-catalyzed azide-alkyne [3+2] cycloaddition (CuAAC) conditions.³³ TSC lysates were robustly labeled with no observable background by western blot (**Figure 2-4**) and the efficiency of capture was assessed by western blot. We also switched the azide-alkyne partners and observed robust metabolic labeling with Ac₄ManNAI. However, Ac₄ManNAz with biotin-alkyne **2** gave more probe-dependent protein identifications and was thus employed for capture of labeled sialoglycoproteins for identification by MS-based proteomics.

Chapter 2: Bioorthogonal labeling of human prostate cancer tissue slice cultures for glycoproteomics

To test that labeling was specific to cell surface glycoproteins, TSCs were fixed and reacted with the commercial fluorescent cyclooctyne reagent dibenzoazacyclooctyne (DIBAC) conjugated to Alexa Fluor 647 (DIBAC-647, **3**, **Figure 2-2**). Fluorescence microscopy of TSCs treated with either Ac₄ManNAz or Ac₄ManNAc followed by 25 μM DIBAC-647 showed robust and azide-specific cell surface labeling (**Figure 2-5a-c**). We observed co-localization of DIBAC labeling with CD47, a cell surface marker of prostate epithelial cells, indicating Ac₄ManNAz labeling is cell surface specific. Different homogenization instruments were evaluated, as well as time of homogenization, detergent used (e.g. T-PER and M-PER from Thermo Scientific), salt concentration, and addition of reducing agents. The effectiveness of the homogenization conditions was evaluated by subsequent reaction of lysate with phosphine-biotin and comparative Western blotting with anti-biotin antibody conjugate to determine which conditions yielded the most total protein labeling. It was found that optimum results were obtained by using a hand-held Tissue Tearor in a lysis buffer containing 1% TritonX-100, 20 mM Tris pH 7.4, 300 mM NaCl, and protease inhibitors.

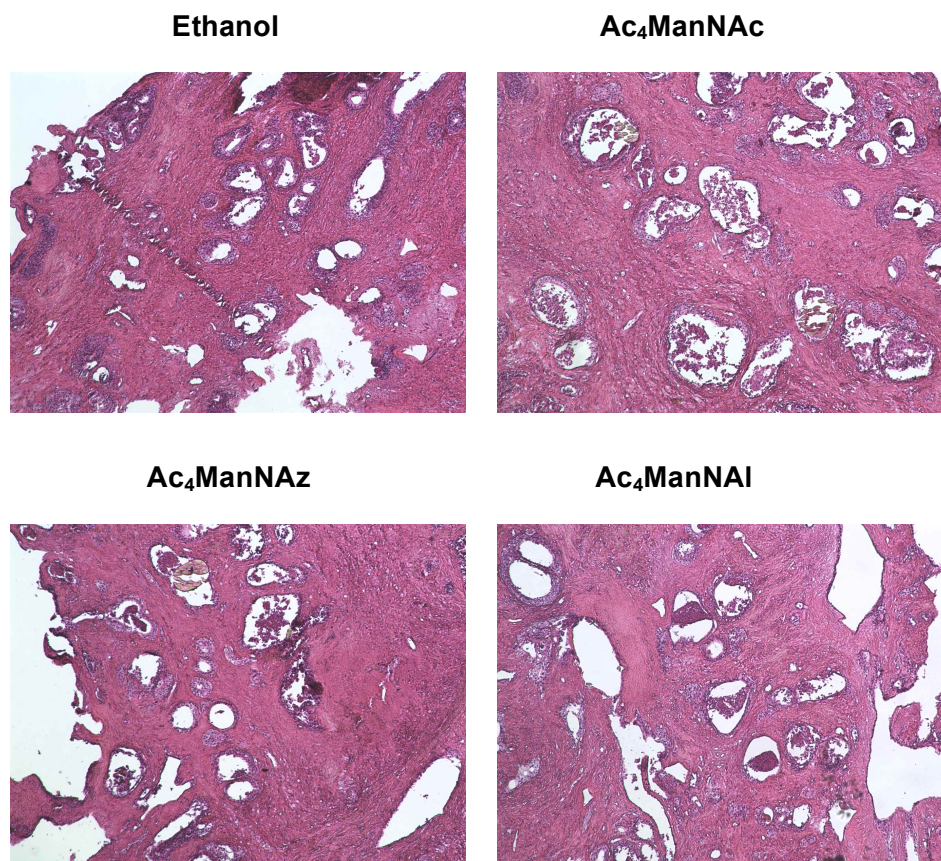


Figure 2-3. Histology of prostate tissue slice cultures (TSCs) by hematoxylin and eosin (H&E) staining. TSCs incubated with either ethanol, Ac₄ManNAc, Ac₄ManNAz or Ac₄ManNAI for 3 days, fixed with paraformaldehyde (PFA) and then stained (magnification 20x). Tissues representative of all TSCs used in this proteomic study.

Chapter 2: Bioorthogonal labeling of human prostate cancer tissue slice cultures for glycoproteomics

To confirm sialoglycoprotein-specificity, we digested TSC lysates with sialidase from *Vibrio cholera* which removes α -2,3- and α -2,6-linked sialic acid substrates,³⁴ reacted with DIBAC-biotin and performed western blot analysis. As shown in **Figure 2-6**, we observed a dose-dependent decrease in signal for sialidase-treated samples, confirming that the azide-specific signal was indeed due to azide incorporation into sialoglycoprotein residues.

Having developed effective labeling conditions, we analyzed human prostate TSCs infiltrated with cancer of Gleason grades 3 and 4 (n=8) and TSCs from normal, noncancerous tissue (n=8), as determined by histological analysis of adjacent tissue slices. TSCs were incubated for 3 days with Ac₄ManNAz or Ac₄ManNAc, lysed, then reacted with biotin-alkyne **2** and carried on to MS-based proteomic analysis. Protein identifications were assigned by searching spectra against the Swiss-Prot human proteome database using the Sequest HT algorithm within the Proteome Discoverer software.

Within Proteome Discoverer we extracted out protein spectral counts which are a semi-quantitative, label-free, measure of protein abundance. Spectral counting has gained wide acceptance in proteomic studies where exact quantitation with a stable isotope is not practical, with several studies demonstrating that spectral counts correlate well with protein abundance even in the presence of complex post-translational modifications (PTMs).³⁴ For validation, in this study we required at least 2 peptides from each protein and with a computational validation of 1% false discovery rate (FDR).

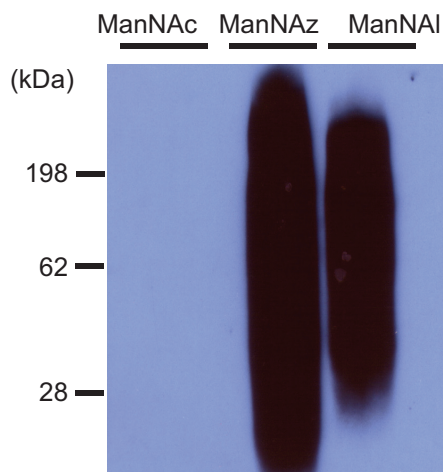


Figure 2-4. Western blot analysis of human prostate TSCs lysate administered azide- and alkyne-functionalized sugars and reacted with corresponding biotin probe under copper-catalyzed azide-alkyne [3+2] cycloaddition (CuAAC) conditions. Ac₄ManNAc and Ac₄ManNAz incubated TSCs reacted with biotin-alkyne and Ac₄ManNAI reacted with biotin-azide. Strong azide and alkyne labeling was observed by HRP-conjugated α -biotin blot. Equal protein was loaded as calculated by bicinchoninic acid (BCA) assay and confirmed by ponceau stain (not shown). No labeling was observed in control Ac₄ManNAc lysate, even when over exposed (not shown).

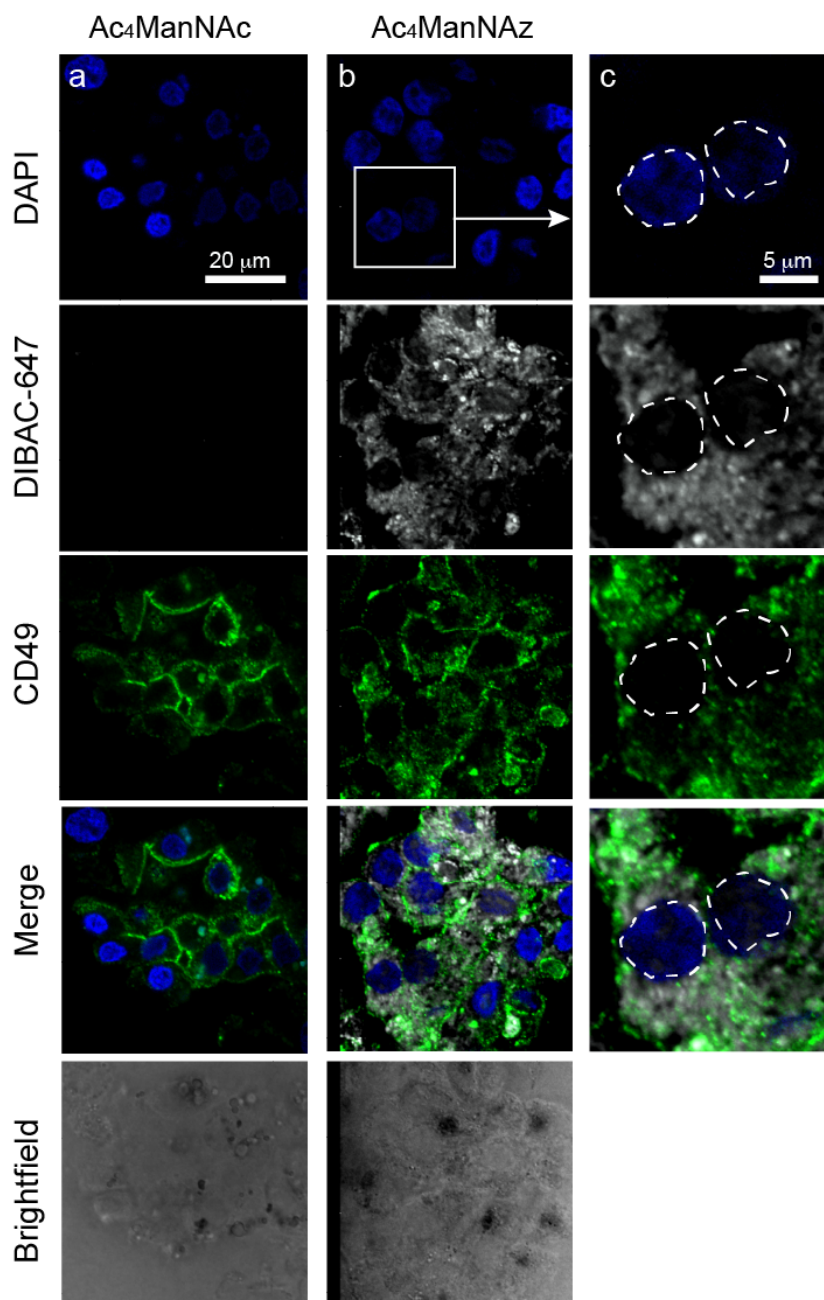


Figure 2-5. Labeling and imaging of cell surface sialoglycoproteins in human prostate tissue slice cultures (TSCs). (a-c) Representative fluorescence microscopy images of TSCs treated either with control sugar Ac₄ManNAc (a, left) or with Ac₄ManNAz (b, center). TSCs stained with DAPI in blue, treated with DIBAC-647 in white, CD47 epithelial cell surface marker in green and merge. Rightmost panel (c) shows zoomed in Ac₄ManNAz labeling.

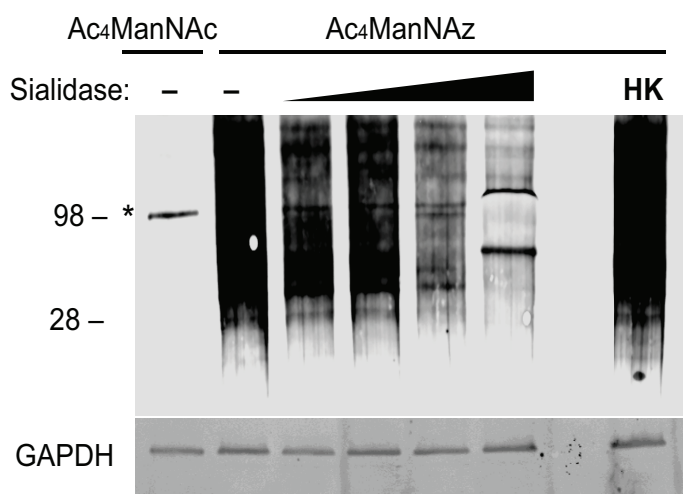


Figure 2-6. Efficient biotinylation of sialoglycoproteins using Ac₄ManNAz. Western blot analysis of sialidase-treated or untreated (-) TSC lysates administered Ac₄ManNAz or control sugar, Ac₄ManNAc. The samples were incubated with active and increasing concentrations of or heat-killed (HK) sialidase from *V. cholerae* (asterisk denotes background labeling of highly abundant sialidase enzyme MW=98 kDA). Total protein loading was confirmed by GAPDH (seen in bottom panel).

In total, 972 non-redundant proteins were observed in the normal and cancer samples with 495 common to both groupings. We found 216 and 261 proteins that were unique to normal and cancer tissue, respectively (**Figure 2-7a**, **Appendix Table A-1**). Although high detergent washes were performed, several highly abundant housekeeping proteins were still identified in the Ac₄ManNAc control groups, such as actin and tubulin (**Figure 2-7b**).

We next analyzed the predicted subcellular compartment for each of the enriched proteins observed in tissue lysates. Over 68% of the proteins were classified as being membrane-bound or secreted (**Figure 2-7c**) and using the Swiss-Prot protein sequence databank annotations, over 45% were known glycoproteins (**Figure 2-7d**). This distribution is consistent with a glycosylation-dependent enrichment method. Based on these results, we compiled a list of proteins that had a greater than 3-fold increase in cancer versus normal tissue (**Table 2-1**).

One such protein was voltage-dependent anion-selective channel 1 (VDAC1). VDAC1 is thought to be a mitochondrial membrane-bound protein; however, there is evidence of additional residence in the plasma membrane.³⁵ Recently, VDAC1 was proposed as a biomarker for gastric cancer,³⁶ and there is evidence of a correlation between VDAC1 expression and breast cancer grade.³⁷ Shoshan-Barmatz *et al.* recently demonstrated that silencing VDAC1 expression in PC-3 prostate cancer cells inhibited cellular proliferation and xenograft tumor growth.³⁸

Chapter 2: Bioorthogonal labeling of human prostate cancer tissue slice cultures for glycoproteomics

We observed a 22-fold increase in VDAC1 in cancer compared to normal TSCs (Table 2-1). This increase could be due to higher protein concentration or, alternatively, to increased glycosylation, which would lead to greater enrichment efficiency. We confirmed that VDAC1 protein levels were dramatically upregulated in cancer TSC lysates whereas we observed weak signal in PC-3 cells and even less in normal TSCs (**Figure 2-8**), strengthening the case for VDAC1 as a potential biomarker and demonstrating the utility of bioorthogonal labeling as a biomarker discovery platform.

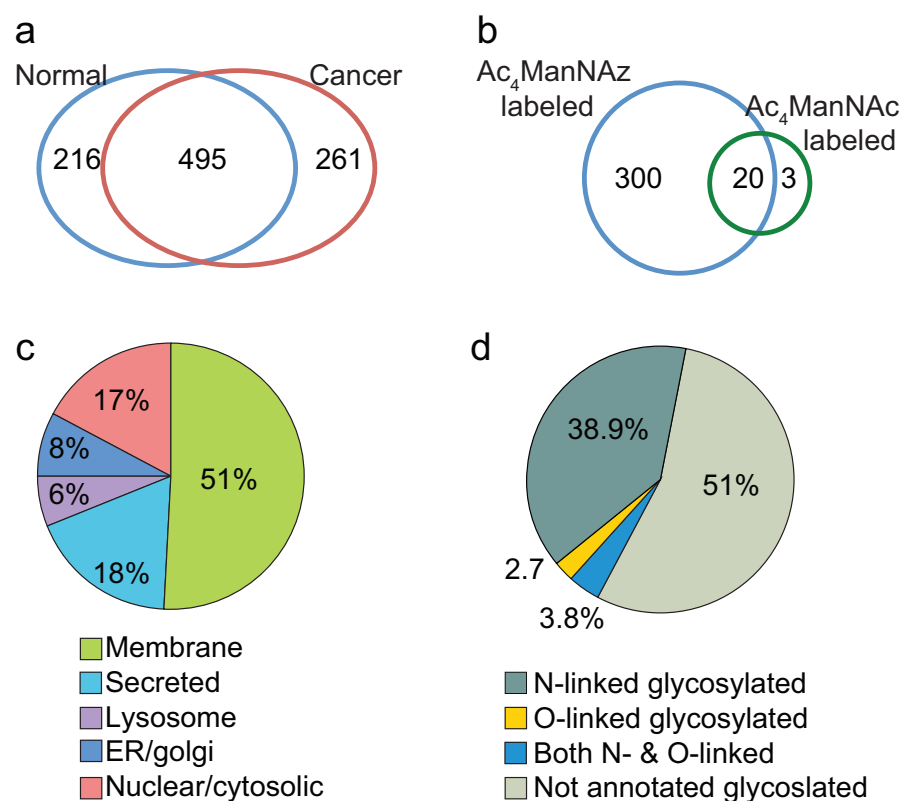


Figure 2-7. Distribution of identified proteins after enrichment. (a) Unique proteins identified over n=8 cancer and normal lysate enrichment. (b) Azide-specific labeling was observed. (c) Subcellular localization was highly specific to sialoglycoproteins. (d) Both N- and O-linked glycoproteins were observed as determined by Swiss-Prot databank annotations.

Chapter 2: Bioorthogonal labeling of human prostate cancer tissue slice cultures for glycoproteomics

Table 2-1. Proteins identified from enriched in cancer (n=8) versus normal (n=8) prostate tissue datasets.

Gene Name	Protein Name	Fold [CA/N]
C4B	Complement C4-B	48
C4A	Complement C4-A	24.7
DPP2	Dipeptidyl peptidase 2	23.0
VDAC	Voltage-dependent anion-selective channel protein 1	22.5
RAB1C	Putative Ras-related protein Rab-1C	18.0
K1324	Estrogen-induced gene 121	18.0
EZRI	Ezrin	17.0
APOE	Apolipoprotein E	10.0
PTPR	Receptor-type tyrosine-protein phosphatase kappa	9.0
GDF15	Growth/differentiation factor 15	8.3
NUCB1	Nucleobindin-1	7.0
VAPA	Plasmalemma vesicle-associated protein	7.0
TRY3	Trypsin-3	7.0
FOLH	Glutamate carboxypeptidase 2	6.5
DRA	HLA class II histocompatibility antigen	6.0
ATPA	ATP synthase subunit alpha	5.4
CATB	Cathepsin B	5.0
GLCM	Glucosylceramidase	5.0
T179	Transmembrane protein 179B	5.0
AMPN	Aminopeptidase N (CD13)	4.8
ENPL	Endoplamin (Tumor rejection antigen 1)	4.6
CERU	Ceruloplasmin	4.5
GGT3	Putative γ -glutamyltranspeptidase 3	4.3
PPAP	Prostatic acid phosphatase	4.1
A1AG	Alpha-1-acid glycoprotein 1	4.0
SODE	Extracellular superoxide dismutase	4.0
FAM3	Protein FAM3B	4.0
TPP1	Tripeptidyl-peptidase 1	4.0
EGLN	Endoglin (CD105)	3.6
ITA1	Integrin alpha-1 (CD49a)	3.3
PIIB	Peptidyl-prolyl cis-trans isomerase	3.2
LYAG	Lysosomal alpha-glucosidase	3.1
DPP4	Dipeptidyl peptidase 4	3.0
MPRI	Cation-independent mannose-6-phosphate receptor	3.0
STEAP4	Metalloreductase STEAP4	3.0
GGT1	γ -glutamyltranspeptidase 1	3.0
GGT2	Inactive γ -glutamyltranspeptidase 2	3.0
TGON	Trans-Golgi network integral membrane protein 2	3.0
AMPE	Glutamyl aminopeptidase (CD249)	3.0
TSN6	Tetraspanin-6	3.0
TCO1	Transcobalamin-1	3.0

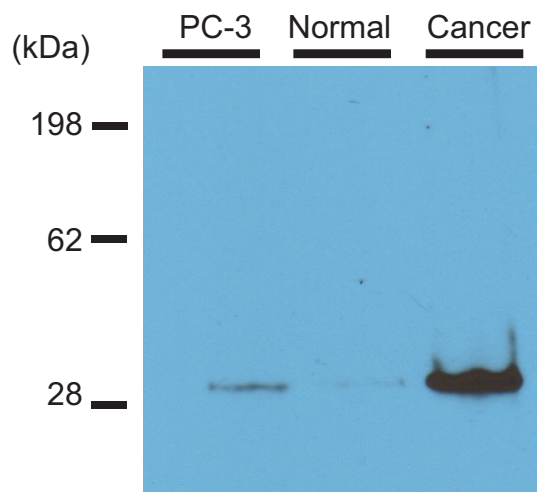


Figure 2-8. Voltage-dependent anion-selective channel 1 (encoded by the gene VDAC1) is overexpressed in human prostate cancer tissue. Lysate from normal and cancer human prostate TSCs and a prostate cell line, PC-3, lysate was probed with an α -VDAC1 mAB. Equal protein was loaded as calculated by BCA assay and confirmed by india ink stain (not shown).

In addition to enrichment of glycoproteins found in cancer versus normal TSCs, we also found proteins that were unique to cancer TSCs (**Table 2-2**). After removing cytosolic proteins, we identified 21 proteins seen in at least half of the cancer patients and none of the normal patients. Some of these proteins were previously implicated in prostate cancer, while others had no previous reported association.

We were particularly interested in legumain (encoded by the gene LGMN), an asparaginyl endopeptidase that is highly expressed in several types of cancer.³⁹ In our studies, it was observed in 5 out of 8 prostate cancer tissue samples but not in any of the 8 patient-derived normal TSCs. Recently, Ohno *et al.* reported that increased legumain expression correlated with prostate cancer invasiveness and aggression.⁴⁰ We did not detect legumain labeling in formalin-fixed, paraffin-embedded (FFPE) normal fixed tissues, whereas in cancer tissue, we observed labeling on malignant epithelial cells (**Figure 2-9a-b**). Western blot analysis after digestion with deglycosylation enzymes confirmed that legumain in prostate cancer TSCs is indeed glycosylated (**Figure 2-9c**). This result supports the conclusion that the proteins in **Table 2-2** are potentially unique to or uniquely glycosylated in cancer TSCs.

Chapter 2: Bioorthogonal labeling of human prostate cancer tissue slice cultures for glycoproteomics

Table 2-2. Proteins identified in prostate cancer proteomic dataset that were absent in normal dataset. All proteins were identified in at least 4 out of 8 cancer patients.

Gene name	Protein name	Previous report
AGR2	Anterior gradient protein 2 homolog	[41]
SYNGR2	Synaptogyrin-2	
ATP6AP1	V-type proton ATPase subunit S1	
LGMN	Legumain	[40]
GUSB	Beta-glucuronidase	
FUCA1	Tissue alpha-L-fucosidase	
HLA-DRB1	HLA class II histocompatibility antigen	[42]
CYB561	Cytochrome b561	
CFB	Complement factor B	[43]
HLA-A	HLA class I histocompatibility antigen	[44]
HLAA		
APMAP	Adipocyte plasma membrane-associated protein	
HLA-H	Putative HLA class I histocompatibility antigen	[26]
HLAH		
PCYOX1	Prenylcysteine oxidase 1	
CALR	Calreticulin	[45]
ORM2	Alpha-1-acid glycoprotein 2	
LMBRD1	Probable lysosomal cobalamin transporter	
PODXL	Podocalyxin	[46]
PLXNB2	Plexin-B2	
TMED10	Transmembrane emp24 domain-containing protein 10	
FAM174B	Membrane protein FAM174B	
SCARB1	Scavenger receptor class B member 1	[47]
LDHA	L-lactate dehydrogenase A	[48]
VAS1	V-type proton ATPase subunit S1	[49]

Finally, we determined whether a statistical modeling of our data could establish a glycoprotein signature that distinguishes cancer from normal tissue. We employed supervised principal component analysis (SPCA) using a method described by Tibshirani and coworkers.⁵⁰ SPCA is a classical dimension reduction and feature extraction tool employed extensively in exploratory analysis⁵¹ and has been used in a wide range of fields.⁵² SPCA reduces dimensionality by projecting experiments (in this case each protein found in a patient's tissue) into a subspace with fewer dimensions than the original space of the variables.

We performed a SPCA on our data treating each protein as a variable. To begin analysis, the data was scaled based on whether or not the protein was from a cancerous or normal patient sample ("y-awareness"), here recoded as -1 (blue) for normal and 1 (red) for cancerous. Scaled observations were used to calculate standard regression coefficients for each feature, which was then used for developing a reduced set of features related to each outcome. Spectral counts, as previously used, were employed

Chapter 2: Bioorthogonal labeling of human prostate cancer tissue slice cultures for glycoproteomics

to scale proteins. Each feature of this reduced set was then projected into the reduced dimensional space of the principal components. A regression analysis shows that the first principal component (PC1) and third (PC3) is sufficient to explain the variability of the dataset (**Figure 2-10a**). The plot of PC1 and the second principal component (PC2) did not allow for distinction between normal and cancer. This is not unexpected for the number of proteins (>400) and the relatively small sample size (n=8 patients, n=16 total). From this analysis we illustrate that tumor derived TSCs were more heterogeneous than normal TSCs and clustered separately (**Figure 2-10c**).

The quantitative data for each of the proteins observed is displayed in a volcano plot (**Figure 2-10b**). We next employed k-1 nested cross validation to extract a set of proteins that could be used to explain the tumorigenic status. We suggest that CD166 antigen (encoded by the gene ALCAM, accession #: Q13740), calcium-activated chloride channel regulator 4 (encoded by the gene CLCA4, accession #: Q14CN2), UPF0577 (encoded by the gene KIAA1324, accession # Q6UXG2), synaptogyrin-2 (encoded by the gene SYNGR2, accession #: O43760), anterior gradient protein 2 homolog (encoded by the gene AGR2, accession #: O95994) together could be used alone to distinguish between a cancer and normal dataset.

More than half these proteins have been previously identified in prostate cancer studies, either *in vitro* or in human derived samples. Interestingly, both synaptogyrin-2 and anterior gradient protein 2 homolog were identified in none of our normal samples and in at least half of the tumor samples (**Table 2-2**). It is also noteworthy that four of these proteins are annotated as cell surface and glycosylated indicating an enrichment of target proteins. It should be noted that this analysis biased away from proteins that simply had significant fold increases and a larger dataset is needed to assert a correlative biomarker.

Chapter 2: Bioorthogonal labeling of human prostate cancer tissue slice cultures for glycoproteomics

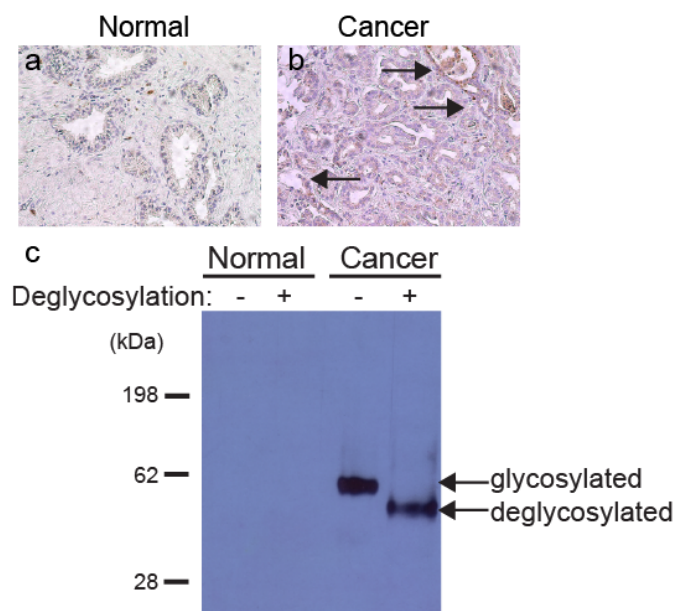


Figure 2-9. Legumain is over-expressed and glycosylated in human prostate cancer tissue. Histological analysis of legumain expression in normal (a) and cancer (b) prostate tissue slice cultures. Arrows indicate epithelial cells with legumain immunoreactivity. Western blot of prostate TSCs lysate probed with a α -legumain mAb (c). Deglycosylation denotes presence or absence of commercial deglycosylation enzyme cocktail. Total protein loading was confirmed by ponceau stain (not shown).

2.3 Conclusion

One of the biggest challenges in the detection and management of cancer remains the lack of prognostic and predictive biomarkers. Of the molecular tissue-based risk classifiers commercially available to predict aggressive prostate cancer at time of diagnosis or post-prostatectomy (Polaris, Decipher, Oncotype Dx, and ProMark), only the latter is protein-based while the others measure RNA expression.⁵³ It is interesting to note that VDAC1, found in our study to be enriched in cancer versus normal prostate TSCs, was one of the 12 prognostic proteins identified by quantitative proteomics of prostate tissues from which the current 8-protein ProMark assay was derived.^{54, 55} Overall, however, few genes or proteins overlap among the current classifiers and clinical value remains to be validated in future prospective studies.

A contributor to this challenge is a lack of preclinical models that accurately recapitulate normal human prostate tissue or primary prostate cancer.³¹ Here we demonstrate that human prostate TSCs can be metabolically labeled for the identification of cell surface and secreted glycoproteins. We performed MS-based proteomics and identified glycoproteins that may be explored further as disease biomarkers.

This platform could be used to interrogate other questions related to cancer. For example, hypersialylation appears to play a role in tumor cell immune evasion.⁵⁶ Merging

Chapter 2: Bioorthogonal labeling of human prostate cancer tissue slice cultures for glycoproteomics

this platform with intact glycoproteome analysis techniques such as IsoTaG^{57, 58} may further augment the information obtained from cancer TSCs. Finally, while in this study we focused on the sialoglycoproteome, there are other sectors of the glycome that can be targeted with this method as well as other post-translational modifications that might change as a function of disease.⁵⁹ Additionally this method could be adapted to quantify human proteomics through one-step metabolic strategies such as stable isotope labeling with amino acids in cell culture (SILAC) which has previously been applied to cell lines and model organisms.⁶⁰ This work therefore extends the use of the methods developed for human tissue slice culture to other metabolic strategies from patients and problems of human clinical relevance.

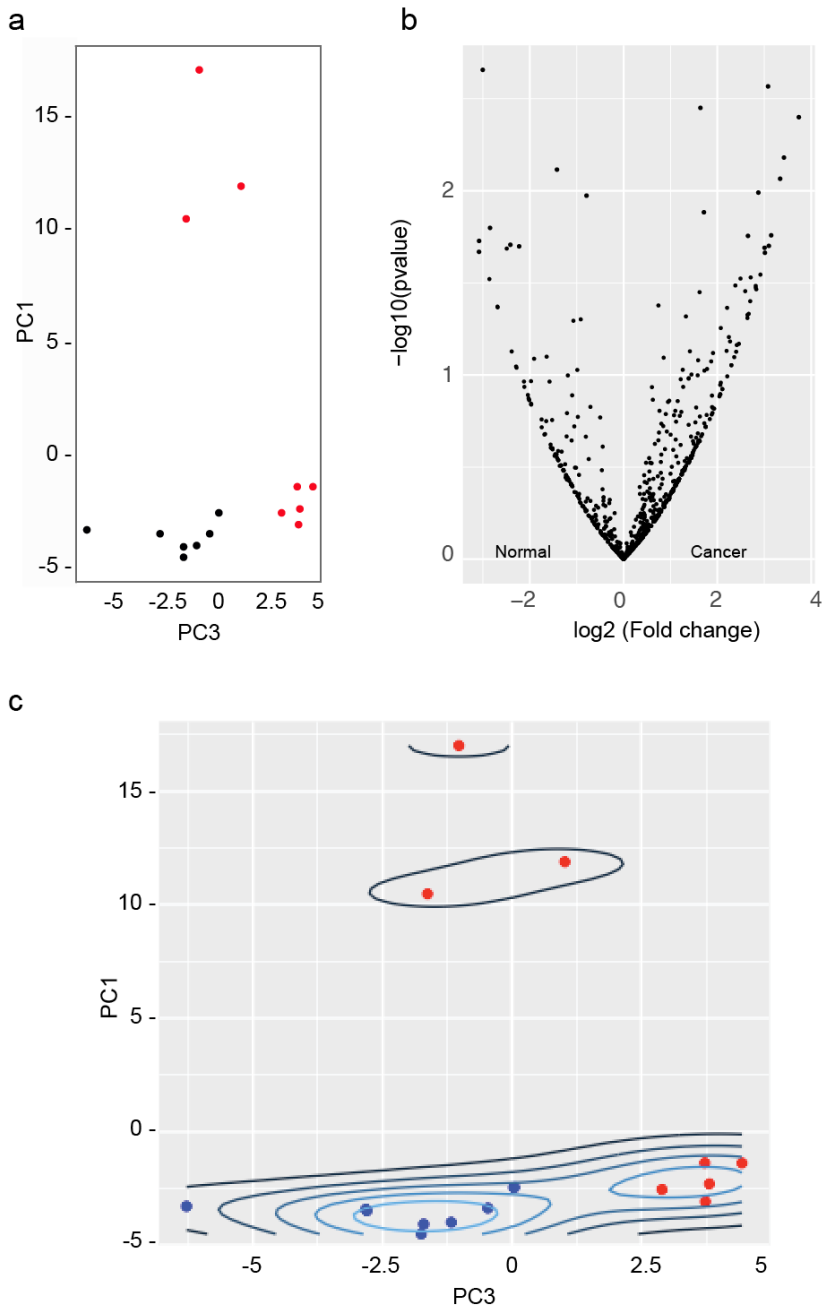


Figure 2-10. Comparative analysis of differentially regulated glycoproteins between normal and cancer TSCs. (a) Supervised principal component analysis of normal (black) and cancer (red) datasets. (b) Volcano plots illustrate differentially observed proteins from normal and cancer TSC samples. The x-axis represents the \log_2 (fold change) whereas y-axis represents the $-\log_{10}$ (p-value) where 'p-value' is the p-value associated to the statistical Welch test. (c) Representation of PCA plot with contour lines.

2.4 Methods and Materials

General reagents. All chemical and biological reagents were of analytical or cell culture grade, obtained from commercial sources, and used without further purification unless otherwise noted. Ac₄ManNAz, Ac₄ManNAI and Ac₄ManNAc were synthesized as previously described.^{23,61}

Metabolic labeling of tissue slice cultures. Tissue slices from healthy and cancerous prostate tissue were obtained with approval from internal review boards from Stanford University (IRB ID13895) and the University of California, Berkeley for use of material from human subjects. Eight-mm diameter cores of normal and cancerous tissue were taken from radical prostatectomy specimens according to needle biopsy maps and gross analysis. Using an automated Krumdieck microtome, the cores were cut into 300 μm thick slices. Slices from the cored section were evaluated by hematoxylin and eosin (H&E) staining to verify the histology of the slices neighboring those used for metabolic labeling. The slices were cultured on titanium screens in 6-well culture plates containing 2.5 mL of supplemented PFMR-4A medium with 50 nM R1881²¹ and 50 μM of monosaccharide (Ac₄ManNAc, Ac₄ManNAz, or Ac₄ManNAI). The plates were set on a rotating platform at a 30 degree angle in a standard tissue culture incubator. The angled rotation at 1 rpm allowed intermittent submersion of the tissue slices in the medium, permitting optimal nutrient and gas diffusion throughout the tissue. Each day, the conditioned media were removed and stored at -80 °C and replaced with fresh media. After 3 d, the media was removed and the slices were washed with phosphate buffered saline (PBS) prior to being snap-frozen in liquid nitrogen.

Preparation of prostate tissue whole cell lysates. Prostate tissue slice cultures were lysed in 1 mL of lysis buffer containing 1% Triton X-100, 20 mM Tris pH 7.4, 300 mM NaCl, and protease inhibitors (inhibitor cocktail III from Calbiochem). While the tissue was cooled on ice, pulverization was performed using a Tissue Tearor (Biospec Products model #780CL-04) on setting 2, with cycles of 20 sec on followed by 20 sec off, 2 min total time. Samples underwent sonication for 1 min total time with cycles of 10 sec on and 10 sec off at 2.0 V setting. Cell surface glycoproteins were collected in the supernatant after centrifugation at 10,000 rpm for 10 min at 4 °C. The supernatant was collected and a bicinchoninic acid (BCA) assay (Thermo Fisher Scientific) was performed to determine protein concentration.

Labeling glycoproteins by biotin-alkyne or biotin-azide via copper (I) catalyzed azide-alkyne [3+2] cycloaddition (CuAAC) reaction. Lysate was reacted in the presence of 1 mM CuSO₄, 5 mM freshly prepared sodium ascorbate and 100 μM tris[(1-benzyl-1H-1,2,3-triazol-4-yl)methyl]amine (TBTA) (Sigma-Aldrich) and 25 μM biotin probe (Invitrogen Life Sciences). Samples were rotated for 1 hour at RT. The reaction was quenched with 10 mM ethylenediaminetetraacetic acid (EDTA).

Immunoblotting. Following preparation and protein concentration normalization by BCA assay, samples were separated by standard SDS-PAGE (Bio-Rad, Criterion system), transferred onto nitrocellulose, blocked in 5% bovine serum albumin (Sigma) in PBS with 0.1% Tween-20, and analyzed by standard enhanced chemiluminescence

Chapter 2: Bioorthogonal labeling of human prostate cancer tissue slice cultures for glycoproteomics

immunoblotting methods (Pierce). Monoclonal mouse anti-biotin HRP reagent (Jackson ImmunoResearch product #200-032-211) was diluted 1:100,000 in blocking buffer.

Cell surface glycoprotein capture and MS analysis. Triton X-100 stock solution diluted to 10% in PBS was added to TSC lysate for 1% final concentration and samples were rotated for 1 h at RT. Samples were then filtered through a PD-10 desalting column (GE Healthcare Life Sciences) and eluted with 3.5 mL PBS. SDS (10%) was added for final concentration of 0.5% SDS and samples were boiled at 90 °C for 8 min. Samples were cooled on ice for 5 min and an additional 8.5 mL of PBS and 100 mL of avidin slurry (Sigma, CAS: 1405-69-2) were added and rotated at RT for 1 h. Beads were concentrated by centrifugation at 1,400 rpm, 3 min at 4 °C, supernatant was removed and beads were transferred to a washed biospin column (Bio Rad Life Sciences) on a vacuum manifold. Beads were washed twice with 1 mL PBS, once with 1 mL 0.2% SDS/PBS, once with 1 mL fresh 6 M urea and twice with 1 mL PBS. Freshly prepared 6 M urea (400 μ L) and 20 μ L 100 μ M tris(2-carboxyethyl)phosphine (TCEP) was delivered and sample was rotated for 30 min at RT. Freshly prepared 20 μ L of 200 μ M iodoacetamide was delivered and the sample was wrapped in foil and rotated for 30 min at RT. Beads were then washed 3 times with 1 mL of PBS and transferred to an RNase-free microcentrifuge tube with 2 washes of 300 μ L PBS. Beads were concentrated by centrifugation at 6000 rpm, 3 min and supernatant was removed. Freshly made 2 M urea (200 μ L) was added and trypsin digestion (Promega Corporation, # V511) was performed overnight in a bench top shaker at 37 °C. The next morning, the beads were pelleted at 6,000 rpm for 3 min. The supernatant was collected and the beads washed with an additional 100 μ L of PBS. LC-MS grade formic acid (16 mL) was added and the resulting peptide mixtures were solid-phase extracted with SPEC PT C18 tips (Agilent, #A57203) according to the manufacturer's instructions and stored at -80°C.

Mass Spectrometry (MS). Released peptides were analyzed by reversed-phase nanoflow liquid chromatography coupled (Thermo Dionex UltiMate3000 RSLC) that was connected in-line with a 15 cm C18 column (Thermo, PM100) to a Thermo LTQ Orbitrap XL mass spectrometer equipped with a nanoelectrospray ionization (nanoESI) source. Full-scan mass spectra were acquired in the positive-ion mode over the range m/z = 400–2,000 using the Orbitrap mass analyzer, in profile format, with a mass resolution setting of 60,000. In the data-dependent mode, the eight most intense ions exceeding an intensity threshold of 50,000 counts were selected from each full-scan mass spectrum for tandem mass spectrometry (MS/MS, i.e., MS²) analysis using collision-induced dissociation (CID). MS² spectra were acquired using the linear ion trap or the Orbitrap analyzer in centroid format. Data acquisition was controlled using Xcalibur software (version 2.0.7, Thermo). The raw data are available upon request.

Data Analysis. LC-MS/MS data was searched using the SequestHT searching algorithm in the Proteome Discover 1.4 software against the human-specific SwissProt-reviewed database downloaded 18 July 2014 with a 1% false discovery rate (FDR).

MudPIT (multidimensional protein identification technology). Samples were subjected to MudPIT analysis as described by Link and coworker,⁶² briefly, a quaternary Hewlett-Packard 1200 series HPLC (running as a 1100 series) was directly coupled to a Thermo LTQ-XL ion trap mass spectrometer equipped with a nano splitflow LC electrospray ionization source. A fused-silica microcapillary column (100 μ m i.d. \times 365

Chapter 2: Bioorthogonal labeling of human prostate cancer tissue slice cultures for glycoproteomics

μm o.d.) was pulled with a Model P-2000 laser puller (Sutter Instrument Co., Novato, CA) as described.⁶³ The microcolumn was first packed with 10 cm of 5 μm C18 reverse-phase material (Magic C-18) followed by 4 cm of 5 μm strong cation exchange material (Partisphere SCX; Whatman, Clifton, NJ). After loading the microcapillary column, the column was placed in-line. A fully automated 15-step chromatography run was carried out on each sample. The four buffer solutions used for the chromatography were 5% ACN/0.1% FA (buffer A), 80% ACN/0.1% FA (buffer B), 250 mM ammonium acetate/5% ACN/0.1% FA (buffer C). The first step of 80 min consisted of a 70 min gradient from 0 to 80% buffer B and a 10 min hold at 80% buffer B. The next 12 steps were 110 min each with the following profile: 5 min of 100% buffer A, 2 min of x% buffer C, 3 min of 100% buffer A, a 10 min gradient from 0 to 10% buffer B, and a 90 min gradient from 10 to 45% buffer B. The 2 min buffer C percentages (x) in steps 2–13 were as follows: 10, 20, 30, 40, 50, 60, 70, 80, 90, 90, 100, and 100%. Step 14 consisted of the following profile: a 5 min 100% buffer A wash, a 20 min 100% buffer C wash, a 5 min 100% buffer A wash, a 10 min gradient from 0 to 10% buffer B, and a 90 min gradient from 10 to 45% buffer B. Step 15 was identical to step 14 except that the 20 min salt wash was with 100% buffer D.

MS/MS data analyzed using the Coon lab OMSSA Proteomics Analysis Software Suite (COMPASS).⁶⁴ Although employed to search spectra prior to database searching with Proteome Discoverer, the Open Mass Spectrometry Search Algorithm (OMSSA; version 2.1.8) was used during optimization of the TSCs. Spectra were searched against the International Protein Index (IPI) human database version 3.85.⁶⁵ For all experiments, carbamidomethylation of cysteine residues was selected as a fixed modification. Oxidation of methionine residues and HexNAc of Serine and Threonine residues was set as a variable modification. Precursor mass tolerance was set to 2.1 Da and monoisotopic mass tolerance was set to 0.5 Da for fragments ions. Results were filtered to a 1% FDR at the peptide and protein level with a maximum precursor mass error of 50 ppm.

Prostate adenocarcinoma tissue slice fluorescence microscopy. Frozen prostate TSCs were placed on slides mounted with 4-tissue culture wells and allowed to thaw for 10 min. Tissue slices were then washed with DPBS + 1% FBS (2 x 0.8 mL), followed by incubation with or without DIBAC-647 (25 μM) in DMEM media for 1 h at 4 °C. Tissue slices were subsequently washed with DPBS + 1% FBS (10 x 0.8 mL) and fixed with 4% paraformaldehyde in PBS (0.4 mL) for 5 min at 4 °C and 20 min at rt and washed with DPBS (4 x 0.4 mL). To demonstrate azide labeling was cell surface-specific, fixed TSCs were blocked in 10% BSA for 1 h and then incubated with CD47 (1:1000, abcam #ab3283) for 1 h RT. TSCs were washed (3 x 0.8 mL) and CD47-labeled proteins were visualized with goat anti-mouse conjugated with Alexa Fluor 488 (1:1000, Abcam #ab150113) for 1 h RT. The tissue slices were washed with DPBS (3 x 0.8 mL) and transferred to a concave microscope slide. DAPI mounting solution (~20 μL) was delivered and a glass coverslip was used to seal the slide, and the tissue slices were imaged.

2.5 R Code

Development of PCA plots in R.

```
### Load Normal/Cancer Datasets
#
#
Protein <- read.csv("~/Documents/machine learning datasets/david -
cancer Proteins/david_cancerProtein.csv")

###Pre-processing necessary to extract state of tissue for each
# observation (tissue)
#
Cancerous <- Protein[, 2]
# need to drop one column so dimensions match
Cancerous <- Cancerous[2:16]

### Explore Data ----
# Basic commands for exploring data
#
View(Protein)
summary(Protein)

### Density plot (violinplot) of observations with each protein
#
#
library(psych)
par(xaxt="n")
violinBy(Protein[3:7],Protein$State, main="Density Plot by Cancerous /
Normal for each Protein" )
legend(5,100, c("Cancerous", "Normal"), text.col = c("blue", "red"),
box.col = "white", text.width = 1.75)

# Example if interested in specific proteins

lablist<-as.vector(c("P35749", "P12111", "P13645", "P04264",
"P21333"))
axis(1, at=seq(1, 10, by=1), labels = FALSE)
text(seq(1, 10, by=2), par("usr")[3] - 0.2, labels = lablist, srt = 45,
pos = 1, xpd = TRUE)
par(xaxt="t")

### Principle Component Analysis ----
# Apply PCA = TRUE is highly advisable, but default is FALSE.
#
# without log transformation
#
pc <- prcomp(na.omit(Protein[, c("P35749", "P12111", "P13645",
"P04264",
"P21333"))], scale=TRUE, center=TRUE,
```

Chapter 2: Bioorthogonal labeling of human prostate cancer tissue slice cultures for glycoproteomics

```
tol=0)

### Summary of results
#
#
summary(pc)

### Plot of principal components
#
#
plot(pc, main="")
title(main="Principal Components Importance")
axis(1, at=seq(0.7, ncol(pc$rotation)*1.2, 1.2),
labels=colnames(pc$rotation), lty=0)

### Alternative plotting
#
#
plot(pc, type="l", main="Principal Component Importance")

### Refined plotting
# observations are plotted on first 2 principal component dimensions
# with protein variable plotted as an overlay
#
library(devtools)
install_github("ggbiplot", "vqv")

library(ggbiplot)
g <- ggbiplot(pc, obs.scale = 1, var.scale = 1,
              groups = Cancerous, ellipse = TRUE,
              circle = TRUE)
g <- g + scale_color_discrete(name = '')
g <- g + theme(legend.direction = 'horizontal',
              legend.position = 'top')
print(g)

### Method to improve results using SPPCA
# Alternative PCA using the Caret library with BoxCox transformation
# of data Box Cox also adjusts for skewness of data
#
require(caret)
trans = preProcess(Protein[,2:7],
                  method=c("BoxCox", "center",
                          "scale", "pca"))
PC = predict(trans, Protein[,2:7])
summary(PC)
print(PC)

### PCA with log transform
#
```

Chapter 2: Bioorthogonal labeling of human prostate cancer tissue slice cultures for glycoproteomics

```
#
log.Protein <- log(Protein[, 3:7])
logpc <- prcomp(na.omit(log.Protein), scale=TRUE, center=TRUE, tol=0)

### Summary of results
#
#
summary(logpc)
print(logpc)

### Plot of principal components
# With data entered, plot. Additional formatting of x- y-axis and
# background color corrected in illustrator)
#
plot(logpc, main="")
title(main="Principal Components Importance")
axis(1, at=seq(0.7, ncol(logpc$rotation)*1.2, 1.2),
labels=colnames(logpc$rotation), lty=0)

### Alternative PCA plotting
# (not used for analysis
#
plot(logpc, type="l", main="Principal Component Importance")

### Refined plotting
# Observations are plotted on first 2 principal component dimensions
with
# Protein variable plotted as an overlay
#
library(devtools)
install_github("ggbiplot", "vqv")

library(ggbiplot)
g <- ggbiplot(logpc, obs.scale = 1, var.scale = 1,
              groups = Cancerous, ellipse = TRUE,
              circle = TRUE)
g <- g + scale_color_discrete(name = '')
g <- g + theme(legend.direction = 'horizontal',
              legend.position = 'top')
print(g)
```

2.6 References

- 1 Spiciarich, D. R., Nolley, R., Maund, S. L., Purcell, S. C., Herschel, J., Iavarone, A. T., Peehl, D. M. & Bertozzi, C. R. Bioorthogonal Labeling of Human Prostate Cancer Tissue Slice Cultures for Glycoproteomics. *Angewandte Chemie International Edition* **56**, 8992-8997 (2017).
- 2 Grammel, M. & Hang, H. C. Chemical reporters for biological discovery. *Nature Chemical Biology* **9**, 475-484 (2013).
- 3 Chuh, K. N. & Pratt, M. R. Chemical Methods for the Proteome-Wide Identification of Posttranslationally Modified Proteins. *Current Opinion in Chemical Biology* **24**, 27 (2015).
- 4 Saxon, E. Cell Surface Engineering by a Modified Staudinger Reaction. *Science* **287**, 2007-2010 (2000).
- 5 Swarts, B. M., Holsclaw, C. M., Jewett, J. C., Alber, M., Fox, D. M., Siegrist, M. S., Leary, J. A., Kalscheuer, R. & Bertozzi, C. R. Probing the mycobacterial trehalose with bioorthogonal chemistry. *Journal of the American Chemical Society* **134**, 16123-16126 (2012).
- 6 Laughlin, S. T. & Bertozzi, C. R. In vivo imaging of *Caenorhabditis elegans* glycans. *ACS Chemical Biology* **4**, 1068-1072 (2009).
- 7 Greiss, S. & Chin, J. W. Expanding the genetic code of an animal. *Journal of the American Chemical Society* **133**, 14196-14199 (2011).
- 8 Bianco, A., Townsley, F. M., Greiss, S., Lang, K. & Chin, J. W. Expanding the genetic code of *Drosophila melanogaster*. *Nature Chemical Biology* **8**, 748-750 (2012).
- 9 Dehnert, K. W., Baskin, J. M., Laughlin, S. T., Beahm, B. J., Naidu, N. N., Amacher, S. L. & Bertozzi, C. R. Imaging the sialose during zebrafish development with copper-free click chemistry. *ChemBiochem* **13**, 353-357 (2012).
- 10 Agarwal, P., Beahm, B. J., Shieh, P. & Bertozzi, C. R. Systemic Fluorescence Imaging of Zebrafish Glycans with Bioorthogonal Chemistry. *Angewandte Chemie International Edition* **54**, 11504-11510 (2015).
- 11 Laughlin, S. T., Baskin, J. M., Amacher, S. L. & Bertozzi, C. R. In Vivo Imaging of Membrane-Associated Glycans in Developing Zebrafish. *Science* **320**, 664 (2008).
- 12 Prescher, J. A., Dube, D. H. & Bertozzi, C. R. Chemical remodelling of cell surfaces in living animals. *Nature* **430**, 873-877 (2004).
- 13 Ernst, R. J., Krogager, T. P., Maywood, E. S., Zanchi, R., Beranek, V., Elliott, T. S., Barry, N. P., Hastings, M. H. & Chin, J. W. Genetic code expansion in the mouse brain. *Nature Chemical Biology* **12**, 776-778 (2016).

Chapter 2: Bioorthogonal labeling of human prostate cancer tissue slice cultures for glycoproteomics

- 14 Pinho, S. S. & Reis, C. A. Glycosylation in cancer: mechanisms and clinical implications. *Nature Reviews Cancer* **15**, 540-555 (2015).
- 15 Stowell, S. R., Ju, T. & Cummings, R. D. Protein glycosylation in cancer. *Annual Review of Pathology* **10**, 473-510 (2015).
- 16 Dube, D. H. & Bertozzi, C. R. Glycans in Cancer and Inflammation--Potential for Therapeutics and Diagnostics. *Nature Review Drug Discovery* **4**, 477 (2005).
- 17 Kailemia, M. J., Park, D. & Lebrilla, C. B. Glycans and glycoproteins as specific biomarkers for cancer. *Analytical and Bioanalytical Chemistry* **409**, 395-410 (2017).
- 18 Hubbard, S. C., Boyce, M., McVaugh, C. T., Peehl, D. M. & Bertozzi, C. R. Cell surface glycoproteomic analysis of prostate cancer-derived PC-3 cells. *Bioorganic & Medicinal Chemistry Letters* **21**, 4945-4950 (2011).
- 19 Hanson, S. R., Hsu, T. L., Weerapana, E., Kishikawa, K., Simon, G. M., Cravatt, B. F. & Wong, C. H. Tailored Glycoproteomics and Glycan Site Mapping Using Saccharide-Selective Bioorthogonal Probes. *Journal of the American Chemical Society* **129**, 7266 (2007).
- 20 Yang, L., Nyalwidhe, J. O., Guo, S., Drake, R. R. & Semmes, O. J. Targeted Identification of Metastasis-associated Cell-surface Sialoglycoproteins in Prostate Cancer. *Molecular & Cellular Proteomics* **10**, M110.007294-M007110.007294 (2011).
- 21 Pan, S., Chen, R., Aebersold, R. & Brentnall, T. A. Mass Spectrometry Based Glycoproteomics--from a Proteomics Perspective. *Molecular & Cellular Proteomics* **10**, R110.003251 (2011).
- 22 Palaniappan, K. K. & Bertozzi, C. R. Chemical Glycoproteomics. *Chemical Reviews* **116**, 14277-14306 (2016).
- 23 Chang, P. V., Chen, X., Smyrniotis, C., Xenakis, A., Hu, T., Bertozzi, C. R. & Wu, P. Metabolic Labeling of Sialic Acids in Living Animals with Alkynyl Sugars. *Angewandte Chemie International Edition* **48**, 4030-4033 (2009).
- 24 Wratil, P. R., Horstkorte, R. & Reutter, W. Metabolic Glycoengineering with N-Acyl Side Chain Modified Mannosamines. *Angewandte Chemie International Edition* **55**, 9482-9512 (2016).
- 25 Sletten, E. M. & Bertozzi, C. R. From Mechanism to Mouse: A Tale of Two Bioorthogonal Reactions. *Accounts of Chemical Research*, 110815072703056 (2011).
- 26 Hsu, T. L., Hanson, S. R., Kishikawa, K., Wang, S. K., Sawa, M. & Wong, C. H. Alkynyl sugar analogs for the labeling and visualization of glycoconjugates in cells. *Proceedings of the National Academy of Sciences* **104**, 2614-2619 (2007).
- 27 Xie, R., Dong, L., Du, Y., Zhu, Y., Hua, R., Zhang, C. & Chen, X. In Vivo Metabolic Labeling of Sialoglycans in the Mouse Brain by Using a Liposome-Assisted

Chapter 2: Bioorthogonal labeling of human prostate cancer tissue slice cultures for glycoproteomics

Bioorthogonal Reporter Strategy. *Proceedings of the National Academy of Sciences USA* **113**, 5173 (2016).

28 de Graaf, I. A. M., Olinga, P., de Jager, M. H., Merema, M. T., de Kanter, R., van de Kerkhof, E. G. & Groothuis, G. M. M. Preparation and incubation of precision-cut liver and intestinal slices for application in drug metabolism and toxicity studies. *Nature Protocols* **5**, 1540-1551 (2010).

29 Kiviharju-af Hallstrom, T. M., Jaamaa, S., Monkkonen, M., Peltonen, K., Andersson, L. C., Medema, R. H., Peehl, D. M. & Laiho, M. Human prostate epithelium lacks Wee1A-mediated DNA damage-induced checkpoint enforcement. *Proceedings of the National Academy of Sciences USA* **104**, 7211-7216 (2007).

30 Vaira, V., Fedele, G., Pyne, S., Fasoli, E., Zadra, G., Bailey, D., Snyder, E., Favarsani, A., Coggi, G., Flavin, R., Bosari, S. & Loda, M. Preclinical model of organotypic culture for pharmacodynamic profiling of human tumors. *Proceedings of the National Academy of Sciences USA* **107**, 8352-8356 (2010).

31 Maund, S. L., Nolley, R. & Peehl, D. M. Optimization and comprehensive characterization of a faithful tissue culture model of the benign and malignant human prostate. *Laboratory Investigation*, 1-14 (2013).

32 Belardi, B., de la Zerda, A. & Spiciarich, D. R. Imaging the Glycosylation State of Cell Surface Glycoproteins by Two - Photon Fluorescence Lifetime Imaging Microscopy. *Angewandte Chemie International Edition* **15**, 259-268 (2013).

33 Rostovtsev, V. V., Green, L. G., Fokin, V. V. & Sharpless, K. B. A Stepwise Huisgen Cycloaddition Process: Copper(I)-Catalyzed Regioselective Ligation of Azides and Terminal Alkynes. *Angewandte Chemie International Edition* **41**, 2596 (2002).

34 Moustafa, I., Connaris, H., Taylor, M., Zaitsev, V., Wilson, J. C., Kiefel, M. J., von Itzstein, M. & Taylor, G. Sialic acid recognition by *Vibrio cholerae* neuraminidase. *Journal of Biological Chemistry* **279**, 40819-40826 (2004).

35 De Pinto, V., Messina, A., Lane, D. J. & Lawen, A. Voltage-dependent anion-selective channel (VDAC) in the plasma membrane. *FEBS Letters* **584**, 1793-1799 (2010).

36 Gao, W., Xua, J., Wang, F., Zhang, L., Peng, R., Zhu, Y., Tang, Q. & Wu, J. Mitochondrial Proteomics Approach Reveals Voltage-Dependent Anion Channel 1 (VDAC1) as a Potential Biomarker of Gastric Cancer. *Cellular Physiology and Biochemistry* **37**, 2339-2354 (2015).

37 Shoshan-Barmatz, V. & Golan, M. Mitochondrial VDAC1: function in cell life and death and a target for cancer therapy. *Current Medicinal Chemistry* **19**, 714-735 (2012).

38 Arif, T., Vasilkovsky, L., Refaely, Y., Konson, A. & Shoshan-Barmatz, V. Silencing VDAC1 Expression by siRNA Inhibits Cancer Cell Proliferation and Tumor Growth In Vivo. *Molecular Therapy - Nucleic Acids* **3**, e159 (2014).

Chapter 2: Bioorthogonal labeling of human prostate cancer tissue slice cultures for glycoproteomics

- 39 Zhen, Y., Chunlei, G., Wenzhi, S., Shuangtao, Z., Na, L., Rongrong, W., Xiaohe, L., Haiying, N., Dehong, L., Shan, J., Xiaoyue, T. & Rong, X. Clinicopathologic significance of legumain overexpression in cancer: a systematic review and meta-analysis. *Science Reports* **5**, 16599 (2015).
- 40 Ohno, Y., Nakashima, J., Izumi, M., Ohori, M., Hashimoto, T. & Tachibana, M. Association of legumain expression pattern with prostate cancer invasiveness and aggressiveness. *World Journal of Urology* **31**, 359-364 (2013).
- 41 Kani, K., Malihi, P. D., Jiang, Y., Wang, H., Wang, Y., Ruderman, D. L., Agus, D. B., Mallick, P. & Gross, M. E. Anterior gradient 2 (AGR2): blood-based biomarker elevated in metastatic prostate cancer associated with the neuroendocrine phenotype. *Prostate* **73**, 306-315 (2013).
- 42 Younger, A. R., Amria, S., Jeffrey, W. A., Mahdy, A. E., Goldstein, O. G., Norris, J. S. & Haque, A. HLA class II antigen presentation by prostate cancer cells. *Prostate Cancer Prostatic Discovery* **11**, 334-341 (2008).
- 43 Hudson, B. D., Kulp, K. S. & Loots, G. G. Prostate cancer invasion and metastasis: insights from mining genomic data. *Brief Functional Genomics* **12**, 397-410 (2013).
- 44 Carlsson, B., Forsberg, O., Bengtsson, M., Totterman, T. H. & Essand, M. Characterization of human prostate and breast cancer cell lines for experimental T cell-based immunotherapy. *Prostate* **67**, 389-395 (2007).
- 45 Lu, Y. C., Weng, W. C. & Lee, H. Functional roles of calreticulin in cancer biology. *Biomedical Research International* **2015**, 526524 (2015).
- 46 Casey, G., Neville, P. J., Liu, X., Plummer, S. J., Cicek, M. S., Krumroy, L. M., Curran, A. P., McGreevy, M. R., Catalona, W. J., Klein, E. A. & Witte, J. S. Podocalyxin variants and risk of prostate cancer and tumor aggressiveness. *Human Molecular Genetics* **15**, 735-741 (2006).
- 47 Schorghofer, D., Kinslechner, K., Preitschopf, A., Schutz, B., Rohrl, C., Hengstschlager, M., Stangl, H. & Mikula, M. The HDL receptor SR-BI is associated with human prostate cancer progression and plays a possible role in establishing androgen independence. *Reprod Biol Endocrinol* **13**, 88 (2015).
- 48 Naruse, K., Yamada, Y., Aoki, S., Taki, T., Nakamura, K., Tobiume, M., Zennami, K., Katsuda, R., Sai, S., Nishio, Y., Inoue, Y., Noguchi, H. & Hondai, N. Lactate dehydrogenase is a prognostic indicator for prostate cancer patients with bone metastasis. *Hinyokika Kyo* **53**, 287-292 (2007).
- 49 Michel, V., Licon-Munoz, Y., Trujillo, K., Bisoffi, M. & Parra, K. J. Inhibitors of vacuolar ATPase proton pumps inhibit human prostate cancer cell invasion and prostate-specific antigen expression and secretion. *International Journal of Cancer* **132**, E1-10 (2013).

Chapter 2: Bioorthogonal labeling of human prostate cancer tissue slice cultures for glycoproteomics

- 50 Bair, E. & Tibshirani, R. Semi-supervised methods to predict patient survival from gene expression data. *PLoS Biol* **2**, E108 (2004).
- 51 Kjaergaard, J., Esbensen, K., Wille-Jorgensen, P., Jorgensen, T., Thorup, J., Berning, H. & Wold, S. A multivariate pattern recognition study of risk-factors indicating postoperative thromboembolism despite low-dose heparin in major abdominal surgery. *Thromb Haemost* **54**, 409-412 (1985).
- 52 Raychaudhuri, S., Stuart, J. M. & Altman, R. B. Principal components analysis to summarize microarray experiments: application to sporulation time series. *Pacific Symposium on Biocomputing*, 455-466 (2000).
- 53 Moschini, M., Spahn, M., Mattei, A., Cheville, J. & Karnes, R. J. Incorporation of tissue-based genomic biomarkers into localized prostate cancer clinics. *BMC Medicine* **14**, 67 (2016).
- 54 Shipitsin, M., Small, C., Choudhury, S., Giladi, E., Friedlander, S., Nardone, J., Hussain, S., Hurley, A. D., Ernst, C., Huang, Y. E., Chang, H., Nifong, T. P., Rimm, D. L., Duniak, J., Loda, M., Berman, D. M. & Blume-Jensen, P. Identification of proteomic biomarkers predicting prostate cancer aggressiveness and lethality despite biopsy-sampling error. *British Journal of Cancer* **111**, 1201-1212 (2014).
- 55 Blume-Jensen, P., Berman, D. M., Rimm, D. L., Shipitsin, M., Putzi, M., Nifong, T. P., Small, C., Choudhury, S., Capela, T., Coupal, L., Ernst, C., Hurley, A., Kaprelyants, A., Chang, H., Giladi, E., Nardone, J., Duniak, J., Loda, M., Klein, E. A., Magi-Galluzzi, C., Latour, M., Epstein, J. I., Kantoff, P. & Saad, F. Development and clinical validation of an in situ biopsy-based multimarker assay for risk stratification in prostate cancer. *Clinical Cancer Research* **21**, 2591-2600 (2015).
- 56 Bull, C., Stoel, M. A., den Brok, M. H. & Adema, G. J. Sialic acids sweeten a tumor's life. *Cancer Research* **74**, 3199-3204 (2014).
- 57 Palaniappan, K. K., Pitcher, A. A., Smart, B. P., Spicciarich, D. R., Iavarone, A. T. & Bertozzi, C. R. Isotopic signature transfer and mass pattern prediction (IsoStamp): an enabling technique for chemically-directed proteomics. *ACS Chemical Biology* **6**, 829-836 (2011).
- 58 Woo, C. M., Iavarone, A. T., Spicciarich, D. R., Palaniappan, K. K. & Bertozzi, C. R. Isotope-targeted glycoproteomics (IsoTaG): a mass-independent platform for intact N- and O-glycopeptide discovery and analysis. *Nature Methods* **12**, 561-567 (2015).
- 59 Yap, M. C., Kostiuik, M. A., Martin, D. D., Perinpanayagam, M. A., Hak, P. G., Siddam, A., Majjigapu, J. R., Rajaiah, G., Keller, B. O., Prescher, J. A., Wu, P., Bertozzi, C. R., Falck, J. R. & Berthiaume, L. G. Rapid and selective detection of fatty acylated proteins using omega-alkynyl-fatty acids and click chemistry. *Journal of Lipid Research* **51**, 1566-1580 (2010).
- 60 Geiger, T., Cox, J., Ostasiewicz, P., Wisniewski, J. R. & Mann, M. Super-SILAC mix for quantitative proteomics of human tumor tissue. *Nature Methods* **7**, 383-385 (2010).

Chapter 2: Bioorthogonal labeling of human prostate cancer tissue slice cultures for glycoproteomics

- 61 Laughlin, S. T. & Bertozzi, C. R. Metabolic labeling of glycans with azido sugars and subsequent glycan-profiling and visualization via Staudinger ligation. *Nature Protocols* **2**, 2930-2944 (2007).
- 62 Link, A. J., Eng, J., Schieltz, D. M., Carmack, E., Mize, G. J., Morris, D. R., Garvik, B. M. & Yates, J. R., 3rd. Direct analysis of protein complexes using mass spectrometry. *Nature Biotechnology* **17**, 676-682 (1999).
- 63 Gatlin, C. L., Kleemann, G. R., Hays, L. G., Link, A. J. & Yates III, J. R. Protein Identification at the Low Femtomole Level from Silver-Stained Gels Using a New Fritless Electrospray Interface for Liquid Chromatography–Microspray and Nanospray Mass Spectrometry. *Analytical Biochemistry* **263**, 93-101 (1998).
- 64 Wenger, C. D., Phanstiel, D. H., Lee, M. V., Bailey, D. J. & Coon, J. J. COMPASS: a suite of pre- and post-search proteomics software tools for OMSSA. *Proteomics* **11**, 1064-1074 (2011).
- 65 Kersey, P. J., Duarte, J., Williams, A., Karavidopoulou, Y., Birney, E. & Apweiler, R. The International Protein Index: an integrated database for proteomics experiments. *Proteomics* **4**, 1985-1988 (2004).

Enrichment of sialoglycoproteins from human prostate tissue slice culture conditioned media

Sean Purcell, Sophia Maund, Anthony Iavarone and Donna Peehl contributed to the work presented in this chapter. Portions of the work described in this chapter have been reported in a separate publication.¹

3.1 Introduction

Classically, the cell secretome refers to the collection of proteins that contain a signal peptide that are processed via the endoplasmic reticulum (ER) and Golgi apparatus through the canonical secretion pathway. The secretome also encompasses proteins shed from the cell surface and intracellular proteins released through a non-classical secretion pathway, e.g. exosomes or multivesicular bodies (MVB).² These secreted proteins include numerous enzymes, growth factors, cytokines and hormones.³ They are fundamental in the processes of cell growth, differentiation,⁴ invasion and angiogenesis due to their influence on cell-cell and cell-extracellular matrix interactions.⁵

Secretome proteins play important roles in regulation of many physiological processes via paracrine/autocrine mechanisms and there is growing evidence of their utility as potential biomarkers and for noninvasive diagnostics and treatment monitoring as well therapeutic targets in diseases.⁶ For example, Semmes and coworkers reported on the profiling of proximal fluids from nine clinical specimens where they looked at seminal plasma and expressed prostatic secretion (EPS) fluids.⁷ They identified 133 significantly differentially expressed proteins in individuals with organ-confined prostate cancer versus extracapsular disease, demonstrating the power of proteomics in identifying secreted proteins related to disease state.

In general, however, identifying unique biomarkers from patients has proven more complicated. This is due in part to patient and disease heterogeneity but also with the technical challenges associated with detection of the presence of as well as changes in the levels of low-abundant proteins in human serum samples. A report by Anderson and Anderson highlights the dynamic range present in serum with albumin present in 8-fold higher concentrations than most proteins associated with tissue leakage (**Figure 3-1**).⁸

To overcome these limitations, many groups study secretome proteins released into the media of cultured cells, termed the conditioned media (CM). These secreted proteins have been studied *in vitro* to better understand the pathological conditions and mechanisms *in vivo*. CM is a rich source of material for biomarker discovery experiments.⁹ – studies of prostate,¹⁰ breast,¹¹ hepatocellular carcinoma¹² and pancreatic¹³ cancer cell lines have all been described.

As discussed in chapter 2, the evolving field of proteomics holds considerable promise for the identification of new disease biomarkers.^{14,15} Based in the technique of mass spectrometry (MS), proteomics discovery methods have the advantage of being highly versatile, sensitive, and accurate.¹⁶ Additionally, two reviews highlight the application of MS in the search for markers of prostate disease states,^{17,18} and specific examples from the literature include reports from Everley and coworkers, who in various reports, employed MS analyses of prostate cancer cell lines with increasing metastatic potential.^{19,20} The results of their studies showed increased levels of proteins associated with cellular proliferation and decreased levels of adhesion molecules – two crucial components of metastatic disease. Another MS-based proteomic study observed specific changes in expression of secreted proteins in response to androgen stimulation in LNCaP cells, an androgen-sensitive human prostate adenocarcinoma cell line.²¹ Identification of changes in serum proteins from androgen-sensitive and androgen-independent prostate tissues could greatly improve initial diagnosis and treatment decisions.

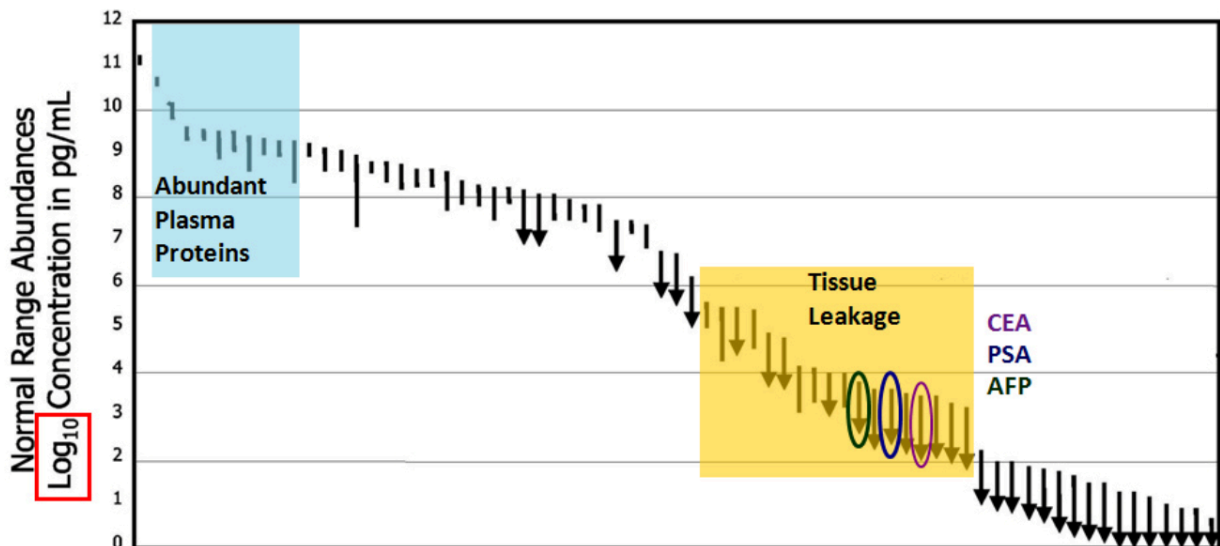


Figure 3-1. Dynamic range of proteins present in serum. Highly abundant proteins such as serum albumin are highlighted in blue, while known cancer biomarkers such as prostate serum antigen (PSA) in blue, Carcinoembryonic antigen (CEA) in purple, and alpha-fetoprotein (AFP) in green are shown in yellow box. This figure was adapted from Anderson and Anderson.⁸

Glycoproteins are an information-rich class of biomolecules with respect to cancer. It has long been appreciated that glycosylation patterns are altered in most cancers.²² Most FDA-approved biomarkers currently in use in the clinic are glycoproteins: carcinoembryonic antigen (CEA) for colon, breast, lung, and pancreatic cancers;²³ cancer antigen 124 (CA125) for ovarian cancer;²⁴ prostate specific antigen (PSA) for prostate cancer;²⁵ herceptin-2 (HER2) for breast cancer;²⁶ among others (**Table 1-1**). Several recent compelling examples support the notion that glycoproteins and, more specifically, their glycosylation state, may be strong predictors of the progression of prostate cancer.²⁷ PSA is a secreted glycoprotein with a single site of glycosylation at

Chapter 3: Enrichment of sialoglycoproteins from conditioned media

asparagine residue N69.²⁸ The structure of the glycan has been elucidated and has been shown to be altered when expressed by malignant cells.^{29,30} Additionally, several groups have observed that in many cancer types, rich, densely packed glycans appended along the protein backbone, correlate with increased metastatic potential and decreased survival rates.^{31,32}

Drake and coworkers recently employed bioorthogonal labeling methods to profile glycoproteins from prostate cancer cell lines using mass spectrometry (MS)-based proteomics. They reported on an alkyne-bead capture of azide-modified glycoproteins from stromal cell culture media that significantly improved the detection of less abundant secreted glycoproteins compared to standard serum-free secretome preparations.³³ They discovered over 100 secreted glycoproteins significantly enriched, several with a no previous association in prostate cancer.

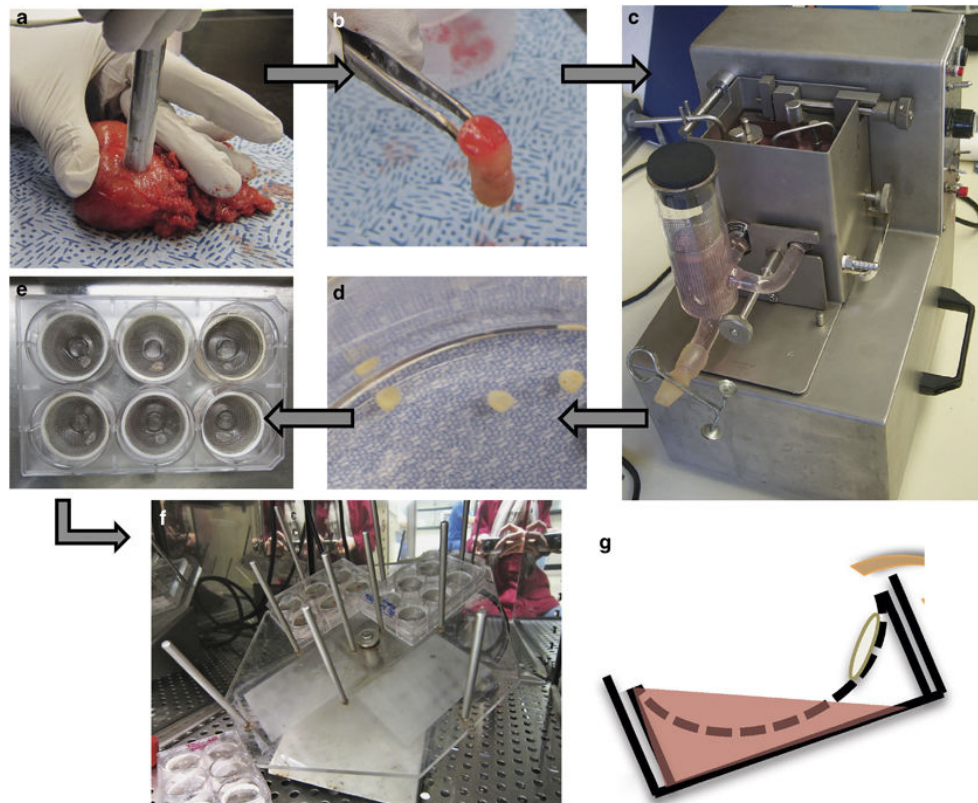


Figure 3-2. Schematic for acquisition of conditioned media (CM) from prostate tissue slice cultures (TSCs). Cores 8-mm in diameter were taken from radical prostatectomy specimens (a, b) and placed in the Krumdieck tissue slicer (c) from which slices emerged in a sequential manner (d). Slices were placed on titanium mesh inserts in six-well plates with 2.5 mL culture medium (e). Plates were mounted on an angled rotating platform in a tissue culture incubator (f). The angled rotation caused intermittent submersion of the tissue slices, facilitating diffusion of gas and nutrients from all sides of the slices (g). Figure adapted from Laboratory Investigation, copyright United States & Canadian Academy of Pathology.³⁴

Building off our success with labeling Ac₄ManNAz-incubated prostate tissue slice cultures (TSCs), as presented in chapter 2, we sought to extend our study to include the

secretome proteins collected from the CM of human prostate TSCs. TSCs can maintain their native *in vivo* cell-cell and cell-matrix interactions for many days while remaining viable and, importantly, metabolically active.^{35,36} As the tissue slices are cultured in the presence of azide-functionalized sugars, the media can be collected and snap-frozen with no observable sample degradation, even years later.

Here we demonstrate that glycoproteins in CM from human prostate TSCs can be metabolically labeled with Ac₄ManNAz, covalently modified with biotin and enriched and identified with MS-based proteomic analysis. This analysis allowed identification of glycoproteins that were secreted at elevated levels in the azide-functionalized TSCs. These data suggest that bioorthogonal labeling methods may be applied to a secretome study of TSCs to reveal disease biomarkers in a more faithful clinical model of human disease.

3.2 Results

In preparation for labeling conditioned media (CM) from human tissue slice cultures (TSC-CM), we used cultured cells to optimize bioorthogonal capture of sialoglycoproteins. CM was collected from PC-3, a prostate cell line, was collected and enriched for sialoglycoproteins by incubating with a modified peracetylated *N*-acetylmannosamine (Ac₄ManNAc) analog such as peracetylated *N*-azidoacetylmannosamine (Ac₄ManNAz) and then subjecting the CM to Staudinger ligation reaction conditions with a phosphine-PEG3-biotin,³⁷ strain-promoted-azide-alkyne-cycloaddition (SPAAC)³⁸ conditions with DIBAC-biotin partner or copper-catalyzed azide-alkyne [3+2] cycloaddition (CuAAC) conditions with a biotin-alkyne partner.³⁹ Labeling was assessed by western blot (**Figure 3-3**).

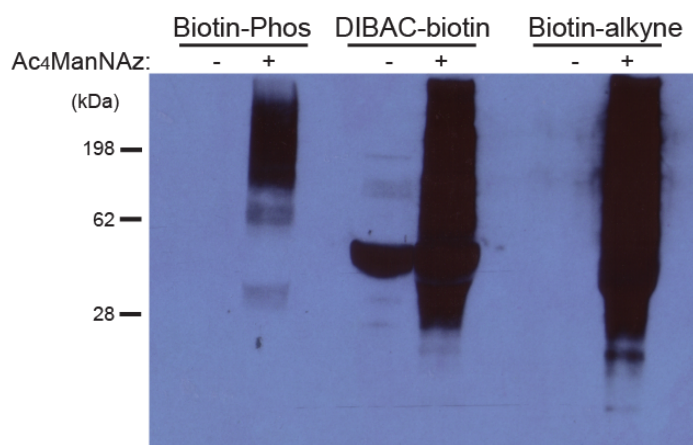


Figure 3-3. Western blot analysis of conditioned media (CM) collected from PC-3 cells incubated with Ac₄ManNAc (-) or Ac₄ManNAz (+) and subsequently reacted with biotin-functionalized reagents. CM collected and reacted with biotin-PEG3-phosphine (left), DIBAC-biotin (center) or biotin-alkyne (right). Protein quantification performed by bicinchoninic acid (BCA) assay and confirmed by ponceau stain (not shown).

Surprisingly, we observed substantial background with the DIBAC reagent and poor labeling with the phosphine probe. In contrast, strong azide-labeling was observed for biotin-alkyne with no labeling of the Ac₄ManNAc control lane was observed, as the Staudinger ligation is known to have substantially lower kinetics than other click reactions,^{40,41} we attempted phosphine reactions for twenty-four hours; however, we still observed less labeling than for one hour under CuAAC conditions (data not shown).

We next sought to reduce the background observed in the DIBAC reaction and were inspired by work by Remon van Geel and coworkers who demonstrated that most of the azide-independent polypeptide labeling in SPAAC reactions could be attributed to thiol-alkyne additions.⁴² Further, they showed that this could be reduced by pretreatment of the peptidyl cysteines (so-called “hot cysteine residues”) with a capping moiety. It was shown that by reacting samples with solutions of iodoacetamide (IAM) ranging from 1-5 mM for 30 min at room temperature, reactive thiols are covalently capped by nucleophilic substitution, blocking thiol-alkyne reactions and reducing background as a result.

Thus we reacted PC-3 CM with iodoacetamide in concentrations ranging from 5-50 mM at both room temperature and 37 °C. Unfortunately, no significant reduction in background labeling was observed using this method (data not shown). Based on these results, it was determined that labeling with biotin-alkyne under CuAAC conditions would be used for all subsequent labeling reactions.

Next we attempted to optimize CuAAC labeling conditions. First we tried several different copper ligands under several (e.g., 3-(4-((bis((1-tert-butyl-1H-1,2,3-triazol-4-yl)methyl)amino)methyl)-1H-1,2,3-triazol-1-yl)propyl hydrogen sulfate (BTTPS), 2-(4-((bis((1-tert-butyl-1H-1,2,3-triazol-4-yl)methyl)amino)methyl)-1H-1,2,3-triazol-1-yl) acetic acid (BTAA) and tris-(benzyltriazolylmethyl)amine (TBTA)). It was found that TBTA found to give robust labeling of PC-3 CM. In addition, TBTA is commercially available and we hoped procedures developed with CM could be translated to other labs. Reaction times were investigated from 30 min to 22 h were investigated. Neither increased labeling nor increased observable background beyond 1 h, and thus we performed all subsequent reactions for 1 hour at room temperature (**Figure 3-4**).

With optimized conditions developed for PC-3 cell lines, we next sought to translate these procedures to prostate TSCs from radical prostatectomies. As previously described, TSCs were derived from an 8 mm in diameter core from a fresh radical prostatectomy specimen, precision-cut into 300-µm-thick slices and incubated in a rotary culture apparatus. Structural and functional fidelity of the TSCs could be maintained for at least five days.³⁴ The TSCs were labeled by incubating with 50 µM Ac₄ManNAz or 50 µM Ac₄ManNAc, a control sugar lacking the chemical reporter functionality. CM was collected for 3 days from the media the TSCs were grown in, flash frozen and stored for biotin capture (**Figure 3-2**).

Ex vivo culture of human prostate TSCs retain physiological properties that are often absent in cell culture and also maintain intra-tissue luminal epithelial and basal cells microheterogeneity. Culturing of tissue core slices from fresh prostatectomy specimens begins in less than hour after the organ is clamped in the operating room. In our work with metabolic labeling, we employed 8 mm cores but 5 mm and 10 mm cores also maintain architecture and reproducibility. Precision slicing of 100 µm – 500µm has been

Chapter 3: Enrichment of sialoglycoproteins from conditioned media

reported but we found that slices of 250-500mm reduce variation in slice thickness and damage to cut surfaces, which maintain optimal nutrient absorption. If you're target is low abundance species, e.g. glycoproteins on extracellular vesicles, larger tissue slices may be desired.

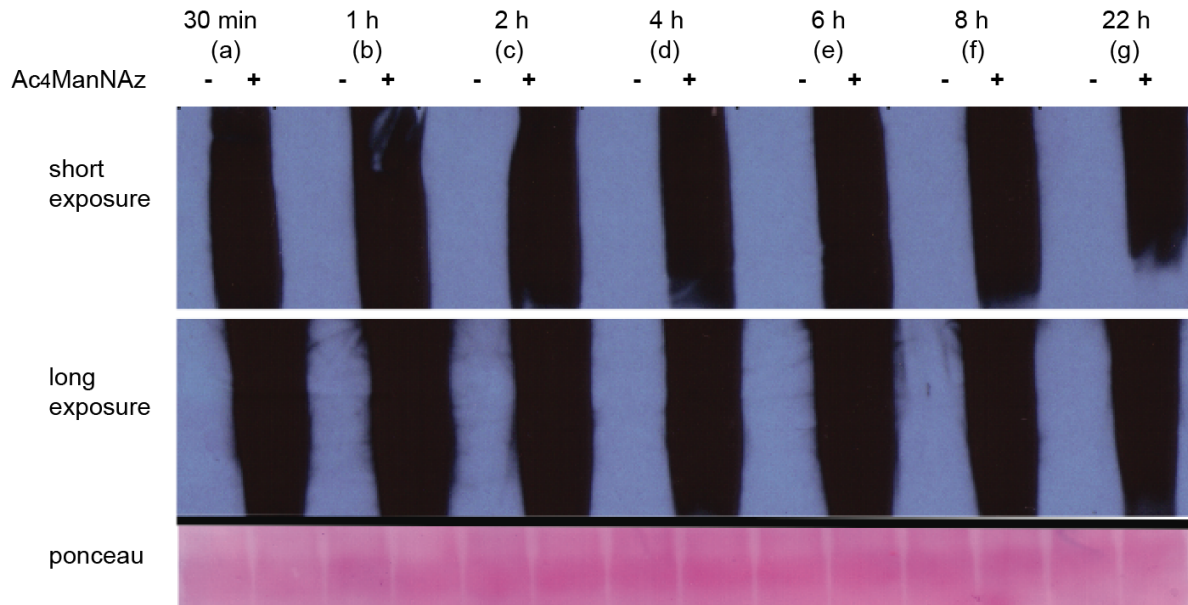


Figure 3-4. Time independence of alkyne-biotin labeling on CM collected from PC-3 cells. PC-3 cells incubated with Ac₄ManNAc (-) or Ac₄ManNAz (+) were lysed and reacted with alkyne-biotin under copper-catalyzed azide-alkyne [3+2] cycloaddition (CuAAAC) conditions for (a) 30 min, (b) 1 h, (c) 2 h, (d) 4 h, (e) 6 h, (f) 8 h, (g) 22 h under. Anti-biotin HRP blot (top panel) short exposure of 1 min (top panel), overnight exposure (middle panel). Protein quantification performed by bicinchoninic acid (BCA) assay and confirmed by ponceau stain (lower panel).

The use of cultured human prostatic tissue slices allows for comparisons of cancerous, normal and other prostatic diseases, for example benign prostate hyperplasia (BPH), tissue from the same patient source.⁴³ We utilized a needle biopsy report available from the surgeon in the operating room providing a schematic view of the patient's area of interest. The schematic view is then taken back with the specimen to the lab to core the areas of interest. Prostate tissue has high heterogeneity and a balance between protein abundance and disease confidence must be considered when selecting core size and location. Palpable areas can also be used to identify regions of cancer tissue. Benign tissue is identified by the needle biopsy pathology report and tissue is taken farthest away from the identified positive cores (cancer). The number of cores that can be taken from a single specimen is dependent the number of overall positive needle biopsies versus the number of benign needle biopsy cores.

Cores are placed in the Krumdieck tissue slicer from which slices emerge in a sequential manner. To slices that were bioorthogonally labelled, histology was performed on both adjacent slices to ensure both tissue architecture and disease state is maintained. Slices were then placed on titanium mesh inserts in six-well plates with 2.5 mL culture medium. Plates are mounted on a rotating platform set at a 30° angle rotating platform in a

Chapter 3: Enrichment of sialoglycoproteins from conditioned media

tissue culture incubator. The angled rotation caused intermittent submersion of the tissue slices, facilitating diffusion of gas and nutrients from all sides of the slices. We have not yet extensively characterized TSCs beyond 5 days, however, preliminary studies³⁴ indicate that overall degeneration of both benign and prostate cancer tissues become apparent after 1 week.

We previously developed a serum-free medium, termed 'Complete PFMR-4A,' for primary culture of human prostatic cells.⁴⁴ In general PFMR-4A components are prepared once a year, aliquoted and stored at -20 °C. The Complete PFMR-4A is prepared and stored at 4 °C for no more than 2 weeks. Increasing the concentration of R1881 in Complete PFMR- 4A revealed that 50 nM prevented luminal epithelial degeneration up to 5 days in culture. Other culture conditions were attempted but we found these culture conditions successfully maintained the structural and functional fidelity of both benign and prostate cancer TSCs for up to 5 days. To the 2.5 mL of Completed PFMR-4A medium with 50 nM R1881, 50 µM of monosaccharide (e.g. Ac₄ManNAc, Ac₄ManNAz, or Ac₄ManNAI) was added.

As previously reported, the tissue viability is enhanced when the culture medium is regularly refreshed to maintain necessary levels of supplements and to remove metabolic waste products that can be damaging when present in the cellular environment.³⁴ Histological analysis of TSC by hematoxylin and eosin (H&E) staining showed that Ac₄ManNAz, Ac₄ManNAc, and Ac₄ManNAI treatments had no obvious effect on TSC morphology. We have also attempted labeling with peracetylated N-azidoacetyl galactosamine (Ac₄GalNAz) for labeling mucin-type glycans and intracellular o-glcNacylation and saw robust labeling by western blot analysis. The azide and alkyne-functionalized sugars were synthesized as previously described,⁴⁵ however, bioorthogonal reagents are now commercially available from several sources (e.g. Invitrogen and Click Chemistry Tools, among others).

Changing the culture medium every day appeared to enhance prostate TSC architecture and survival over changing the culture medium every other day and there was no perceived benefit to changing the medium more than once per day and this is particularly important for metabolic studies. In addition to the TSCs that were collected after 3 days of incubation with bioorthogonal chemical reporters, conditioned media were collected, after each day, spun down, and stored at -80 °C.

We applied our robust reaction conditions developed in cell lines for labeling CM to human derived TSC-CM. Surprisingly, low biotin signal was observed by immunoblotting. Additionally, when samples were carried on to MS-based proteomics, very few glycoproteins were observed. One potential reason for this unexpected difference in labeling is TSCs are quite heterogeneous and the media they are grown in is optimized around survival rather than copper click labeling conditions. It was suspected that labeling suppression was in part due to oxidizing and chelating agents in the complex media, which could lead to poor copper reactivity.

Chapter 3: Enrichment of sialoglycoproteins from conditioned media

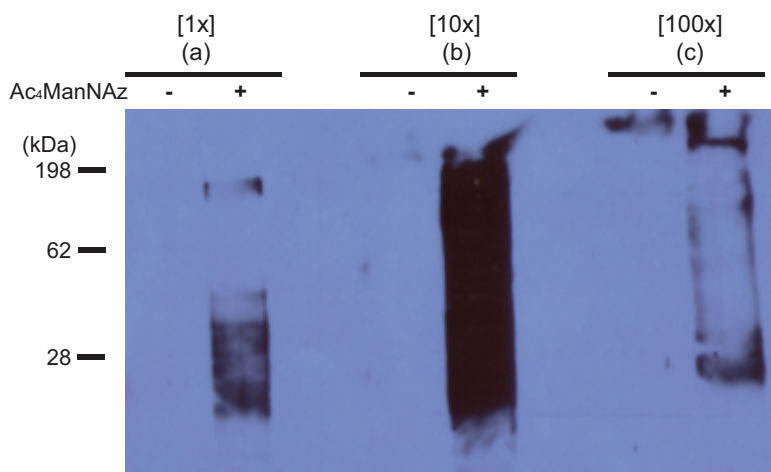


Figure 3-5. Concentration dependence of biotin-alkyne reaction on CM derived from human TSC CM. TSCs labeled with either incubated with $Ac_4ManNAz$ (+) or with $Ac_4ManNAc$ (-), CM was isolated, reacted a base concentration of 100 μM (TBTA) and 25 μM alkyne-biotin and corresponding 1mM copper sulfate and 5mM sodium ascorbate and then protein precipitated with acetone. 1x (a), 10x (b), or a 100x cocktail of CuAAc reagents (c). Protein quantification performed by BCA assay and confirmed confirmed by Ponceau stain (not shown).

To overcome low labeling we attempted different concentrations of copper ligand and alkyne probe, ranging from 0.1x to 100x of a base CuAAc labeling cocktail. Higher labeling was achieved with a 10x click cocktail concentration, whereas 100x concentration of copper led to obvious protein precipitation which in turn led to reduced labeling (**Figure 3-5, Table 3-1**). Many methods were attempted to remove excess biotin and small molecule reagents (e.g., 5 kDa size exclusion columns, protein precipitation with trichloroacetic acid (TCA), methanol or acetone). It was found that acetone precipitation following labeling retained substantial labeled proteins. Interestingly, we did not observe background in control sugar lacking the azide-functionality even under the 100x labeling conditions.

Table 3-1. Concentration of CuAAC reagents tested for covalently conjugating biotin to azide-labeled glycoproteins. Tris-(benzyltriazolylmethyl)amine (TBTA), copper sulfate ($CuSO_4$), sodium ascorbate, biotin-PEG4-alkyne make up the labeling reagents, reactions were quenched with ethylenediaminetetraacetic acid (EDTA).

Concentration	TBTA [mM]	$CuSO_4$ [mM]	Sodium ascorbate [mM]	Biotin alkyne [mM]	EDTA [mM]
0.1 x	0.01	0.1	0.5	0.0025	0.04
1 x	0.1	1	5	0.025	0.4
10 x	1	10	50	0.25	4
100 x	10	100	500	2.5	40

Surprisingly, CM collected on different days exhibited varied protein concentration and labeling profiles. Across CM collected from several patients, CM collected after 1 day showed the greatest protein concentration. However, it was CM collected on the second day that resulted in the most robust labeling. CM collected after 3 days of labeling showed reduced labeling and concentration, indicating changes in the glycoproteome could be occurring that are not observable by histology. For this study, only CM collected after 2 days of incubation was used for subsequent enrichment (**Figure 3-6**).

Capture procedures previously described for prostate TSCs lysate¹ was employed for labeled-CM. In brief, following covalent labeling and desalting, biotinylated proteins were captured on avidin resin, washed and then digested on-bead with trypsin. The samples were then carried onto MS-based proteomic analysis. High resolution data was obtained on an LTQ-Orbitrap and analyzed with Proteome Discoverer 1.4 suite by searching spectra against the reviewed Swiss-Prot human proteome database using the Sequest HT algorithm.

Within Proteome Discoverer we extracted out protein spectral counts which, as previously described, are a semi-quantitative, label-free measure of protein abundance.⁴⁶ For validation, in this study we used the commonly accepted practice of requiring at least 2 peptides from each protein with a 1% computational false discovery rate (FDR).

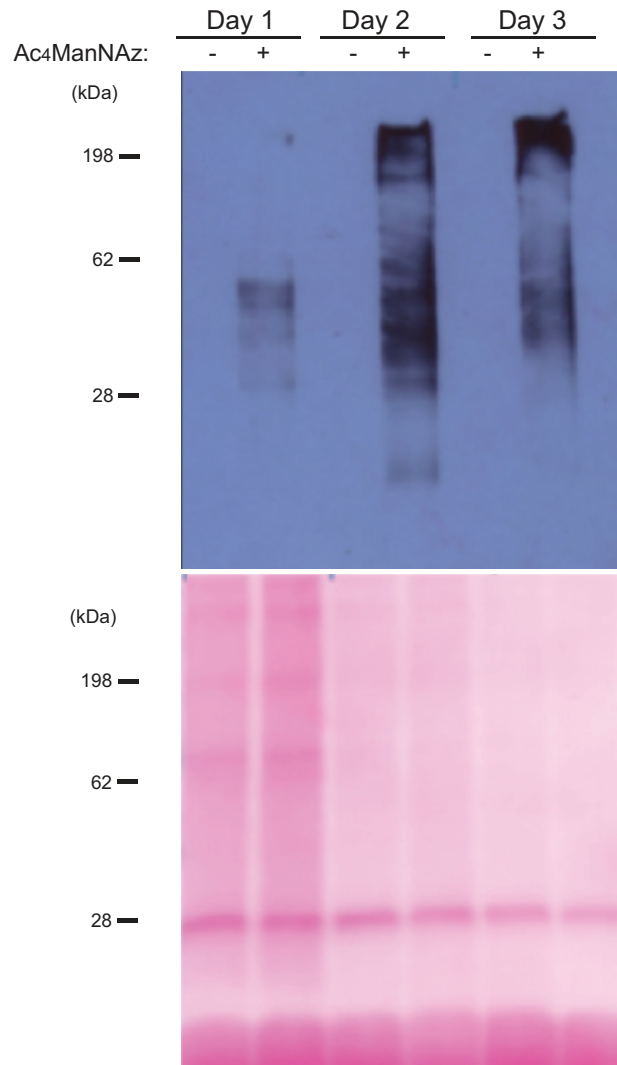


Figure 3-6. Labeling of CM harvested from human prostate TSCs varies by collection time. Equal volumes of CM labeling over days, with different overall protein quantitation seen by Ponceau stain (lower panel).

Unfortunately, we observed high background, 118 non-redundant proteins were observed in the normal and cancer samples with 77 common to both groupings. We found 41 proteins that were unique to the azide-labeled and none that were unique to the Ac₄ManNAc control sample (**Figure 3-7**). Although detergent washes were performed, only abundant housekeeping proteins were identified in the Ac₄ManNAz-labeled CM. Although more than 95% of proteins identified were secreted only 40% had an annotation of glycosylation. Additionally, the number of background proteins (e. g. 35% unique v. 65% common) identified as labeled ones was deemed high, necessitating further optimization performed. This was repeated several times with similar results.

To reduce capture of steady-state proteins and enrich for less abundant glycoproteins, more stringent washes with higher concentrations of urea or sodium dodecyl sulfate

Chapter 3: Enrichment of sialoglycoproteins from conditioned media

(SDS) were attempted along with an acid-cleavable detergent, ProteaseMAX Surfactant. Additionally, different anti-biotin conjugated resins (e. g., avidin, NeutrAvidin, Streptavidin and Streptavidin Plus UltraLink Resin) were tested.

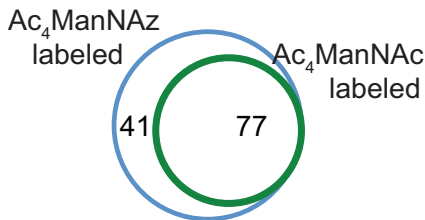


Figure 3-7. Labeled glycoproteins from conditioned media administered Ac₄ManNAz or Ac₄ManNAc. The conditioned media from prostate TSC incubated with Ac₄ManNAz or Ac₄ManNAc was collected and purified to remove excess sugar. Samples were treated with biotin-alkyne probe, enriched and carried on to MS-based proteomic analysis. Number indicates proteins observed with at least two peptides and 1% false discovery rate (FDR).

With harsher washes during enrichment, background observed by mass spectrometry was reduced. On application of our optimized procedures to enrich sialylated glycoproteins from CM of TSCs, we identified 146 proteins unique to azide-labeled samples, 1 unique to control group, and 36 in common (**Figure 3-8**). Of the 146 found in the azide-group, 64% were annotated as glycosylated in Uniprot; in contrast, of the 36 proteins found in common, only ~10% had this glycosylation annotation. Further comparisons of proteins identified in normal and cancer conditioned media samples are still on going and anticipated to yield new potential biomarkers for prostate cancer (**Table 3-2**).

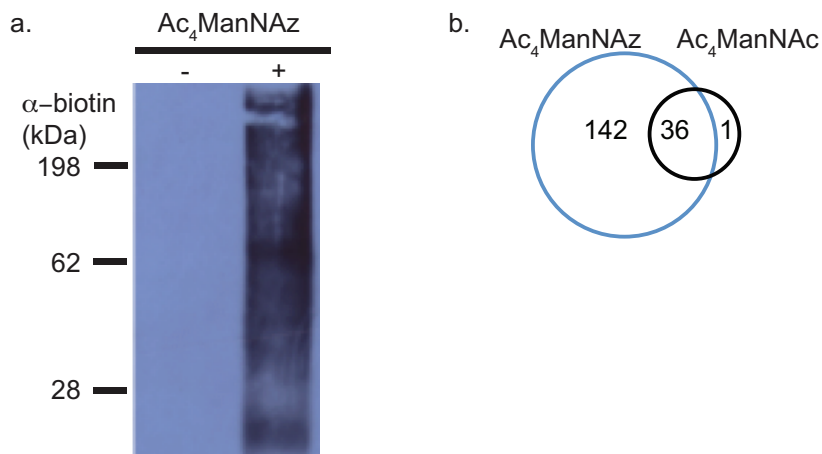


Figure 3-8: Optimized enrichment of labeled glycoproteins from conditioned media administered Ac₄ManNAz or Ac₄ManNAc. (a) The conditioned media from prostate TSC incubated with Ac₄ManNAz (+) or Ac₄ManNAc(-) was collected and purified to remove excess sugar. Samples were treated with biotin-alkyne probe and analyzed by western blot using an HRP-conjugated anti-biotin antibody. Strong azide labeling was observed over background. (b) Proteomic analysis revealed azide-dependent labeling.

3.3 Discussion

With approximately 180,000 new prostate cancer diagnoses annually, there is a need for reliable biomarkers for disease detection and prognosis.⁴⁷ Currently, PSA is used as a clinical biomarker for prostate detection. PSA screening, however, suffers from a high rate of false results, both positive and negative, that often leads to an incomplete or incorrect diagnosis.⁴⁸ PSA levels in blood serum are correlated with prostate size rather than cancer, and many factors including age and race, can lead to increased PSA levels.⁴⁹

Although further optimization of the method to label CM is desired, we believe that with the robust labeling and capture conditions developed herein, CM from cancerous and normal TSCs can now be employed to identify proteins related to disease state. Previous CM studies have often relied on depleting albumin or growing cells in a serum-free media.⁵⁰ This, however, can have a deleterious effect on cell growth and their glycoproteomes, problems that our approach circumvents.

One of the biggest challenges in the management and detection of cancer and disease remains the lack of prognostic and predictive biomarkers that can help in the design of therapeutic strategies as well as in monitoring tumor progression. A new approach toward biomarker discovery is emerging, where pathways instead of individual proteins are monitored and targeted.^{51,52} Often referred to as interaction networks, these pathways can be analyzed using statistical modeling and protein concentration to infer information. Our studies, which could be employed to identify protein classes that exhibit significant modulation in the diseased state, could be further used to elucidate this type of pathway information.⁵³

Once proteins or classes of proteins are identified, they can then be correlated with patient prognosis. Upon determining the identities and specific localization of putative glycoprotein biomarkers in tissues and sera, comparisons of the expression level and localization of the markers to disease progression and patient survival can be made. We will seek to establish whether any trends exist between marker expression in the serum and PSA level, potentially providing for a more accurate diagnosis prior to treatment.

More generally, we view this model as a useful source of information to guide targeted experiments, aimed at the discovery of yet unknown carcinogenesis mechanisms and therapeutic strategies. Furthermore we believe that this model may prove useful for the study of non-malignant prostatic tissue that is more difficult to propagate in traditional cell culture models. Finally, we envision that this platform could be employed for capturing extracellular vesicles (e. g. exosomes) which have been shown to change during tumorigenesis.⁵⁴

3.4 Table

Table 3-2. Proteins identified in Normal Ac₄ManNAz-incubated CM dataset that were absent in Normal Ac₄ManNAc dataset.

Accession	Gene	Protein
P98160	PGBM	Basement membrane-specific heparan sulfate proteoglycan protein
P12111	CO6A3	Collagen alpha-3
Q9Y6R7	FCGBP	IgGfC-binding protein
P00450	CERU	Ceruloplasmin
Q9NPR2	SEM4B	Semaphorin-4B
P24821	TENA	Tenascin
P05067	A4	Amyloid beta A4 protein
P02671	FIBA	Fibrinogen alpha chain
P02790	HEMO	Hemopexin
P15941	MUC1	Mucin-1
P07996	TSP1	Thrombospondin-1
Q14118	DAG1	Dystroglycan
P01023	A2MG	Alpha-2-macroglobulin
Q16610	ECM1	Extracellular matrix protein 1
O43286	B4GT5	Beta-1,4-galactosyltransferase 5
P07858	CATB	Cathepsin B
P00738	HPT	Haptoglobin
P01833	PIGR	Polymeric immunoglobulin receptor
Q12841	FSTL1	Follistatin-related protein 1
P04196	HRG	Histidine-rich glycoprotein
P27487	DPP4	Dipeptidyl peptidase 4
P02675	FIBB	Fibrinogen beta chain
O94985	CSTN1	Calsyntenin-1
P00751	CFAB	Complement factor B
Q9UBX7	KLK11	Kallikrein-11
P02751	FINC	Fibronectin
P23142	FBLN1	Fibulin-1
P07686	HEXB	Beta-hexosaminidase subunit beta
P10909	CLUS	Clusterin
P09668	CATH	Cathepsin H
O00584	RNT2	Ribonuclease T2
P08253	MMP2	72 kDa type IV collagenase
P0C0L4	CO4A	Complement C4-A
Q13510	ASAH1	Acid ceramidase
P09758	TACD2	Tumor-associated calcium signal transducer 2
P06731	CEAM5	Carcinoembryonic antigen-related cell adhesion molecule 5

Chapter 3: Enrichment of sialoglycoproteins from conditioned media

Accession	Gene	Protein
P01876	IGHA1	Ig alpha-1 chain C region
P01008	ANT3	Antithrombin-III
P18827	SDC1	Syndecan-1
Q16270	IBP7	Insulin-like growth factor-binding protein 7
P31431	SDC4	Syndecan-4
Q08380	LG3BP	Galectin-3-binding protein
O00391	QSOX1	Sulfhydryl oxidase 1
P01024	CO3	Complement C3
P01859	IGHG2	Ig gamma-2 chain C region
P07093	GDN	Glia-derived nexin
P01033	TIMP1	Metalloproteinase inhibitor 1
P01860	IGHG3	Ig gamma-3 chain C region
P17900	SAP3	Ganglioside GM2 activator
P07339	CATD	Cathepsin D
P02647	APOA1	Apolipoprotein A-I
P62937	PPIA	Peptidyl-prolyl cis-trans isomerase A
P02750	A2GL	Leucine-rich alpha-2-glycoprotein
P36955	PEDF	Pigment epithelium-derived factor
P51884	LUM	Lumican
P05155	IC1	Plasma protease C1 inhibitor
P68871	HBB	Hemoglobin subunit beta
Q6UX06	OLFM4	Olfactomedin-4
P25311	ZA2G	Zinc-alpha-2-glycoprotein
P69905	HBA	Hemoglobin subunit alpha
P41222	PTGDS	Prostaglandin-H2 D-isomerase
P15309	PPAP	Prostatic acid phosphatase
P05121	PAI1	Plasminogen activator inhibitor 1
P80188	NGAL	Neutrophil gelatinase-associated lipocalin
P01011	AACT	Alpha-1-antichymotrypsin

3.5 Methods and Materials

General methods

Human Embryonic Kidney (HEK) 293T cells (ATCC) were maintained in a 5% CO₂, water-saturated atmosphere at 37 °C in DMEM supplemented with 10 % FBS, penicillin (100 U/mL), and streptomycin (0.1 mg/mL). Adherent cell densities were maintained between 1 x 10⁵ and 2 x 10⁶ cells.

Preparation of prostate tissue whole cell lysates. Prostate tissue slice cultures were lysed in 1 mL of lysis buffer containing 1% Triton X-100, 20 mM Tris pH 7.4, 300 mM NaCl, and protease inhibitors (inhibitor cocktail III from Calbiochem). While the tissue was cooled on ice, pulverization was performed using a Tissue Tearor (Biospec Products model #780CL-04) on setting 2, with cycles of 20 sec on followed by 20 sec off, 2 min total time. Samples underwent sonication for 1 min total time with cycles of 10 sec on and 10 sec off at 2.0 V setting. Cell surface glycoproteins were collected in the supernatant after centrifugation at 10,000 rpm for 10 min at 4 °C. The supernatant was collected and a bicinchoninic acid (BCA) assay (Thermo Fisher Scientific) was performed to determine protein concentration.

Gel analyses. All sodium dodecyl sulfate polyacrylamide gel electrophoresis (SDS-PAGE) was performed with the Criterion System (Bio-Rad) using either 4-12% or 12% Criterion XT Bis-Tris precast gels and XT MES running buffer. The See Blue Plus 2 marker (Invitrogen) was used to determine the apparent molecular weights of resolved proteins. Visualization of protein bands was accomplished by staining with Coomassie Brilliant Blue G-250 (Fluka) or silver stain (Bio-Rad, 1610449). Unless otherwise noted, all SDS-PAGE analysis was performed under reducing conditions by incubating protein samples with loading buffer containing 100 µM 2-mercaptoethanol and heating at 95 °C for 5 min.

Silver stain. After running, the gel was removed from the cartridge and washed twice in ultrapure water, each wash requiring 5 min. of gentle shaking at RT. The water is then discarded and a fixing solution of 30% ethanol (Sigma Aldrich), 10% acetic acid (Sigma Aldrich), and 60% ultrapure water is added until the gel is submerged. The gel is fixed for 15 min. shaking gently at RT before the solution is replaced and fixing continues for an additional 15 min. The fixing solution is discarded and gel is washed in twice in 10% ethanol, each wash requiring 5 min. of gentle shaking at RT. The gel is then washed twice in ultrapure water for 5 min at RT. A solution of 50 µL Silver Stain Sensitizer (Pierce, 24612) in 25 mL ultrapure water is prepared and gel is sensitized for 1 min at RT. Immediately after sensitizing the gel is washed twice with ultrapure water for 1 min. each. A staining solution of 0.5 mL Enhancer (Pierce, 24612) and 25 mL Silver Stain (Pierce, 24612) is mixed and added to the gel. The gel is then stained for 30 min. at RT with gentle shaking. While the gel is staining, a developing solution of 0.5 mL Enhancer and 25 mL Developer (Pierce, 24612) is prepared. A stop solution of 5% acetic acid in ultrapure water is also prepared. The gel is washed twice for 20 sec. each with ultrapure water before the developing solution is added. The gel is gently rocked in the developing solution for 2-3 min. until bands appear (gel box is held above standard light source for enhanced visualization). As soon as bands appear developing solution is discarded and

developing stopped with two washes of 5% acetic acid; the first only for 30 sec. and the second for 10 min. at RT with gentle shaking.

Protein precipitation with Trichloroacetic acid (TCA). Labeled conditioned media (1.15 mL) is added to a 1.5 mL protein low-bind tube (Eppendorf) and chilled on ice for 10 min. Trichloroacetic acid (Sigma Aldrich) is pre-chilled on ice and then 287.5 μ L is added to each sample such that final concentration is 20% trichloroacetic acid. The tube is then submerged in a dry ice and isopropanol (Sigma Aldrich) bath that was prepared 30 min prior to freezing. Once frozen (typically after a duration of 1-2 min.) sample is thawed on ice until liquid. Samples are spun at 13,200 rpm for 10 min at 4 °C. Supernatant is discarded and samples are washed with 800 μ L of 1% trichloroacetic acid, pre chilled on ice. Samples are centrifuged under the same conditions and supernatant is again discarded. Pellet is dried by Speedvac at 40 °C under vacuum for approximately 25 min.

Protein precipitation by Acetone. Labeled conditioned media (1 mL) is added to a 5 mL protein low-bind tube (Eppendorf) and chilled on ice for 10 min. Acetone (Sigma Aldrich) is pre-chilled to -20 °C and then added to each sample such that final volume is 80% acetone (2.5 mL). The tube is then submerged in a dry ice and isopropanol (Sigma Aldrich) bath that was prepared 30 min prior to freezing. Once frozen (typically after a duration of 15 min) sample is thawed at RT until liquid. Samples are spun at 15,000 rpm for 10 min at 4 °C. Supernatant is discarded and samples are washed with another 2.5 mL acetone (Sigma Aldrich) pre-chilled to -20 C. Samples are centrifuged under the same conditions and supernatant is again discarded. Pellet is dried by leaving Eppendorf tube uncapped and allowing residual acetone to evaporate for approximately 20 min with gentle heating at 40 C.

Protein precipitation by 40:40:20 ACN:MeOH:H₂O. Labeled conditioned media (1 mL) is added to a 5 mL protein low-bind tube (Eppendorf) and chilled on ice for 10 min. A precipitation solution of 40% acetonitrile (Sigma Aldrich), 40% methanol (Sigma Aldrich) and ultrapure water is mixed and pre-chilled to -20 °C. The solution is then added to each sample such that final volume is 80% precipitation solution (2.5 mL). The tubes are then submerged in a dry ice and isopropanol (Sigma Aldrich) bath that was prepared 30 min prior to freezing. Once frozen (typically after a duration of 15 min) sample is thawed at RT until liquid. Samples are spun at 15,000 rpm for 10 min at 4 C. Supernatant is discarded and samples are washed with another 2.5 mL precipitation solution pre-chilled to -20 °C. Samples are centrifuged under the same conditions and supernatant is again discarded. Pellets are dried by leaving tubes uncapped and allowing residual precipitation solution to evaporate for approximately 20 min with gentle heating at 40 °C.

DIBAC labeling. Conditioned media is thawed on ice and an ethylenediaminetetraacetic acid (EDTA) free protease inhibitor cocktail (Millipore, 539134) is added in a volume equal to 10% that of the conditioned media. The samples (sizes ranging from 50 μ L to 1 mL) are then transferred to a protein low-bind tube (Eppendorf). Azadibenzocyclooctyne-(polyethylene glycol)₄-biotin (DIBAC-PEG₄-Biotin, Jena Bioscience) is added such that the final concentration is 20 μ M in solution. Samples are vortexed and then rotated at 37 °C for 1 h. Reaction is quenched by placing sample tubes in dry ice bath until samples are frozen (approximately 2-4 min).

Preventing thiol-yne addition with iodoacetamide pretreatment prior and to DIBAC labeling. Conditioned media is thawed on ice and an ethylenediaminetetraacetic acid (EDTA)-free protease inhibitor cocktail (Millipore, 539134) is added in a volume equal to 10% that of the conditioned media. The samples are then transferred (sample sizes ranging from 50 μ L to 1 mL) to a protein low-bind tube (Eppendorf). Iodoacetamide (Sigma-Aldrich) is added such that a final concentration of 5 mM is achieved. Samples are vortexed and then rotate at either RT, 37 °C, or a gradient from RT to 37 °C for 30 min in no ambient light. Azadibenzocyclooctyne-(polyethylene glycol)₄-Biotin (DIBAC-PEG₄-Biotin, Jena Bioscience) is then added such that the final concentration is 20 μ M in solution. Samples are vortexed and then rotated at RT for 1 h. Reaction is quenched by placing sample tubes in dry ice until samples are frozen (approximately 2-4 min).

Staudinger ligation methods. Conditioned media is thawed on ice and an ethylenediaminetetraacetic acid (EDTA)-free protease inhibitor cocktail (Millipore, 539134) is added in a volume equal to 10% that of the conditioned media. The samples (sample sizes ranging from 50 μ L to 1 mL) are then transferred to a protein low-bind tube (Eppendorf) under an argon gas source. Phosphine-(polyethylene glycol)₃-biotin (Life Technologies) is added such that the final concentration in solution is 250 μ M. Samples are sealed, vortexed, and incubated at 37 °C (reaction time varies from 8-24 h). Reactions are quenched by placing samples in dry ice until frozen (2-4 min).

TPPO / Staudinger. Conditioned media is thawed on ice and an ethylenediaminetetraacetic acid (EDTA) free protease inhibitor cocktail (Millipore, 539134) is added in a volume equal to 10% that of the conditioned media. The samples (100 μ L) are then transferred to protein low-bind tubes (Eppendorf) under an argon gas source. Triphenylphosphine oxide (TPPO, Sigma Aldrich) is added to samples until a final concentration of 1.25 mM is achieved. TPPO was used a pre-treatment to reduce background associated with Staudinger ligation reaction. Phosphine-(polyethylene glycol)₃-Biotin (Life Technologies) is added such that the final concentration in solution is 250 μ M. Samples are sealed, vortexed, and incubated at 37 °C for 24 h. Reactions are quenched by placing samples in dry ice until frozen (2-4 min).

Copper Click (1x, 10x, or 100x). Conditioned media is thawed on ice and an ethylenediaminetetraacetic acid-free protease inhibitor cocktail (Millipore, 539134) is added in a volume equal to 10% that of the conditioned media. The samples are vortexed and then 50 μ L to 1 mL is transferred to a protein low-bind tube (Eppendorf). A solution of tris(benzyltriazolylmethyl)amine (TBTA) (Sigma Aldrich) is added such that the final concentration is 0.1 mM (1x), 1mM (10x), or 10mM (100x). Next a solution of copper (II) Sulfate (Sigma Aldrich) in ultrapure water is added such that the final concentration is 1 mM (1x), 10 mM (10x), or 100 mM (100x). A solution of sodium ascorbate (Spectrum) in ultra pure water is prepared immediately before being added to the sample such that a final concentration of 5 mM (1x), 50 mM (10x), or 500 mM (100x). Lastly, a solution of biotin-(polyethylene glycol)₄-alkyne is added such that the final concentration in solution is 25 μ M (1x), 0.25 mM (10x), or 2.5 mM (100x). The samples are vortexed and rotated at 37 °C for 1 hr. After incubation the reaction is quenched with a solution of EDTA such that the final concentration is 0.4 mM (1x), 4 mM (10x), or 40 mM (100x). Samples are again vortexed and then placed on ice.

Enrichment of secretome sialoglycoproteins in conditioned media. Cell pellets are dried by gentle heating (at or lower than 40 °C) and 184 µL of 10% SDS (Sigma-Aldrich) in phosphate buffered saline without calcium or magnesium (PBS) (preheated to 95 °C) is added. An additional 3.5 mL of PBS preheated to 95 °C is added to samples and the samples are heated at 95 °C for 8 min. Samples are then removed from the heat, sealed, and chilled on ice for 5 min. After cooling samples are then transferred to a 15 mL Falcon tube and 8.5 mL of PBS, at RT, is added such that SDS is at a final concentration of 0.5%. Resin (Avidin or Streptavidin UltraLink) is added to the tubes and samples are rotated for 90 min at RT. Samples are then centrifuged at 1400 rpm, RT, for 3 min and supernatant solution is removed. A small fraction of the resin (1.25 - 5%) is removed for analysis by Western blot by suspension in PBS. Samples are centrifuged under identical conditions and supernatant discarded. The resin is transferred to a Micro-BioSpin column (BioRad) on a vacuum manifold using two 500 µL PBS washes, stepwise. Resin is washed on vacuum manifold with various detergents (as specified in table) in aliquots of no more than 1 mL, vigorously pipetted onto samples. Two additional washes each of 200 µL PBS at RT are used to remove bubbles formed on walls of BioSpin column. Once the washes are complete columns are removed from manifold and capped. Each sample is rotated at RT in a solution of 400 µL 6M Urea (Sigma Aldrich) and 20 µL 113 mM tris(2-carboxylethyl)phosphine (Life Technologies). After rotating for 30 min 20 µL of 200mM iodoacetamide (Sigma Aldrich) is added and samples are rotated an additional 30 min at RT in the dark. Samples are uncapped and placed on vacuum manifold where they are washed with 1 mL of PBS (RT) 3 times to remove tris(2-carboxylethyl)phosphine, urea, and iodoacetamide. Resin is transferred to a protein low bind tube (Eppendorf) using two 300 µL PBS washes, stepwise. Samples are spun at 6000 rpm for 3 min at RT in a micro centrifuge and supernatant is removed. A small fraction of the resin (1.25 - 5%) is removed for analysis by western blot by suspension in PBS. Samples are centrifuged under the same conditions and supernatant discarded.

Protein Digestion. On-bead digestion was performed with the digestion solution of 200 µL 2M Urea (Sigma Aldrich), 2 µL 0.1M CaCl₂ (Sigma Aldrich), 4 µL Trypsin (Promega), 4 µL Protease Max (Promega, V5111) is gently mixed by pipette and preheated to 30 C for 5-10 min before being delivered to samples. To prepare the Trypsin, 40 µL of Trypsin buffer (Promega) at 30C is delivered to 20 µg of Trypsin and incubated at 30 C for 15 min. The solution of ProteaseMax is prepared to a concentration of 0.01% in 0.55 mM ammonium bicarbonate (Sigma Aldrich). After digestion, samples are spun at 6000 rpm for 3 min at RT. Supernatant is carefully transferred to a new protein low-bind sample tube. Resin is washed with 100 µL RT PBS and centrifuged for an additional 3 min. Supernatant is added to the protein low-bind tube. A small fraction of the resin (1.25 - 5%) is removed for analysis by western blot by suspension in PBS. 15 µL of formic acid is added to the supernatant (digested sample) and samples are vortexed.

Peptide desalting prior to MS analysis. SPEC C-18 columns (A57203, Agilent Technologies – Santa Clara, CA) are conditioned with 200 µL methanol and three 200 µL washes of 5% acetonitrile and 5% formic acid in ddH₂O under positive pressure applied by syringe. Acidified samples are loaded onto columns in six 200 µL steps by reloading flow-through onto the column. The samples are washed in triplicate with 200 µL of 5% acetonitrile and 5% formic acid in ddH₂O and flow-through is collected in a labeled wash

Chapter 3: Enrichment of sialoglycoproteins from conditioned media

eppendorf. Peptides are eluted from the SPEC C-18 tips using three 100 μ L washes of 80% acetonitrile and 5% formic acid in ddH₂O. Samples are then dried by SpeedVac at 45 °C under vacuum for a duration of 1-3 h.

3.6 References

- 1 Spiciarich, D. R., Nolley, R., Maund, S. L., Purcell, S. C., Herschel, J., Iavarone, A. T., Peehl, D. M. & Bertozzi, C. R. Bioorthogonal Labeling of Human Prostate Cancer Tissue Slice Cultures for Glycoproteomics. *Angewandte Chemie International Edition* **56**, 8992-8997 (2017).
- 2 Klee, E. W. & Sosa, C. P. Computational classification of classically secreted proteins. *Drug Discovery Today* **12**, 234-240 (2007).
- 3 Mukherjee, P. & Mani, S. Methodologies to decipher the cell secretome. *Biochimica et Biophysica Acta* **1834**, 2226-2232 (2013).
- 4 Teixeira, F. G., Panchalingam, K. M., Assuncao-Silva, R., Serra, S. C., Mendes-Pinheiro, B., Patricio, P., Jung, S., Anjo, S. I., Manadas, B., Pinto, L., Sousa, N., Behie, L. A. & Salgado, A. J. Modulation of the Mesenchymal Stem Cell Secretome Using Computer-Controlled Bioreactors: Impact on Neuronal Cell Proliferation, Survival and Differentiation. *Science Reports* **6**, 27791 (2016).
- 5 van Dijk, M., Goransson, S. A. & Stromblad, S. Cell to extracellular matrix interactions and their reciprocal nature in cancer. *Experimental Cell Research* **319**, 1663-1670 (2013).
- 6 Stastna, M. & Van Eyk, J. E. Secreted proteins as a fundamental source for biomarker discovery. *Proteomics* **12**, 722-735 (2012).
- 7 Drake, R. R., Elschenbroich, S., Lopez-Perez, O., Kim, Y., Ignatchenko, V., Ignatchenko, A., Nyalwidhe, J. O., Basu, G., Wilkins, C. E., Gjurich, B., Lance, R. S., Semmes, O. J., Medin, J. A. & Kislinger, T. In-depth proteomic analyses of direct expressed prostatic secretions. *Journal of Proteome Research* **9**, 2109-2116 (2010).
- 8 Anderson, N. L. & Anderson, N. G. The Human Plasma Proteome: History, Character, and Diagnostic Prospects. *Molecular & Cellular Proteomics* **1**, 845 (2002).
- 9 Xue, H., Lu, B. & Lai, M. The cancer secretome: a reservoir of biomarkers. *Journal Translational Medicine* **6**, 52 (2008).
- 10 Sardana, G., Jung, K., Stephan, C. & Diamandis, E. P. Proteomic analysis of conditioned media from the PC3, LNCaP, and 22Rv1 prostate cancer cell lines: discovery and validation of candidate prostate cancer biomarkers. *Journal of Proteome Research* **7**, 3329-3338 (2008).
- 11 Mbeunkui, F., Metge, B. J., Shevde, L. A. & Pannell, L. K. Identification of differentially secreted biomarkers using LC-MS/MS in isogenic cell lines representing a progression of breast cancer. *Journal of Proteome Research* **6**, 2993-3002 (2007).
- 12 Li, X., Jiang, J., Zhao, X., Zhao, Y., Cao, Q., Zhao, Q., Han, H., Wang, J., Yu, Z., Peng, B., Ying, W. & Qian, X. In-depth analysis of secretome and N-glycosylated secretome of human hepatocellular carcinoma metastatic cell lines shed light on metastasis correlated proteins. *Oncotarget* **7**, 22031-22049 (2016).

Chapter 3: Enrichment of sialoglycoproteins from conditioned media

- 13 Song, G., Cui, Y., Zhong, N. & Han, J. Proteomic characterisation of pancreatic islet beta-cells stimulated with pancreatic carcinoma cell conditioned medium. *Journal of Clinical Pathology* **62**, 802-807 (2009).
- 14 Conrads, T. P., Zhou, M., Petricoin, E. F., 3rd, Liotta, L. & Veenstra, T. D. Cancer diagnosis using proteomic patterns. *Expert Review Molecular Design* **3**, 411-420 (2003).
- 15 Veenstra, T. D., Conrads, T. P., Hood, B. L., Avellino, A. M., Ellenbogen, R. G. & Morrison, R. S. Biomarkers: mining the biofluid proteome. *Molecular Cellular Proteomics* **4**, 409-418 (2005).
- 16 Mann, M. & Kelleher, N. L. Precision proteomics: the case for high resolution and high mass accuracy. *Proceedings of the National Academy of Sciences USA* **105**, 18132-18138 (2008).
- 17 Banez, L. L., Srivastava, S. & Moul, J. W. Proteomics in prostate cancer. *Current Opinions in Urology* **15**, 151-156 (2005).
- 18 Palaniappan, K. K. & Bertozzi, C. R. Chemical Glycoproteomics. *Chemical Reviews* **116**, 14277-14306 (2016).
- 19 Everley, P. A., Krijgsveld, J., Zetter, B. R. & Gygi, S. P. Quantitative cancer proteomics: stable isotope labeling with amino acids in cell culture (SILAC) as a tool for prostate cancer research. *Molecular & Cellular Proteomics* **3**, 729-735 (2004).
- 20 Everley, P. A., Bakalarski, C. E., Elias, J. E., Waghorne, C. G., Beausoleil, S. A., Gerber, S. A., Faherty, B. K., Zetter, B. R. & Gygi, S. P. Enhanced analysis of metastatic prostate cancer using stable isotopes and high mass accuracy instrumentation. *Journal of Proteome Research* **5**, 1224-1231 (2006).
- 21 Martin, D. B., Gifford, D. R., Wright, M. E., Keller, A., Yi, E., Goodlett, D. R., Aebersold, R. & Nelson, P. S. Quantitative proteomic analysis of proteins released by neoplastic prostate epithelium. *Cancer Research* **64**, 347-355 (2004).
- 22 Pinho, S. S. & Reis, C. A. Glycosylation in cancer: mechanisms and clinical implications. *Nature Reviews Cancer* **15**, 540-555 (2015).
- 23 Cho-Chung, Y. S. Autoantibody biomarkers in the detection of cancer. *Biochimica et Biophysica Acta* **1762**, 587-591 (2006).
- 24 Scholler, N. & Urban, N. CA125 in ovarian cancer. *Biomark Med* **1**, 513-523 (2007).
- 25 Catalona, W. J., Richie, J. P., Ahmann, F. R., Hudson, M. A., Scardino, P. T., Flanigan, R. C., DeKernion, J. B., Ratliff, T. L., Kavoussi, L. R., Dalkin, B. L., Waters, W. B., MacFarlane, M. T. & Southwick, P. C. Comparison of Digital Rectal Examination and Serum Prostate Specific Antigen in the Early Detection of Prostate Cancer: Results of a Multicenter Clinical Trial of 6,630 Men. *Journal Urology* **197**, S200-S207 (2017).

Chapter 3: Enrichment of sialoglycoproteins from conditioned media

- 26 Piccart, M., Lohrisch, C., Di Leo, A. & Larsimont, D. The predictive value of HER2 in breast cancer. *Oncology* **61 Suppl 2**, 73-82 (2001).
- 27 Munkley, J., Mills, I. G. & Elliott, D. J. The role of glycans in the development and progression of prostate cancer. *Nature Review Urology* **13**, 324-333 (2016).
- 28 Song, E., Hu, Y., Hussein, A., Yu, C. Y., Tang, H. & Mechref, Y. Characterization of the Glycosylation Site of Human PSA Prompted by Missense Mutation using LC-MS/MS. *Journal of Proteome Research* **14**, 2872-2883 (2015).
- 29 Tajiri, M., Ohyama, C. & Wada, Y. Oligosaccharide profiles of the prostate specific antigen in free and complexed forms from the prostate cancer patient serum and in seminal plasma: a glycopeptide approach. *Glycobiology* **18**, 2-8 (2008).
- 30 Tabares, G., Jung, K., Reiche, J., Stephan, C., Lein, M., Peracaula, R., de Llorens, R. & Hoesel, W. Free PSA forms in prostatic tissue and sera of prostate cancer patients: analysis by 2-DE and western blotting of immunopurified samples. *Clinical Biochemistry* **40**, 343-350 (2007).
- 31 Matull, W. R., Andreola, F., Loh, A., Adiguzel, Z., Deheragoda, M., Qureshi, U., Batra, S. K., Swallow, D. M. & Pereira, S. P. MUC4 and MUC5AC are highly specific tumour-associated mucins in biliary tract cancer. *British Journal of Cancer* **98**, 1675-1681 (2008).
- 32 Lugli, A., Zlobec, I., Baker, K., Minoo, P., Tornillo, L., Terracciano, L. & Jass, J. R. Prognostic significance of mucins in colorectal cancer with different DNA mismatch-repair status. *Journal of Clinical Pathology* **60**, 534-539 (2007).
- 33 Roper, S. M., Zemskova, M., Neely, B. A., Martin, A., Gao, P., Jones, E. E., Kraft, A. S. & Drake, R. R. Targeted glycoprotein enrichment and identification in stromal cell secretomes using azido sugar metabolic labeling. *Proteomics Clinical Applications* **7**, 367-371 (2013).
- 34 Maund, S. L., Nolley, R. & Peehl, D. M. Optimization and comprehensive characterization of a faithful tissue culture model of the benign and malignant human prostate. *Laboratory Investigation*, 1-14 (2013).
- 35 de Graaf, I. A. M., Olinga, P., de Jager, M. H., Merema, M. T., de Kanter, R., van de Kerkhof, E. G. & Groothuis, G. M. M. Preparation and incubation of precision-cut liver and intestinal slices for application in drug metabolism and toxicity studies. *Nature Protocols* **5**, 1540-1551 (2010).
- 36 Kiviharju-af Hallstrom, T. M., Jaamaa, S., Monkkonen, M., Peltonen, K., Andersson, L. C., Medema, R. H., Peehl, D. M. & Laiho, M. Human prostate epithelium lacks Wee1A-mediated DNA damage-induced checkpoint enforcement. *Proceedings of the National Academy of Sciences USA* **104**, 7211-7216 (2007).
- 37 Saxon, E. Cell Surface Engineering by a Modified Staudinger Reaction. *Science* **287**, 2007-2010 (2000).

Chapter 3: Enrichment of sialoglycoproteins from conditioned media

- 38 Debets, M. F., van Hest, J. C. & Rutjes, F. P. Bioorthogonal Labelling of Biomolecules: New Functional Handles and Ligation Methods. *Organic and Biomolecular Chemistry* **11**, 6439 (2013).
- 39 Rostovtsev, V. V., Green, L. G., Fokin, V. V. & Sharpless, K. B. A Stepwise Huisgen Cycloaddition Process: Copper(I)-Catalyzed Regioselective "Ligation" of Azides and Terminal Alkynes. *Angewandte Chemie International Edition* **41**, 2596 (2002).
- 40 Hackenberger, C. P. R. & Schwarzer, D. Chemoselective ligation and modification strategies for peptides and proteins. *Angewandte Chemie International Edition* **47**, 10030-10074 (2008).
- 41 Serwa, R., Wilkening, I., Del Signore, G., Muhlberg, M., Clausnitzer, I., Weise, C., Gerrits, M. & Hackenberger, C. P. Chemoselective Staudinger-phosphite reaction of azides for the phosphorylation of proteins. *Angewandte Chemie International Edition* **48**, 8234-8239 (2009).
- 42 van Geel, R., Pruijn, G. J., van Delft, F. L. & Boelens, W. C. Preventing thiol-yne addition improves the specificity of strain-promoted azide-alkyne cycloaddition. *Bioconjugation Chemistry* **23**, 392-398 (2012).
- 43 Vaira, V., Fedele, G., Pyne, S., Fasoli, E., Zadra, G., Bailey, D., Snyder, E., Favarsani, A., Coggi, G., Flavin, R., Bosari, S. & Loda, M. Preclinical model of organotypic culture for pharmacodynamic profiling of human tumors. *Proceedings of the National Academy of Sciences USA* **107**, 8352-8356 (2010).
- 44 Peehl, D. M. *Culture of Epithelial Cells* 171-194 (John Wiley & Sons, Inc., 2002).
- 45 Laughlin, S. T. & Bertozzi, C. R. Metabolic labeling of glycans with azido sugars and subsequent glycan-profiling and visualization via Staudinger ligation. *Nature Protocols* **2**, 2930-2944 (2007).
- 46 Lundgren, D. H., Hwang, S. I., Wu, L. & Han, D. K. Role of spectral counting in quantitative proteomics. *Expert Rev Proteomics* **7**, 39-53 (2010).
- 47 Filella, X. & Foj, L. Prostate Cancer Detection and Prognosis: From Prostate Specific Antigen (PSA) to Exosomal Biomarkers. *International Journal Molecular Science* **17** (2016).
- 48 Stamey, T. A., Caldwell, M., McNeal, J. E., Nolley, R., Hemenez, M. & Downs, J. The prostate specific antigen era in the United States is over for prostate cancer: what happened in the last 20 years? *Journal of Urology* **172**, 1297-1301 (2004).
- 49 Canby-Hagino, E., Hernandez, J., Brand, T. C. & Thompson, I. Looking back at PCPT: looking forward to new paradigms in prostate cancer screening and prevention. *European Urology* **51**, 27-33 (2007).
- 50 Woo, C. M., Felix, A., Byrd, W. E., Zuegel, D. K., Ishihara, M., Azadi, P., Iavarone, A. T., Pitteri, S. J. & Bertozzi, C. R. Development of IsoTaG, a Chemical

Chapter 3: Enrichment of sialoglycoproteins from conditioned media

Glycoproteomics Technique for Profiling Intact N- and O-Glycopeptides from Whole Cell Proteomes. *Journal of Proteome Research* **16**, 1706-1718 (2017).

51 Lawlor, K., Nazarian, A., Lacomis, L., Tempst, P. & Villanueva, J. Pathway-based biomarker search by high-throughput proteomics profiling of secretomes. *Journal of Proteome Research* **8**, 1489-1503 (2009).

52 Gromov, P., Gromova, I., Bunkenborg, J., Cabezon, T., Moreira, J. M., Timmermans-Wielenga, V., Roepstorff, P., Rank, F. & Celis, J. E. Up-regulated proteins in the fluid bathing the tumour cell microenvironment as potential serological markers for early detection of cancer of the breast. *Molecular Oncology* **4**, 65-89 (2010).

53 Wu, C. C., Hsu, C. W., Chen, C. D., Yu, C. J., Chang, K. P., Tai, D. I., Liu, H. P., Su, W. H., Chang, Y. S. & Yu, J. S. Candidate serological biomarkers for cancer identified from the secretomes of 23 cancer cell lines and the human protein atlas. *Molecular & Cellular Proteomics* **9**, 1100-1117 (2010).

54 Azmi, A. S., Bao, B. & Sarkar, F. H. Exosomes in cancer development, metastasis, and drug resistance: a comprehensive review. *Cancer Metastasis Reviews* **32**, 623-642 (2013).

A novel germline variant in CSF3R reveals a N-glycosylation site that is important in receptor regulation

Julia Maxson, Stephen T. Oh, Amy Foley, Michael J. Mauro, and, Rosa Viner, contributed to the work presented in this chapter. Portions of the work described in this chapter have been compiled in a manuscript that is in preparation.

4.1 Introduction

Mutations in the CSF3 granulocyte colony-stimulating factor 3 receptor (CSF3R), also known as G-CSFR, occur in the majority of patients with chronic neutrophilic leukemia (CNL)¹ and also are rarely found in acute myeloid leukemia (AML).^{2,3} Truncation mutations that lead to a premature stop in the cytoplasmic domain are also found in CNL¹ and result in increased expression of CSF3R on the cell surface.⁴ However, the most common CSF3R mutation in CNL is T618I a point mutation in the membrane-proximal extracellular domain that causes ligand independence.⁵ T618I also known as T595I using the historical numbering system, which doesn't include the 23 amino acid signal peptide. Recently, CSF3R T618I mutation became a part of the world health organization (WHO) criteria for diagnosis of CNL.⁶

Although CSF3R T618I is the most common mutation in CNL, there are other rarer variants that also cause profound receptor activation. For example, a rare mutation seen in the membrane proximal domain, T615A (also known as T592A), also causes ligand-independent activation of the receptor.¹ In the transmembrane domain, a point mutation at T640N (also known as T617N), was reported in a family with congenital neutrophilia and in a few patients with CNL.^{7,8} This mutation, is predicted to cause intramolecular hydrogen-bonding, thus driving dimerization.⁷ Furthermore, biochemical studies showed that there is increased ligand-independent receptor dimerization in the presence of this mutation.⁸ While this understanding has greatly improved our ability to diagnosis and treat the disease, there are rare variants for which their significance is not clear.

In this study we identified a patient with a rare germline CSF3R N610H mutation. This patient has a condition most consistent with primary myelofibrosis with mild leukocytosis. Given its proximity to other oncogenic CSF3R point mutations found in CNL we were interested in understanding whether the N610H mutation might contribute to disease biology.

Previously we reported that the most common CNL mutation in CSF3R, T618I, is glycosylated with mucin-type O-glycosylation.⁹ There is a substantive body of literature that correlates changes in glycosylation with cancer progression.^{10,11} The Asn residue at 610 is part of an N-linked glycosylation consensus motif N-X-(S/T), where X denotes a

Chapter 4: A novel germline variant in CSF3R reveals a N-glycosylation site that is important in receptor regulation

non-proline residue consensus motif for N-linked glycosylation.¹² N-glycans are typically destined for exposure to the extracellular space where they contribute to folding, trafficking, and thermodynamic stability of proteins.¹³ We employed mass spectrometry (MS) analysis to confirm the occupancy the glycosylation. We determined that N610 is occupied with a sialylated bisecting complex N-glycan. We further found that the N610H mutation and a more conservative N610Q substitution are highly activating in CSF3R, leading to cytokine-independent growth in the murine Ba/F3 cell line. Like the T618I mutation, these mutations render the receptor ligand-independent. N610H and N610Q lead to a robust increase in downstream signaling through the JAK/STAT pathway as demonstrated by an increase in the levels of phospho-STAT3. The loss of N-glycosylation in the membrane-proximal region of CSF3R may therefore increase ligand-independent receptor activation and promote oncogenesis. This study highlights the insight that rare human mutations can provide into the relationship between receptor structure and function.

4.2 Results

The CSF3R N610H mutation was identified in a patient with a myeloproliferative neoplasm through sequencing on the GeneTrails AML/MDS Gene Panel, which encompasses selected exons or entire coding regions for 42 genes with biological importance in myeloid malignancies. This sequencing of the patient's bone marrow using an Ion Torrent PGM platform revealed a mutation at N610H in CSF3R at a 50% mutant allele frequency. This myeloproliferative neoplasm was most consistent with a JAK2, CALR, MPL mutation-negative primary myelofibrosis. This patient had a history of mild leukocytosis for several years with most recent white blood cell counts between 13.3 and 15.3 x 10³/μL. A bone marrow biopsy revealed 90% cellularity with a mild increase in reticulin fibrosis, increased myeloid to erythroid ratio, no overt dysplasia, and less than 5% blasts. The cells were karyotypically normal with a micro deletion of the 3' end of PDGFRB (5q) identified by FISH at 59%.

The patient has had minimal symptoms with no anemia or thrombocytopenia and is currently being monitored but not receiving any intervention. The 50% allele fraction of the N610H mutation prompted us to determine whether the mutation was germline or somatic. Sanger sequencing confirmed the presence of a heterozygous N610H mutation in a sample of blood as well as in a skin biopsy (**Figure 4-1A**). This data confirms the presence of a novel CSF3R N610H germline mutation in this patient with an unusual myeloproliferative neoplasm.

Chapter 4: A novel germline variant in CSF3R reveals a N-glycosylation site that is important in receptor regulation

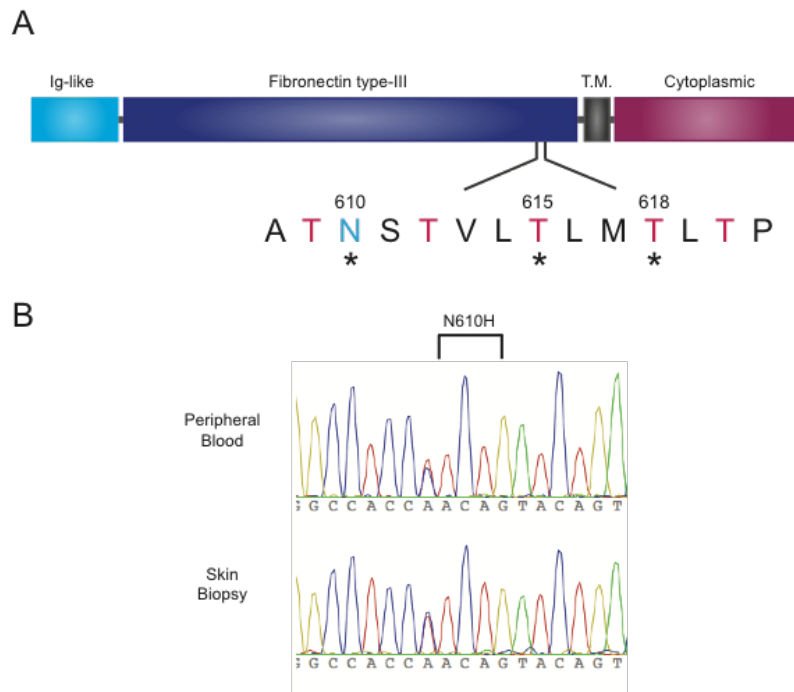


Figure 4-1. A novel germline mutation in CSF3R. (A) Schematic of the membrane-proximal location of the N610H mutation and nearby leukemia-associated CSF3R T615A and T618I mutations. (B) Sanger sequencing of CSF3R exon 14 confirms the presence of the CSF3R N610H mutation in both the peripheral blood and skin biopsy from a patient with a myeloproliferative neoplasm.

Given its proximity to the most common CSF3R mutation found in Chronic Neutrophilic Leukemia (T618I, aka T595I), we were interested in understanding whether the N610H mutation might contribute to disease biology (**Figure 4-1B**). To test the oncogenic capacity of this novel mutation we used a cytokine-independent growth assay. In this assay the murine pro-B cell line, Ba/F3, was transduced with a retrovirus expressing the WT or mutant CSF3R using a vector containing an IRES-GFP. GFP positive cells expressing the gene of interest are then sorted, allowed to recover, then washed to remove cytokine support and further cultured in the absence of exogenous cytokines. Native Ba/F3 cells and those expressing WT CSF3R are dependent on cytokines for growth, and die when they are removed. We found that the N610H mutation, which results in a positive charge, and a more conservative N610Q substitution are highly activating in CSF3R, leading to cytokine-independent growth in the murine Ba/F3 cell line (**Figure 4-2a**).

Glutamine (Q) was chosen because it is structurally similar asparagine (N) and is also uncharged. The CSF3R T618I mutation, which is commonly found in CNL, confers ligand-independent receptor activation. To test whether the N610H mutation also conferred cytokine-independent growth we grew Ba/F3 cells transduced with WT or mutant forms of CSF3R in decreasing concentrations of GCSF, the ligand for CSF3R. Like the T618I mutant, both the N610H and N610S mutations exhibit ligand independence, while WT CSF3R has a dose dependent decrease in cell viability with decreasing concentrations of GCSF (**Figure 4-2-b**).

Chapter 4: A novel germline variant in CSF3R reveals a N-glycosylation site that is important in receptor regulation

One feature of the CSF3R T618I mutation is robust activation of the JAK/STAT pathway. Here we assessed the ability of the CSF3R N610H and N610Q mutations to activate this pathway using phosphorylated STAT3 as a marker. Both of these mutations lead to robust phosphorylation of STAT3 above and beyond the increase in signaling with WT CSF3R (**Figure 4-2c**).

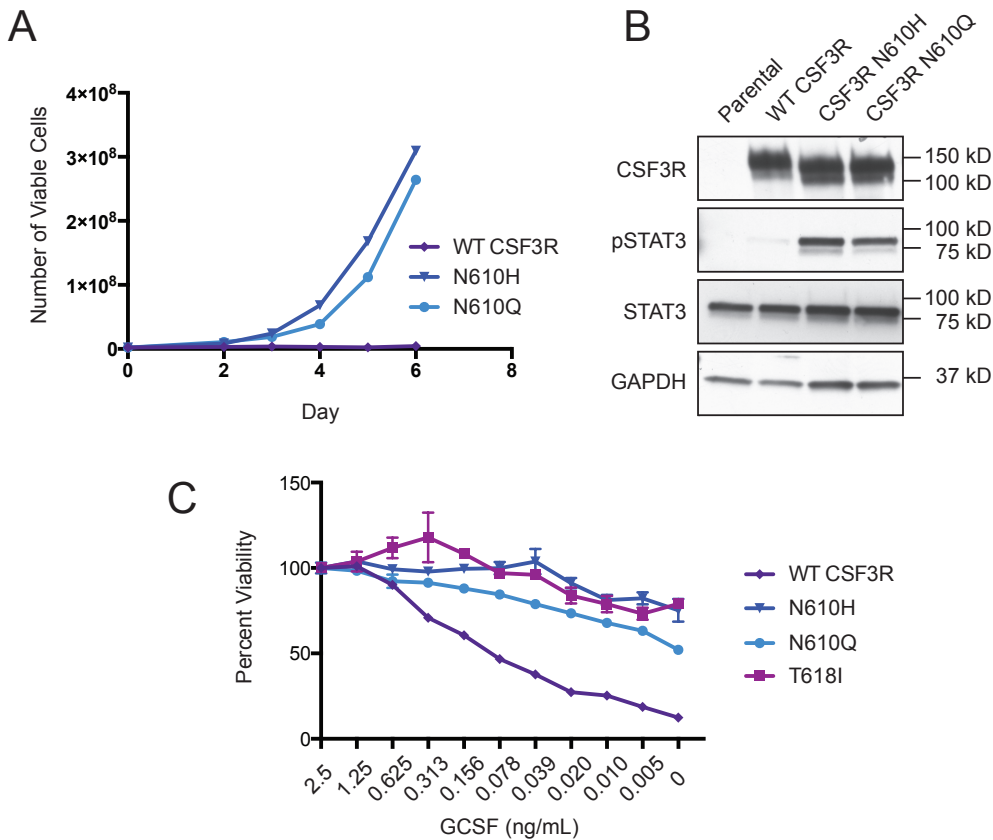


Figure 4-2. The CSF3R N610H mutation is transforming and activates the JAK-STAT pathway in a ligand-independent manner. (A) Transforming capacity of the CSF3R N610H (and a conservative N610Q) mutations in the murine Ba/F3 cytokine-independent growth assays. (B) The CSF3R N610H mutation activates the JAK/STAT pathway as measured by immunoblotting of phosphorylated-STAT3 (pSTAT3) in 293T17 cells transiently transfected with WT or CSF3R mutants. T.M. transmembrane domain, N610H (the CSF3R N610H mutation), N610Q (CSF3R N610Q mutation, a conservative substitution) and T618I (the CSF3R T618I mutation found commonly in CNL). (C) The CSF3R N610H mutation confers ligand-independence to the receptor as measured by a titration of GCSF in Ba/F3 cells expressing WT CSF3R, and the CSF3R N610H, N610Q and T618I mutations. Cell lines were plated in decreasing concentrations of GCSF and then cell viability was measured after 72 hours using a tetrazolamine based assay (CellTiter Aqueous one solution cell proliferation MTS assay).

We previously reported that CSF3R T618 site is O-glycosylated, a loss of glycosylation accompanies ligand independence and neutrophil proliferation.⁹ Interestingly, N610 is part of an N-X-T motif, which is a consensus sequence for N-linked glycosylation. Hanju

Chapter 4: A novel germline variant in CSF3R reveals a N-glycosylation site that is important in receptor regulation

et al demonstrated that N610 is one of 8 sites that results in a lower molecular weight gel shift when treated with a cocktail of deglycosylation enzymes, indicating that it is likely a site of N-glycosylation.¹⁴ We were interested in confirming the glycosite occupancy and identifying the glycan structure at N610. We began by performing free glycan analysis of. In brief, this was achieved by digesting WT CSF3R-purified proteins with trypsin, and N-glycans were released enzymatically from the crude mixture by PNGase F. Released N-glycans were permethylated with methyl iodide and analyzed by MS (**Figure 4-3a**). Interestingly, we observed complex, biantennary as well as high mannose glycan structures (**Figure 4-3b**). We confirmed the connectivity of these glycan structures with electrospray ionization mass spectrometry (ESI-MS). Although this analysis allows for accurate structure assignment, it does not allow for determination of the N-linked glycosite on CSF3R which we were particularly interested in (complete list of glycan ratios for CSF3R WT compiled in **Table 4-2**).

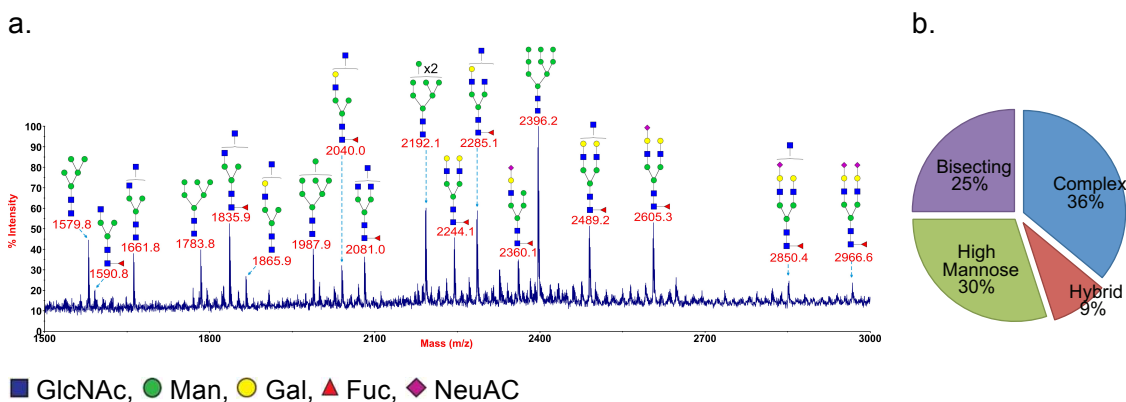


Figure 4-3. Annotated MALDI-TOF MS spectra of permethylated N-glycans from CSF3R WT. (a) Released permethylated N-glycan analysis by MALDI (m/z 1500-3000). Glycan structures identified were confirmed by electrospray ionization mass spectrometry (ESI-MS/MS). Putative structures are based on the molecular weight and N-glycan biosynthesis pathway. (b) The ratio indicates a comparison of the glycan relative abundance to those identified.

Free glycan analysis revealed several glycan structures on native CSF3R with sialic acid, also known as N-Acetylneuraminic acid (Neu5Ac). Aberrant expression of sialic acid on proteins has been observed in many types of cancer,¹⁵ to confirm that WT CSF3R is indeed sialylated at N610, we performed a metabolic glycosylation assay. As previously described, sialoglycoproteins are specifically targeted by metabolically labeling cells with a modified peracetylated *N*-acetylmannosamine (Ac₄ManNAc) analog such as peracetylated *N*-azidoacetylmannosamine (Ac₄ManNAz, **1**) that incorporates into sialic acid glycoproteins.¹⁶ The azide-modified sugar passively diffuses through the cell and is converted by the Roseman-Warren pathway into the corresponding azidosialic acid,¹⁷ which allows for the site-specific labeling with a cyclooctyne reagent dibenzoazacyclooctyne (DIBAC) conjugated to biotin. HEK 293T cells were transfected with WT, N610H or T618I FLAG-tagged constructs and incubated with 50 μ M Ac₄ManNAz or DMSO, as a control. The FLAG-tagged constructs were then immunoprecipitated from whole cell lysates and biotin-labeled. Western blot analysis revealed robust labeling of WT CSF3R and T618I, whereas we did not observe labeling

Chapter 4: A novel germline variant in CSF3R reveals a N-glycosylation site that is important in receptor regulation

in the N610H mutant, suggesting that N610 is the only site of sialylation in CSF3R (**Figure 4-4a**).

To confirm the glycan structure at the N610 site, we performed a glycoproteomic experiment on digested purified protein. Although tryptic digestion was performed, we were not able to observe the resulting peptide as the asparagine site sits in a rather large 71 amino acid residue peptide. Peptides of this size are challenging to analyze by mass-spectrometry based methods. However, chymotrypsin, which cleaves on the N-terminal side of hydrophobic amino acid (tyrosine, tryptophan, and phenylalanine/leucine and also leucine residues) proved successful. FLAG-purified WT and N610H constructs allowed us to identify, *in vitro*, several sites of N-glycosylation with both complex and bisecting glycan structures (**Figure 4-4 c,d**). We observed HexNAc oxonium ions *m/z* at 138, 168, 186 and 204, Neu5Ac oxonium ions at 274 and 292 and the intensity of HexHexNAc oxonium ion at 366. Here we report to sialylated glycan structures we observed at N-610. As with T618I, the loss of glycosylation in the membrane-proximal region of CSF3R may therefore increase ligand-independent receptor activation and promote oncogenesis.

Besides identifying changes in glycosylation, we were also interested in looking protein changes between our these constructs. Several methods for quantifying protein changes by mass spectrometry have been developed. While each have their advantages, SILAC (stable isotope labeling by amino acids in cell culture) remains a robust and commercial choice to analyze simultaneously multiple samples in different conditions.¹⁸ Proteins from samples differentially labeled after metabolic incorporation of isotopic amino acids are pooled before further sample processing, minimizing bias due to handling, and thus increases reproducibility over chemical labeling or label-free quantification approaches.¹⁹ 293T cells were incubated with either light or heavy media containing arginine and lysine, either with normal isotopes of carbon and nitrogen (i.e. ¹²C¹⁴N, light) or L-arginine-¹³C₆-¹⁵N₄ and L-lysine-¹³C₆-¹⁵N₂ (heavy) (**Figure 4-5**).

Cells were then transformed with WT, N610 or T618I CSF3R constructs, enriched and digested with recombinant Lys-C. After desalting, samples were separated by high-pH separation and analyzed on a nano-electrospray ionization in-line with a high resolution mass spectrometer. (nESI-MS-MS). Data compiled in (**Table 4-1**) and reveals proteins that may be upregulated in CSF3R N610 compared to WT. As the pathway for CSF3R remains unknown, this analysis could help elucidate the drivers of neutrophil production.

Subsequent to these initial studies, a CSF3R N610S mutation was detected in a patient with chronic phase CML. This patient was in deep molecular remission after therapy with nilotinib, with minimally evident (>4 log reduction from untreated International Standard baseline) or undetectable BCR/ABL sequentially, who developed increasing thrombocytosis; evaluation for typical myeloproliferative drivers was unrevealing and bone marrow pathology noted mild myeloid hyperplasia and megakaryocytic MPN-like changes (clustering, increased nuclear-cytoplasmic ratio). In this context the patient had previously had a DNMT3A mutation (R882H), and in a subsequent biopsy there was the emergence of a clone harboring the CSF3R N610S mutation (**Figure 4-6a**).

Chapter 4: A novel germline variant in CSF3R reveals a N-glycosylation site that is important in receptor regulation

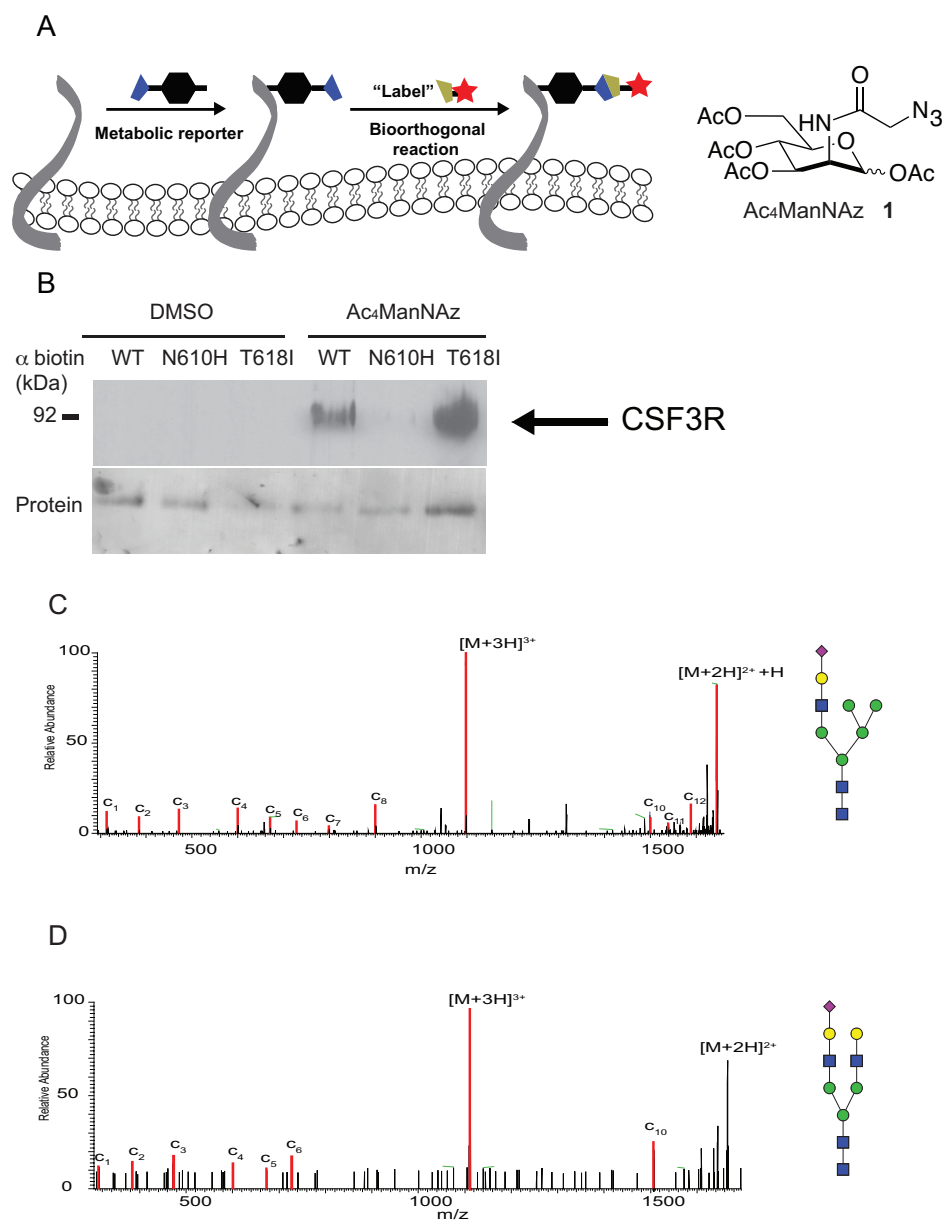


Figure 4-4. Identification of sialic acid glycosylation on N610. (A) Schematic of labeling of sialic acid glycoproteins with an azide-functionalized sugar. (B) Wild-type, N610H or T618I CSF3R were transfected in 293T cells and then incubated with either Ac₄ManNAz, **1** or DMSO, as a control. After incubation, cells were lysed and reacted with a DIBCAC-functionalized biotin probe. Sialoglycoproteins (biotinylated) were immunoprecipitated using an avidin resin and visualized with an HRP-conjugated anti-FLAG. Equal avidin resin was loaded. (c,d) The MS/MS spectra of electron transfer dissociation (ETD) fragmented N610 peptide “AASQAGATNSTVL”. (c) The most intense peak corresponds to the peptide with a HexNAc₃Hexose₆NeuAc. (d) Spectrum corresponds to glycan structure HexNAc₃Hexose₆NeuAc. The illustrated glycans depict possible structures for each glycan composition HexNAc₃Hexose₆NeuAc. The illustrated glycans depict possible structures for each glycan composition HexNAc₃Hexose₆NeuAc. The illustrated glycans depict possible structures for each glycan composition HexNAc₃Hexose₆NeuAc. Glycoworkbench²⁰ was used for creating the glycan structure figures. Galactose; green circle; mannose; white circle: Hexose; purple diamond: N-Acetylneuraminic acid (Neu5Ac).

Chapter 4: A novel germline variant in CSF3R reveals a N-glycosylation site that is important in receptor regulation

At this time point the DNMT3A R882H mutation (c. 2645 G>A) was found at a VAF of 6.4% and the CSF3R N610H mutation (c. 1829 A>G) mutations was at 53%. To test whether the serine substitution was also transforming at the 610 position we ran a cytokine independent growth assay as described above. In this assay, the N610S mutation was robustly transforming, and allowed for a similar growth capacity as the N610H and T618I mutations in CSF3R (**Figure 4-6b**). Finally to confirm the transforming potential of this mutation and assess ligand independence we performed a mouse bone marrow colony assay (**Figure 4-6c**). In this assay primary mouse bone marrow is transduced with a retroviral vector expressing WT or mutant CSF3R or an empty vector control (mig empty). The cells are then plated in methylcellulose without any added cytokine support. In this assay WT CSF3R produces very few colonies but the CSF3R T618I mutant, which is able to signal in the absence of ligand produces abundant colonies. Both the CSF3R N610H and N610S were able to induce colony formation at a similar levels at T618I, indicating that they are robustly oncogenic.

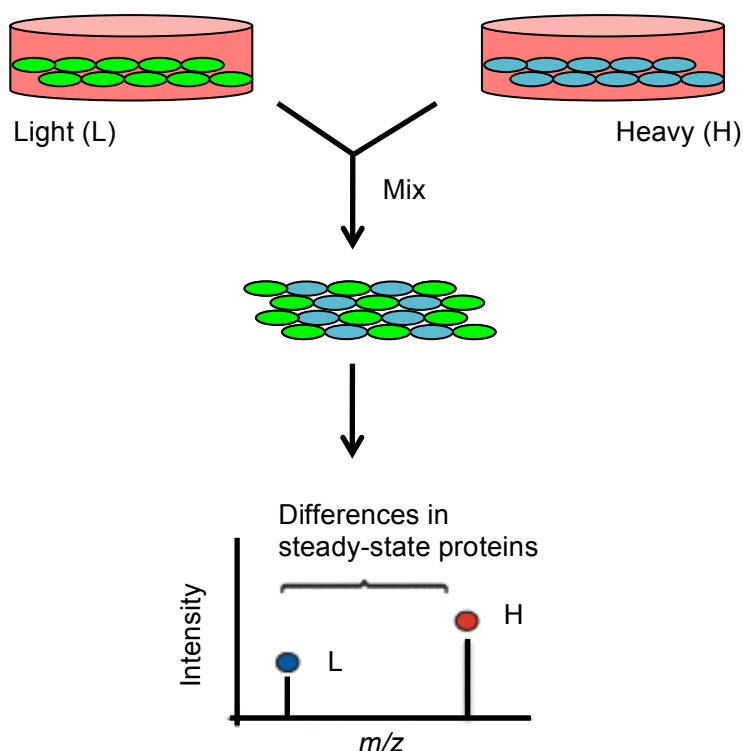


Figure 4-5. General scheme for stable isotope labeling by amino acids in cell culture (SILAC) analysis of cellular proteome dynamics. Typical SILAC labeling uses lysine and arginine, which in combination with trypsin digestion results in labeling of every peptide in the mixture (except for the c-terminal peptide of the protein). SILAC experiments involve differential labeling of two to three cell types: cells grown with the natural amino acids, with $^2\text{H}_4$ -lysine and $^{13}\text{C}_6$ -arginine and with $^{15}\text{N}_2$ $^{13}\text{C}_6$ -lysine and $^{15}\text{N}_4$ $^{13}\text{C}_6$ -arginine. The SILAC method relies on the complete incorporation of heavy amino acids during protein turnover.

We previously identified the JAK kinase inhibitor, ruxolitinib, as a potential therapeutic strategy for patients with CSF3R mutations. Additionally, a recent study identified the MEK inhibitor, trametinib, as being efficacious in a mouse bone marrow transplant model

Chapter 4: A novel germline variant in CSF3R reveals a N-glycosylation site that is important in receptor regulation

of the CSF3R T618I mutation. We tested the ability of both ruxolitinib and trametinib to inhibit the viability of Ba/F3 cells expressing the CSF3R N610H and N610S mutations and found them to be sensitive to both compounds to a similar or greater extent than for the CSF3R T618I mutation. Taken together the similar properties of N610 and T618 substitutions along with similar drug sensitivity, indicate that the CSF3R N610H and N610S variants are rare but clinically targetable mutations. Of note, the WT CSF3R and Mig empty vector control cells are grown in medium containing IL3 for the drug studies (as they would die in its absence), which is known to exert its pro-survival effects on Ba/F3 cells through the JAK/STAT pathway. And thus the growth inhibition of these cells by ruxolitinib is an on-target effect.

Table 4-1. Proteins identified with greater than 2-fold increase in N610 CSF3R compared to WT in SILAC-based proteomics. Accession number (Accn#), gene name, protein name and subcellular localization determined in Uniprot, Fold change determined through SILAC ratio. N610 CSF3R grown in “heavy” media containing $^{15}\text{N}_2^{13}\text{C}_6$ -lysine and WT grown in “light” media containing natural abundant amino acids. Fractions were combined, digested with LysC and further separated by pH chromatography before MS-MS and analysis with MaxQuant software suite.

Accn #	Gene names	Protein names	Subcellular location	Fold
P63151	PPP2R2A	Serine/threonine-protein phosphatase 2A		20.3
Q01081	U2AF1	Splicing factor U2AF 35 kDa subunit	Nucleus	12.9
P50552	VASP	Vasodilator-stimulated phosphoprotein	Cytoplasm	14.1
Q9Y6Y8	SEC23IP	SEC23-interacting protein	Cytoplasmic vesicle	11.4
Q13084	MRPL28	39S ribosomal protein L28, mitochondrial	Mitochondrion	10.4
P61006	RAB8A	Ras-related protein Rab-8A	Cell membrane	10.0
Q9BSH4	TACO1	Translational activator of cytochrome c oxidase 1	Mitochondrion	9.7
Q9Y570	PPME1	Protein phosphatase methylesterase 1		9.4
Q7KZ85	SUPT6H	Transcription elongation factor SPT6	Nucleus	8.8
P52306	RAP1GDS1	Rap1 GTPase-GDP dissociation stimulator 1		8.7
P63267	ACTG2	Actin, gamma-enteric smooth muscle	Cytoplasm	8.5
P40616	ARL1	ADP-ribosylation factor-like protein 1	Golgi apparatus membrane	8.5
Q12996	CSTF3	Cleavage stimulation factor subunit 3	Nucleus	7.9
P21283	ATP6V1C1	V-type proton ATPase subunit C 1		7.7
Q9P210	CPSF2	Cleavage and polyadenylation factor subunit 2	Nucleus	7.2
P19525	EIF2AK2	Interferon-induced, double-stranded RNA-activated protein kinase	Cytoplasm, Nucleus	7.2
P13861	PRKAR2A	cAMP-dependent protein kinase type II-alpha	Cytoplasm	6.8
P38606	VPP2	V-type proton ATPase catalytic subunit A		6.4
Q15056	WSC1	Eukaryotic translation initiation factor 4H	Cytoplasm, perinuclear region	6.3
Q8N684	CPSF7	Cleavage and polyadenylation specificity factor subunit 7	Nucleus	6.1

Chapter 4: A novel germline variant in CSF3R reveals a N-glycosylation site that is important in receptor regulation

Accn #	Gene names	Protein names	Subcellular location	Fold
Q5VYK3	ECM29	Proteasome-associated protein ECM29 homolog	Endoplasmic reticulum.	5.7
Q5H9R7	SAPS3	Serine/threonine-protein phosphatase 6 regulatory subunit 3	Cytoplasm, Nucleus	5.5
Q9NUJ1	ABHD10	Mycophenolic acid acyl-glucuronide esterase	Mitochondrion	5.2
O00629	QIP1	Importin subunit alpha-3	Cytoplasm	5.1
P20810	CAST	Calpastatin		4.8
Q9BTT0	ANP32E	Acidic leucine-rich nuclear phosphoprotein	Cytoplasm	4.8
Q14181	POLA2	DNA polymerase alpha subunit B	Nucleus	4.8
P52701	GTBP	DNA mismatch repair protein Msh6	Nucleus	4.4
P50851	LRBA	Lipopolysaccharide-responsive like anchor protein	Cell membrane	4.0
P49770	EIF2B2	Translation initiation factor eIF-2B subunit beta		3.9
O94874	RCAD	E3 UFM1-protein ligase 1	Endoplasmic reticulum Late endosome membrane	3.9
O43633	CHMP2	Charged multivesicular body protein 2a		3.8
O60739	EIF1B	Eukaryotic translation initiation factor 1b		3.7
O00232	PSMD12	26S proteasome non-ATPase subunit		3.7
P60983	GMFB	Glia maturation factor beta		3.6
Q99538	LGMN	Legumain	Lysosome	3.6
O75937	DNAJC8	DnaJ homolog subfamily C member 8	Nucleus	3.4
Q6UX04	CWC2	Peptidyl-prolyl cis-trans isomerase CWC27 homolog		3.4
Q9Y4Y9	LSM5	U6 snRNA-associated Sm-like protein LSm5	Nucleus	3.3
P49643	PRIM2	DNA primase large subunit		3.1
Q9UKM9	RALY	RNA-binding protein Raly	Nucleus	3.0
P36957	DLST	Dihydrolipoyllysine-residue succinyltransferase	Mitochondrion	2.9
P47755	CAPZA2	F-actin-capping protein subunit alpha-2		2.9
P52294	KPNA1	Importin subunit alpha-5	Cytoplasm Endoplasmic reticulum lumen	2.9
Q15293	RCN1	Reticulocalbin-1		2.9
P30085	CMPK1	UMP-CMP kinase	Nucleus	2.6
Q14203	DCTN1	Dynactin subunit 1	Cytoplasm Golgi apparatus membrane	2.6
P36405	ARL3	ADP-ribosylation factor-like protein 3		2.4
Q04760	GLO1	Lactoylglutathione lyase		2.3
P35241	RDX	Radixin	Cell membrane	2.3
P28161	GSTM2	Glutathione S-transferase Mu 2	Cytoplasm.	2.2
Q16222	UAP1	UDP-N-acetylhexosamine pyrophosphorylase	Cytoplasm.	2.2
Q96G03	PGM2	Phosphoglucomutase-2	Cytoplasm.	2.2
P54136	RARS	Arginine--tRNA ligase	Cytoplasm.	2.2
P21912	SDHB	Succinate dehydrogenase	Mitochondrion inner membrane	2.1

Chapter 4: A novel germline variant in CSF3R reveals a N-glycosylation site that is important in receptor regulation

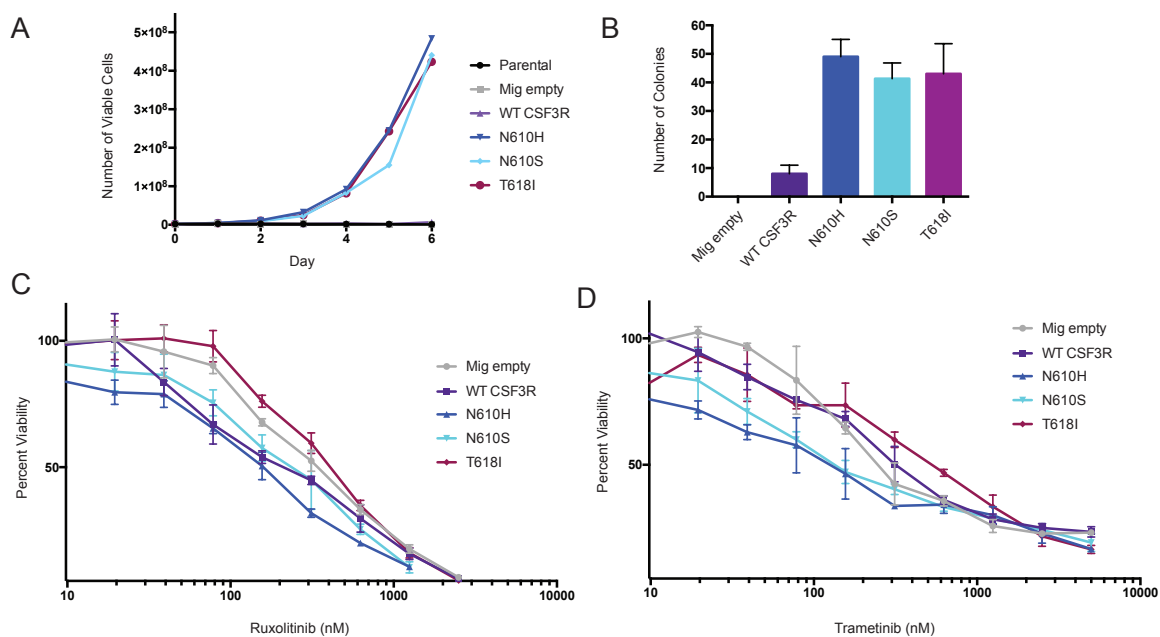


Figure 4-6. A somatic N610S mutation identified in a patient with CNL is transforming and therapeutically targetable. **(A)** The CSF3R N610S mutation is transforming in the Ba/F3 cytokine independent growth assay. **(B)** The CSF3R N610H and N610S mutations confer cytokine-independent growth in a mouse bone marrow colony assay. **(C)** Sensitivity of CSF3R expressing Ba/F3 cells to the JAK kinase inhibitor ruxolitinib. Ba/F3 cells were grown in the presence (Mig empty and WT CSF3R) and absence (N610H, N610S and T618I) of the cytokine, IL3 in 96 well format. Cell lines were plated in triplicate and were treated with a dose curve of ruxolitinib. After 72 hours cell viability/proliferation was measured using a tetrazolium based CellTiter Aqueous One Solution and read on a plate reader. Viability is represented as a percentage of the untreated control. **(D)** Sensitivity of cells expressing CSF3R mutants to the MEK inhibitor trametinib as outlined in panel. **(C)** Parental (untransformed cells), Mig empty (empty vector control), N610H (the CSF3R N610H mutation), N610S (the CSF3R N610S mutation) and T618I (the CSF3R T618I mutation).

4.3 Discussion

The main classes of CSF3R mutations are membrane proximal point mutations, e.g. T618I and T615A and the truncation mutations in the cytoplasmic domain, e.g. Q741 and S783fs, and are generally thought to be somatic mutations that are transforming in CNL patients. We were therefore surprised to identify a germline N610H mutation in CSF3R in a patient with unusual myelofibrosis. This mutation has not previously been described and warranted further mechanistic exploration. We subsequently identified another patient with a different substitution at this same site, N610S. This patient had previously had BCR/ABL positive CML, and then in relapse with a greatly reduced BCR/ABL burden, a DNMT3A mutation with apparent transformation to CNL. It is essential to understand whether this mutational event in CSF3R is oncogenic and have prognostic or therapeutic relevance. The N610H, N610Q and N610S mutations are highly transformative in both cell line studies (**Figure 4-2**) and in primary murine bone marrow (**Figure 4-6**). The germline nature of the N610H mutation and also familial

Chapter 4: A novel germline variant in CSF3R reveals a N-glycosylation site that is important in receptor regulation

germline T640N mutations identified in a family with neutrophilia⁷ suggest that additional mutations are likely to be necessary to drive the full clinical phenotype of CNL. Additional mutations in SETBP1, TET2 and other genes may contribute to the pathobiology of CNL.⁷

In previous studies it was noted that wild-type CSF3R treated with N-glycosidases results in a 17kDA band shift, indicating glycosylation is a significant portion of the protein.¹⁴ The N610 site sits in an N-linked glycosylation consensus sequence which had previously been proposed but whose structure was not known. Using mass spectrometry-based glycoproteomics, we describe the glycan heterogeneity at the N610 site (**Figure 4-4**). As with T618I, the loss of glycosylation in the membrane-proximal region of CSF3R may therefore increase ligand-independent receptor activation, promoting oncogenesis. Although, it is known that there can be an interplay between neighboring and nearby sites of phosphorylation²¹ but this has not been described for proximal N and O linked glycosylation sites. Interestingly, mass-spectrometry analysis of the CSF3R T618I mutant protein showed that the N610 site was still occupied in that at least one of the glycan structures was the same between the mutant and wild-type protein. Although, this does not rule out subtle differences in N-linked glycosylation at this site, it does indicate that the T618I mutation does not grossly alter the occupancy of the nearby N-linked glycosylation site.

CSF3R N610 mutations are activating and causes ligand-independence with increased phosphorylation of STAT3. We verified that both ruxolitinib and trametinib inhibit the viability of Ba/F3 cells expressing the CSF3R N610H and N610S mutations and found them to be sensitive to both compounds at similar or greater extent than the well-characterized CSF3R T618I mutation.

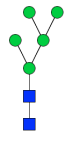
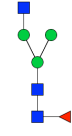
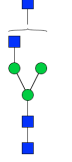
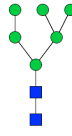
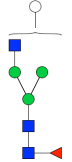
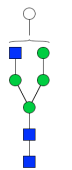
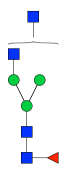
In the age of widespread sequencing of samples from patients with hematologic malignancies, a lack of functional annotation for less common variants represent a major challenge. In this study we employ functional and biochemical analysis of CSF3R to provide strong evidence that N610 substitutions activate the receptor. Furthermore, this study provides evidence that although they are rare, substitutions at N610 are likely to be therapeutically targetable. Finally, these clinically identified N610 substitution shine light on the importance of membrane proximal N-glycosylation to regulation of CSF3R activity. CSF3R mutations are the first example of a cancer-associated mutation that alters glycosylation in a site-specific manner to cause oncogenic transformation. This study highlights how careful investigation of cancer-associated mutations can provide critical insight into the relationship between protein structure and function.

Chapter 4: A novel germline variant in CSF3R reveals a N-glycosylation site that is important in receptor regulation

4.4 Table

Table 4-2. Compositional assignments of mono charged molecular ions, $[M+Na]^+$, observed in MALDI-TOF spectrum of permethylated N-glycans from CSF3R WT. The relative intensity was obtained from Data Explorer which performed baseline correction and Gaussian smoothed (filter width 9 points) on the spectrum; the ratio indicates a rough comparison of the glycan relative abundance to the whole group.

■GlcNAc, □HexNAc, ●Man, Gal, Hexose, Fuc, ◆NeuAc.

Observed m/z	Theoretical value	Component	Structure	Ratio	Percentage
1579.8	1579.8	2GlcNAc5Man		0.049	4.9%
1590.8	1590.8	3GlcNAc3Man1Fuc		0.021	2.1%
1661.6	1661.8	4GlcNAc3Man		0.042	4.2%
1783.8	1783.9	2GlcNAc6Man		0.044	4.4%
1794.9	1794.9	3GlcNAc3Man1Hexose1Fuc		0.023	2.3%
1824.9	1824.9	3GlcNAc4Man1Hexose		0.024	2.4%
1835.9	1835.9	4GlcNAc3Man1Fuc		0.058	5.8%

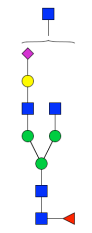
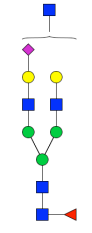
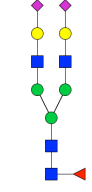
Chapter 4: A novel germline variant in CSF3R reveals a N-glycosylation site that is important in receptor regulation

Observed m/z	Theoretical value	Component	Structure	Ratio	Percentage
1865.9	1865.9	3GlcNAc1HexNAc3Man1Hexose		0.030	3.0%
1906.9	1907.0	4GlcNAc1HexNAc3Man		0.019	1.9%
1987.9	1988.0	2GlcNAc7Man		0.045	4.5%
1999.0	1999.0	3GlcNAc4Man1Hexose1Fuc		0.024	2.4%
2040.0	2040.0	3GlcNAc1HexNAc3Man1Hexose1Fuc		0.035	3.5%
2081.0	2081.0	4GlcNAc1HexNAc3Man1Fuc		0.040	4.0%
2192.1	2192.1	2GlcNAc8Man		0.065	6.5%

Chapter 4: A novel germline variant in CSF3R reveals a N-glycosylation site that is important in receptor regulation

Observed m/z	Theoretical value	Component	Structure	Ratio	Percentage
2244.1	2244.1	4GlcNAc3Man2Gal1Fuc		0.044	4.4%
2285.1	2285.1	4GlcNAc1HexNAc3Man1Gal1Fuc		0.060	6.0%
2326.1	2326.2	4GlcNAc2HexNAc3Man1Fuc		0.033	3.3%
2360.1	2360.2	3GlcNAc4Man1Gal1Fuc1NeuAc		0.037	3.7%
2396.2	2396.2	2GlcNAc9Man		0.099	9.9%
2489.2	2489.3	5GlcNAc3Man2Gal1Fuc		0.050	5.0%
2605.3	2605.3	4GlcNAc3Man2Gal1Fuc1NeuAc		0.050	5.0%

Chapter 4: A novel germline variant in CSF3R reveals a N-glycosylation site that is important in receptor regulation

Observed m/z	Theoretical value	Component	Structure	Ratio	Percentage
2646.3	2646.3	5GlcNAc3Man1Gal1Fuc1NeuAc		0.025	2.5%
2850.4	2850.4	5GlcNAc3Man2Gal1Fuc1NeuAc		0.024	2.4%
2966.6	2966.5	4GlcNAc3Man2Gal1Fuc2NeuAc		0.020	2.0%

4.5 Methods

Sanger Sequencing of CSF3R

Genomic DNA from a skin biopsy or peripheral blood was sequenced. Exon 14 of CSF3R was amplified using the following M13F and M13R tagged primers (F-(GTAAAACGACGGCCAGTCCACGGAGGCAGCTTTAC and R-CAGGAAACAGCTATGACCAAATCAGCATCCTTTGGGTG), purified on an Amicon Ultra 0.5 mL Centrifugal Filter (Millipore) followed by Sanger Sequencing (Eurofins genomics) using M13F and M13R primers.

Plasmid Construction

MSCV-IRES-GFP (MigR1) was made compatible for Gateway cloning using the Gateway Vector Conversion Kit (Invitrogen). A gateway pDONR vector for CSF3R transcript variant 1 (NM_00760.2 was purchased (GeneCopoeia). CSF3R was mutagenized as described previously for the CSF3R T618I mutation¹ or using the Quikchange II XL Site Directed Mutagenesis Kit (Agilent Genomics). The following primers were used for site directed mutagenesis—N610H (F-ggctggggccaccacagtagctct, R-aggactgtactgtgggtggccccagcc), N610Q (F-gtgaggactgtactctgggtggccccagcct, R-aggctggggccaccagtagctctctac), N610S (F-gaggactgtactctgggtggccccagc, R-gctggggccaccagtagctctctc). After sequence conformation of the mutagenesis, CSF3R mutants were subcloned into Gateway-MSCV-IRES-GFP using LR Clonease II, a recombination based strategy (Invitrogen).

Cell Culture

Ba/F3 cells were grown in RPMI 1640 with 10% fetal bovine serum (FBS, HyClone), Pen/Strep, 15% WEHI conditioned medium (which contains IL3) and L-glutamine. 293T17 cells were grown in DMEM containing GlutaMAX (Gibco) with 10% FBS and Pen/Strep. 293T17 cells were transfected with Fugene 6 (Promega) at a 5:1 ratio of lipid to DNA. Retrovirus was made by co-transfection of MigR1 constructs with pEcopac.

Ba/F3 cytokine independent growth assays

Viral supernatants were filtered using 0.45 micron filters and then Ba/F3 cells or mouse bone marrow were spinoculated in the presence of polybrene and hepes buffer. Cells were spun at 2500 rpms, for 90 minutes at 30°C (brake turned off). GFP+ cells were sorted on a BD FACSAria II sorter, and then sorted cells were allowed to expand for 2-4 days. GFP+ Ba/F3 cells expressing CSF3R mutants or controls were washed three times, and plated at 5×10^5 cells/mL in the absence of cytokine support (RPMI 1640 media, with 10% FBS, L-glutamine and Pen/Strep). Cell viability and number were monitored on a Bio-Rad TC20 cell counter. For drug treatment studies, Mig empty (control vector) and WT CSF3R were grown in the presence of IL3 (WEHI conditioned medium) and CSF3R mutant constructs were grown in the absence of IL3. Cells in 96 well plate format were treated with increasing doses of Ruxolitinib (Selleckchem) or Trametinib (Selleckchem). GCSF-independence assays were performed with GFP-sorted cells maintained in IL3-containing media. Cells were washed three times in media without IL3 and then grown in 96 well format with increasing doses of GCSF to determine the extent to which each cell type required GCSF for growth.

Mouse bone marrow colony assays

Mouse bone marrow was harvested from a 6-10 week old C57/BL6 mice. Marrow was cultured overnight in the presence of SCF, IL6 and IL3. Virus was prepared as described in the cell culture section and then filtered using 0.45 micron filters. 1×10^6 mouse bone marrow cells were spinoculated with viral supernatant, hepes buffer and polybrene on two subsequent days. For the spinoculation, cells were spun at 2500 rpms, for 90 minutes at 30°C (brake turned off). One day after the second sorting, GFP percentage was assessed by flow cytometry to determine that all vectors had infected the bone marrow cell. 10,000 cell were plated in triplicate in 1 mL mouse methylcellulose without added cytokines (MethoCult M3234, Stemcell Technologies). Cells were imaged using STEMvision (Stemcell Technologies) at day 14, blinded, and then manually counted.

Immunoblot analysis

293T17 cells transfected with the indicated CSF3R-MigR1 constructs as described under cell culture, were lysed 48h post-transfection in Cell Lysis Buffer (Cell Signaling Technologies) containing Complete Protease Inhibitor Cocktail Tablets (Roche) and Phosphatase Inhibitor Cocktail II (Sigma). Lysates were centrifuged at 14,000 rpms for 10 minutes at 4°C. Supernatant was transferred to a new tube then mixed with 3x SDS sample buffer (75 mM Tris pH 6.8, 3% SCS, 15% glycerol, 8% beta-mercaptoethanol, 0.1% bromophenol blue) and then heated for 5 minutes at 95°C. Lysates were run on 4-15% criterion TGX Precast Mini Protein Gels, 12 + 2 wells (Bio-Rad). Gels were transferred using the Trans-Blot Turbo Transfer System (Bio-Rad). After blocking in TBST with 5% milk, blots were probed in anti-GCSFR (38643, R&D Systems), Rb anti-pSTAT3 (9131, Cell Signaling Technologies), Rb anti-Stat3 (9132, Cell Signaling

Chapter 4: A novel germline variant in CSF3R reveals a N-glycosylation site that is important in receptor regulation

Technologies), or GAPDH (#25778, Santa Cruz Biotechnology). Blots were washed in TBST and then incubated with anti-mouse or anti-rabbit IgG, HRP-linked antibodies (Cell Signaling Technologies), followed by incubation with SuperSignal West Dura Substrate (Thermo) and imaged using a ChemiDoc Gel Imaging System (Bio-rad).

Immunoprecipitation

Purified protein was performed as previously described but in brief, 293T cells from American Type Culture Collection (ATCC) were maintained at 37 °C and 5% CO₂ in a water-saturated incubator in DMEM with 10% FBS (Atlanta Biologicals) and penicillin/streptomycin (Invitrogen). 293T cells were transfected using FuGENE 6 (Promega) in Optimem. Transfected cells were lysed using cell lysis buffer (Cell Signaling Technologies) containing complete protease inhibitor 3 (CalBioChem), spun at 10,000 rpm for 10 min to pellet cell debris and supernatant collected. FLAG-tagged constructs were immunoprecipitated from cell lysates by incubation with anti- FLAG M2 affinity gel (Sigma-Aldrich) for 1 h at 4 °C on a rotator. Beads were washed with cell lysis buffer. Proteins were disassociated from beads by incubating with FLAG peptide at room temperature for 1 hour and then subjected to immunoblotting analysis.

MALDI-TOF MS analysis of released N-linked profiling

Direct MS analysis of the released N-glycans was performed on whole HEK 293T transfected cells based on the method of Aoki et al.²² The released N-glycans were prepared from purified WT CSF3R as described previously. Released glycans were permethylated based on the method of Anumula and Taylor²³ and profiled directly by mass spectrometry. MALDI-TOF mass spectra of the permethylated N-glycans were acquired in the reflector positive ion mode using α -dihydroxybenzoic acid (DHBA, 20 mg/mL solution in 50% methanol-water) as a matrix. Dried samples were resuspended in 200 μ L glycoprotein denaturing buffer (New England Biosciences), then 5 μ L of PNGase F was added, and each sample was incubated at 37 °C for 24 hours (another 5 μ L of PNGase F was added after the first 12-hour incubation). After incubation the samples were lyophilized and desalted on a Sep-Pak C18 1 cc cartridge ESI MS analysis was performed by direct into the mass spectrometer at a constant flow rate of 0.25 μ L/min. The spectra were acquired using a TOF/TOF 5800 System (AB SCIEX).

Digestion for MS/MS analysis

CSF3R was digested by first denaturing 10 μ g of purified protein in 1 μ L of freshly made 1% protease max (Promega) and 15 μ L of 8M urea and incubated at 37 °C for 60 min. Reduction occurred with 1 μ L DTT at 60 °C or 20 min and alkylation was performed with 2.7 μ L of .55 M Iodoacetamide (IAA). This was mixed in the dark at room temperature for 15 minutes. To prepare samples for digestion, 24 μ L of 500 mM Tris-HCl pH8 and 1.2 μ L of 1M calcium chloride was added and then enough PBS so final volume is at 94.05 μ L. Chymotrypsin (Promega) was reconstituted in 25 μ L of 1 mM HCl, then 5.95 μ L was delivered to each sample. Samples were rotated for 18 hours at 25 °C. Prior to TMT labeling, samples were desalted and speed vacuumed until dry.

TMT labeling of chymotrypsin-digested peptides

The chymotrypsin digested samples were then labeled with TMT0 (Thermo Scientific). Immediately before use, equilibrate the TMT Label Reagents (Thermo scientific) to RT. For the 0.8mg vials, 41 μ L of anhydrous acetonitrile was added to each tube. The tubes with reagent are allowed to sit for 5 min with occasional vortexing. Next, 41 μ L TMT Label

Chapter 4: A novel germline variant in CSF3R reveals a N-glycosylation site that is important in receptor regulation

Reagent was added to each sample. The reaction was allowed to incubate for 1 hour at RT. To quench the reaction, 8 μ L 5% hydroxylamine was added. The samples were then desalted and speed vacuumed until dry.

Glycoproteomics on TMT-labeled peptides

Chymotrypsin-digested proteins were analyzed using with a Lumos Orbitrap mass spectrometer equipped with a nanoelectrospray ionization (nanoESI) source (Thermo Fisher Scientific, Waltham, MA). The LC was a Thermo Dionex UltiMate3000 RSLCnano liquid chromatograph that was connected in-line with a C18 precolumn (Acclaim PepMap 100, 20 mm length \times 0.075 mm inner diameter, 3 μ m particles, 75 Å pores, Thermo). Solvent A was 99.9% water/0.1% formic acid and solvent B was 99.9% acetonitrile/0.1% formic acid (v/v). The elution program consisted of isocratic flow at 2% B for 4 min, a linear gradient to 50% B over 50 min, isocratic flow at 95% B for 6 min, and isocratic flow at 2% B for 12 min, at a flow rate of 300 nL/min.

Full-scan mass spectra were acquired in the positive ion mode over the range m/z = 400 to 1800 using the Orbitrap mass analyzer, in profile format, with a mass resolution setting of 60 000 (at m/z = 400, measured at full width at half-maximum peak height, fwhm). In the data-dependent mode, the three most intense ions exceeding an intensity threshold of 50 000 counts were selected from each full-scan mass spectrum for tandem mass spectrometry (MS/MS, i.e., MS2) analysis using HCD. MS2 spectra were acquired using the linear ion trap or the Orbitrap analyzer (in the latter case, with a resolution setting of 7500 at m/z = 400, fwhm), in centroid format, with the following parameters: isolation width 4 m/z units, normalized collision energy 28%, default charge state 3+, activation Q 0.25, and activation time 30 ms. Ions were selected for electron transfer dissociation (ETD) that contained m/z 204 (HexNAc + H)⁺, m/z 163 (Hex + H)⁺, and m/z 366 (HexNAc + Hex + H)⁺. With sialylation, m/z 292 (Neu5Ac + H)⁺, m/z 274 (Neu5Ac - H₂O + H)⁺ and m/z 657 (HexNAc + Hex + Neu5Ac + H)⁺ are also present in each HCD MS2 spectrum. To avoid the occurrence of redundant MS/MS measurements, real-time dynamic exclusion was enabled to preclude reselection of previously analyzed precursor ions, with the following parameters: repeat count 1, repeat duration 30 s, exclusion list size 500, exclusion duration 60 s, and exclusion mass width \pm 1.5 m/z units. Data acquisition was controlled using Xcalibur software (version 4.0.0, Thermo).

The raw data was processed using Proteome Discoverer software (version 2.0 Thermo Fisher Scientific) and searched against either the human-specific SwissProt-reviewed protein database downloaded on July 18, 2014 or CSF3R (uniprot accession # Q99062). allowing for up to three missed cleavages, one fixed modification (carboxyamidomethylcysteine, + 57.021 Da), and variable modifications (methionine oxidation, + 15.995 Da; TMT, 224.1524). Precursor ion mass tolerances for spectra acquired using the Orbitrap Lumos and linear ion trap (LTQ) were set to 10 ppm and 1.5 Da, respectively. The fragment ion mass tolerance was set to 0.2 Da. Spectra were searched using the Byonic search algorithm v2.0 as a node in Proteome Discoverer 2.0. Computational assignments of all spectra were validated by manual inspection for glycan and peptide fragments. Only spectra for which the glycan structure was fully characterized were included in the final analysis.x

SILAC/Mass Spectrometry

Chapter 4: A novel germline variant in CSF3R reveals a N-glycosylation site that is important in receptor regulation

HEK293T cells were cultured in SILAC DMEM (Pierce) lacking lysine and arginine that was supplemented with isotopically enriched forms of L-Leucine ($^{13}\text{C}_6$, 50 $\mu\text{g}/\text{mL}$), L-lysine ($^{13}\text{C}_6$, $^{15}\text{N}_2$ hydrochloride; 50 $\mu\text{g}/\text{mL}$), and L-arginine ($^{13}\text{C}_6$, $^{15}\text{N}_4$ hydrochloride; 40 $\mu\text{g}/\text{mL}$) (heavy) or the corresponding unlabeled form of each at the same concentration (light). Both heavy and light forms of DMEM were further supplemented with L-proline (200 $\mu\text{g}/\text{mL}$; to prevent metabolic conversion of Arg \rightarrow Pro), L-glutamine (2 mM), and 10% dialyzed FBS (Pierce). After 5 days of metabolic labeling, cells were transfected with the denoted constructs and allowed to express the constructs for 48 hr. Cells were lysed and immunoprecipitated as described above. Proteins were subjected to overnight in digestion with 10 ng/ μL Lys-C enzyme in the presence of 50 mM ammonium bicarbonate/5% acetonitrile. Peptides were extracted with 50% acetonitrile/5% formic acid and then dried to completion, resuspended in 4% acetonitrile/5% formic acid and then heavy and light samples were combined for analysis.

The peptide quantification was performed in MaxQuant software as previously described^{18,24} with default parameters. Mascot Distiller quantification was performed with the following parameters. The extracted ion chromatogram (XIC) threshold was set from 0.1 to 0.3, XIC smooth was set from 3 to 1 and maximum XIC width was set to 250. The correlation score, a quantification quality parameter was set from 0.7 to 0.9.

4.6 References

- 1 Maxson, J. E., Gotlib, J., Pollyea, D. A., Fleischman, A. G., Agarwal, A., Eide, C. A., Bottomly, D., Wilmot, B., McWeeney, S. K., Tognon, C. E., Pond, J. B., Collins, R. H., Goueli, B., Oh, S. T., Deininger, M. W., Chang, B. H., Loriaux, M. M., Druker, B. J. & Tyner, J. W. Oncogenic CSF3R mutations in chronic neutrophilic leukemia and atypical CML. *The New England Journal of Medicine* **368**, 1781-1790 (2013).
- 2 Beekman, R., Valkhof, M., van Strien, P., Valk, P. J. & Touw, I. P. Prevalence of a new auto-activating colony stimulating factor 3 receptor mutation (CSF3R-T595I) in acute myeloid leukemia and severe congenital neutropenia. *Haematologica* **98**, e62-63 (2013).
- 3 Maxson, J. E., Ries, R. E., Wang, Y. C., Gerbing, R. B., Kolb, E. A., Thompson, S. L., Guidry Auvil, J. M., Marra, M. A., Ma, Y., Zong, Z., Mungall, A. J., Moore, R., Long, W., Gesuwan, P., Davidsen, T. M., Hermida, L. C., Hughes, S. B., Farrar, J. E., Radich, J. P., Smith, M. A., Gerhard, D. S., Gamis, A. S., Alonzo, T. A. & Meshinchi, S. CSF3R mutations have a high degree of overlap with CEBPA mutations in pediatric AML. *Blood* **127**, 3094-3098 (2016).
- 4 Ward, A. C., van Aesch, Y. M., Schelen, A. M. & Touw, I. P. Defective internalization and sustained activation of truncated granulocyte colony-stimulating factor receptor found in severe congenital neutropenia/acute myeloid leukemia. *Blood* **93**, 447-458 (1999).
- 5 Beekman, R., Valkhof, M. G., Sanders, M. A., van Strien, P. M., Haanstra, J. R., Broeders, L., Geertsma-Kleinekoort, W. M., Veerman, A. J., Valk, P. J., Verhaak, R. G., Lowenberg, B. & Touw, I. P. Sequential gain of mutations in severe congenital neutropenia progressing to acute myeloid leukemia. *Blood* **119**, 5071-5077 (2012).
- 6 Arber, D. A., Orazi, A., Hasserjian, R., Thiele, J., Borowitz, M. J., Le Beau, M. M., Bloomfield, C. D., Cazzola, M. & Vardiman, J. W. The 2016 revision to the World Health Organization classification of myeloid neoplasms and acute leukemia. *Blood* **127**, 2391-2405 (2016).
- 7 Plo, I., Zhang, Y., Le Couedic, J. P., Nakatake, M., Boulet, J. M., Itaya, M., Smith, S. O., Debili, N., Constantinescu, S. N., Vainchenker, W., Louache, F. & de Botton, S. An activating mutation in the CSF3R gene induces a hereditary chronic neutrophilia. *J Exp Med* **206**, 1701-1707 (2009).
- 8 Maxson, J. E., Luty, S. B., MacManiman, J. D., Paik, J. C., Gotlib, J., Greenberg, P., Bahamadi, S., Savage, S. L., Abel, M. L., Eide, C. A., Loriaux, M. M., Stevens, E. A. & Tyner, J. W. The Colony-Stimulating Factor 3 Receptor T640N Mutation Is Oncogenic, Sensitive to JAK Inhibition, and Mimics T618I. *Clinical Cancer Research* **22**, 757-764 (2016).
- 9 Maxson, J. E., Luty, S. B., MacManiman, J. D., Abel, M. L., Druker, B. J. & Tyner, J. W. Ligand independence of the T618I mutation in the colony-stimulating factor 3

Chapter 4: A novel germline variant in CSF3R reveals a N-glycosylation site that is important in receptor regulation

receptor (CSF3R) protein results from loss of O-linked glycosylation and increased receptor dimerization. *Journal of Biological Chemistry* **289**, 5820-5827 (2014).

10 Pinho, S. S. & Reis, C. A. Glycosylation in cancer: mechanisms and clinical implications. *Nature Reviews Cancer* **15**, 540-555 (2015).

11 Dube, D. H. & Bertozzi, C. R. Glycans in Cancer and Inflammation--Potential for Therapeutics and Diagnostics. *Nature Review Drug Discovery* **4**, 477 (2005).

12 Weerapana, E. & Imperiali, B. Asparagine-linked protein glycosylation: from eukaryotic to prokaryotic systems. *Glycobiology* **16**, 91R-101R (2006).

13 Imperiali, B. & Rickert, K. W. Conformational implications of asparagine-linked glycosylation. *Proceedings of the National Academy of Sciences USA* **92**, 97-101 (1995).

14 Haniu, M., Horan, T., Arakawa, T., Le, J., Katta, V., Hara, S. & Rohde, M. F. Disulfide structure and N-glycosylation sites of an extracellular domain of granulocyte-colony stimulating factor receptor. *Biochemistry* **35**, 13040-13046 (1996).

15 Bull, C., Stoel, M. A., den Brok, M. H. & Adema, G. J. Sialic acids sweeten a tumor's life. *Cancer Res* **74**, 3199-3204 (2014).

16 Saxon, E. Cell Surface Engineering by a Modified Staudinger Reaction. *Science* **287**, 2007-2010 (2000).

17 Wratil, P. R., Horstkorte, R. & Reutter, W. Metabolic Glycoengineering with N-Acyl Side Chain Modified Mannosamines. *Angewandte Chemie International Edition* **55**, 9482-9512 (2016).

18 Everley, P. A., Krijgsveld, J., Zetter, B. R. & Gygi, S. P. Quantitative cancer proteomics: stable isotope labeling with amino acids in cell culture (SILAC) as a tool for prostate cancer research. *Molecular Cellular Proteomics* **3**, 729-735 (2004).

19 Geiger, T., Cox, J., Ostasiewicz, P., Wisniewski, J. R. & Mann, M. Super-SILAC mix for quantitative proteomics of human tumor tissue. *Nature Methods* **7**, 383-385 (2010).

20 Damerell, D., Ceroni, A., Maass, K., Ranzinger, R., Dell, A. & Haslam, S. M. Annotation of glycomics MS and MS/MS spectra using the GlycoWorkbench software tool. *Methods Mol Biol* **1273**, 3-15 (2015).

21 Schweiger, R. & Linial, M. Cooperativity within proximal phosphorylation sites is revealed from large-scale proteomics data. *Biol Direct* **5**, 6 (2010).

22 Aoki, K., Perlman, M., Lim, J. M., Cantu, R., Wells, L. & Tiemeyer, M. Dynamic developmental elaboration of N-linked glycan complexity in the *Drosophila melanogaster* embryo. *Journal of Biological Chemistry* **282**, 9127-9142 (2007).

Chapter 4: A novel germline variant in CSF3R reveals a N-glycosylation site that is important in receptor regulation

- 23 Anumula, K. R. & Taylor, P. B. A comprehensive procedure for preparation of partially methylated alditol acetates from glycoprotein carbohydrates. *Analytical Biochemistry* **203**, 101-108 (1992).
- 24 Tyanova, S., Temu, T. & Cox, J. The MaxQuant computational platform for mass spectrometry-based shotgun proteomics. *Nat Protoc* **11**, 2301-2319 (2016).

APPENDICES

Appendix Table 1. Proteomic dataset of proteins found in normal and cancer prostate tissue slice cultures (TSCs). Proteins found in normal (n1-8) proteomic dataset. Columns include uniprot accession numbers (ACCN), gene names, protein names, Swiss-Prot databank annotations of glycosylation. The total number of identified peptide sequences (peptide spectrum matches) for the protein, including those redundantly identified.

ACCN	Gene Name	Protein Name	Annotated Glycosylated	N1	N2	N3	N4	N5	N6	N7	N8
P35749	MYH11	Myosin-11		24	13	41	36	37	31	22	85
P12111	COL6A3	Collagen alpha-3	N-linked, O-linked	11	6	35	28	23	21	2	102
P13645	KRT10	Keratin, type I cytoskeletal 10		15	14	23	19	10	1	27	42
P04264	KRT1	Keratin, type II cytoskeletal 1		15	12	23	14	11	8	30	35
P21333	FLNA	Filamin-A		18	4	20	16	27	4	11	16
P35908	KRT2	Keratin, type II cytoskeletal 2 epidermal		9	14	19	11	10	4	25	20
Q7Z5K2	WAPL	Wings apart-like protein homolog		22	2	35	11	29			
P05556	ITGB1	Integrin beta-1	N-linked	10	7	11	15	9	9	14	22
P18206	VCL	Vinculin		7	7	24	7	21	11	7	9
P35527	KRT9	Keratin, type I cytoskeletal 9		9	3	13	5	8	3	14	35
P01011	SERPINA3	Alpha-1-antichymotrypsin	N-linked	12	12	5	6	6	7	17	15
P17301	ITGA2	Integrin alpha-2	N-linked	10	8	11	10	7	11	7	15
P17661	DES	Desmin		2	1	10	7	12	9	7	29
P24821	TNC	Tenascin	N-linked	8	12	10	8	8	7	6	17
P06756	ITGAV	Integrin alpha-V	N-linked	7	10	10	10	7	10	9	10
P51884	LUM	Lumican	N-linked	9	6	8	9	4	5	8	22
Q01995	TAGLN	Transgelin		7	5	9	6	6	6	19	10
P63267	ACTG2	Actin, gamma-enteric smooth muscle		8	5	8	6	7	4	5	24
P08195	SLC3A2	4F2 cell-surface antigen heavy chain	N-linked	7	9	7	7	5	7	11	13
P07093	SERPINE2	Glia-derived nexin	N-linked	6	6	6	8	1	7	12	14
Q9Y490	TLN1	Talin-1		7	4	20	13	11	2	1	
P08758	ANXA5	Annexin A5		5	3	10	8	2	6	5	18
P35579	MYH9	Myosin-9				11	9	7	10		20
P68871	HBB	Hemoglobin subunit beta	N-linked	2	4	10	8	5	4	10	12
P23229	ITGA6	Integrin alpha-6	N-linked	5	9	8	7	6	5	7	6
P60660	MYL6	Myosin light polypeptide 6		7	1	5	7	3	2	7	20
P09758	TACSTD2	Tumor-associated calcium signal transducer 2	N-linked	3	6	7	7	3	6	11	5
P08133	ANXA6	Annexin A6			1	10	4	5	1		26
Q08380	LGALS3BP	Galectin-3-binding protein	N-linked	11	4	5	7	4	2	7	6
Q09666	AHNAK	Neuroblast differentiation-associated protein AHNAK		1	6	9	12	5	3	7	2
Q16853	AOC3	Membrane primary amine oxidase	N-linked, O-linked		2	10	5	2	3	11	12
P13647	KRT5	Keratin, type II cytoskeletal 5			4	8	3	6	2	11	9
Q13740	ALCAM	CD166 antigen	N-linked	5	5	3	5	5	4	8	8
P02768	ALB	Serum albumin	N-linked	1	2	6	4	4	3	8	14

Appendix Table 1. Proteomic dataset of proteins found in normal prostate tissue slice cultures (TSCs)

ACCN	Gene Name	Protein Name	Annotated Glycosylated	N1	N2	N3	N4	N5	N6	N7	N8
P09493	TPM1	Tropomyosin alpha-1 chain		4	3	8	6	5	3	8	5
P10909	CLU	Clusterin	N-linked	4	3	7	5	6	3	9	5
P60709	ACTB	Actin, cytoplasmic 1		5	5	6	4	5			17
P02533	KRT14	Keratin, type I cytoskeletal 14		1	7	8	4			14	6
Q15758	SLC1A5	Neutral amino acid transporter B	N-linked	6	3	4	7	2	6	5	7
P11142	HSPA8	Heat shock cognate 71 kDa protein		6	6	4	3	6	5	4	4
P11021	HSPA5	78 kDa glucose-regulated protein		3	9	9	3		4	4	5
P51888	PRELP	Prolargin	N-linked	3	2	2	5	3	2		20
P25311	AZGP1	Zinc-alpha-2-glycoprotein	N-linked	3	5	3	3	1	4	13	4
P05362	ICAM1	Intercellular adhesion molecule 1	N-linked	6	4	5	4	3	2	6	4
P08779	KRT16	Keratin, type I cytoskeletal 16			7	7				14	6
P12109	COL6A1	Collagen alpha-1	N-linked	1	1	3	1	3	1	1	23
P08648	ITGA5	Integrin alpha-5	N-linked	1	5	5	4	5	3	6	4
P62805	HIST1H4A	Histone H4		2	1	5	4	2	4	4	11
P04259	KRT6B	Keratin, type II cytoskeletal 6B		4	5					12	11
P05787	KRT8	Keratin, type II cytoskeletal 8				6	5	2	4	8	7
P07355	ANXA2	Annexin A2		4	3	7	5	3	3		7
P26006	ITGA3	Integrin alpha-3	N-linked	5	3	3	5	1	3	4	8
O75976	CPD	Carboxypeptidase D	N-linked	1	10	2	9	2	5	1	1
P15144	ANPEP	Aminopeptidase N	N-linked	6	10		2		1	12	
P62736	ACTA2	Actin, aortic smooth muscle								5	26
P02788	LTF	Lactotransferrin	N-linked	9	12	1	2			4	2
P63104	YWHAZ	14-3-3 protein zeta/delta		5	3	7	6	3	4		2
P11279	LAMP1	Lysosome-associated membrane glycoprotein 1	N-linked, O-linked	4	2	4	3	2	3	7	4
P68032	ACTC1	Actin, alpha cardiac muscle 1								5	24
Q14108	SCARB2	Lysosome membrane protein 2	N-linked	2	3	4	5	1	3	7	4
P02545	LMNA	Prelamin-A/C [Cleaved into: Lamin-A/C		3	2	3	5	4	7	2	2
P02751	FN1	Fibronectin	N-linked, O-linked	1	6	6	4	8			1
P07951	TPM2	Tropomyosin beta chain			3	5	7		3	6	2
P11047	LAMC1	Laminin subunit gamma-1	N-linked	1		3	3	2	5		12
P54709	ATP1B3	Sodium/potassium-transporting ATPase subunit beta-3	N-linked	3	2	3	2	3	2	4	7
P08962	CD63	CD63 antigen	N-linked	2	1	3	3	1	2	5	8
P35613	BSG	Basigin	N-linked	4	3	4	5	1	2	5	1
Q06830	PRDX1	Peroxiredoxin-1		1	2	3	3	2	3	7	4
Q8NBJ4	GOLM1	Golgi membrane protein 1	N-linked		4	2	3	1	4	11	
P05026	ATP1B1	Sodium/potassium-transporting ATPase subunit beta-1	N-linked	4	1	3	3	2	2	3	6

Appendix Table 1. Proteomic dataset of proteins found in normal prostate tissue slice cultures (TSCs)

ACCN	Gene Name	Protein Name	Annotated Glycosylated	N1	N2	N3	N4	N5	N6	N7	N8
P05090	APOD	Apolipoprotein D	N-linked	1	4	3	2	1	4	5	4
P06733	ENO1	Alpha-enolase		4	6	5	3	2	3		1
Q14126	DSG2	Desmoglein-2	N-linked	4	2	4	6	3	1	2	2
Q96KK5	HIST1H2A H	Histone H2A type 1-H		2	1	2	3	3	2	2	9
P06731	CEACAM5	Carcinoembryonic antigen-related cell adhesion molecule 5	N-linked	3		4	4	3	3	3	3
P08473	MME	Neprilysin	N-linked		1	2	7		2	11	
P12110	COL6A2	Collagen alpha-2	N-linked			2	3	3	2		13
P13473	LAMP2	Lysosome-associated membrane glycoprotein 2	N-linked, O-linked	2	1	3	4	2	3	3	5
P27348	YWHAQ	14-3-3 protein theta		5		4	4		4	3	3
P27701	CD82	CD82 antigen	N-linked	4	1	5	4			8	1
P68133	ACTA1	Actin, alpha skeletal muscle								5	18
Q13641	TPBG	Trophoblast glycoprotein	N-linked	3	2	2	5	1	2	2	6
P04792	HSPB1	Heat shock protein beta-1		3	2	2	2	2	1	4	6
P16284	PECAM1	Platelet endothelial cell adhesion molecule	N-linked	4	2	5	4		1	2	4
P21810	BGN	Biglycan	N-linked, O-linked	2	1	1	1	3	1	2	11
P51911	CNN1	Calponin-1		2	3	4	4	4		2	3
Q05707	COL14A1	Collagen alpha-1	N-linked, O-linked	1		9	2	2	2		6
P20774	OGN	Mimecan	N-linked, O-linked	2		2	2	1	3		11
P24844	MYL9	Myosin regulatory light polypeptide 9			3	5	4			3	6
P68104	EEF1A1	Elongation factor 1-alpha 1		4	2	2	2	2	1	3	5
Q13510	ASAH1	Acid ceramidase	N-linked	1	4	3	2	2	2	5	2
Q92542	NCSTN	Nicastrin	N-linked	1	3	2	5	1	3	5	1
Q9BQE3	TUBA1C	Tubulin alpha-1C chain			1	3	1	2	1		13
O60814	HIST1H2B K	Histone H2B type 1-K	O-linked	1	2	4	2	3	3	1	4
P01033	TIMP1	Metalloproteinase inhibitor 1	N-linked	3	3	2	2	2	1	4	3
P02538	KRT6A	Keratin, type II cytoskeletal 6A				11					9
P02794	FTH1	Ferritin heavy chain			1	4	3		2	4	6
P05121	SERPINE1	Plasminogen activator inhibitor 1	N-linked	2	5	5	2	2	1	3	
P08670	VIM	Vimentin	O-linked			3	2	2	2		11
P10809	HSPD1	60 kDa heat shock protein, mitochondrial			1	6	5	2	2		4
Q14CN2	CLCA4	Calcium-activated chloride channel regulator 4	N-linked	4	1	4	4	2	3	2	
P07237	P4HB	Protein disulfide-isomerase			1	5	2	2	1	7	1
P07339	CTSD	Cathepsin D	N-linked, O-linked	3	6	1	5	1	2		1
P0DMV8	HSPA1A	Heat shock 70 kDa protein 1A			6		4	5	2		2
P0CG48	UBC	Polyubiquitin-C		2	1	1	2	2	1	4	6
P13688	CEACAM1	Carcinoembryonic antigen-related cell adhesion molecule 1	N-linked	2	3	2	4	3			5

Appendix Table 1. Proteomic dataset of proteins found in normal prostate tissue slice cultures (TSCs)

ACCN	Gene Name	Protein Name	Annotated Glycosylated	N1	N2	N3	N4	N5	N6	N7	N8
P62258	YWHAE	14-3-3 protein epsilon		4		4	4	2	4		1
P06753	TPM3	Tropomyosin alpha-3 chain		2		5	5		2	4	
Q06323	PSME1	Proteasome activator complex subunit 1		1	1	4	5		3	4	
P23528	CFL1	Cofilin-1		3	3	2	3	1	1	2	2
P32119	PRDX2	Peroxiredoxin-2		1		2	2	2	2	5	3
P43121	MCAM	Cell surface glycoprotein MUC18	N-linked	1	1	4	4	2	1		4
P50895	BCAM	Basal cell adhesion molecule	N-linked	1	3	3	3		3	4	
P63261	ACTG1	Actin, cytoplasmic 2									17
Q03135	CAV1	Caveolin-1		3		4	2	1			7
P02786	TFRC	Transferrin receptor protein 1	N-linked, O-linked	3	4	2	4		3		
P04406	GAPDH	Glyceraldehyde-3-phosphate dehydrogenase		1	2	2	2	2	1		6
P14625	HSP90B1	Endoplasmic	N-linked		4	2	1	4	4		1
P15586	GNS	N-acetylglucosamine-6-sulfatase	N-linked	2	3	2	3		1	5	
P18827	SDC1	Syndecan-1	N-linked, O-linked	2	2	1	1	2	2	2	4
P45880	VDAC2	Voltage-dependent anion-selective channel protein 2		5		4	3	1	1		2
P55268	LAMB2	Laminin subunit beta-2	N-linked			2	4	1	1		8
Q08722	CD47	Leukocyte surface antigen CD47	N-linked	1	1	1		1	1	7	4
Q15746	MYLK	Myosin light chain kinase, smooth muscle		4		1	3	3	2	2	1
P04179	SOD2	Superoxide dismutase [Mn], mitochondrial			1	2	3		3	4	2
P08238	HSP90AB1	Heat shock protein HSP 90-beta	O-linked	2	3	2	2		3	2	1
P08727	KRT19	Keratin, type I cytoskeletal 19				3		3	4		5
P13796	LCP1	Plastin-2		2	3	5	3	1	1		
Q14BN4	SLMAP	Sarcolemmal membrane-associated protein				7	4	4			
Q9P2B2	PTGFRN	Prostaglandin F2 receptor negative regulator	N-linked	1	4	3	3	1	1	2	
P15309	ACPP	Prostatic acid phosphatase	N-linked	1	2	2	2	3	1	3	
P16070	CD44	CD44 antigen	N-linked, O-linked	3	2	1	2	1	1	2	2
P21589	NT5E	5'-nucleotidase	N-linked	1	1	2	3	1	1		5
P60174	TPI1	Triosephosphate isomerase		2	1	3	1	2	1	2	2
Q07065	CKAP4	Cytoskeleton-associated protein 4				6	1	3	1		3
P02792	FTL	Ferritin light chain		1	1	2	1	2	1	3	2
P09382	LGALS1	Galectin-1			2	2	2		1	4	2
P27824	CANX	Calnexin		1		1	1	1	1	5	3
P31947	SFN	14-3-3 protein sigma				4	4		4		1
P68363	TUBA1B	Tubulin alpha-1B chain									13
P69905	HBA1;	Hemoglobin subunit alpha	N-linked		1	5	2	3			2
Q6YHK3	CD109	CD109 antigen	N-linked	2	3	2	2		2		2

Appendix Table 1. Proteomic dataset of proteins found in normal prostate tissue slice cultures (TSCs)

ACCN	Gene Name	Protein Name	Annotated Glycosylated	N1	N2	N3	N4	N5	N6	N7	N8
Q99715	COL12A1	Collagen alpha-1	N-linked, O-linked		1	1	2	1	2		6
P27105	STOM	Erythrocyte band 7 integral membrane protein			1	4	4	1			2
P30048	PRDX3	Thioredoxin-dependent peroxide reductase, mitochondrial				2	2	2	1		5
P38646	HSPA9	Stress-70 protein, mitochondrial			6	1		2	1	1	1
Q15063	POSTN	Periostin	N-linked			2	3		2		5
Q8IV08	PLD3	Phospholipase D3	N-linked	2	2	1	3		2	2	
Q92520	FAM3C	Protein FAM3C		1	4		2	1	1	2	1
Q9UIQ6	LNPEP	Leucyl-cystinyl aminopeptidase	N-linked	2		2	3	1	2		2
O14494	PLPP1	Phospholipid phosphatase 1	N-linked		2	2	3	2	2		
P00558	PGK1	Phosphoglycerate kinase 1		2	4		1	2	2		
P01009	SERPINA1	Alpha-1-antitrypsin	N-linked	1	3	2	2			2	1
P02042	HBD	Hemoglobin subunit delta				5					6
P02750	LRG1	Leucine-rich alpha-2-glycoprotein	N-linked, O-linked		1	1	3			6	
P04083	ANXA1	Annexin A1				3		1			7
P04908	HIST1H2A B	Histone H2A type 1-B/E								2	9
P06703	S100A6	Protein S100-A6			1	1	1		1	5	2
P08253	MMP2	72 kDa type IV collagenase	N-linked	3	1	3	4				
P0C0S8	HIST1H2A G	Histone H2A type 1								2	9
P12830	CDH1	Cadherin-1	N-linked	1		4	3	2	1		
P13987	CD59	CD59 glycoprotein	N-linked, O-linked	1	1	1	2	1	1	2	2
P20671	HIST1H2A D	Histone H2A type 1-D								2	9
P23142	FBLN1	Fibulin-1	N-linked	2	2	2	3			2	
Q16777	HIST2H2A C	Histone H2A type 2-C								2	9
Q53GD3	SLC44A4	Choline transporter-like protein 4	N-linked	1	2	1	2	1	2	2	
Q6FI13	HIST2H2A A3	Histone H2A type 2-A								2	9
Q7L7L0	HIST3H2A	Histone H2A type 3								2	9
Q8NFD2	ANKK1	Ankyrin repeat and protein kinase domain-containing protein 1					4	7			
Q93077	HIST1H2A C	Histone H2A type 1-C								2	9
Q99878	HIST1H2AJ	Histone H2A type 1-J								2	9
Q9BTM1	H2AFJ	Histone H2A.J								2	9
Q9Y6C2	EMILIN1	EMILIN-1	N-linked			5	3	2	1		
O00391	QSOX1	Sulfhydryl oxidase 1	N-linked	3	1	1	2	2		1	
P00750	PLAT	Tissue-type plasminogen activator	N-linked, O-linked	1	2		1	1	1	4	
P05155	SERPING1	Plasma protease C1 inhibitor	N-linked, O-linked	1	2	1	1		1	4	
P06576	ATP5B	ATP synthase subunit beta, mitochondrial	O-linked		1	2	2	1	2		2
P07195	LDHB	L-lactate dehydrogenase B chain		1		2	1	2	2		2

Appendix Table 1. Proteomic dataset of proteins found in normal prostate tissue slice cultures (TSCs)

ACCN	Gene Name	Protein Name	Annotated Glycosylated	N1	N2	N3	N4	N5	N6	N7	N8
P0CG47	UBB	Polyubiquitin-B [Cleaved into: Ubiquitin]								4	6
P16422	EPCAM	Epithelial cell adhesion molecule	N-linked	1	1	1	1	1	1	2	2
P19105	MYL12A	Myosin regulatory light chain 12A						1	1	4	4
P29401	TKT	Transketolase		1	1	2		5	1		
P35580	MYH10	Myosin-10									10
P42892	ECE1	Endothelin-converting enzyme 1	N-linked	3	1		3		1		2
P62979	RPS27A	Ubiquitin-40S ribosomal protein S27a								4	6
P62987	UBA52	Ubiquitin-60S ribosomal protein L40								4	6
P78310	CXADR	Coxsackievirus and adenovirus receptor	N-linked	2	1	1	2		1	3	
Q05682	CALD1	Caldesmon		2	3	2	1	1		1	
Q14315	FLNC	Filamin-C		2				4			4
Q16563	SYPL1	Synaptophysin-like protein 1	N-linked	1	1	1	1	1	1	2	2
Q6UX06	OLFM4	Olfactomedin-4	N-linked	5	1		4				
Q71U36	TUBA1A	Tubulin alpha-1A chain									10
Q7Z406	MYH14	Myosin-14									10
Q9H5V8	CDCP1	CUB domain-containing protein 1	N-linked		1	3	3	2	1		
O15118	NPC1	Niemann-Pick C1 protein	N-linked	1	1	1	3		2		1
P04075	ALDOA	Fructose-bisphosphate aldolase A		1	2	3		2	1		
P07602	PSAP	Prosaposin	N-linked	2		1	2			4	
P07996	THBS1	Thrombospondin-1	N-linked, O-linked	2	3	1	3				
P27487	DPP4	Dipeptidyl peptidase 4	N-linked		1	2	2	1	1	2	
P39060	COL18A1	Collagen alpha-1	N-linked, O-linked	1	1	2	2		1	2	
P48668	KRT6C	Keratin, type II cytoskeletal 6C									9
Q04695	KRT17	Keratin, type I cytoskeletal 17				5					4
A5A3E0	POTEF	POTE ankyrin domain family member F									8
O14950	MYL12B	Myosin regulatory light chain 12B								4	4
O60487	MPZL2	Myelin protein zero-like protein 2	N-linked	1		1	2	1	1	2	
O95858	TSPAN15	Tetraspanin-15	N-linked		1	1	2		1	3	
P01019	AGT	Angiotensinogen	N-linked		2		1		2	3	
P07737	PFN1	Profilin-1		1	1	2	1		1		2
P10253	GAA	Lysosomal alpha-glucosidase	N-linked		1	3	1	1		2	
P31949	S100A11	Protein S100-A11		1		2	1		2		2
P34931	HSPA1L	Heat shock 70 kDa protein 1-like		4							4
P37802	TAGLN2	Transgelin-2		2	1	2	2		1		
P54652	HSPA2	Heat shock-related 70 kDa protein 2								4	4
P80188	LCN2	Neutrophil gelatinase-associated lipocalin	N-linked		1	1	2	1	2		1

Appendix Table 1. Proteomic dataset of proteins found in normal prostate tissue slice cultures (TSCs)

ACCN	Gene Name	Protein Name	Annotated Glycosylated	N1	N2	N3	N4	N5	N6	N7	N8
P98160	HSPG2	Basement membrane-specific heparan sulfate proteoglycan core protein	N-linked, O-linked			1	1	2			4
Q15365	PCBP1	Poly		1	1	1	1		1	2	1
Q16787	LAMA3	Laminin subunit alpha-3	N-linked			1	3	2	2		
Q5VTE0	EEF1A1P5	Putative elongation factor 1-alpha-like 3								3	5
Q6S8J3	POTEE	POTE ankyrin domain family member E									8
Q7Z2Q7	LRRC70	Leucine-rich repeat-containing protein 70	N-linked		2	4		2			
Q8N271	PROM2	Prominin-2	N-linked	2	1	1	4				
Q8NBN3	TMEM87A	Transmembrane protein 87A	N-linked	1	1	1	3	1	1		
Q8WUH2	TGFBRAP1	Transforming growth factor-beta receptor-associated protein 1				4	4				
Q96KP4	CNDP2	Cytosolic non-specific dipeptidase				3	1	1	1	2	
Q9BVK6	TMED9	Transmembrane emp24 domain-containing protein 9	N-linked	1	1	2		1	1	2	
O00461	GOLIM4	Golgi integral membrane protein 4	N-linked		1	1	1	1	1		2
O43653	PSCA	Prostate stem cell antigen	N-linked		1	1			1	2	2
O75369	FLNB	Filamin-B						4			3
O94919	ENDOD1	Endonuclease domain-containing 1 protein			1	1	1	1	1	2	
P00533	EGFR	Epidermal growth factor receptor	N-linked		2		1		1	2	1
P01889	HLA-B	HLA class I histocompatibility antigen, B-7 alpha chain	N-linked	3						4	
P05023	ATP1A1	Sodium/potassium-transporting ATPase subunit alpha-1				3	2				2
P07288	KLK3	Prostate-specific antigen	N-linked		1		1	1	1	2	1
P07585	DCN	Decorin	N-linked, O-linked	1		3					3
P15941	MUC1	Mucin-1	N-linked, O-linked	1	1	1	1		1	2	
P19256	CD58	Lymphocyte function-associated antigen 3	N-linked	1		1	1		1	2	1
P25705	ATP5A1	ATP synthase subunit alpha, mitochondrial	O-linked			3	2		2		
P37837	TALDO1	Transaldolase		1	1	1	1	1	1	1	
P40926	MDH2	Malate dehydrogenase, mitochondrial	O-linked	1		3	1	1	1		
P49748	ACADVL	Very long-chain specific acyl-CoA dehydrogenase, mitochondrial				4		3			
P62937	PPIA	Peptidyl-prolyl cis-trans isomerase A	N-linked	2		1	1	1	1	1	
P68366	TUBA4A	Tubulin alpha-4A chain		1							6
Q00765	REEP5	Receptor expression-enhancing protein 5			1	2	1	1	1	1	
Q12841	FSTL1	Follistatin-related protein 1	N-linked	1		1	1		1	3	
Q15323	KRT31	Keratin, type I cuticular Ha1				5					2
Q16363	LAMA4	Laminin subunit alpha-4	N-linked			1	2		1		3
Q8IWA5	SLC44A2	Choline transporter-like protein 2	N-linked	2		1	2		1		1
Q8NFI5	GPRC5A	Retinoic acid-induced protein 3	N-linked	1	1	1	1		1	2	
Q92896	GLG1	Golgi apparatus protein 1	N-linked		1	1	1		1	3	

Appendix Table 1. Proteomic dataset of proteins found in normal prostate tissue slice cultures (TSCs)

ACCN	Gene Name	Protein Name	Annotated Glycosylated	N1	N2	N3	N4	N5	N6	N7	N8
Q9NRX5	SERINC1	Serine incorporator 1	N-linked		1	1	1	1	1	2	
Q9UL46	PSME2	Proteasome activator complex subunit 2				2	2		1	2	
Q9Y277	VDAC3	Voltage-dependent anion-selective channel protein 3		1	2		3				1
Q9Y624	F11R	Junctional adhesion molecule A	N-linked	1		2	1		1	2	
O15230	LAMA5	Laminin subunit alpha-5	N-linked				1				5
O75915	ARL6IP5	PRA1 family protein 3		1		1	2			2	
P00450	CP	Ceruloplasmin	N-linked		1	2	2		1		
P07900	HSP90AA1	Heat shock protein HSP 90-alpha						3		2	1
P08729	KRT7	Keratin, type II cytoskeletal 7					2		1		3
P12814	ACTN1	Alpha-actinin-1				3			1		2
P15088	CPA3	Mast cell carboxypeptidase A									6
P21291	CSRP1	Cysteine and glycine-rich protein 1			1	1	1	2		1	
P31629	HIVEP2	Transcription factor HIVEP2		1	1		2	2			
P48960	CD97	CD97 antigen	N-linked		1	1	2		2		
P67936	TPM4	Tropomyosin alpha-4 chain					6				
P98088	MUC5AC	Mucin-5AC	N-linked			1		1	2		2
Q05639	EEF1A2	Elongation factor 1-alpha 2								3	3
Q15149	PLEC	Plectin					3	1	2		
Q92764	KRT35	Keratin, type I cuticular Ha5				4					2
Q9BYX7	POTEKP	Putative beta-actin-like protein 3									6
Q9NY65	TUBA8	Tubulin alpha-8 chain									6
A6NIZ1		Ras-related protein Rap-1b-like protein		1			1		1		2
O00468	AGRN	Agrin	N-linked, O-linked	1			1		1		2
O14493	CLDN4	Claudin-4				1	1		1	2	
O43707	ACTN4	Alpha-actinin-4						3			2
O43852	CALU	Calumenin	N-linked			1			1	3	
O60664	PLIN3	Perilipin-3			3	2					
P00505	GOT2	Aspartate aminotransferase, mitochondrial				3		2			
P04040	CAT	Catalase				3		2			
P06899	HIST1H2BJ	Histone H2B type 1-J	O-linked							1	4
P10319	HLA-B	HLA class I histocompatibility antigen, B-58 alpha chain	N-linked		1		2		2		
P10599	TXN	Thioredoxin				1	2			2	
P13646	KRT13	Keratin, type I cytoskeletal 13									5
P15151	PVR	Poliovirus receptor	N-linked	1	1	1	2				
P15259	PGAM2	Phosphoglycerate mutase 2					1		1	2	1
P16870	CPE	Carboxypeptidase E	N-linked		1			1	1	2	

Appendix Table 1. Proteomic dataset of proteins found in normal prostate tissue slice cultures (TSCs)

ACCN	Gene Name	Protein Name	Annotated Glycosylated	N1	N2	N3	N4	N5	N6	N7	N8
P17813	ENG	Endoglin	N-linked		1	2	2				
P23284	PPIB	Peptidyl-prolyl cis-trans isomerase B	N-linked		3	1	1				
P23527	HIST1H2B O	Histone H2B type 1-O	O-linked							1	4
P30041	PRDX6	Peroxiredoxin-6		1	2						2
P31946	YWHAB	14-3-3 protein beta/alpha		4							1
P33778	HIST1H2B B	Histone H2B type 1-B	O-linked							1	4
P36269	GGT5	Gamma-glutamyltransferase 5	N-linked		1	1	1				2
P40199	CEACAM6	Carcinoembryonic antigen-related cell adhesion molecule 6	N-linked			2	2	1			
P55083	MFAP4	Microfibril-associated glycoprotein 4	N-linked								5
P57053	H2BFS	Histone H2B type F-S	O-linked							1	4
P58876	HIST1H2B D	Histone H2B type 1-D	O-linked							1	4
P62807	HIST1H2B C	Histone H2B type 1-C/E/F/G/I	O-linked							1	4
Q03405	PLAUR	Urokinase plasminogen activator surface receptor	N-linked	1			1		1	2	
Q13308	PTK7	Inactive tyrosine-protein kinase 7	N-linked		1	1	1	1	1		
Q13748	TUBA3C	Tubulin alpha-3C/D chain									5
Q15223	NECTIN1	Nectin-1	N-linked	1			2		1		1
Q16778	HIST2H2B E	Histone H2B type 2-E	O-linked							1	4
Q5QNW6	HIST2H2BF	Histone H2B type 2-F	O-linked							1	4
Q6P4E1	CASC4	Protein CASC4			1		1		1	2	
Q6PEY2	TUBA3E	Tubulin alpha-3E chain									5
Q8N257	HIST3H2B B	Histone H2B type 3-B	O-linked							1	4
Q92692	NECTIN2	Nectin-2	N-linked			1	1		1	2	
Q93079	HIST1H2B H	Histone H2B type 1-H	O-linked							1	4
Q99877	HIST1H2B N	Histone H2B type 1-N	O-linked							1	4
Q99879	HIST1H2B M	Histone H2B type 1-M	O-linked							1	4
Q99880	HIST1H2BL	Histone H2B type 1-L	O-linked							1	4
Q9BYK8	HELZ2	Helicase with zinc finger domain 2		1			2	1			1
Q9Y5Z0	BACE2	Beta-secretase 2	N-linked		3					2	
Q9Y639	NPTN	Neuroplastin	N-linked	1	1		1		1	1	
A6NMY6	ANXA2P2	Putative annexin A2-like protein									4
O00264	PGRMC1	Membrane-associated progesterone receptor component 1		1			1			2	
O00299	CLIC1	Chloride intracellular channel protein 1		1	1	1	1				
O00754	MAN2B1	Lysosomal alpha-mannosidase	N-linked		2	1	1				
O43790	KRT86	Keratin, type II cuticular Hb6				4					
O60635	TSPAN1	Tetraspanin-1	N-linked			1	1			2	

Appendix Table 1. Proteomic dataset of proteins found in normal prostate tissue slice cultures (TSCs)

ACCN	Gene Name	Protein Name	Annotated Glycosylated	N1	N2	N3	N4	N5	N6	N7	N8
O60637	TSPAN3	Tetraspanin-3	N-linked			1	1		1		1
O75503	CLN5	Ceroid-lipofuscinosis neuronal protein 5	N-linked		2		2				
P04080	CSTB	Cystatin-B			1	1	1		1		
P04439	HLA-A	HLA class I histocompatibility antigen, A-3 alpha chain	N-linked	4							
P05067	APP	Amyloid beta A4 protein	N-linked, O-linked	1	1	1	1				
P05386	RPLP1	60S acidic ribosomal protein P1		1			1		1		1
P05976	MYL1	Myosin light chain 1/3, skeletal muscle isoform									4
P07437	TUBB	Tubulin beta chain									4
P08590	MYL3	Myosin light chain 3									4
P0C0S5	H2AFZ	Histone H2A.Z									4
P0CG38	POTEI	POTE ankyrin domain family member I									4
P0CG39	POTEJ	POTE ankyrin domain family member J									4
P11117	ACP2	Lysosomal acid phosphatase	N-linked		2		1		1		
P11166	SLC2A1	Solute carrier family 2, facilitated glucose transporter member 1	N-linked	3					1		
P11717	IGF2R	Cation-independent mannose-6-phosphate receptor	N-linked		1				1	2	
P14314	PRKCSH	Glucosidase 2 subunit beta	N-linked	1			1			2	
P16104	H2AFX	Histone H2AX									4
P16144	ITGB4	Integrin beta-4	N-linked	1			2		1		
P16190	HLA-A	HLA class I histocompatibility antigen, A-33 alpha chain	N-linked							4	
P19012	KRT15	Keratin, type I cytoskeletal 15									4
P20645	M6PR	Cation-dependent mannose-6-phosphate receptor	N-linked	3			1				
P23141	CES1	Liver carboxylesterase 1	N-linked			2	2				
P30453	HLA-A	HLA class I histocompatibility antigen, A-34 alpha chain	N-linked								4
P30457	HLA-A	HLA class I histocompatibility antigen, A-66 alpha chain	N-linked								4
P30460	HLA-B	HLA class I histocompatibility antigen, B-8 alpha chain	N-linked								4
P30479	HLA-B	HLA class I histocompatibility antigen, B-41 alpha chain	N-linked								4
P30480	HLA-B	HLA class I histocompatibility antigen, B-42 alpha chain	N-linked								4
P35052	GPC1	Glypican-1	N-linked, O-linked			2	1		1		
P35573	AGL	Glycogen debranching enzyme			1	1	1		1		
P51572	BCAP31	B-cell receptor-associated protein 31				1	2			1	
P55072	VCP	Transitional endoplasmic reticulum ATPase					2	2			
P56199	ITGA1	Integrin alpha-1	N-linked			1	1				2
Q00796	SORD	Sorbitol dehydrogenase						2	1	1	
Q01650	SLC7A5	Large neutral amino acids transporter small subunit 1	N-linked	2	1						1
Q04826	HLA-B	HLA class I histocompatibility antigen, B-40 alpha chain	N-linked							4	

Appendix Table 1. Proteomic dataset of proteins found in normal prostate tissue slice cultures (TSCs)

ACCN	Gene Name	Protein Name	Annotated Glycosylated	N1	N2	N3	N4	N5	N6	N7	N8
Q13336	SLC14A1	Urea transporter 1	N-linked	1		1	1				1
Q13751	LAMB3	Laminin subunit beta-3	N-linked	1			2		1		
Q2M2I5	KRT24	Keratin, type I cytoskeletal 24									4
Q5XKE5	KRT79	Keratin, type II cytoskeletal 79									4
Q71UI9	H2AFV	Histone H2A.V									4
Q92187	ST8SIA4	CMP-N-acetylneuraminate-poly-alpha-2,8-sialyltransferase	N-linked		1	1	1	1			
Q92485	SMPDL3B	Acid sphingomyelinase-like phosphodiesterase 3b	N-linked				1		1	2	
Q969L2	MAL2	Protein MAL2	N-linked							2	2
Q96QV6	HIST1H2A A	Histone H2A type 1-A									4
Q96S97	MYADM	Myeloid-associated differentiation marker				1			1		2
Q9BVC6	TMEM109	Transmembrane protein 109			1	1	1				1
Q9NSB4	KRT82	Keratin, type II cuticular Hb2				4					
Q9Y5Y6	ST14	Suppressor of tumorigenicity 14 protein	N-linked		1		1			2	
A6NGU5	GGT3P	Putative gamma-glutamyltranspeptidase 3	N-linked		1					2	
A7E2Y1	MYH7B	Myosin-7B				1	2				
O43240	KLK10	Kallikrein-10	N-linked			1	1	1			
O95678	KRT75	Keratin, type II cytoskeletal 75									3
P02763	ORM1	Alpha-1-acid glycoprotein 1	N-linked							3	
P04233	CD74	HLA class II histocompatibility antigen gamma chain	N-linked, O-linked		1	1	1				
P04350	TUBB4A	Tubulin beta-4A chain									3
P07492	GRP	Gastrin-releasing peptide		1				2			
P08123	COL1A2	Collagen alpha-2	N-linked	1							2
P09238	MMP10	Stromelysin-2		1			1		1		
P09525	ANXA4	Annexin A4				2		1			
P0C0L4	C4A	Complement C4-A	N-linked, O-linked						1	2	
P12277	CKB	Creatine kinase B-type					1		2		
P13726	F3	Tissue factor	N-linked						1	2	
P14618	PKM	Pyruvate kinase PKM							1		2
P17693	HLA-G	HLA class I histocompatibility antigen, alpha chain G	N-linked							3	
P18084	ITGB5	Integrin beta-5	N-linked				1		2		
P18669	PGAM1	Phosphoglycerate mutase 1								2	1
P19013	KRT4	Keratin, type II cytoskeletal 4									3
P30456	HLA-A	HLA class I histocompatibility antigen, A-43 alpha chain	N-linked	3							
P30501	HLA-C	HLA class I histocompatibility antigen, Cw-2 alpha chain	N-linked			3					
P49221	TGM4	Protein-glutamine gamma-glutamyltransferase 4				2		1			
P50336	PPOX	Protoporphyrinogen oxidase								1	2

Appendix Table 1. Proteomic dataset of proteins found in normal prostate tissue slice cultures (TSCs)

ACCN	Gene Name	Protein Name	Annotated Glycosylated	N1	N2	N3	N4	N5	N6	N7	N8
P55058	PLTP	Phospholipid transfer protein	N-linked				2		1		
P68371	TUBB4B	Tubulin beta-4B chain									3
P98172	EFNB1	Ephrin-B1	N-linked		2	1					
Q01518	CAP1	Adenylyl cyclase-associated protein 1				1	1	1			
Q12767	TMEM94	Transmembrane protein 94	N-linked	1							2
Q13228	SELENBP1	Selenium-binding protein 1				2		1			
Q13813	SPTAN1	Spectrin alpha chain, non-erythrocytic 1				1		2			
Q14118	DAG1	Dystroglycan	N-linked, O-linked		1					2	
Q14512	FGFBP1	Fibroblast growth factor-binding protein 1		1	1		1				
Q14956	GNPMB	Transmembrane glycoprotein NMB	N-linked		1	1	1				
Q5T9S5	CCDC18	Coiled-coil domain-containing protein 18					1		1		1
Q5VU43	PDE4DIP	Myomegalin				1		2			
Q687X5	STEAP4	Metalloreductase STEAP4	N-linked		2				1		
Q6EMK4	VASN	Vasorin	N-linked	1	1		1				
Q7Z794	KRT77	Keratin, type II cytoskeletal 1b									3
Q8IXW5	RPAP2	Putative RNA polymerase II subunit B1 CTD phosphatase RPAP2					2		1		
Q8N0Y7	PGAM4	Probable phosphoglycerate mutase 4								2	1
Q969P0	IGSF8	Immunoglobulin superfamily member 8	N-linked	1			1		1		
Q96DA0	ZG16B	Zymogen granule protein 16 homolog B	N-linked		1		2				
Q99456	KRT12	Keratin, type I cytoskeletal 12								1	2
Q99988	GDF15	Growth/differentiation factor 15	N-linked		1					2	
Q9C0H2	TTYH3	Protein tweety homolog 3	N-linked	1	1		1				
Q9H853	TUBA4B	Putative tubulin-like protein alpha-4B									3
Q9HBA9	FOLH1B	Putative N-acetylated-alpha-linked acidic dipeptidase	N-linked				1			2	
Q9NQC3	RTN4	Reticulon-4				1	2				
Q9UDY6	TRIM10	Tripartite motif-containing protein 10		3							
Q9Y3E0	GOLT1B	Vesicle transport protein GOT1B		1		1	1				
Q9Y653	ADGRG1	Adhesion G-protein coupled receptor G1	N-linked	1			1				1
A6NNZ2		Tubulin beta-8 chain-like protein LOC260334									2
B3KS81	SRRM5	Serine/arginine repetitive matrix protein 5						2			
O00584	RNASET2	Ribonuclease T2	N-linked						1	1	
O00746	NME4	Nucleoside diphosphate kinase, mitochondrial				1	1				
O14880	MGST3	Microsomal glutathione S-transferase 3					1				1
O15519	CFLAR	CASP8 and FADD-like apoptosis regulator					1		1		
O15551	CLDN3	Claudin-3								2	

Appendix Table 1. Proteomic dataset of proteins found in normal prostate tissue slice cultures (TSCs)

ACCN	Gene Name	Protein Name	Annotated Glycosylated	N1	N2	N3	N4	N5	N6	N7	N8
O43493	TGOLN2	Trans-Golgi network integral membrane protein 2	N-linked			1	1				
O75106	AOC2	Retina-specific copper amine oxidase	N-linked								2
O94886	TMEM63A	CSC1-like protein 1				1			1		
O94985	CLSTN1	Calsyntenin-1	N-linked	1			1				
O95197	RTN3	Reticulon-3									2
O95484	CLDN9	Claudin-9								2	
O95786	DDX58	Probable ATP-dependent RNA helicase DDX58		2							
P00403	MT-CO2	Cytochrome c oxidase subunit 2					1				1
P01574	IFNB1	Interferon beta	N-linked								2
P01833	PIGR	Polymeric immunoglobulin receptor	N-linked	1			1				
P01903	HLA-DRA	HLA class II histocompatibility antigen, DR alpha chain	N-linked		1	1					
P02100	HBE1	Hemoglobin subunit epsilon									2
P04921	GYPC	Glycophorin-C	N-linked, O-linked		2						
P05783	KRT18	Keratin, type I cytoskeletal 18	O-linked								2
P06396	GSN	Gelsolin				1		1			
P06748	NPM1	Nucleophosmin		1		1					
P07686	HEXB	Beta-hexosaminidase subunit beta	N-linked			1	1				
P08572	COL4A2	Collagen alpha-2	N-linked								2
P0C0L5	C4B	Complement C4-B	N-linked							2	
P12035	KRT3	Keratin, type II cytoskeletal 3									2
P12757	SKIL	Ski-like protein					1		1		
P13639	EEF2	Elongation factor 2				1		1			
P13747	HLA-E	HLA class I histocompatibility antigen, alpha chain E	N-linked				2				
P14136	GFAP	Glial fibrillary acidic protein									2
P14649	MYL6B	Myosin light chain 6B									2
P17066	HSPA6	Heat shock 70 kDa protein 6									2
P18564	ITGB6	Integrin beta-6	N-linked		1		1				
P19440	GGT1	Gamma-glutamyltranspeptidase 1	N-linked							2	
P20073	ANXA7	Annexin A7									2
P21796	VDAC1	Voltage-dependent anion-selective channel protein 1				1					1
P23946	CMA1	Chymase	N-linked								2
P29034	S100A2	Protein S100-A2								1	1
P30461	HLA-B	HLA class I histocompatibility antigen, B-13 alpha chain	N-linked						2		
P30825	SLC7A1	High affinity cationic amino acid transporter 1	N-linked				1		1		
P31997	CEACAM8	Carcinoembryonic antigen-related cell adhesion molecule 8	N-linked								2
P33151	CDH5	Cadherin-5	N-linked			1	1				

Appendix Table 1. Proteomic dataset of proteins found in normal prostate tissue slice cultures (TSCs)

ACCN	Gene Name	Protein Name	Annotated Glycosylated	N1	N2	N3	N4	N5	N6	N7	N8
P36268	GGT2	Inactive gamma-glutamyltranspeptidase 2	N-linked							2	
P45877	PPIC	Peptidyl-prolyl cis-trans isomerase C			1	1					
P48741	HSPA7	Putative heat shock 70 kDa protein 7									2
P50995	ANXA11	Annexin A11				2					
P56747	CLDN6	Claudin-6								2	
P60033	CD81	CD81 antigen		1		1					
P61224	RAP1B	Ras-related protein Rap-1b									2
P62834	RAP1A	Ras-related protein Rap-1A									2
P68431	HIST1H3A	Histone H3.1								1	1
P69891	HBG1	Hemoglobin subunit gamma-1									2
P69892	HBG2	Hemoglobin subunit gamma-2									2
P84243	H3F3A	Histone H3.3								1	1
Q01546	KRT76	Keratin, type II cytoskeletal 2 oral									2
Q02818	NUCB1	Nucleobindin-1								2	
Q04609	FOLH1	Glutamate carboxypeptidase 2	N-linked							2	
Q04941	PLP2	Proteolipid protein 2	N-linked			1	1				
Q07507	DPT	Dermatopontin									2
Q10589	BST2	Bone marrow stromal antigen 2	N-linked	1							1
Q12805	EFEMP1	EGF-containing fibulin-like extracellular matrix protein 1	N-linked			1	1				
Q13162	PRDX4	Peroxiredoxin-4				2					
Q13509	TUBB3	Tubulin beta-3 chain									2
Q13561	DCTN2	Dynactin subunit 2					2				
Q13753	LAMC2	Laminin subunit gamma-2	N-linked	1			1				
Q13885	TUBB2A	Tubulin beta-2A chain									2
Q14103	HNRNPD	Heterogeneous nuclear ribonucleoprotein D0				1		1			
Q14525	KRT33B	Keratin, type I cuticular Ha3-II									2
Q14532	KRT32	Keratin, type I cuticular Ha2									2
Q14568	HSP90AA2 P	Heat shock protein HSP 90-alpha A2								2	
Q15124	PGM5	Phosphoglucomutase-like protein 5						2			
Q15406	NR6A1	Nuclear receptor subfamily 6 group A member 1				2					
Q15582	TGFBI	Transforming growth factor-beta-induced protein ig-h3				1	1				
Q16695	HIST3H3	Histone H3.1t								1	1
Q16836	HADH	Hydroxyacyl-coenzyme A dehydrogenase, mitochondrial				2					
Q16881	TXNRD1	Thioredoxin reductase 1, cytoplasmic						2			
Q3ZCM7	TUBB8	Tubulin beta-8 chain									2
Q58FF8	HSP90AB2 P	Putative heat shock protein HSP 90-beta 2								2	

Appendix Table 1. Proteomic dataset of proteins found in normal prostate tissue slice cultures (TSCs)

ACCN	Gene Name	Protein Name	Annotated Glycosylated	N1	N2	N3	N4	N5	N6	N7	N8
Q5T5P2	KIAA1217	Sickle tail protein homolog	O-linked			2					
Q6KB66	KRT80	Keratin, type II cytoskeletal 80									2
Q6KC79	NIPBL	Nipped-B-like protein		2							
Q6NXT2	H3F3C	Histone H3.3C								1	1
Q6PCB0	VWA1	von Willebrand factor A domain-containing protein 1	N-linked								2
Q6UVK1	CSPG4	Chondroitin sulfate proteoglycan 4	N-linked, O-linked				1	1			
Q6UWR7	ENPP6	Ectonucleotide pyrophosphatase/phosphodiesterase family member 6	N-linked	1		1					
Q6UXS9	CASP12	Inactive caspase-12				1	1				
Q6ZT07	TBC1D9	TBC1 domain family member 9		2							
Q71DI3	HIST2H3A;	Histone H3.2								1	1
Q7Z3Y7	KRT28	Keratin, type I cytoskeletal 28									2
Q7Z7H5	TMED4	Transmembrane emp24 domain-containing protein 4	N-linked				2				
Q86TE4	LUZP2	Leucine zipper protein 2	N-linked		1	1					
Q8IUE6	HIST2H2A B	Histone H2A type 2-B									2
Q8IZP2	ST13P4	Putative protein FAM10A4				1		1			
Q8N129	CNPY4	Protein canopy homolog 4				1	1				
Q8NCM8	DYNC2H1	Cytoplasmic dynein 2 heavy chain 1			1				1		
Q8NFW5	DMBX1	Diencephalon/mesencephalon homeobox protein 1		1			1				
Q8TAF7	ZNF461	Zinc finger protein 461				1			1		
Q96QD8	SLC38A2	Sodium-coupled neutral amino acid transporter 2	N-linked	2							
Q99439	CNN2	Calponin-2		1		1					
Q9BUF5	TUBB6	Tubulin beta-6 chain									2
Q9BVA1	TUBB2B	Tubulin beta-2B chain									2
Q9BX97	PLVAP	Plasmalemma vesicle-associated protein	N-linked								2
Q9BY67	CADM1	Cell adhesion molecule 1	N-linked							2	
Q9BZJ3	TPSD1	Tryptase delta	N-linked			1	1				
Q9C0G6	DNAH6	Dynein heavy chain 6, axonemal				1		1			
Q9H4B7	TUBB1	Tubulin beta-1 chain									2
Q9HBR0	SLC38A10	Putative sodium-coupled neutral amino acid transporter 10			1		1				
Q9NUB1	ACSS1	Acetyl-coenzyme A synthetase 2-like, mitochondrial				1			1		
Q9NZU0	FLRT3	Leucine-rich repeat transmembrane protein FLRT3	N-linked		1				1		
Q9P273	TENM3	Teneurin-3	N-linked			1		1			
Q9P2M7	CGN	Cingulin			1		1				
Q9UBG0	MRC2	C-type mannose receptor 2	N-linked				1		1		
Q9UQC9	CLCA2	Calcium-activated chloride channel regulator 2	N-linked		1		1				

Appendix Table 1. Proteomic dataset of proteins found in normal prostate tissue slice cultures (TSCs)

ACCN	Gene Name	Protein Name	Annotated Glycosylated	N1	N2	N3	N4	N5	N6	N7	N8
Q9Y6X5	ENPP4	Bis	N-linked						1	1	
A7XYQ1	SOBP	Sine oculis-binding protein homolog							1		
B1APH4	ZNF487	Putative zinc finger protein 487		1							
C9JVV0	INAFM1	Putative transmembrane protein INAFM1							1		
O14495	PLPP3	Phospholipid phosphatase 3	N-linked			1					
O14558	HSPB6	Heat shock protein beta-6						1			
O14672	ADAM10	Disintegrin and metalloproteinase domain-containing protein 10	N-linked		1						
O14773	TPP1	Tripeptidyl-peptidase 1	N-linked					1			
O43570	CA12	Carbonic anhydrase 12	N-linked				1				
O43657	TSPAN6	Tetraspanin-6	N-linked	1							
O60347	TBC1D12	TBC1 domain family member 12						1			
O95425	SVIL	Supervillin							1		
P00441	SOD1	Superoxide dismutase [Cu-Zn]					1				
P00915	CA1	Carbonic anhydrase 1				1					
P01834	IGKC	Immunoglobulin kappa constant		1							
P01857	IGHG1	Immunoglobulin heavy constant gamma 1	N-linked			1					
P02649	APOE	Apolipoprotein E	N-linked, O-linked	1							
P02743	APCS	Serum amyloid P-component	N-linked								1
P02787	TF	Serotransferrin	N-linked, O-linked						1		
P04004	VTN	Vitronectin	N-linked								1
P04062	GBA	Glucosylceramidase	N-linked						1		
P05141	SLC25A5	ADP/ATP translocase 2									1
P05937	CALB1	Calbindin									1
P07196	NEFL	Neurofilament light polypeptide	O-linked								1
P07197	NEFM	Neurofilament medium polypeptide	O-linked								1
P07858	CTSB	Cathepsin B	N-linked				1				
P07942	LAMB1	Laminin subunit beta-1	N-linked	1							
P08294	SOD3	Extracellular superoxide dismutase [Cu-Zn]	N-linked							1	
P09211	GSTP1	Glutathione S-transferase P			1						
P11766	ADH5	Alcohol dehydrogenase class-3				1					
P12036	NEFH	Neurofilament heavy polypeptide									1
P12235	SLC25A4	ADP/ATP translocase 1									1
P12236	SLC25A6	ADP/ATP translocase 3									1
P13489	RNH1	Ribonuclease inhibitor							1		
P13598	ICAM2	Intercellular adhesion molecule 2	N-linked			1					
P13637	ATP1A3	Sodium/potassium-transporting ATPase subunit alpha-3			1						

Appendix Table 1. Proteomic dataset of proteins found in normal prostate tissue slice cultures (TSCs)

ACCN	Gene Name	Protein Name	Annotated Glycosylated	N1	N2	N3	N4	N5	N6	N7	N8
P14543	NID1	Nidogen-1	N-linked						1		
P15311	EZR	Ezrin							1		
P15529	CD46	Membrane cofactor protein	N-linked, O-linked				1				
P15924	DSP	Desmoplakin				1					
P17900	GM2A	Ganglioside GM2 activator	N-linked							1	
P18085	ARF4	ADP-ribosylation factor 4					1				
P19338	NCL	Nucleolin							1		
P20061	TCN1	Transcobalamin-1	N-linked						1		
P20701	ITGAL	Integrin alpha-L	N-linked			1					
P21266	GSTM3	Glutathione S-transferase Mu 3		1							
P22626	HNRNPA2 B1	Heterogeneous nuclear ribonucleoproteins A2/B1						1			
P27816	MAP4	Microtubule-associated protein 4				1					
P30086	PEBP1	Phosphatidylethanolamine-binding protein 1				1					
P30408	TM4SF1	Transmembrane 4 L6 family member 1	N-linked	1							
P31948	STIP1	Stress-induced-phosphoprotein 1						1			
P35030	PRSS3	Trypsin-3					1				
P35626	GRK3	Beta-adrenergic receptor kinase 2							1		
P36957	DLST	Dihydrolypoyllysine-residue succinyltransferase component of 2-oxoglutarate dehydrogenase complex, mitochondrial				1					
P39059	COL15A1	Collagen alpha-1	N-linked, O-linked			1					
P39880	CUX1	Homeobox protein cut-like 1						1			
P43007	SLC1A4	Neutral amino acid transporter A	N-linked	1							
P46063	RECQL	ATP-dependent DNA helicase Q1			1						
P48454	PPP3CC	Serine/threonine-protein phosphatase 2B catalytic subunit gamma isoform							1		
P48509	CD151	CD151 antigen	N-linked				1				
P48552	NRIP1	Nuclear receptor-interacting protein 1									1
P50991	CCT4	T-complex protein 1 subunit delta				1					
P52565	ARHGDI A	Rho GDP-dissociation inhibitor 1							1		
P55011	SLC12A2	Solute carrier family 12 member 2									1
P56539	CAV3	Caveolin-3									1
P56962	STX17	Syntaxin-17					1				
P58499	FAM3B	Protein FAM3B	N-linked		1						
P60981	DSTN	Destrin			1						
P61026	RAB10	Ras-related protein Rab-10			1						
P61803	DAD1	Dolichyl-diphosphooligosaccharide-protein glycosyltransferase subunit DAD1			1						

Appendix Table 1. Proteomic dataset of proteins found in normal prostate tissue slice cultures (TSCs)

ACCN	Gene Name	Protein Name	Annotated Glycosylated	N1	N2	N3	N4	N5	N6	N7	N8
P61981	YWHAG	14-3-3 protein gamma									1
P62072	TIMM10	Mitochondrial import inner membrane translocase subunit Tim10						1			
P78417	GSTO1	Glutathione S-transferase omega-1				1					
Q00325	SLC25A3	Phosphate carrier protein, mitochondrial									1
Q00597	FANCC	Fanconi anemia group C protein					1				
Q04760	GLO1	Lactoylglutathione lyase				1					
Q04917	YWHAH	14-3-3 protein eta									1
Q07021	C1QBP	Complement component 1 Q subcomponent-binding protein, mitochondrial				1					
Q07075	ENPEP	Glutamyl aminopeptidase	N-linked						1		
Q08174	PCDH1	Protocadherin-1	N-linked						1		
Q10472	GALNT1	Polypeptide N-acetylgalactosaminyltransferase 1	N-linked			1					
Q12769	NUP160	Nuclear pore complex protein Nup160						1			
Q12931	TRAP1	Heat shock protein 75 kDa, mitochondrial									1
Q13126	MTAP	S-methyl-5'-thioadenosine phosphorylase				1					
Q13136	PPFIA1	Liprin-alpha-1									1
Q13315	ATM	Serine-protein kinase ATM						1			
Q13642	FHL1	Four and a half LIM domains protein 1		1							
Q14112	NID2	Nidogen-2	N-linked								1
Q14116	IL18	Interleukin-18							1		
Q14204	DYNC1H1	Cytoplasmic dynein 1 heavy chain 1						1			
Q14232	EIF2B1	Translation initiation factor eIF-2B subunit alpha		1							
Q14974	KPNB1	Importin subunit beta-1				1					
Q14980	NUMA1	Nuclear mitotic apparatus protein 1	O-linked		1						
Q15084	PDIA6	Protein disulfide-isomerase A6							1		
Q15262	PTPRK	Receptor-type tyrosine-protein phosphatase kappa	N-linked			1					
Q15366	PCBP2	Poly			1						
Q15836	VAMP3	Vesicle-associated membrane protein 3				1					
Q16352	INA	Alpha-internexin									1
Q3MIR4	TMEM30B	Cell cycle control protein 50B	N-linked		1						
Q4KMZ1	IQCC	IQ domain-containing protein C								1	
Q53HC0	CCDC92	Coiled-coil domain-containing protein 92			1						
Q5SYB0	FRMPD1	FERM and PDZ domain-containing protein 1			1						
Q5VWN6	FAM208B	Protein FAM208B				1					
Q68DK2	ZFYVE26	Zinc finger FYVE domain-containing protein 26									1
Q6NZI2	PTRF	Polymerase I and transcript release				1					

Appendix Table 1. Proteomic dataset of proteins found in normal prostate tissue slice cultures (TSCs)

ACCN	Gene Name	Protein Name	Annotated Glycosylated	N1	N2	N3	N4	N5	N6	N7	N8
		factor									
Q6P1J6	PLB1	Phospholipase B1, membrane-associated	N-linked					1			
Q6PI98	INO80C	INO80 complex subunit C				1					
Q6UWU2	GLB1L	Beta-galactosidase-1-like protein	N-linked				1				
Q6UXG2	KIAA1324	UPF0577 protein KIAA1324	N-linked		1						
Q6ZRP7	QSOX2	Sulfhydryl oxidase 2	N-linked	1							
Q6ZS30	NBEAL1	Neurobeachin-like protein 1									1
Q7Z5A9	FAM19A1	Protein FAM19A1				1					
Q7Z7N9	TMEM179B	Transmembrane protein 179B		1							
Q86U37	LINC01551	Uncharacterized protein encoded by LINC01551		1							
Q86VD9	PIGZ	GPI mannosyltransferase 4					1				
Q86Y46	KRT73	Keratin, type II cytoskeletal 73									1
Q8IUG5	MYO18B	Unconventional myosin-XVIIIb							1		
Q8IVB5	LIX1L	LIX1-like protein					1				
Q8N300	SVBP	Small vasohibin-binding protein							1		
Q8N4G2	ARL14	ADP-ribosylation factor-like protein 14					1				
Q8N715	CCDC185	Coiled-coil domain-containing protein 185			1						
Q8N8G6	C15orf54	Putative uncharacterized protein C15orf54			1						
Q8NEL9	DDHD1	Phospholipase DDHD1			1						
Q8NG11	TSPAN14	Tetraspanin-14	N-linked				1				
Q8TD19	NEK9	Serine/threonine-protein kinase Nek9				1					
Q92667	AKAP1	A-kinase anchor protein 1, mitochondrial									1
Q92928	RAB1C	Putative Ras-related protein Rab-1C		1							
Q96A08	HIST1H2B A	Histone H2B type 1-A								1	
Q96A26	FAM162A	Protein FAM162A				1					
Q96EE4	CCDC126	Coiled-coil domain-containing protein 126	N-linked				1				
Q96FQ6	S100A16	Protein S100-A16					1				
Q96JG8	MAGED4	Melanoma-associated antigen D4							1		
Q96Q06	PLIN4	Perilipin-4		1							
Q99102	MUC4	Mucin-4	N-linked, O-linked				1				
Q99592	ZBTB18	Zinc finger and BTB domain-containing protein 18						1			
Q9BQ52	ELAC2	Zinc phosphodiesterase ELAC protein 2					1				
Q9BTV4	TMEM43	Transmembrane protein 43				1					
Q9BYB0	SHANK3	SH3 and multiple ankyrin repeat domains protein 3					1				
Q9BYG4	PARD6G	Partitioning defective 6 homolog gamma					1				
Q9GZN1	ACTR6	Actin-related protein 6									1

Appendix Table 1. Proteomic dataset of proteins found in normal prostate tissue slice cultures (TSCs)

ACCN	Gene Name	Protein Name	Annotated Glycosylated	N1	N2	N3	N4	N5	N6	N7	N8
Q9GZZ9	UBA5	Ubiquitin-like modifier-activating enzyme 5						1			
Q9H0C2	SLC25A31	ADP/ATP translocase 4									1
Q9NQ84	GPRC5C	G-protein coupled receptor family C group 5 member C	N-linked		1						
Q9NQX4	MYO5C	Unconventional myosin-Vc							1		
Q9NR09	BIRC6	Baculoviral IAP repeat-containing protein 6							1		
Q9NVN3	RIC8B	Synembryn-B									1
Q9NX62	IMPAD1	Inositol monophosphatase 3	N-linked						1		
Q9NY35	CLDND1	Claudin domain-containing protein 1	N-linked	1							
Q9NYZ2	SLC25A37	Mitoferrin-1		1							
Q9NZK5	CECR1	Adenosine deaminase CECR1	N-linked							1	
Q9P2E9	RRBP1	Ribosome-binding protein 1					1				
Q9UBY0	SLC9A2	Sodium/hydrogen exchanger 2	N-linked			1					
Q9UBZ9	REV1	DNA repair protein REV1				1					
Q9UGC7	MTRF1L	Peptide chain release factor 1-like, mitochondrial		1							
Q9UGM3	DMBT1	Deleted in malignant brain tumors 1 protein	N-linked	1							
Q9UHL4	DPP7	Dipeptidyl peptidase 2	N-linked				1				
Q9UKX3	MYH13	Myosin-13			1						
Q9ULX5	RNF112	RING finger protein 112			1						
Q9UMS6	SYNPO2	Synaptopodin-2		1							
Q9UNN8	PROCR	Endothelial protein C receptor	N-linked							1	
Q9Y6M5	SLC30A1	Zinc transporter 1	N-linked				1				
Q9Y6R7	FCGBP	IgGfC-binding protein	N-linked				1				

Appendix Table 2. Proteomic dataset of proteins found in normal and cancer prostate tissue slice cultures (TSCs). Proteins found in prostate cancer (c1-8) proteomic dataset. Columns include uniprot accession numbers (ACCN), gene names, protein names, Swiss-Prot databank annotations of glycosylation. The total number of identified peptide sequences (peptide spectrum matches) for the protein, including those redundantly identified.

ACCN	Gene Name	Protein Name	Annotated Glycosylated	C1	C2	C3	C4	C5	C6	C7	C8
P35749	MYH11	Myosin-11		13	14	12	13	28	42	66	56
P12111	COL6A3	Collagen alpha-3	N-linked, O-linked	4	8	3	11	5	28	40	67
P13645	KRT10	Keratin, type I cytoskeletal 10		16	14	12	13	17	42	45	38
P04264	KRT1	Keratin, type II cytoskeletal 1		25	15	14	13	15	41	45	37
P21333	FLNA	Filamin-A			18	9	9	19	5	6	57
P35908	KRT2	Keratin, type II cytoskeletal 2 epidermal		16	8	8	11	9	24	31	26
Q7Z5K2	WAPL	Wings apart-like protein homolog		25	28	27	3	20			
P05556	ITGB1	Integrin beta-1	N-linked	11	11	13	8	10	24	26	22
P18206	VCL	Vinculin			8	6	17	14	4	1	45
P35527	KRT9	Keratin, type I cytoskeletal 9		19	11	13	4	11	25	30	31
P01011	SERPINA3	Alpha-1-antichymotrypsin	N-linked	15	8	11	17	21	36	48	12
P17301	ITGA2	Integrin alpha-2	N-linked	3	8	9	6	4	18	21	12
P17661	DES	Desmin		4	6	2	3	7	12	11	19
P24821	TNC	Tenascin	N-linked	2	1	2	6	7	21	19	4
P06756	ITGAV	Integrin alpha-V	N-linked	2	6	7	8	12	14	16	9
P51884	LUM	Lumican	N-linked	2	9	9	6	8	8	10	22
Q01995	TAGLN	Transgelin		4	9	10	6	7	16	18	22
P63267	ACTG2	Actin, gamma-enteric smooth muscle			5	5	5	5			31
P08195	SLC3A2	4F2 cell-surface antigen heavy chain	N-linked	2	5	6	6	6	23	26	27
P07093	SERPINE2	Glia-derived nexin	N-linked	11	5	5	4	8	6	9	9
Q9Y490	TLN1	Talin-1			10	6	11	6			7
P08758	ANXA5	Annexin A5		3	7	6	4	4	13	19	21
P35579	MYH9	Myosin-9			3		1	15			24
P68871	HBB	Hemoglobin subunit beta	N-linked	3	2	3	5	10	24	25	22
P23229	ITGA6	Integrin alpha-6	N-linked	2	2	1	5	2	7	8	
P60660	MYL6	Myosin light polypeptide 6		4	6	4	3	4	7	8	10
P09758	TACSTD2	Tumor-associated calcium signal transducer 2	N-linked	3	4	4	6	6	13	18	11
P08133	ANXA6	Annexin A6									9
Q08380	LGALS3BP	Galectin-3-binding protein	N-linked	8	11	14	3	8	15	18	6
Q09666	AHNAK	Neuroblast differentiation-associated protein AHNAK		8	6	7	11	13	5	7	4
Q16853	AOC3	Membrane primary amine oxidase	N-linked, O-linked	4	2		3	6	7	10	11
P13647	KRT5	Keratin, type II cytoskeletal 5		9	2		5	5	10	10	9
Q13740	ALCAM	CD166 antigen	N-linked	8	7	8	7	10	20	23	19
P02768	ALB	Serum albumin	N-linked	5	1	1	3	5	12	13	15

Appendix Table 2. Proteomic dataset of proteins found in cancer prostate tissue slice cultures (TSCs)

ACCN	Gene Name	Protein Name	Annotated Glycosylated	C1	C2	C3	C4	C5	C6	C7	C8
P09493	TPM1	Tropomyosin alpha-1 chain		3	6	5	3	7	10	9	13
P10909	CLU	Clusterin	N-linked	5	3	4	4	8	12	14	9
P60709	ACTB	Actin, cytoplasmic 1		3	6	3	5	6	23	29	25
P02533	KRT14	Keratin, type I cytoskeletal 14		11	3		5	3	8	9	11
Q15758	SLC1A5	Neutral amino acid transporter B	N-linked	7	6	6	2	3	10	11	9
P11142	HSPA8	Heat shock cognate 71 kDa protein					7	3	14	14	12
P11021	HSPA5	78 kDa glucose-regulated protein		2	5	6	10	11	19	23	29
P51888	PRELP	Prolargin	N-linked		1		3	5	8	16	25
P25311	AZGP1	Zinc-alpha-2-glycoprotein	N-linked	4	2	2	3	5	22	30	14
P05362	ICAM1	Intercellular adhesion molecule 1	N-linked	6	7	7	5	4	13	16	17
P08779	KRT16	Keratin, type I cytoskeletal 16		8			5		8	9	11
P12109	COL6A1	Collagen alpha-1	N-linked				1	3	2	8	8
P08648	ITGA5	Integrin alpha-5	N-linked	4	4	5	3	4	16	11	16
P62805	HIST1H4A	Histone H4		2	3	2	3	3	7	10	10
P04259	KRT6B	Keratin, type II cytoskeletal 6B		11			5	5	14		
P05787	KRT8	Keratin, type II cytoskeletal 8					7	5	16	20	33
P07355	ANXA2	Annexin A2			5	5			24	32	18
P26006	ITGA3	Integrin alpha-3	N-linked	2	2	2	2	1	6	6	
O75976	CPD	Carboxypeptidase D	N-linked	3	5	2	11	11	19	25	10
P15144	ANPEP	Aminopeptidase N	N-linked	15	3	4	18	10	51	56	24
P62736	ACTA2	Actin, aortic smooth muscle							23	32	33
P02788	LTF	Lactotransferrin	N-linked	1		1	25	6			
P63104	YWHAZ	14-3-3 protein zeta/delta		3	8	6	4	6	10	11	17
P11279	LAMP1	Lysosome-associated membrane glycoprotein 1	N-linked, O-linked	3	4	3	4	4	7	8	9
P68032	ACTC1	Actin, alpha cardiac muscle 1							23		33
Q14108	SCARB2	Lysosome membrane protein 2	N-linked	3	4	4	2	5	16	15	9
P02545	LMNA	Prelamin-A/C [Cleaved into: Lamin-A/C		2	3	4	6	4	4	12	35
P02751	FN1	Fibronectin	N-linked, O-linked		1	1	10	8		1	1
P07951	TPM2	Tropomyosin beta chain				5	3	5	8	5	12
P11047	LAMC1	Laminin subunit gamma-1	N-linked				1	2			2
P54709	ATP1B3	Sodium/potassium-transporting ATPase subunit beta-3	N-linked	1	1	2	2	2	8	10	6
P08962	CD63	CD63 antigen	N-linked	3	2	3	2	3	8	12	8
P35613	BSG	Basigin	N-linked	3	4	4	2	5	5	10	6
Q06830	PRDX1	Peroxiredoxin-1		2	2	2	3	3	6	8	9
Q8NBJ4	GOLM1	Golgi membrane protein 1	N-linked	5	6	8	7	7	6	14	2
P05026	ATP1B1	Sodium/potassium-transporting ATPase subunit beta-1	N-linked	1	4	3	2	3	3	4	2

Appendix Table 2. Proteomic dataset of proteins found in cancer prostate tissue slice cultures (TSCs)

ACCN	Gene Name	Protein Name	Annotated Glycosylated	C1	C2	C3	C4	C5	C6	C7	C8
P05090	APOD	Apolipoprotein D	N-linked	3	4	5	3	3	7	7	7
P06733	ENO1	Alpha-enolase		1	4	4	6	3	12	24	10
Q14126	DSG2	Desmoglein-2	N-linked	2	7	5	3	3	6	4	
Q96KK5	HIST1H2A H	Histone H2A type 1-H			2	2	2	2	7	8	8
P06731	CEACAM5	Carcinoembryonic antigen-related cell adhesion molecule 5	N-linked	3	2	2			4	5	2
P08473	MME	Neprilysin	N-linked	2			1	8	7	8	4
P12110	COL6A2	Collagen alpha-2	N-linked					2	3	4	6
P13473	LAMP2	Lysosome-associated membrane glycoprotein 2	N-linked, O-linked	2	2	2	1	5	6	6	6
P27348	YWHAQ	14-3-3 protein theta		3	5	5					8
P27701	CD82	CD82 antigen	N-linked	5	2	3	1	4		1	
P68133	ACTA1	Actin, alpha skeletal muscle							23		27
Q13641	TPBG	Trophoblast glycoprotein	N-linked	1	1	2	2	2	4	5	7
P04792	HSPB1	Heat shock protein beta-1			5	3	1	2	6	8	7
P16284	PECAM1	Platelet endothelial cell adhesion molecule	N-linked	2	5	5	1	6	4	8	9
P21810	BGN	Biglycan	N-linked, O-linked	1	1	1	1	2	5	10	17
P51911	CNN1	Calponin-1			3	3	4	6	2	5	6
Q05707	COL14A1	Collagen alpha-1	N-linked, O-linked					3			12
P20774	OGN	Mimecan	N-linked, O-linked		1	1		1			4
P24844	MYL9	Myosin regulatory light polypeptide 9					3	4	4	4	6
P68104	EEF1A1	Elongation factor 1-alpha 1		2	2	1	1	3	12	17	8
Q13510	ASAH1	Acid ceramidase	N-linked	6	1	3	7	3	12	11	8
Q92542	NCSTN	Nicastrin	N-linked	4	2	5	3	8	9	12	3
Q9BQE3	TUBA1C	Tubulin alpha-1C chain					1	1	15	20	11
O60814	HIST1H2B K	Histone H2B type 1-K	O-linked		1	1	1	3		3	5
P01033	TIMP1	Metalloproteinase inhibitor 1	N-linked	2	2	2	2	2	4	4	4
P02538	KRT6A	Keratin, type II cytoskeletal 6A									
P02794	FTH1	Ferritin heavy chain			2	1	2	3	9	10	14
P05121	SERPINE1	Plasminogen activator inhibitor 1	N-linked		1	1	1	1	2	3	4
P08670	VIM	Vimentin	O-linked				2	2	10	13	21
P10809	HSPD1	60 kDa heat shock protein, mitochondrial		2	4	4	8	11	19	24	29
Q14CN2	CLCA4	Calcium-activated chloride channel regulator 4	N-linked	1			1				
P07237	P4HB	Protein disulfide-isomerase					1	8	17	22	28
P07339	CTSD	Cathepsin D	N-linked, O-linked	4	3	4	6	3	12	13	4
P0DMV8	HSPA1A	Heat shock 70 kDa protein 1A					5		10	15	11
P0CG48	UBC	Polyubiquitin-C		1	3	3	2	2	5	6	5
P13688	CEACAM1	Carcinoembryonic antigen-related cell adhesion molecule 1	N-linked				2	3	8	10	4

Appendix Table 2. Proteomic dataset of proteins found in cancer prostate tissue slice cultures (TSCs)

ACCN	Gene Name	Protein Name	Annotated Glycosylated	C1	C2	C3	C4	C5	C6	C7	C8
P62258	YWHAE	14-3-3 protein epsilon			5	3	4	3	9	10	9
P06753	TPM3	Tropomyosin alpha-3 chain		3	5	5	2	6		4	5
Q06323	PSME1	Proteasome activator complex subunit 1		1	4	3	4	6	5	7	2
P23528	CFL1	Cofilin-1		1	4	4	3	3	7	8	4
P32119	PRDX2	Peroxiredoxin-2		1	2	2	3	2		4	3
P43121	MCAM	Cell surface glycoprotein MUC18	N-linked	2	1	1	1	5	1	2	3
P50895	BCAM	Basal cell adhesion molecule	N-linked	7	2	2	6	5	10	11	2
P63261	ACTG1	Actin, cytoplasmic 2							23	29	25
Q03135	CAV1	Caveolin-1			1	1		1	2	2	2
P02786	TFRC	Transferrin receptor protein 1	N-linked, O-linked	2	5	5	3		3	4	10
P04406	GAPDH	Glyceraldehyde-3-phosphate dehydrogenase			1	1	3	2	8	11	10
P14625	HSP90B1	Endoplasmic	N-linked		3	1	4	2	22	25	33
P15586	GNS	N-acetylglucosamine-6-sulfatase	N-linked	2	3	4	3	5	9	10	4
P18827	SDC1	Syndecan-1	N-linked, O-linked	1	1	1		1	2	2	2
P45880	VDAC2	Voltage-dependent anion-selective channel protein 2		1	6	5	3	1	10	10	10
P55268	LAMB2	Laminin subunit beta-2	N-linked					1			
Q08722	CD47	Leukocyte surface antigen CD47	N-linked	2	1	1	1	1	6	7	6
Q15746	MYLK	Myosin light chain kinase, smooth muscle		1	4	3	2	2			
P04179	SOD2	Superoxide dismutase [Mn], mitochondrial		2			2	3	9	14	7
P08238	HSP90AB1	Heat shock protein HSP 90-beta	O-linked				3	2	13	24	15
P08727	KRT19	Keratin, type I cytoskeletal 19						2	9	12	15
P13796	LCP1	Plastin-2			2	4	3	3	6	7	11
Q14BN4	SLMAP	Sarcolemmal membrane-associated protein		1				2			
Q9P2B2	PTGFRN	Prostaglandin F2 receptor negative regulator	N-linked	3			2	2	7	9	1
P15309	ACPP	Prostatic acid phosphatase	N-linked	2	1		3	5	19	28	13
P16070	CD44	CD44 antigen	N-linked, O-linked	4	2	2	1	1	4	6	6
P21589	NT5E	5'-nucleotidase	N-linked			1		1			
P60174	TPI1	Triosephosphate isomerase		1	3	2	1	2	7	9	7
Q07065	CKAP4	Cytoskeleton-associated protein 4					3	1			8
P02792	FTL	Ferritin light chain		1	1	1	1	1	6	8	10
P09382	LGALS1	Galectin-1		1		1	1	3	2	2	4
P27824	CANX	Calnexin		2	2	1	1	3	8	9	14
P31947	SFN	14-3-3 protein sigma							6		7
P68363	TUBA1B	Tubulin alpha-1B chain							15	20	11
P69905	HBA1;	Hemoglobin subunit alpha	N-linked					3	11	12	11
Q6YHK3	CD109	CD109 antigen	N-linked		2	1	2				

Appendix Table 2. Proteomic dataset of proteins found in cancer prostate tissue slice cultures (TSCs)

ACCN	Gene Name	Protein Name	Annotated Glycosylated	C1	C2	C3	C4	C5	C6	C7	C8
Q99715	COL12A1	Collagen alpha-1	N-linked, O-linked					6	2	4	5
P27105	STOM	Erythrocyte band 7 integral membrane protein					3				
P30048	PRDX3	Thioredoxin-dependent peroxide reductase, mitochondrial					2	3	4	6	8
P38646	HSPA9	Stress-70 protein, mitochondrial					7	4	4	5	4
Q15063	POSTN	Periostin	N-linked		1	1					24
Q8IV08	PLD3	Phospholipase D3	N-linked	1	2	1	2	1	4	4	
Q92520	FAM3C	Protein FAM3C		1	1	1	2	3			
Q9UIQ6	LNPEP	Leucyl-cystinyl aminopeptidase	N-linked		1	2	4	2	3	7	1
O14494	PLPP1	Phospholipid phosphatase 1	N-linked		1	2	2	2	4	6	3
P00558	PGK1	Phosphoglycerate kinase 1			2	1	5	2	15	20	7
P01009	SERPINA1	Alpha-1-antitrypsin	N-linked	2	1	1	3	4	5	6	2
P02042	HBD	Hemoglobin subunit delta					2	5	14	15	12
P02750	LRG1	Leucine-rich alpha-2-glycoprotein	N-linked, O-linked	2		3	5	7	7	9	2
P04083	ANXA1	Annexin A1							5	8	8
P04908	HIST1H2A B	Histone H2A type 1-B/E							7	8	8
P06703	S100A6	Protein S100-A6		2	1	2		1	4	4	3
P08253	MMP2	72 kDa type IV collagenase	N-linked	3	2	2	3				
P0C0S8	HIST1H2A G	Histone H2A type 1							7	8	8
P12830	CDH1	Cadherin-1	N-linked		1	2		4		3	
P13987	CD59	CD59 glycoprotein	N-linked, O-linked	1	1	1	1	1	2	2	2
P20671	HIST1H2A D	Histone H2A type 1-D							7	8	8
P23142	FBLN1	Fibulin-1	N-linked	1	2	2	1		3	3	
Q16777	HIST2H2A C	Histone H2A type 2-C							7	8	8
Q53GD3	SLC44A4	Choline transporter-like protein 4	N-linked	2	2	2	2	1	3	7	2
Q6FI13	HIST2H2A A3	Histone H2A type 2-A							7	8	8
Q7L7L0	HIST3H2A	Histone H2A type 3							7	8	8
Q8NFD2	ANKK1	Ankyrin repeat and protein kinase domain-containing protein 1						1			
Q93077	HIST1H2A C	Histone H2A type 1-C							7	8	8
Q99878	HIST1H2AJ	Histone H2A type 1-J							7	8	8
Q9BTM1	H2AFJ	Histone H2A.J							7	8	8
Q9Y6C2	EMILIN1	EMILIN-1	N-linked					3			
O00391	QSOX1	Sulfhydryl oxidase 1	N-linked		1	3				2	
P00750	PLAT	Tissue-type plasminogen activator	N-linked, O-linked	1			1				
P05155	SERPING1	Plasma protease C1 inhibitor	N-linked, O-linked	3		1	3	2	14	16	
P06576	ATP5B	ATP synthase subunit beta, mitochondrial	O-linked			1	6	1	12	20	14
P07195	LDHB	L-lactate dehydrogenase B chain			1		1		2	5	4

Appendix Table 2. Proteomic dataset of proteins found in cancer prostate tissue slice cultures (TSCs)

ACCN	Gene Name	Protein Name	Annotated Glycosylated	C1	C2	C3	C4	C5	C6	C7	C8
P0CG47	UBB	Polyubiquitin-B [Cleaved into: Ubiquitin]							5	6	5
P16422	EPCAM	Epithelial cell adhesion molecule	N-linked	3	2	2	1	2	2	4	
P19105	MYL12A	Myosin regulatory light chain 12A		1				4	6	4	8
P29401	TKT	Transketolase					1	1		7	7
P35580	MYH10	Myosin-10									9
P42892	ECE1	Endothelin-converting enzyme 1	N-linked	2	3	2	3	4	2	7	3
P62979	RPS27A	Ubiquitin-40S ribosomal protein S27a							5	6	5
P62987	UBA52	Ubiquitin-60S ribosomal protein L40							5	6	5
P78310	CXADR	Coxsackievirus and adenovirus receptor	N-linked	2	2	3	1	4	2	2	
Q05682	CALD1	Caldesmon		4	6	10	4	2			6
Q14315	FLNC	Filamin-C									3
Q16563	SYPL1	Synaptophysin-like protein 1	N-linked	1	1	2	1	1	2	2	2
Q6UX06	OLFM4	Olfactomedin-4	N-linked	1	2	2	2		10	13	
Q71U36	TUBA1A	Tubulin alpha-1A chain									9
Q7Z406	MYH14	Myosin-14									6
Q9H5V8	CDCP1	CUB domain-containing protein 1	N-linked	1	2	1		3	6	1	
O15118	NPC1	Niemann-Pick C1 protein	N-linked	1	2	2	1	2	8	6	3
P04075	ALDOA	Fructose-bisphosphate aldolase A			1		2	2	7	8	7
P07602	PSAP	Prosaposin	N-linked	2	1	2		3			
P07996	THBS1	Thrombospondin-1	N-linked, O-linked	1	2	4	2	1	2	2	
P27487	DPP4	Dipeptidyl peptidase 4	N-linked	3			2	6	8	8	9
P39060	COL18A1	Collagen alpha-1	N-linked, O-linked		1			2			2
Q04695	KRT17	Keratin, type I cytoskeletal 17		5							6
A5A3E0	POTEF	POTE ankyrin domain family member F									12
O14950	MYL12B	Myosin regulatory light chain 12B							6	4	8
O60487	MPZL2	Myelin protein zero-like protein 2	N-linked		2	2	1	1	2		
O95858	TSPAN15	Tetraspanin-15	N-linked	2			1	1	3	2	
P01019	AGT	Angiotensinogen	N-linked		1		2	1	4	6	
P07737	PFN1	Profilin-1			1	2	3	1	2	6	3
P10253	GAA	Lysosomal alpha-glucosidase	N-linked		1	1	3	5	10	13	
P31949	S100A11	Protein S100-A11		1	2	2			4	4	4
P37802	TAGLN2	Transgelin-2			3	3	1	1	2	2	7
P54652	HSPA2	Heat shock-related 70 kDa protein 2			3	3					10
P80188	LCN2	Neutrophil gelatinase-associated lipocalin	N-linked	1			2	1	5	6	
Q15365	PCBP1	Poly		1	2	1	1		2	2	2
Q5VTE0	EEF1A1P5	Putative elongation factor 1-alpha-like 3							12	17	8

Appendix Table 2. Proteomic dataset of proteins found in cancer prostate tissue slice cultures (TSCs)

ACCN	Gene Name	Protein Name	Annotated Glycosylated	C1	C2	C3	C4	C5	C6	C7	C8
Q6S8J3	POTEE	POTE ankyrin domain family member E									12
Q7Z2Q7	LRRC70	Leucine-rich repeat-containing protein 70	N-linked					2			
Q8N271	PROM2	Prominin-2	N-linked		3	1	3				
Q8NBN3	TMEM87A	Transmembrane protein 87A	N-linked		1	1		2	4	5	2
Q96KP4	CNDP2	Cytosolic non-specific dipeptidase					3	3	9	12	9
Q9BVK6	TMED9	Transmembrane emp24 domain-containing protein 9	N-linked		1	1	2	3	8	7	3
O00461	GOLIM4	Golgi integral membrane protein 4	N-linked				1	1			
O43653	PSCA	Prostate stem cell antigen	N-linked		1						
O75369	FLNB	Filamin-B								4	3
O94919	ENDOD1	Endonuclease domain-containing 1 protein			1		3	1	2	2	
P00533	EGFR	Epidermal growth factor receptor	N-linked			1	1		2	2	
P01889	HLA-B	HLA class I histocompatibility antigen, B-7 alpha chain	N-linked		3				6		
P05023	ATP1A1	Sodium/potassium-transporting ATPase subunit alpha-1							9	5	9
P07288	KLK3	Prostate-specific antigen	N-linked	1		1	2	2	7	9	5
P07585	DCN	Decorin	N-linked, O-linked		1	1		2		1	5
P15941	MUC1	Mucin-1	N-linked, O-linked	1	2	3	1	2	5	8	1
P19256	CD58	Lymphocyte function-associated antigen 3	N-linked	1		1	1	1	2	2	
P25705	ATP5A1	ATP synthase subunit alpha, mitochondrial	O-linked				5		13	15	12
P37837	TALDO1	Transaldolase			1	1	2	1	5	7	3
P40926	MDH2	Malate dehydrogenase, mitochondrial	O-linked		1		4	3	4	8	16
P49748	ACADVL	Very long-chain specific acyl-CoA dehydrogenase, mitochondrial								1	
P62937	PPIA	Peptidyl-prolyl cis-trans isomerase A	N-linked		2		1	1	4	4	4
P68366	TUBA4A	Tubulin alpha-4A chain									6
Q00765	REEP5	Receptor expression-enhancing protein 5		1	1			2			
Q12841	FSTL1	Follistatin-related protein 1	N-linked			2			2	2	
Q15323	KRT31	Keratin, type I cuticular Ha1									2
Q8IWA5	SLC44A2	Choline transporter-like protein 2	N-linked				1	1	3	5	2
Q8NFJ5	GPRC5A	Retinoic acid-induced protein 3	N-linked	1	1	1	1	1	2	2	1
Q92896	GLG1	Golgi apparatus protein 1	N-linked		1	2	2	1	5	6	2
Q9NRX5	SERINC1	Serine incorporator 1	N-linked		1		1	1	2	2	1
Q9UL46	PSME2	Proteasome activator complex subunit 2		2	1	1	1	2	2	2	
Q9Y277	VDAC3	Voltage-dependent anion-selective channel protein 3		1	1	1	4	3	9	10	9
Q9Y624	F11R	Junctional adhesion molecule A	N-linked	2	1	2	2	1	1	3	2
O75915	ARL6IP5	PRA1 family protein 3		1	2	3	4	1		1	2
P00450	CP	Ceruloplasmin	N-linked	2			6	4	7	14	
P07900	HSP90AA1	Heat shock protein HSP 90-alpha			3				14	26	18

Appendix Table 2. Proteomic dataset of proteins found in cancer prostate tissue slice cultures (TSCs)

ACCN	Gene Name	Protein Name	Annotated Glycosylated	C1	C2	C3	C4	C5	C6	C7	C8
P08729	KRT7	Keratin, type II cytoskeletal 7									4
P12814	ACTN1	Alpha-actinin-1							2	5	13
P21291	CSRP1	Cysteine and glycine-rich protein 1			1	3	1	1		3	1
P31629	HIVEP2	Transcription factor HIVEP2		1				4			
P48960	CD97	CD97 antigen	N-linked	1				1			
P67936	TPM4	Tropomyosin alpha-4 chain			3	3					9
Q05639	EEF1A2	Elongation factor 1-alpha 2									4
Q15149	PLEC	Plectin					2				
Q92764	KRT35	Keratin, type I cuticular Ha5									2
Q9BYX7	POTEKP	Putative beta-actin-like protein 3									8
Q9NY65	TUBA8	Tubulin alpha-8 chain									6
A6NIZ1		Ras-related protein Rap-1b-like protein			1	1				2	
O14493	CLDN4	Claudin-4		1	1	1	1	1	2	2	2
O43707	ACTN4	Alpha-actinin-4							2	5	12
O43852	CALU	Calumenin	N-linked		1	1			3	4	5
O60664	PLIN3	Perilipin-3				1	4	3			
P00505	GOT2	Aspartate aminotransferase, mitochondrial							1	4	10
P06899	HIST1H2BJ	Histone H2B type 1-J	O-linked							3	3
P10319	HLA-B	HLA class I histocompatibility antigen, B-58 alpha chain	N-linked					2			4
P10599	TXN	Thioredoxin		3				2	2	2	2
P13646	KRT13	Keratin, type I cytoskeletal 13									11
P15151	PVR	Poliovirus receptor	N-linked	1	1		1	2	2		2
P15259	PGAM2	Phosphoglycerate mutase 2			1				2	2	2
P16870	CPE	Carboxypeptidase E	N-linked				1		2	2	
P17813	ENG	Endoglin	N-linked		3	1	2	2	4	4	7
P23284	PPIB	Peptidyl-prolyl cis-trans isomerase B	N-linked				4	1	4	5	7
P23527	HIST1H2B O	Histone H2B type 1-O	O-linked							3	3
P30041	PRDX6	Peroxiredoxin-6		1	1	2	1		3	6	5
P31946	YWHAB	14-3-3 protein beta/alpha			3	4					3
P33778	HIST1H2B B	Histone H2B type 1-B	O-linked							3	3
P36269	GGT5	Gamma-glutamyltransferase 5	N-linked		1	1	2	1	2	2	4
P40199	CEACAM6	Carcinoembryonic antigen-related cell adhesion molecule 6	N-linked	2							
P55083	MFAP4	Microfibril-associated glycoprotein 4	N-linked								2
P57053	H2BFS	Histone H2B type F-S	O-linked							3	5
P58876	HIST1H2B D	Histone H2B type 1-D	O-linked							3	5
P62807	HIST1H2B C	Histone H2B type 1-C/E/F/G/I	O-linked							3	5

Appendix Table 2. Proteomic dataset of proteins found in cancer prostate tissue slice cultures (TSCs)

ACCN	Gene Name	Protein Name	Annotated Glycosylated	C1	C2	C3	C4	C5	C6	C7	C8
Q03405	PLAUR	Urokinase plasminogen activator surface receptor	N-linked	1		1		1	2		2
Q13308	PTK7	Inactive tyrosine-protein kinase 7	N-linked	1			1	1	2	2	
Q13748	TUBA3C	Tubulin alpha-3C/D chain									5
Q15223	NECTIN1	Nectin-1	N-linked	2						1	
Q16778	HIST2H2B E	Histone H2B type 2-E	O-linked							3	3
Q5QNW6	HIST2H2BF	Histone H2B type 2-F	O-linked							3	5
Q6P4E1	CASC4	Protein CASC4		1	1	1	2	1	4	2	
Q6PEY2	TUBA3E	Tubulin alpha-3E chain									5
Q8N257	HIST3H2B B	Histone H2B type 3-B	O-linked							3	3
Q92692	NECTIN2	Nectin-2	N-linked	1			1	2		2	
Q93079	HIST1H2B H	Histone H2B type 1-H	O-linked							3	5
Q99877	HIST1H2B N	Histone H2B type 1-N	O-linked							3	5
Q99879	HIST1H2B M	Histone H2B type 1-M	O-linked							3	5
Q99880	HIST1H2BL	Histone H2B type 1-L	O-linked							3	5
Q9BYK8	HELZ2	Helicase with zinc finger domain 2		1				1			
Q9Y5Z0	BACE2	Beta-secretase 2	N-linked	3			3	1		1	
Q9Y639	NPTN	Neuroplastin	N-linked	1	1	1		1	2	2	
A6NMY6	ANXA2P2	Putative annexin A2-like protein					1				16
O00264	PGRMC1	Membrane-associated progesterone receptor component 1								1	
O00299	CLIC1	Chloride intracellular channel protein 1			1		1	1	2	2	2
O00754	MAN2B1	Lysosomal alpha-mannosidase	N-linked				3	2	1	2	
O60635	TSPAN1	Tetraspanin-1	N-linked				1	2			
O60637	TSPAN3	Tetraspanin-3	N-linked			1		2		1	
O75503	CLN5	Ceroid-lipofuscinosis neuronal protein 5	N-linked				2	1	3	4	
P04080	CSTB	Cystatin-B		1		1	1	1	2	4	2
P04439	HLA-A	HLA class I histocompatibility antigen, A-3 alpha chain	N-linked	3	3		3				6
P05067	APP	Amyloid beta A4 protein	N-linked, O-linked	3	1	1	1				
P05386	RPLP1	60S acidic ribosomal protein P1			1	1		1	2	2	2
P07437	TUBB	Tubulin beta chain							7	19	
P0C0S5	H2AFZ	Histone H2A.Z									5
P0CG38	POTEI	POTE ankyrin domain family member I									6
P0CG39	POTEJ	POTE ankyrin domain family member J									4
P11117	ACP2	Lysosomal acid phosphatase	N-linked				2	2	2	6	
P11166	SLC2A1	Solute carrier family 2, facilitated glucose transporter member 1	N-linked						5	4	1
P11717	IGF2R	Cation-independent mannose-6-phosphate receptor	N-linked				5	1		3	7

Appendix Table 2. Proteomic dataset of proteins found in cancer prostate tissue slice cultures (TSCs)

ACCN	Gene Name	Protein Name	Annotated Glycosylated	C1	C2	C3	C4	C5	C6	C7	C8
P14314	PRKCSH	Glucosidase 2 subunit beta	N-linked	1	2	2		1	4	5	6
P16104	H2AFX	Histone H2AX									4
P16190	HLA-A	HLA class I histocompatibility antigen, A-33 alpha chain	N-linked							6	6
P20645	M6PR	Cation-dependent mannose-6-phosphate receptor	N-linked	1	2	1			1	4	
P23141	CES1	Liver carboxylesterase 1	N-linked				1				
P30453	HLA-A	HLA class I histocompatibility antigen, A-34 alpha chain	N-linked							6	6
P30457	HLA-A	HLA class I histocompatibility antigen, A-66 alpha chain	N-linked							6	6
P30460	HLA-B	HLA class I histocompatibility antigen, B-8 alpha chain	N-linked						6		
P30480	HLA-B	HLA class I histocompatibility antigen, B-42 alpha chain	N-linked						6		
P35573	AGL	Glycogen debranching enzyme		1				1	1		1
P51572	BCAP31	B-cell receptor-associated protein 31					1	1	2	2	2
P56199	ITGA1	Integrin alpha-1	N-linked	1	1	4		3			8
Q00796	SORD	Sorbitol dehydrogenase					1	2	6	9	1
Q2M2I5	KRT24	Keratin, type I cytoskeletal 24									4
Q71UI9	H2AFV	Histone H2A.V									5
Q92187	ST8SIA4	CMP-N-acetylneuraminate-poly-alpha-2,8-sialyltransferase	N-linked	1		1		1			
Q92485	SMPDL3B	Acid sphingomyelinase-like phosphodiesterase 3b	N-linked	1			2	2	1	2	
Q969L2	MAL2	Protein MAL2	N-linked				1	1	2	2	2
Q96QV6	HIST1H2A A	Histone H2A type 1-A									4
Q96S97	MYADM	Myeloid-associated differentiation marker					1	1			
Q9BVC6	TMEM109	Transmembrane protein 109				1	1	1	2	1	2
Q9Y5Y6	ST14	Suppressor of tumorigenicity 14 protein	N-linked				1				
A6NGU5	GGT3P	Putative gamma-glutamyltranspeptidase 3	N-linked	2			3	3	2	3	3
A7E2Y1	MYH7B	Myosin-7B		1							
O95678	KRT75	Keratin, type II cytoskeletal 75									5
P02763	ORM1	Alpha-1-acid glycoprotein 1	N-linked	4				2	2	7	
P04233	CD74	HLA class II histocompatibility antigen gamma chain	N-linked, O-linked	1			2	1	2	2	
P07492	GRP	Gastrin-releasing peptide				1					
P08123	COL1A2	Collagen alpha-2	N-linked					1			
P09238	MMP10	Stromelysin-2					2		2	2	
P09525	ANXA4	Annexin A4							3	4	3
P0C0L4	C4A	Complement C4-A	N-linked, O-linked	1			5	7		63	1
P12277	CKB	Creatine kinase B-type					2		5	6	1
P13726	F3	Tissue factor	N-linked	1						1	
P14618	PKM	Pyruvate kinase PKM					1		11	14	1
P17693	HLA-G	HLA class I histocompatibility antigen, alpha chain G	N-linked								2

Appendix Table 2. Proteomic dataset of proteins found in cancer prostate tissue slice cultures (TSCs)

ACCN	Gene Name	Protein Name	Annotated Glycosylated	C1	C2	C3	C4	C5	C6	C7	C8
P18084	ITGB5	Integrin beta-5	N-linked	1							
P18669	PGAM1	Phosphoglycerate mutase 1							2	2	2
P19013	KRT4	Keratin, type II cytoskeletal 4									7
P30456	HLA-A	HLA class I histocompatibility antigen, A-43 alpha chain	N-linked								4
P30501	HLA-C	HLA class I histocompatibility antigen, Cw-2 alpha chain	N-linked	3							5
P50336	PPOX	Protoporphyrinogen oxidase							2	2	2
P55058	PLTP	Phospholipid transfer protein	N-linked				3				
P68371	TUBB4B	Tubulin beta-4B chain							7	18	
Q01518	CAP1	Adenylyl cyclase-associated protein 1						1	2	2	3
Q13228	SELENBP1	Selenium-binding protein 1					1				
Q13813	SPTAN1	Spectrin alpha chain, non-erythrocytic 1									1
Q14118	DAG1	Dystroglycan	N-linked, O-linked				1	1			
Q14512	FGFBP1	Fibroblast growth factor-binding protein 1	O-linked			1	1				
Q14956	GNPMB	Transmembrane glycoprotein NMB	N-linked				1	2	1		
Q5T9S5	CCDC18	Coiled-coil domain-containing protein 18					1				
Q687X5	STEAP4	Metalloreductase STEAP4	N-linked			1	2		2	7	
Q6EMK4	VASN	Vasorin	N-linked	1	1	1	1	1		1	5
Q7Z794	KRT77	Keratin, type II cytoskeletal 1b									3
Q8N0Y7	PGAM4	Probable phosphoglycerate mutase 4							2	2	2
Q969P0	IGSF8	Immunoglobulin superfamily member 8	N-linked		2	2	1				
Q96DA0	ZG16B	Zymogen granule protein 16 homolog B	N-linked	3					3	4	
Q99456	KRT12	Keratin, type I cytoskeletal 12									2
Q99988	GDF15	Growth/differentiation factor 15	N-linked				2	1	10	11	4
Q9C0H2	TTYH3	Protein tweety homolog 3	N-linked		1	3	1	2			
Q9H853	TUBA4B	Putative tubulin-like protein alpha-4B									2
Q9HBA9	FOLH1B	Putative N-acetylated-alpha-linked acidic dipeptidase	N-linked								1
Q9NQC3	RTN4	Reticulon-4						2	1	2	1
Q9UDY6	TRIM10	Tripartite motif-containing protein 10			5	5					
Q9Y3E0	GOLT1B	Vesicle transport protein GOT1B		1	1	1		1	1	2	
O00584	RNASET2	Ribonuclease T2	N-linked						1	1	4
O14880	MGST3	Microsomal glutathione S-transferase 3								1	
O15551	CLDN3	Claudin-3							2	2	3
O43493	TGOLN2	Trans-Golgi network integral membrane protein 2	N-linked	2	1	2	1	1		1	
O75106	AOC2	Retina-specific copper amine oxidase	N-linked								4
O94886	TMEM63A	CSC1-like protein 1					1		1	2	
O95197	RTN3	Reticulon-3							2	2	2

Appendix Table 2. Proteomic dataset of proteins found in cancer prostate tissue slice cultures (TSCs)

ACCN	Gene Name	Protein Name	Annotated Glycosylated	C1	C2	C3	C4	C5	C6	C7	C8
O95484	CLDN9	Claudin-9							2	2	2
P00403	MT-CO2	Cytochrome c oxidase subunit 2					1		2	2	2
P01833	PIGR	Polymeric immunoglobulin receptor	N-linked		2	1		1			
P01903	HLA-DRA	HLA class II histocompatibility antigen, DR alpha chain	N-linked		2	2	2	2	2	4	
P02100	HBE1	Hemoglobin subunit epsilon									1
P04921	GYPE	Glycophorin-C	N-linked, O-linked		1		1				
P05783	KRT18	Keratin, type I cytoskeletal 18	O-linked				2		6	6	14
P06396	GSN	Gelsolin							1	2	2
P06748	NPM1	Nucleophosmin			1	2	1	2		4	
P07686	HEXB	Beta-hexosaminidase subunit beta	N-linked						2	3	
P08572	COL4A2	Collagen alpha-2	N-linked								2
P0C0L5	C4B	Complement C4-B	N-linked						34	63	1
P12035	KRT3	Keratin, type II cytoskeletal 3									5
P12757	SKIL	Ski-like protein				4					
P13639	EEF2	Elongation factor 2							4	7	7
P13747	HLA-E	HLA class I histocompatibility antigen, alpha chain E	N-linked					2			2
P14136	GFAP	Glial fibrillary acidic protein									3
P14649	MYL6B	Myosin light chain 6B									2
P18564	ITGB6	Integrin beta-6	N-linked				1			2	
P19440	GGT1	Gamma-glutamyltranspeptidase 1	N-linked						2	3	3
P20073	ANXA7	Annexin A7							1	1	
P21796	VDAC1	Voltage-dependent anion-selective channel protein 1		2		1	3		13	12	16
P23946	CMA1	Chymase	N-linked						2	4	
P29034	S100A2	Protein S100-A2								1	
P30825	SLC7A1	High affinity cationic amino acid transporter 1	N-linked				1	1			
P31997	CEACAM8	Carcinoembryonic antigen-related cell adhesion molecule 8	N-linked								2
P36268	GGT2	Inactive gamma-glutamyltranspeptidase 2	N-linked						2	3	3
P45877	PPIC	Peptidyl-prolyl cis-trans isomerase C					1				
P48741	HSPA7	Putative heat shock 70 kDa protein 7									5
P56747	CLDN6	Claudin-6							2	2	2
P60033	CD81	CD81 antigen			2	2					1
P61224	RAP1B	Ras-related protein Rap-1b								2	
P62834	RAP1A	Ras-related protein Rap-1A								2	
P68431	HIST1H3A	Histone H3.1								2	3
P69891	HBG1	Hemoglobin subunit gamma-1									1
P69892	HBG2	Hemoglobin subunit gamma-2									1

Appendix Table 2. Proteomic dataset of proteins found in cancer prostate tissue slice cultures (TSCs)

ACCN	Gene Name	Protein Name	Annotated Glycosylated	C1	C2	C3	C4	C5	C6	C7	C8
P84243	H3F3A	Histone H3.3								2	3
Q01546	KRT76	Keratin, type II cytoskeletal 2 oral									7
Q02818	NUCB1	Nucleobindin-1		2	3	3	1	1	2	2	
Q04609	FOLH1	Glutamate carboxypeptidase 2	N-linked	4			5	5			1
Q10589	BST2	Bone marrow stromal antigen 2	N-linked	1		1					
Q13162	PRDX4	Peroxiredoxin-4					2	3	5	10	11
Q14103	HNRNPD	Heterogeneous nuclear ribonucleoprotein D0					1	1		1	1
Q14525	KRT33B	Keratin, type I cuticular Ha3-II									2
Q14532	KRT32	Keratin, type I cuticular Ha2									2
Q14568	HSP90AA2 P	Heat shock protein HSP 90-alpha A2		1							6
Q15124	PGM5	Phosphoglucomutase-like protein 5									1
Q15582	TGFBI	Transforming growth factor-beta-induced protein ig-h3							1	2	2
Q16695	HIST3H3	Histone H3.1t								2	3
Q58FF8	HSP90AB2 P	Putative heat shock protein HSP 90-beta 2									4
Q6KB66	KRT80	Keratin, type II cytoskeletal 80									3
Q6KC79	NIPBL	Nipped-B-like protein			3	1					
Q6NXT2	H3F3C	Histone H3.3C								2	3
Q6ZT07	TBC1D9	TBC1 domain family member 9			1	1					
Q71DI3	HIST2H3A;	Histone H3.2								2	3
Q7Z3Y7	KRT28	Keratin, type I cytoskeletal 28									6
Q7Z7H5	TMED4	Transmembrane emp24 domain-containing protein 4	N-linked					3	2	2	
Q86TE4	LUZP2	Leucine zipper protein 2	N-linked				1	1			
Q8IUE6	HIST2H2A B	Histone H2A type 2-B									2
Q8IZP2	ST13P4	Putative protein FAM10A4					2	1			
Q8N129	CNPY4	Protein canopy homolog 4		1				1			
Q8NCM8	DYNC2H1	Cytoplasmic dynein 2 heavy chain 1		1				1			
Q8NFW5	DMBX1	Diencephalon/mesencephalon homeobox protein 1				1	1	1			
Q8TAF7	ZNF461	Zinc finger protein 461						1			
Q9BX97	PLVAP	Plasmalemma vesicle-associated protein	N-linked	1	1	2	1		2	4	5
Q9BZJ3	TPSD1	Tryptase delta	N-linked					1			1
Q9C0G6	DNAH6	Dynein heavy chain 6, axonemal						1			
Q9HBR0	SLC38A10	Putative sodium-coupled neutral amino acid transporter 10			1	1		1			
Q9NUB1	ACSS1	Acetyl-coenzyme A synthetase 2-like, mitochondrial		1	1						
Q9P2M7	CGN	Cingulin					1				
Q9Y6X5	ENPP4	Bis	N-linked	1		1			2		
B1APH4	ZNF487	Putative zinc finger protein 487				1					

Appendix Table 2. Proteomic dataset of proteins found in cancer prostate tissue slice cultures (TSCs)

ACCN	Gene Name	Protein Name	Annotated Glycosylated	C1	C2	C3	C4	C5	C6	C7	C8
O14558	HSPB6	Heat shock protein beta-6			1						
O14672	ADAM10	Disintegrin and metalloproteinase domain-containing protein 10	N-linked				1	1			
O14773	TPP1	Tripeptidyl-peptidase 1	N-linked						2	3	
O43657	TSPAN6	Tetraspanin-6	N-linked	1	1	1		1			
O95425	SVIL	Supervillin						1			
P00441	SOD1	Superoxide dismutase [Cu-Zn]						1		2	
P00915	CA1	Carbonic anhydrase 1							2	3	
P02649	APOE	Apolipoprotein E	N-linked, O-linked		5	5		1			
P02743	APCS	Serum amyloid P-component	N-linked								1
P02787	TF	Serotransferrin	N-linked, O-linked					1			
P04062	GBA	Glucosylceramidase	N-linked				2		2	2	
P05141	SLC25A5	ADP/ATP translocase 2							2	4	4
P07196	NEFL	Neurofilament light polypeptide	O-linked								1
P07197	NEFM	Neurofilament medium polypeptide	O-linked								1
P07858	CTSB	Cathepsin B	N-linked	1	1				1	3	
P07942	LAMB1	Laminin subunit beta-1	N-linked		1	1					
P08294	SOD3	Extracellular superoxide dismutase [Cu-Zn]	N-linked				1		2	2	
P09211	GSTP1	Glutathione S-transferase P							1	5	
P12036	NEFH	Neurofilament heavy polypeptide									1
P12235	SLC25A4	ADP/ATP translocase 1							2		4
P12236	SLC25A6	ADP/ATP translocase 3							2	4	4
P13637	ATP1A3	Sodium/potassium-transporting ATPase subunit alpha-3					1	1			2
P14543	NID1	Nidogen-1	N-linked								2
P15311	EZR	Ezrin							7	7	4
P15529	CD46	Membrane cofactor protein	N-linked, O-linked		1						
P15924	DSP	Desmoplakin		1							
P18085	ARF4	ADP-ribosylation factor 4					1		1	4	
P19338	NCL	Nucleolin					2	1			
P20061	TCN1	Transcobalamin-1	N-linked		1	2	1				
P22626	HNRNPA2 B1	Heterogeneous nuclear ribonucleoproteins A2/B1						1	2	2	2
P27816	MAP4	Microtubule-associated protein 4						1			
P30086	PEBP1	Phosphatidylethanolamine-binding protein 1					1	1	1	2	3
P30408	TM4SF1	Transmembrane 4 L6 family member 1	N-linked		1	1					
P31948	STIP1	Stress-induced-phosphoprotein 1					1	1			
P35030	PRSS3	Trypsin-3		1				1	2	2	2
P36957	DLST	Dihydrolypoyllysine-residue succinyltransferase component of					6	1			5

Appendix Table 2. Proteomic dataset of proteins found in cancer prostate tissue slice cultures (TSCs)

ACCN	Gene Name	Protein Name	Annotated Glycosylated	C1	C2	C3	C4	C5	C6	C7	C8
		2-oxoglutarate dehydrogenase									
P48509	CD151	CD151 antigen	N-linked						1	2	
P52565	ARHGDI A	Rho GDP-dissociation inhibitor 1					1		2	3	2
P58499	FAM3B	Protein FAM3B	N-linked				1		2	2	
P60981	DSTN	Destrin			1	1			2	2	1
P61026	RAB10	Ras-related protein Rab-10								6	3
P61803	DAD1	Dolichyl-diphosphooligosaccharide-protein glycosyltransferase subunit DAD1					2		4	4	4
P61981	YWHAG	14-3-3 protein gamma							6	5	5
P78417	GSTO1	Glutathione S-transferase omega-1								2	2
Q00325	SLC25A3	Phosphate carrier protein, mitochondrial							2	2	2
Q04760	GLO1	Lactoylglutathione lyase							2		
Q04917	YWHAH	14-3-3 protein eta									3
Q07021	C1QBP	Complement component 1 Q subcomponent-binding protein						1		1	2
Q07075	ENPEP	Glutamyl aminopeptidase	N-linked				2				2
Q12769	NUP160	Nuclear pore complex protein Nup160		1							
Q12931	TRAP1	Heat shock protein 75 kDa, mitochondrial				1			2	2	2
Q13642	FHL1	Four and a half LIM domains protein 1									2
Q14232	EIF2B1	Translation initiation factor eIF-2B subunit alpha						1			
Q14974	KPNB1	Importin subunit beta-1			1						
Q14980	NUMA1	Nuclear mitotic apparatus protein 1	O-linked				1				
Q15084	PDIA6	Protein disulfide-isomerase A6					1		8	7	6
Q15262	PTPRK	Receptor-type tyrosine-protein phosphatase kappa	N-linked				1	3	2	4	
Q16352	INA	Alpha-intermexin									1
Q3MIR4	TMEM30B	Cell cycle control protein 50B	N-linked				1		1		
Q4KMZ1	IQCC	IQ domain-containing protein C									
Q53HC0	CCDC92	Coiled-coil domain-containing protein 92				1					
Q6P1J6	PLB1	Phospholipase B1, membrane-associated	N-linked					1			
Q6UXG2	KIAA1324	UPF0577 protein KIAA1324	N-linked	2	1	1	1		6	6	2
Q6ZRP7	QSOX2	Sulfhydryl oxidase 2	N-linked		1						
Q7Z7N9	TMEM179B	Transmembrane protein 179B		1	1	1	1			2	
Q86Y46	KRT73	Keratin, type II cytoskeletal 73		2							1
Q8NG11	TSPAN14	Tetraspanin-14	N-linked		1	1	1				
Q92928	RAB1C	Putative Ras-related protein Rab-1C			1	1	2		5	6	3
Q96Q06	PLIN4	Perilipin-4			1	1					
Q9BQ52	ELAC2	Zinc phosphodiesterase ELAC protein 2		1				1			

Appendix Table 2. Proteomic dataset of proteins found in cancer prostate tissue slice cultures (TSCs)

ACCN	Gene Name	Protein Name	Annotated Glycosylated	C1	C2	C3	C4	C5	C6	C7	C8
Q9H0C2	SLC25A31	ADP/ATP translocase 4							2		4
Q9NQ84	GPRC5C	G-protein coupled receptor family C group 5 member C	N-linked				1				
Q9NYZ2	SLC25A37	Mitoferrin-1				1					
Q9P2E9	RRBP1	Ribosome-binding protein 1		5	1		3	6			
Q9UBY0	SLC9A2	Sodium/hydrogen exchanger 2	N-linked	1							
Q9UHL4	DPP7	Dipeptidyl peptidase 2	N-linked					7	6	10	1
Q9UMS6	SYNPO2	Synaptopodin-2		1	2	3					
Q9UNN8	PROCR	Endothelial protein C receptor	N-linked							2	
A1L1A6	IGSF23	Immunoglobulin superfamily member 23	N-linked		1						
A6NMS3	OR5K4	Olfactory receptor 5K4	N-linked	1							
A8MQT2	GOLGA8B	Golgin subfamily A member 8B						1			
A8MTJ3	GNAT3	Guanine nucleotide-binding protein G							2	2	
B2RTY4	MYO9A	Unconventional myosin-IXa						1			
O00161	SNAP23	Synaptosomal-associated protein 23		1				1			
O00459	PIK3R2	Phosphatidylinositol 3-kinase regulatory subunit beta						1			
O00533	CHL1	Neural cell adhesion molecule L1-like protein	N-linked				4				
O00592	PODXL	Podocalyxin	N-linked						1	1	2
O14497	ARID1A	AT-rich interactive domain-containing protein 1A			1						
O14556	GAPDHS	Glyceraldehyde-3-phosphate dehydrogenase, testis-specific									2
O14617	AP3D1	AP-3 complex subunit delta-1						2			
O15031	PLXNB2	Plexin-B2	N-linked		1				1	2	
O43278	SPINT1	Kunitz-type protease inhibitor 1	N-linked				1				
O43286	B4GALT5	Beta-1,4-galactosyltransferase 5	N-linked						2	2	2
O43505	B4GAT1	Beta-1,4-glucuronyltransferase 1	N-linked				1				
O43567	RNF13	E3 ubiquitin-protein ligase RNF13	N-linked			1				2	
O43760	SYNGR2	Synaptogyrin-2		2			2	2	1	1	6
O43829	ZBTB14	Zinc finger and BTB domain-containing protein 14									1
O60264	SMARCA5	SWI/SNF-related matrix-associated actin-dependent regulator of chromatin subfamily A member 5							1		
O60293	ZFC3H1	Zinc finger C3H1 domain-containing protein						3			
O60361	NME2P1	Putative nucleoside diphosphate kinase									2
O60888	CUTA	Protein CutA					1				
O75071	EFCAB14	EF-hand calcium-binding domain-containing protein 14						1			
O75144	ICOSLG	ICOS ligand	N-linked	1				1	1		
O75185	ATP2C2	Calcium-transporting ATPase type 2C member 2			1						
O75223	GGCT	Gamma-glutamylcyclotransferase					1				

Appendix Table 2. Proteomic dataset of proteins found in cancer prostate tissue slice cultures (TSCs)

ACCN	Gene Name	Protein Name	Annotated Glycosylated	C1	C2	C3	C4	C5	C6	C7	C8
O75390	CS	Citrate synthase, mitochondrial									1
O75874	IDH1	Isocitrate dehydrogenase [NADP] cytoplasmic							6	10	4
O75947	ATP5H	ATP synthase subunit d, mitochondrial									1
O95295	SNAPIN	SNARE-associated protein Snapin						1			
O95297	MPZL1	Myelin protein zero-like protein 1	N-linked			1			1		
O95994	AGR2	Anterior gradient protein 2 homolog			1	1	2		4	4	5
P00338	LDHA	L-lactate dehydrogenase A chain			1		1		3	6	4
P00367	GLUD1	Glutamate dehydrogenase 1, mitochondrial							2	7	15
P00738	HP	Haptoglobin	N-linked				4				
P00751	CFB	Complement factor B	N-linked				1		12	19	
P00846	MT-ATP6	ATP synthase subunit a								2	2
P01036	CST4	Cystatin-S									1
P01037	CST1	Cystatin-SN									1
P01876	IGHA1	Immunoglobulin heavy constant alpha 1	N-linked, O-linked								1
P01877	IGHA2	Immunoglobulin heavy constant alpha 2	N-linked			1					1
P01891	HLA-A	HLA class I histocompatibility antigen, A-68 alpha chain	N-linked							6	6
P01892	HLA-A	HLA class I histocompatibility antigen, A-2 alpha chain	N-linked						6	6	4
P01893	HLA-H	Putative HLA class I histocompatibility antigen, α chain H	N-linked			4				6	4
P01906	HLA-DQA2	HLA class II histocompatibility antigen, DQ alpha 2 chain	N-linked						2		
P01911	HLA-DRB1	HLA class II histocompatibility antigen, DRB1-15 beta chain	N-linked		1						4
P01912	HLA-DRB1	HLA class II histocompatibility antigen, DRB1-3 chain	N-linked								4
P04066	FUCA1	Tissue alpha-L-fucosidase	N-linked				1		6	6	1
P04216	THY1	Thy-1 membrane glycoprotein	N-linked		1						
P04222	HLA-C	HLA class I histocompatibility antigen, Cw-3 alpha chain	N-linked								3
P04229	HLA-DRB1	HLA class II histocompatibility antigen, DRB1-1 beta chain	N-linked								2
P04440	HLA-DPB1	HLA class II histocompatibility antigen, DP beta 1 chain	N-linked					1			2
P04899	GNAI2	Guanine nucleotide-binding protein G							2	2	
P05107	ITGB2	Integrin beta-2	N-linked			1					
P05165	PCCA	Propionyl-CoA carboxylase alpha chain, mitochondrial									11
P05534	HLA-A	HLA class I histocompatibility antigen, A-24 alpha chain	N-linked								6
P06702	S100A9	Protein S100-A9								2	
P06744	GPI	Glucose-6-phosphate isomerase							2	10	12
P07099	EPHX1	Epoxide hydrolase 1							3	7	
P07332	FES	Tyrosine-protein kinase Fes/Fps							1		1
P08236	GUSB	Beta-glucuronidase	N-linked					1	5	6	8

Appendix Table 2. Proteomic dataset of proteins found in cancer prostate tissue slice cultures (TSCs)

ACCN	Gene Name	Protein Name	Annotated Glycosylated	C1	C2	C3	C4	C5	C6	C7	C8
P08254	MMP3	Stromelysin-1	N-linked		2						
P08571	CD14	Monocyte differentiation antigen CD14	N-linked, O-linked		1						
P08754	GNAI3	Guanine nucleotide-binding protein G							2	2	
P09104	ENO2	Gamma-enolase									4
P09237	MMP7	Matrilysin								1	
P09471	GNAO1	Guanine nucleotide-binding protein G							2	2	
P09619	PDGFRB	Platelet-derived growth factor receptor beta	N-linked								1
P09622	DLD	Dihydrolipoyl dehydrogenase, mitochondrial						2			4
P10314	HLA-A	HLA class I histocompatibility antigen, A-32 alpha chain	N-linked								4
P10316	HLA-A	HLA class I histocompatibility antigen, A-69 alpha chain	N-linked							6	6
P10321	HLA-C	HLA class I histocompatibility antigen, Cw-7 alpha chain	N-linked								3
P10412	HIST1H1E	Histone H1.4								4	
P10620	MGST1	Microsomal glutathione S-transferase 1								2	
P10645	CHGA	Chromogranin-A	O-linked					1			
P10915	HAPLN1	Hyaluronan and proteoglycan link protein 1	N-linked	1							
P11488	GNAT1	Guanine nucleotide-binding protein G							2	2	
P12429	ANXA3	Annexin A3							2	3	
P13073	COX4I1	Cytochrome c oxidase subunit 4 isoform 1, mitochondrial							1		2
P13611	VCAN	Versican core protein	N-linked			1					6
P13667	PDIA4	Protein disulfide-isomerase A4							8	10	13
P13746	HLA-A	HLA class I histocompatibility antigen, A-11 alpha chain	N-linked								6
P13760	HLA-DRB1	HLA class II histocompatibility antigen, DRB1-4 beta chain	N-linked								2
P13797	PLS3	Plastin-3									3
P13929	ENO3	Beta-enolase									4
P14209	CD99	CD99 antigen		1	1	1					
P15291	B4GALT1	Beta-1,4-galactosyltransferase 1	N-linked						2	2	2
P15531	NME1	Nucleoside diphosphate kinase A							2	6	4
P15907	ST6GAL1	Beta-galactoside alpha-2,6-sialyltransferase 1	N-linked						1	1	
P16188	HLA-A	HLA class I histocompatibility antigen, A-30 alpha chain	N-linked								6
P16189	HLA-A	HLA class I histocompatibility antigen, A-31 alpha chain	N-linked								4
P16234	PDGFRA	Platelet-derived growth factor receptor alpha	N-linked						1		
P16278	GLB1	Beta-galactosidase	N-linked				1				2
P16402	HIST1H1D	Histone H1.3									4
P16403	HIST1H1C	Histone H1.2									4
P17174	GOT1	Aspartate aminotransferase, cytoplasmic					2				

Appendix Table 2. Proteomic dataset of proteins found in cancer prostate tissue slice cultures (TSCs)

ACCN	Gene Name	Protein Name	Annotated Glycosylated	C1	C2	C3	C4	C5	C6	C7	C8
P17405	SMPD1	Sphingomyelin phosphodiesterase	N-linked				1				
P18428	LBP	Lipopolysaccharide-binding protein	N-linked				1				
P18462	HLA-A	HLA class I histocompatibility antigen, A-25 alpha chain	N-linked							6	6
P18463	HLA-B	HLA class I histocompatibility antigen, B-37 alpha chain	N-linked						6		
P18465	HLA-B	HLA class I histocompatibility antigen, B-57 alpha chain	N-linked								4
P18615	NELFE	Negative elongation factor E									3
P19075	TSPAN8	Tetraspanin-8	N-linked	1							
P19087	GNAT2	Guanine nucleotide-binding protein G							2	2	
P19447	ERCC3	TFIIH basal transcription factor complex helicase XPB						2			
P19652	ORM2	Alpha-1-acid glycoprotein 2	N-linked	3					2	5	
P20039	HLA-DRB1	HLA class II histocompatibility antigen, DRB1-11 beta chain	N-linked	2					6	4	2
P20336	RAB3A	Ras-related protein Rab-3A									2
P20337	RAB3B	Ras-related protein Rab-3B									2
P20338	RAB4A	Ras-related protein Rab-4A									2
P20340	RAB6A	Ras-related protein Rab-6A							2	2	2
P20674	COX5A	Cytochrome c oxidase subunit 5A, mitochondrial								2	2
P20810	CAST	Calpastatin		1		1					
P21397	MAOA	Amine oxidase [flavin-containing] A									7
P21926	CD9	CD9 antigen	N-linked								1
P22392	NME2	Nucleoside diphosphate kinase B							2	6	4
P24752	ACAT1	Acetyl-CoA acetyltransferase, mitochondrial					2				
P25815	S100P	Protein S100-P		1	1	1				1	
P26038	MSN	Moesin									6
P26641	EEF1G	Elongation factor 1-gamma							2	2	
P27797	CALR	Calreticulin	N-linked						2	4	5
P29508	SERPINB3	Serpin B3					2			1	
P30040	ERP29	Endoplasmic reticulum resident protein 29								2	
P30044	PRDX5	Peroxiredoxin-5, mitochondrial							2	2	
P30101	PDIA3	Protein disulfide-isomerase A3							17	21	20
P30443	HLA-A	HLA class I histocompatibility antigen, A-1 alpha chain	N-linked								6
P30447	HLA-A	HLA class I histocompatibility antigen, A-23 alpha chain	N-linked								6
P30450	HLA-A	HLA class I histocompatibility antigen, A-26 alpha chain	N-linked							6	6
P30455	HLA-A	HLA class I histocompatibility antigen, A-36 alpha chain	N-linked								6
P30459	HLA-A	HLA class I histocompatibility antigen, A-74 alpha chain	N-linked								4
P30462	HLA-B	HLA class I histocompatibility antigen, B-14 alpha chain	N-linked						6		
P30475	HLA-B	HLA class I histocompatibility antigen, B-39 alpha chain	N-linked						6		

Appendix Table 2. Proteomic dataset of proteins found in cancer prostate tissue slice cultures (TSCs)

ACCN	Gene Name	Protein Name	Annotated Glycosylated	C1	C2	C3	C4	C5	C6	C7	C8
P30486	HLA-B	HLA class I histocompatibility antigen, B-48 alpha chain	N-linked								2
P30492	HLA-B	HLA class I histocompatibility antigen, B-54 alpha chain	N-linked								4
P30499	HLA-C	HLA class I histocompatibility antigen, Cw-1 alpha chain	N-linked								1
P30504	HLA-C	HLA class I histocompatibility antigen, Cw-4 alpha chain	N-linked								5
P30505	HLA-C	HLA class I histocompatibility antigen, Cw-8 alpha chain	N-linked								5
P30508	HLA-C	HLA class I histocompatibility antigen, Cw-12 alpha chain	N-linked								7
P30510	HLA-C	HLA class I histocompatibility antigen, Cw-14 alpha chain	N-linked								5
P30512	HLA-A	HLA class I histocompatibility antigen, A-29 alpha chain	N-linked								4
P35232	PHB	Prohibitin							6	10	9
P35237	SERPINB6	Serpin B6					1	1			
P35241	RDX	Radixin									4
P35442	THBS2	Thrombospondin-2	N-linked				1	1			
P35609	ACTN2	Alpha-actinin-2									3
P37198	NUP62	Nuclear pore glycoprotein p62	O-linked					1			
P38405	GNAL	Guanine nucleotide-binding protein G							2	2	
P39656	DDOST	Dolichyl-diphosphooligosaccharide-protein glycosyltransferase 48 kDa subunit							4	4	
P40189	IL6ST	Interleukin-6 receptor subunit beta	N-linked					1			
P40925	MDH1	Malate dehydrogenase, cytoplasmic							2	2	2
P41219	PRPH	Peripherin									2
P41222	PTGDS	Prostaglandin-H2 D-isomerase	N-linked, O-linked				1				
P41250	GARS	Glycine--tRNA ligase								1	1
P42126	ECI1	Enoyl-CoA delta isomerase 1, mitochondrial					1				4
P43251	BTD	Biotinidase	N-linked				1	1			
P43490	NAMPT	Nicotinamide phosphoribosyltransferase								12	
P47755	CAPZA2	F-actin-capping protein subunit alpha-2							2		
P47756	CAPZB	F-actin-capping protein subunit beta								1	2
P47895	ALDH1A3	Aldehyde dehydrogenase family 1 member A3							2	4	
P49447	CYB561	Cytochrome b561		1				1		2	1
P49448	GLUD2	Glutamate dehydrogenase 2, mitochondrial							2	7	15
P49721	PSMB2	Proteasome subunit beta type-2								1	1
P49755	TMED10	Transmembrane emp24 domain-containing protein 10	N-linked						1	1	2
P49908	SELENOP	Selenoprotein P	N-linked	1							
P50281	MMP14	Matrix metalloproteinase-14									2
P50897	PPT1	Palmitoyl-protein thioesterase 1	N-linked				1				
P50993	ATP1A2	Sodium/potassium-transporting ATPase subunit alpha-2									2

Appendix Table 2. Proteomic dataset of proteins found in cancer prostate tissue slice cultures (TSCs)

ACCN	Gene Name	Protein Name	Annotated Glycosylated	C1	C2	C3	C4	C5	C6	C7	C8
P51571	SSR4	Translocon-associated protein subunit delta							1		2
P51659	HSD17B4	Peroxisomal multifunctional enzyme type 2								4	
P51688	SGSH	N-sulphoglucosamine sulphohydrolase	N-linked				1	3			
P52799	EFNB2	Ephrin-B2	N-linked			1					
P52823	STC1	Stanniocalcin-1	N-linked	1	1	1					
P52907	CAPZA1	F-actin-capping protein subunit alpha-1							2		
P54289	CACNA2D1	Voltage-dependent calcium channel subunit alpha-2/delta-1	N-linked				1				
P54802	NAGLU	Alpha-N-acetylglucosaminidase	N-linked							1	
P54826	GAS1	Growth arrest-specific protein 1	N-linked					1			
P54852	EMP3	Epithelial membrane protein 3	N-linked			1					
P55290	CDH13	Cadherin-13	N-linked			1					
P55291	CDH15	Cadherin-15	N-linked						1		1
P56134	ATP5J2	ATP synthase subunit f								2	1
P58335	ANTXR2	Anthrax toxin receptor 2	N-linked	2							
P59190	RAB15	Ras-related protein Rab-15							4	4	3
P59998	ARPC4	Actin-related protein 2/3 complex subunit 4									4
P60842	EIF4A1	Eukaryotic initiation factor 4A-I							2	2	
P61088	UBE2N	Ubiquitin-conjugating enzyme E2 N							1	1	
P61106	RAB14	Ras-related protein Rab-14									2
P61204	ARF3	ADP-ribosylation factor 3							2	4	
P61457	PCBD1	Pterin-4-alpha-carbinolamine dehydratase									3
P62820	RAB1A	Ras-related protein Rab-1A							5	6	3
P62826	RAN	GTP-binding nuclear protein Ran								2	
P63092	GNAS	Guanine nucleotide-binding protein G							2	2	
P63096	GNAI1	Guanine nucleotide-binding protein G							2	2	
P68036	UBE2L3	Ubiquitin-conjugating enzyme E2 L3		1							
P78504	JAG1	Protein jagged-1	N-linked		1						
P81605	DCD	Dermcidin		2							
P84077	ARF1	ADP-ribosylation factor 1							2	4	
P84085	ARF5	ADP-ribosylation factor 5							2	4	
P98095	FBLN2	Fibulin-2	N-linked, O-linked								1
Q01469	FABP5	Fatty acid-binding protein, epidermal						1		2	
Q01638	IL1RL1	Interleukin-1 receptor-like 1	N-linked	1				1			
Q03113	GNA12	Guanine nucleotide-binding protein subunit alpha-12							2	2	
Q07000	HLA-C	HLA class I histocompatibility antigen, Cw-15 alpha chain	N-linked								5
Q07157	TJP1	Tight junction protein ZO-1		1			1				

Appendix Table 2. Proteomic dataset of proteins found in cancer prostate tissue slice cultures (TSCs)

ACCN	Gene Name	Protein Name	Annotated Glycosylated	C1	C2	C3	C4	C5	C6	C7	C8
Q08043	ACTN3	Alpha-actinin-3									2
Q09160	HLA-A	HLA class I histocompatibility antigen, A-80 alpha chain	N-linked								2
Q12907	LMAN2	Vesicular integral-membrane protein VIP36	N-linked				1				2
Q12913	PTPRJ	Receptor-type tyrosine-protein phosphatase eta	N-linked					1			
Q13011	ECH1	Delta									4
Q13033	STRN3	Striatin-3									2
Q13443	ADAM9	Disintegrin metalloproteinase domain-containing protein 9	N-linked					1			
Q14240	EIF4A2	Eukaryotic initiation factor 4A-II							2	2	
Q14344	GNA13	Guanine nucleotide-binding protein subunit alpha-13							2	2	
Q14651	PLS1	Plastin-1									2
Q14697	GANAB	Neutral alpha-glucosidase AB	N-linked							3	5
Q14814	MEF2D	Myocyte-specific enhancer factor 2D					1				
Q14964	RAB39A	Ras-related protein Rab-39A							2	2	2
Q15075	EEA1	Early endosome antigen 1					1				
Q15125	EBP	3-beta-hydroxysteroid-Delta							2	2	
Q15181	PPA1	Inorganic pyrophosphatase								2	
Q15286	RAB35	Ras-related protein Rab-35							4	4	3
Q15661	TPSAB1	Tryptase alpha/beta-1	N-linked							3	2
Q15771	RAB30	Ras-related protein Rab-30									2
Q15904	ATP6AP1	V-type proton ATPase subunit S1	N-linked			1	1	1	3	4	
Q16181	SEPT7	Septin-7									1
Q16270	IGFBP7	Insulin-like growth factor-binding protein 7	N-linked			1					
Q16651	PRSS8	Prostasin	N-linked		1						
Q16706	MAN2A1	Alpha-mannosidase 2	N-linked				1			2	
Q16799	RTN1	Reticulon-1				1					
Q29718	HLA-B	HLA class I histocompatibility antigen, B-82 alpha chain	N-linked						6		
Q29836	HLA-B	HLA class I histocompatibility antigen, B-67 alpha chain	N-linked						6		
Q29865	HLA-C	HLA class I histocompatibility antigen, Cw-18 alpha chain	N-linked								3
Q29960	HLA-C	HLA class I histocompatibility antigen, Cw-16 alpha chain	N-linked								6
Q29963	HLA-C	HLA class I histocompatibility antigen, Cw-6 alpha chain	N-linked							6	5
Q29974	HLA-DRB1	HLA class II histocompatibility antigen, DRB1-16 beta chain	N-linked			3					2
Q30134	HLA-DRB1	HLA class II histocompatibility antigen, DRB1-8 beta chain	N-linked	2							
Q30154	HLA-DRB5	HLA class II histocompatibility antigen, DR beta 5 chain	N-linked								2
Q30167	HLA-DRB1	HLA class II histocompatibility antigen, DRB1-10 beta chain	N-linked								2
Q31610	HLA-B	HLA class I histocompatibility antigen, B-81 alpha chain	N-linked								2

Appendix Table 2. Proteomic dataset of proteins found in cancer prostate tissue slice cultures (TSCs)

ACCN	Gene Name	Protein Name	Annotated Glycosylated	C1	C2	C3	C4	C5	C6	C7	C8
Q31612	HLA-B	HLA class I histocompatibility antigen, B-73 alpha chain	N-linked			4					
Q3KNS1	PTCHD3	Patched domain-containing protein 3	N-linked				1				
Q3ZCQ3	FAM174B	Membrane protein FAM174B	N-linked						1	2	1
Q53TN4	CYBRD1	Cytochrome b reductase 1	N-linked				1				2
Q562R1	ACTBL2	Beta-actin-like protein 2									6
Q58FF3	HSP90B2P	Putative endoplasmic-like protein									3
Q58FF6	HSP90AB4 P	Putative heat shock protein HSP 90-beta 4									3
Q58FF7	HSP90AB3 P	Putative heat shock protein HSP 90-beta-3									5
Q58FG0	HSP90AA5 P	Putative heat shock protein HSP 90-alpha A5									1
Q5BJF6	ODF2	Outer dense fiber protein 2						2			
Q5JR59	MTUS2	Microtubule-associated tumor suppressor candidate 2						1			
Q5JWF2	GNAS	Guanine nucleotide-binding protein G							2	2	
Q5JXB2	UBE2NL	Putative ubiquitin-conjugating enzyme E2 N-like							1	1	
Q5TZA2	CROCC	Rootletin							1	2	
Q5VZ19	TDRD10	Tudor domain-containing protein 10		2	2	2		2			
Q5Y7A7	HLA-DRB1	HLA class II histocompatibility antigen, DRB1-13 beta chain	N-linked								4
Q5ZPR3	CD276	CD276 antigen	N-linked								1
Q6IQ22	RAB12	Ras-related protein Rab-12									2
Q6TFL3	CCDC171	Coiled-coil domain-containing protein 171							2		
Q6UWV6	ENPP7	Ectonucleotide pyrophosphatase/phosphodiesterase family member 7	N-linked						2		
Q6UXD5	SEZ6L2	Seizure 6-like protein 2	N-linked	1							
Q6WRI0	IGSF10	Immunoglobulin superfamily member 10	N-linked						1		
Q7Z7M0	MEGF8	Multiple epidermal growth factor-like domains protein 8	N-linked								1
Q86YS6	RAB43	Ras-related protein Rab-43									2
Q86YS7	C2CD5	C2 domain-containing protein 5					2				
Q8IYM9	TRIM22	E3 ubiquitin-protein ligase TRIM22		1			1				
Q8IZA0	KIAA0319L	Dyslexia-associated protein KIAA0319-like protein	N-linked	1							
Q8IZF2	ADGRF5	Adhesion G protein-coupled receptor F5	N-linked		1	1					
Q8N8E3	CEP112	Centrosomal protein of 112 kDa		1			1				
Q8NBS9	TXNDC5	Thioredoxin domain-containing protein 5									4
Q8NC54	KCT2	Keratinocyte-associated transmembrane protein 2	N-linked					1			
Q8NDX2	SLC17A8	Vesicular glutamate transporter 3	N-linked					1			
Q8NFZ8	CADM4	Cell adhesion molecule 4	N-linked				1				
Q8NHP8	PLBD2	Putative phospholipase B-like 2	N-linked				1				
Q8TD06	AGR3	Anterior gradient protein 3									2

Appendix Table 2. Proteomic dataset of proteins found in cancer prostate tissue slice cultures (TSCs)

ACCN	Gene Name	Protein Name	Annotated Glycosylated	C1	C2	C3	C4	C5	C6	C7	C8
Q8TDR0	TRAF3IP1	TRAF3-interacting protein 1					1	1			
Q8TEQ0	SNX29	Sorting nexin-29		2		2					
Q8WTV0	SCARB1	Scavenger receptor class B member 1	N-linked			1		1		2	
Q92930	RAB8B	Ras-related protein Rab-8B									3
Q95365	HLA-B	HLA class I histocompatibility antigen, B-38 alpha chain	N-linked						6		
Q95604	HLA-C	HLA class I histocompatibility antigen, Cw-17 alpha chain	N-linked								4
Q95IE3	HLA-DRB1	HLA class II histocompatibility antigen, DRB1-12 beta chain	N-linked								2
Q969X5	ERGIC1	Endoplasmic reticulum-Golgi intermediate compartment protein 1	N-linked						1	2	1
Q96AX2	RAB37	Ras-related protein Rab-37									2
Q96DA2	RAB39B	Ras-related protein Rab-39B									2
Q96DC7	TMCO6	Transmembrane and coiled-coil domain-containing protein 6									2
Q96E17	RAB3C	Ras-related protein Rab-3C									2
Q96HE7	ERO1A	ERO1-like protein alpha	N-linked				1		1	1	
Q96HL8	SH3YL1	SH3 domain-containing YSC84-like protein 1		1							
Q96HR9	REEP6	Receptor expression-enhancing protein 6					1	1			1
Q96NY8	NECTIN4	Nectin-4	N-linked	1							
Q96PQ0	SORCS2	VPS10 domain-containing receptor SorCS2	N-linked						1		
Q99538	LGMN	Legumain	N-linked		1	1	1	1		2	
Q99623	PHB2	Prohibitin-2								2	8
Q9BQ51	PDCD1LG2	Programmed cell death 1 ligand 2	N-linked							1	
Q9BTY2	FUCA2	Plasma alpha-L-fucosidase	N-linked							1	
Q9BYT9	ANO3	Anoctamin-3	N-linked				1				
Q9H082	RAB33B	Ras-related protein Rab-33B							2	2	2
Q9H0U4	RAB1B	Ras-related protein Rab-1B							5	6	3
Q9H0V1	TMEM168	Transmembrane protein 168	N-linked		1						
Q9H3K2	GHITM	Growth hormone-inducible transmembrane protein					1				
Q9H3R2	MUC13	Mucin-13	N-linked				1				
Q9H3Z4	DNAJC5	DnaJ homolog subfamily C member 5									1
Q9H8J5	MANSC1	MANSC domain-containing protein 1	N-linked	1				1			
Q9HAU0	PLEKHA5	Pleckstrin homology domain-containing family A member 5					1				
Q9HB40	SCPEP1	Retinoid-inducible serine carboxypeptidase	N-linked							2	
Q9HC07	TMEM165	Transmembrane protein 165								2	
Q9HD45	TM9SF3	Transmembrane 9 superfamily member 3	N-linked						1	2	
Q9HDC9	APMAP	Adipocyte plasma membrane-associated protein	N-linked						4	4	7
Q9NPR9	GPR108	Protein GPR108	N-linked							1	
Q9NQH7	XPNPEP3	Probable Xaa-Pro aminopeptidase								1	1

Appendix Table 2. Proteomic dataset of proteins found in cancer prostate tissue slice cultures (TSCs)

ACCN	Gene Name	Protein Name	Annotated Glycosylated	C1	C2	C3	C4	C5	C6	C7	C8
		3									
Q9NRW1	RAB6B	Ras-related protein Rab-6B							2	2	2
Q9NUN5	LMBRD1	Probable lysosomal cobalamin transporter	N-linked						2	2	1
Q9NV96	TMEM30A	Cell cycle control protein 50A	N-linked		1	1			1		
Q9NYL4	FKBP11	Peptidyl-prolyl cis-trans isomerase FKBP11					1	1			
Q9NZ56	FMN2	Formin-2									2
Q9P2G4	MAP10	Microtubule-associated protein 10			1	1					
Q9TNN7	HLA-C	HLA class I histocompatibility antigen, Cw-5 alpha chain	N-linked								4
Q9UFN0	NIPSNAP3 A	Protein NipSnap homolog 3A								1	2
Q9UHC9	NPC1L1	Niemann-Pick C1-like protein 1	N-linked						1	2	
Q9UHG3	PCYOX1	Prenylcysteine oxidase 1	N-linked						4	6	3
Q9UPA5	BSN	Protein bassoon	O-linked				1				
Q9UPZ6	THSD7A	Thrombospondin type-1 domain-containing protein 7A	N-linked				1				
Q9Y281	CFL2	Cofilin-2									2
Q9Y394	DHRS7	Dehydrogenase/reductase SDR family member 7							2	6	2
Q9Y646	CPQ	Carboxypeptidase Q	N-linked				1	3			
Q9Y6N5	SQRDL	Sulfide:quinone oxidoreductase, mitochondrial							1	1	1
Q9Y6R1	SLC4A4	Electrogenic sodium bicarbonate cotransporter 1	N-linked							4	

Appendix Table 3. Proteomic dataset of proteins found in benign prostate hyperplasia prostatic tissue slice cultures (TSCs)

Appendix Table 3. Proteomic dataset of proteins found in benign prostate hyperplasia prostatic tissue slice cultures (TSCs). Proteins found in prostate BPH (BPH1-6) proteomic dataset. Columns include uniprot accession numbers (Accn #), gene names and protein names. The total number of identified peptide sequences (peptide spectrum matches) for the proteins identified.

Accn#	Gene name	Protein Name	B1	B2	B3	B4	B5	B6
P01011	SERPINA3	Alpha-1-antichymotrypsin	57	62	48	86	20	30
P13645	KRT10	Keratin, type I cytoskeletal 10	22	24	37	27	23	25
P04264	KRT1	Keratin, type II cytoskeletal 1	18	14	31	21	25	24
P35908	KRT2	Keratin, type II cytoskeletal 2 epidermal	12	14	24	20	20	24
P35527	KRT9	Keratin, type I cytoskeletal 9	8	7	13	10	8	12
P11021	HSPA5	78 kDa glucose-regulated protein	11	8	6	8	7	15
Q7Z5K2	WAPL	Wings apart-like protein homolog	18	14	13		1	9
P17301	ITGA2	Integrin alpha-2	8	7	7	7	4	10
P02533	KRT14	Keratin, type I cytoskeletal 14	5	4	11	3	7	12
P13647	KRT5	Keratin, type II cytoskeletal 5	5	4	12	4	8	8
P23229	ITGA6	Integrin alpha-6	9	8	8	4	5	6
P08779	KRT16	Keratin, type I cytoskeletal 16	4	5	11	4	5	10
P08195	SLC3A2	4F2 cell-surface antigen heavy chain	8	6	8	3	5	8
P11142	HSPA8	Heat shock cognate 71 kDa protein	9	10	4	6	1	8
Q09666	AHNAK	Neuroblast differentiation-associated protein AHNAK	5	7	7	5	6	8
Q6YHK3	CD109	CD109 antigen	12	9	5	1	1	9
P07093	SERPINE2	Glia-derived nexin	8	5	5	6	2	9
P04259	KRT6B	Keratin, type II cytoskeletal 6B	4	3	11	3	4	7
P06756	ITGAV	Integrin alpha-V	8	7	8	1		8
P50895	BCAM	Basal cell adhesion molecule	6	7	5	4	5	5
P07355	ANXA2	Annexin A2	7	6	6	4		8
P08648	ITGA5	Integrin alpha-5	6	5	7	3	3	7
P05556	ITGB1	Integrin beta-1	6	3	5	5	6	5
P51884	LUM	Lumican	6	4	5	6	3	6
P02538	KRT6A	Keratin, type II cytoskeletal 6A	3	3	9	4	4	6
P16070	CD44	CD44 antigen	5	5	6	4	3	6
P35749	MYH11	Myosin-11	2	8	17		2	
P63104	YWHAZ	14-3-3 protein zeta/delta	5	7	5	5	3	4
P68871	HBB	Hemoglobin subunit beta	7	5	5	2	3	7
O75976	CPD	Carboxypeptidase D	3	6	5	2	5	6
Q01995	TAGLN	Transgelin	6	5	5	4	4	3
P02751	FN1	Fibronectin	4	5	3	3	5	6
P18206	VCL	Vinculin	3	2		6	3	12
Q92520	FAM3C	Protein FAM3C	4	8	3	4	3	4
P07339	CTSD	Cathepsin D	4	4	5	2	3	7
P35613	BSG	Basigin	5	6	3	3	1	6
P01019	AGT	Angiotensinogen	4	4	3	5	3	4
P43121	MCAM	Cell surface glycoprotein MUC18	4	4	5	2	4	4
Q7Z794	KRT77	Keratin, type II cytoskeletal 1b	3	3	4	3	5	5
P08107	HSPA1A	Heat shock 70 kDa protein 1A	4	4	3	3	1	7
P15144	ANPEP	Aminopeptidase N	6	5	2	2	3	4
P25311	AZGP1	Zinc-alpha-2-glycoprotein	5	4	4	5	2	2
P27348	YWHAQ	14-3-3 protein theta	5	3	3	4	2	5
P60174	TPI1	Triosephosphate isomerase	4	4	4	4	2	4
P06733	ENO1	Alpha-enolase	5	4	2	4		6

Appendix Table 3. Proteomic dataset of proteins found in benign prostate hyperplasia prostatic tissue slice cultures (TSCs)

Accn#	Gene name	Protein Name	B1	B2	B3	B4	B5	B6
P23528	CFL1	Cofilin-1	3	3	4	4	3	4
P02788	LTF	Lactotransferrin	15	4				1
P08758	ANXA5	Annexin A5	3	2	3	3	2	7
Q08380	LGALS3BP	Galectin-3-binding protein	3	2	5	5	2	3
Q8NBJ4	GOLM1	Golgi membrane protein 1	5	2	4	2	4	3
O15118	NPC1	Niemann-Pick C1 protein	5	2	3	4	1	4
P02786	TFRC	Transferrin receptor protein 1	3	3	2	3	1	7
P07737	PFN1	Profilin-1	2	2	3	4	2	6
P16284	PECAM1	Platelet endothelial cell adhesion molecule	3	4	5	2	1	4
P63267	ACTG2	Actin, gamma-enteric smooth muscle	4	4	3	2	1	5
P62736	ACTA2	Actin, aortic smooth muscle	4	4	3	2	1	5
P68032	ACTC1	Actin, alpha cardiac muscle 1	4	4	3	2	1	5
Q9UIQ6	LNPEP	Leucyl-cystinyl aminopeptidase	4	4	5	2		4
O60664	PLIN3	Perilipin-3	2	5	2	1	3	5
P01009	SERPINA1	Alpha-1-antitrypsin	2	2	3	5	3	3
P05534	HLA-A	HLA class I histocompatibility antigen, A-24 alpha chain	4	5	3	2		4
P09758	TACSTD2	Tumor-associated calcium signal transducer 2	5	4	3	2	2	2
P12111	COL6A3	Collagen alpha-3	1	1	14		1	1
P23142	FBLN1	Fibulin-1	4	4	2	3	1	4
P30508	HLA-C	HLA class I histocompatibility antigen, Cw-12 alpha chain	5	3	5	2		3
P08473	MME	Neprilysin		3	4	4	3	3
Q04695	KRT17	Keratin, type I cytoskeletal 17	1	1	5	2	2	6
Q05707	COL14A1	Collagen alpha-1	4	3	8		1	1
Q13740	ALCAM	CD166 antigen	3	4	3	2	1	4
P01889	HLA-B	HLA class I histocompatibility antigen, B-7 alpha chain	4	3	7	1		1
P30460	HLA-B	HLA class I histocompatibility antigen, B-8 alpha chain	4	3	7	1		1
P30480	HLA-B	HLA class I histocompatibility antigen, B-42 alpha chain	4	3	7	1		1
P26006	ITGA3	Integrin alpha-3	4	3	6			3
Q29963	HLA-C	HLA class I histocompatibility antigen, Cw-6 alpha chain	5	2	5	2		2
P01893	HLA-H	Putative HLA class I histocompatibility antigen, alpha chain H	4	2	4	2		3
P07951	TPM2	Tropomyosin beta chain	3	3	5	1	2	1
P13688	CEACAM1	Carcinoembryonic antigen-related cell adhesion molecule 1	3	2	3	3	2	2
P21333	FLNA	Filamin-A		7	5	1		2
P21589	NT5E	5'-nucleotidase	2	3	4		2	4
P23141	CES1	Liver carboxylesterase 1	2	2	3	3	1	4
P30510	HLA-C	HLA class I histocompatibility antigen, Cw-14 alpha chain	4	3	5	1		2
P38646	HSPA9	Stress-70 protein, mitochondrial	4	3	3			5
P68133	ACTA1	Actin, alpha skeletal muscle	3	3	3	2	1	3
P78310	CXADR	Coxsackievirus and adenovirus receptor	3	3	3	2	1	3
P00450	CP	Ceruloplasmin	2	2	3	2	2	3
P00558	PGK1	Phosphoglycerate kinase 1	3	2	1	3		5
P30479	HLA-B	HLA class I histocompatibility antigen, B-41 alpha chain	3	3	6	1		1
Q04826	HLA-B	HLA class I histocompatibility antigen, B-40 alpha chain	3	3	6	1		1
O95678	KRT75	Keratin, type II cytoskeletal 75	1	2	3	3	3	2

Appendix Table 3. Proteomic dataset of proteins found in benign prostate hyperplasia prostatic tissue slice cultures (TSCs)

Accn#	Gene name	Protein Name	B1	B2	B3	B4	B5	B6
P05023	ATP1A1	Sodium/potassium-transporting ATPase subunit alpha-1	3	4	2	1	1	3
P05362	ICAM1	Intercellular adhesion molecule 1	2	2	3	2	2	3
P18827	SDC1	Syndecan-1	3	3	2	1	3	2
P24821	TNC	Tenascin	5	4	3			2
P30501	HLA-C	HLA class I histocompatibility antigen, Cw-2 alpha chain	4	2	4	2		2
P30504	HLA-C	HLA class I histocompatibility antigen, Cw-4 alpha chain	3	3	5	1		2
P54709	ATP1B3	Sodium/potassium-transporting ATPase subunit beta-3	2	2	4	3	1	2
Q9P2B2	PTGFRN	Prostaglandin F2 receptor negative regulator	3	4	1	2	1	3
O00299	CLIC1	Chloride intracellular channel protein 1	3	3	2	2	2	1
P01033	TIMP1	Metalloproteinase inhibitor 1	3	2	3	2	1	2
P01892	HLA-A	HLA class I histocompatibility antigen, A-2 alpha chain	5	2	1	1		4
P02787	TF	Serotransferrin	4	3	1	5		
P30447	HLA-A	HLA class I histocompatibility antigen, A-23 alpha chain	3	3	2	2		3
P07996	THBS1	Thrombospondin-1	4	3	1	2		3
P09382	LGALS1	Galectin-1	3	2	2	2		4
P16190	HLA-A	HLA class I histocompatibility antigen, A-33 alpha chain	3	2	5	1		2
P18462	HLA-A	HLA class I histocompatibility antigen, A-25 alpha chain	3	2	5	1		2
P30450	HLA-A	HLA class I histocompatibility antigen, A-26 alpha chain	3	2	5	1		2
P30453	HLA-A	HLA class I histocompatibility antigen, A-34 alpha chain	3	2	5	1		2
P30457	HLA-A	HLA class I histocompatibility antigen, A-66 alpha chain	3	2	5	1		2
P29508	SERPINB3	Serpin B3	4	3	4	1		1
P30505	HLA-C	HLA class I histocompatibility antigen, Cw-8 alpha chain	3	2	4	2		2
Q07000	HLA-C	HLA class I histocompatibility antigen, Cw-15 alpha chain	3	2	4	2		2
P51911	CNN1	Calponin-1	3	3	1			6
P60709	ACTB	Actin, cytoplasmic 1	3	2	3	2	1	2
P63261	ACTG1	Actin, cytoplasmic 2	3	2	3	2	1	2
Q01650	SLC7A5	Large neutral amino acids transporter small subunit 1	3	2	2	2	2	2
Q06323	PSME1	Proteasome activator complex subunit 1	2	2	2	3	2	2
Q14CN4	KRT72	Keratin, type II cytoskeletal 72	2	2	3	2	2	2
Q3SY84	KRT71	Keratin, type II cytoskeletal 71	2	2	3	2	2	2
Q7RTS7	KRT74	Keratin, type II cytoskeletal 74	2	2	3	2	2	2
Q86Y46	KRT73	Keratin, type II cytoskeletal 73	2	2	3	2	2	2
Q9P2E9	RRBP1	Ribosome-binding protein 1	1	6	3	1	1	1
Q9UL46	PSME2	Proteasome activator complex subunit 2	4	1	3	1	2	2
Q9Y5Z0	BACE2	Beta-secretase 2	2	2	3	2	2	2
P00751	CFB	Complement factor B	2	5	2	2		1
P01130	LDLR	Low-density lipoprotein receptor	2	2	2	2	2	2
Q29865	HLA-C	HLA class I histocompatibility antigen, Cw-18 alpha chain	3	2	5	1		1
P04075	ALDOA	Fructose-bisphosphate aldolase A	2	3	2	2		3
P07237	P4HB	Protein disulfide-isomerase	2	2	2	2	1	3
P54652	HSPA2	Heat shock-related 70 kDa protein 2	3	3	2	1	1	2

Appendix Table 3. Proteomic dataset of proteins found in benign prostate hyperplasia prostatic tissue slice cultures (TSCs)

Accn#	Gene name	Protein Name	B1	B2	B3	B4	B5	B6
P11717	IGF2R	Cation-independent mannose-6-phosphate receptor	4	2	3	1		2
P16422	EPCAM	Epithelial cell adhesion molecule	2	2	2	2	2	2
P16188	HLA-A	HLA class I histocompatibility antigen, A-30 alpha chain	3	1	3	2		3
P37802	TAGLN2	Transgelin-2	3	1	5	1	1	1
P60660	MYL6	Myosin light polypeptide 6	2	2	4	1	1	2
A5A3E0	POTEF	POTE ankyrin domain family member F	3	2	2	2	1	2
Q6S8J3	POTEE	POTE ankyrin domain family member E	3	2	2	2	1	2
Q15084	PDIA6	Protein disulfide-isomerase A6	3	2	1	2		4
Q5ZPR3	CD276	CD276 antigen	2	2	2	2	2	2
Q8N271	PROM2	Prominin-2	5	2	1	1	1	2
Q92896	GLG1	Golgi apparatus protein 1	3	2	1	1	2	3
Q96KK5	HIST1H2A H	Histone H2A type 1-H	2	2	2	2	2	2
P04908	HIST1H2A B	Histone H2A type 1-B/E	2	2	2	2	2	2
P0C0S8	HIST1H2A G	Histone H2A type 1	2	2	2	2	2	2
P20671	HIST1H2A D	Histone H2A type 1-D	2	2	2	2	2	2
Q16777	HIST2H2A C	Histone H2A type 2-C	2	2	2	2	2	2
Q6FI13	HIST2H2A A3	Histone H2A type 2-A	2	2	2	2	2	2
Q7L7L0	HIST3H2A	Histone H2A type 3	2	2	2	2	2	2
Q93077	HIST1H2A C	Histone H2A type 1-C	2	2	2	2	2	2
Q99878	HIST1H2AJ	Histone H2A type 1-J	2	2	2	2	2	2
Q9BTM1	H2AFJ	Histone H2A.J	2	2	2	2	2	2
P19012	KRT15	Keratin, type I cytoskeletal 15	1	1	3	1	1	4
Q29960	HLA-C	HLA class I histocompatibility antigen, Cw-16 alpha chain	3	1	2	2		3
P07585	DCN	Decorin	2	1	2	3	2	1
P08238	HSP90AB1	Heat shock protein HSP 90-beta	2	1	2	3	1	2
P08253	MMP2	72 kDa type IV collagenase	3	1	2	1	1	3
P09525	ANXA4	Annexin A4	2	2	2			5
P10809	HSPD1	60 kDa heat shock protein, mitochondrial	1	4	1	2		3
P13796	LCP1	Plastin-2	2	1	2	3		3
P15309	ACPP	Prostatic acid phosphatase			2	4		5
P30461	HLA-B	HLA class I histocompatibility antigen, B-13 alpha chain	4	2	3	1		1
P36871	PGM1	Phosphoglucomutase-1	2	3		3		3
P51888	PRELP	Prolargin	3	2	2	1	1	2
Q562R1	ACTBL2	Beta-actin-like protein 2	2	2	2	2	1	2
Q9BYX7	POTEKP	Putative beta-actin-like protein 3	2	2	2	2	1	2
P04222	HLA-C	HLA class I histocompatibility antigen, Cw-3 alpha chain	2	2	4	1		1
P18463	HLA-B	HLA class I histocompatibility antigen, B-37 alpha chain	3	1	4	1		1
P30462	HLA-B	HLA class I histocompatibility antigen, B-14 alpha chain	3	1	4	1		1
P30475	HLA-B	HLA class I histocompatibility antigen, B-39 alpha chain	3	1	4	1		1
Q29718	HLA-B	HLA class I histocompatibility antigen, B-82 alpha chain	3	1	4	1		1
Q29836	HLA-B	HLA class I histocompatibility antigen,	3	1	4	1		1

Appendix Table 3. Proteomic dataset of proteins found in benign prostate hyperplasia prostatic tissue slice cultures (TSCs)

Accn#	Gene name	Protein Name	B1	B2	B3	B4	B5	B6
		B-67 alpha chain						
Q95365	HLA-B	HLA class I histocompatibility antigen, B-38 alpha chain	3	1	4	1		1
P04406	GAPDH	Glyceraldehyde-3-phosphate dehydrogenase	2	2	1	1	1	3
P05155	SERPING1	Plasma protease C1 inhibitor	4	3	2		1	
A6NMY6	ANXA2P2	Putative annexin A2-like protein	2	2	2	1		3
P09211	GSTP1	Glutathione S-transferase P	2	2	1	1		4
P13667	PDIA4	Protein disulfide-isomerase A4	3	2		2		3
P69905	HBA1;	Hemoglobin subunit alpha	2	2	2	1	1	2
P80188	LCN2	Neutrophil gelatinase-associated lipocalin	2	1	4	1	1	1
Q13228	SELENBP1	Selenium-binding protein 1	3	2		2	1	2
Q14108	SCARB2	Lysosome membrane protein 2	2	1	3	1	2	1
Q6EMK4	VASN	Vasorin	2	1	2	2		3
P00738	HP	Haptoglobin	3	3		1	1	1
Q09160	HLA-A	HLA class I histocompatibility antigen, A-80 alpha chain	2	2	2	1		2
P02768	ALB	Serum albumin	2	2		3	1	1
P04179	SOD2	Superoxide dismutase [Mn], mitochondrial	2	1	2		2	2
P17066	HSPA6	Heat shock 70 kDa protein 6	2	3	1	1		2
P10319	HLA-B	HLA class I histocompatibility antigen, B-58 alpha chain	3	1	2	1		2
P18465	HLA-B	HLA class I histocompatibility antigen, B-57 alpha chain	3	1	2	1		2
P10909	CLU	Clusterin	2	1	2		1	3
P14625	HSP90B1	Endoplasmic reticulum chaperone protein 90B	1	2	1	3	1	1
P15907	ST6GAL1	Beta-galactoside alpha-2,6-sialyltransferase 1	1	3	1	1	1	2
P10314	HLA-A	HLA class I histocompatibility antigen, A-32 alpha chain	2	1	3	1		2
P16189	HLA-A	HLA class I histocompatibility antigen, A-31 alpha chain	2	1	3	1		2
P30456	HLA-A	HLA class I histocompatibility antigen, A-43 alpha chain	2	1	3	1		2
P30459	HLA-A	HLA class I histocompatibility antigen, A-74 alpha chain	2	1	3	1		2
P20645	M6PR	Cation-dependent mannose-6-phosphate receptor	2	2	3	1		1
P21796	VDAC1	Voltage-dependent anion-selective channel protein 1	3	3		2		1
P48594	SERPINB4	Serpin B4	3	2	2	1		1
P67936	TPM4	Tropomyosin alpha-4 chain	1	3	3	1	1	
Q05682	CALD1	Caldesmon	2	2		1	1	3
Q14126	DSG2	Desmoglein-2	1	2	2	2	1	1
Q16853	AOC3	Membrane primary amine oxidase	1		1	2	1	4
Q53GD3	SLC44A4	Choline transporter-like protein 4	1	1	1	2	2	2
O14786	NRP1	Neuropilin-1	2	1	1	2		2
P01834	IGKC	Immunoglobulin kappa constant	2		2	2	1	1
P03989	HLA-B	HLA class I histocompatibility antigen, B-27 alpha chain	2	1	3	1		1
P30466	HLA-B	HLA class I histocompatibility antigen, B-18 alpha chain	2	1	3	1		1
P30481	HLA-B	HLA class I histocompatibility antigen, B-44 alpha chain	2	1	3	1		1
P30483	HLA-B	HLA class I histocompatibility antigen, B-45 alpha chain	2	1	3	1		1
P30485	HLA-B	HLA class I histocompatibility antigen, B-47 alpha chain	2	1	3	1		1

Appendix Table 3. Proteomic dataset of proteins found in benign prostate hyperplasia prostatic tissue slice cultures (TSCs)

Accn#	Gene name	Protein Name	B1	B2	B3	B4	B5	B6
P30487	HLA-B	HLA class I histocompatibility antigen, B-49 alpha chain	2	1	3	1		1
P30488	HLA-B	HLA class I histocompatibility antigen, B-50 alpha chain	2	1	3	1		1
P30499	HLA-C	HLA class I histocompatibility antigen, Cw-1 alpha chain	2	2	4			
Q9TNN7	HLA-C	HLA class I histocompatibility antigen, Cw-5 alpha chain	2		2	2		2
P04083	ANXA1	Annexin A1	1	1	1	2		3
P04233	CD74	HLA class II histocompatibility antigen gamma chain	1	3	2	1		1
P04792	HSPB1	Heat shock protein beta-1	2	1	2	1		2
P05121	SERPINE1	Plasminogen activator inhibitor 1	3	1		1	1	2
P30492	HLA-B	HLA class I histocompatibility antigen, B-54 alpha chain	2	1	2	1		2
P05787	KRT8	Keratin, type II cytoskeletal 8	1		5	1	1	
P09493	TPM1	Tropomyosin alpha-1 chain	1	2	2	1	1	1
P0C0L4	C4A	Complement C4-A	2	2	1	2		1
P0C0L5	C4B	Complement C4-B	2	2	1	2		1
P0CG48	UBC	Polyubiquitin-C [Cleaved into: Ubiquitin]	1	2	1	1	2	1
P0CG47	UBB	Polyubiquitin-B [Cleaved into: Ubiquitin]	1	2	1	1	2	1
P62979	RPS27A	Ubiquitin-40S ribosomal protein S27a	1	2	1	1	2	1
P62987	UBA52	Ubiquitin-60S ribosomal protein L40	1	2	1	1	2	1
P13164	IFITM1	Interferon-induced transmembrane protein 1	2	2		2	1	1
Q01628	IFITM3	Interferon-induced transmembrane protein 3	2	2		2	1	1
Q01629	IFITM2	Interferon-induced transmembrane protein 2	2	2		2	1	1
P30512	HLA-A	HLA class I histocompatibility antigen, A-29 alpha chain	2	1	2	1		2
P17813	ENG	Endoglin	2	1	2		1	2
P27105	STOM	Erythrocyte band 7 integral membrane protein	2	2	2	1		1
P30086	PEBP1	Phosphatidylethanolamine-binding protein 1	3	2	1	1		1
P30101	PDIA3	Protein disulfide-isomerase A3	1	3		2	1	1
P35579	MYH9	Myosin-9		1	7			
Q5XKE5	KRT79	Keratin, type II cytoskeletal 79	1	1	2	1	1	2
P56199	ITGA1	Integrin alpha-1	1	1	2	1	1	2
P98172	EFNB1	Ephrin-B1		3	3			2
Q01638	IL1RL1	Interleukin-1 receptor-like 1	2		2	2		2
Q13510	ASAH1	Acid ceramidase	2		2	1	1	2
Q8NFJ5	GPRC5A	Retinoic acid-induced protein 3	2	2	1	1	1	1
Q99536	VAT1	Synaptic vesicle membrane protein VAT-1 homolog	1	3		1		3
O43291	SPINT2	Kunitz-type protease inhibitor 2	1	1	2	1	1	1
P01023	A2M	Alpha-2-macroglobulin	2	1		1	1	2
P30486	HLA-B	HLA class I histocompatibility antigen, B-48 alpha chain	2	1	4			
Q31610	HLA-B	HLA class I histocompatibility antigen, B-81 alpha chain	2	1	4			
P02042	HBD	Hemoglobin subunit delta	1	1	1		2	2
P08729	KRT7	Keratin, type II cytoskeletal 7	1		4	1	1	
P14136	GFAP	Glial fibrillary acidic protein	1		4	1	1	
Q6KB66	KRT80	Keratin, type II cytoskeletal 80	1		4	1	1	
P05026	ATP1B1	Sodium/potassium-transporting	1		3	1		2

Appendix Table 3. Proteomic dataset of proteins found in benign prostate hyperplasia prostatic tissue slice cultures (TSCs)

Accn#	Gene name	Protein Name	B1	B2	B3	B4	B5	B6
		ATPase subunit beta-1						
P07195	LDHB	L-lactate dehydrogenase B chain	1	1	2	1		2
P10253	GAA	Lysosomal alpha-glucosidase	1	1	1	1	1	2
P15941	MUC1	Mucin-1	1		4			2
P27701	CD82	CD82 antigen	2	1	2			2
P35030	PRSS3	Trypsin-3	1	1	1	2	1	1
P40926	MDH2	Malate dehydrogenase, mitochondrial	1	2		1		3
P42892	ECE1	Endothelin-converting enzyme 1			1	1		5
P61019	RAB2A	Ras-related protein Rab-2A	1	1	1	1	2	1
Q07954	LRP1	Prolow-density lipoprotein receptor-related protein 1	3		1			3
Q6UXG2	KIAA1324	UPF0577 protein KIAA1324	2	2	1		1	1
Q8IZP2	ST13P4	Putative protein FAM10A4	1	1	1	1	1	2
P50502	ST13	Hsc70-interacting protein	1	1	1	1	1	2
Q99497	PARK7	Protein/nucleic acid deglycase DJ-1	1	2		1	1	2
Q9H5V8	CDCP1	CUB domain-containing protein 1	2	1	1	1		2
Q9NRX5	SERINC1	Serine incorporator 1	2	1	1	1	1	1
P31944	CASP14	Caspase-14			2	2	2	1
O00461	GOLIM4	Golgi integral membrane protein 4	1	1		1	1	2
O14494	PLPP1	Phospholipid phosphatase 1	2	1	1	1		1
O15173	PGRMC2	Membrane-associated progesterone receptor component 2	1	1	1	1	1	1
O94919	ENDOD1	Endonuclease domain-containing 1 protein	1	1	1	1	1	1
P00533	EGFR	Epidermal growth factor receptor	1	1	1	1	1	1
P13747	HLA-E	HLA class I histocompatibility antigen, alpha chain E	2		2	1		1
P01903	HLA-DRA	HLA class II histocompatibility antigen, DR alpha chain	1	1	1	1		2
P02545	LMNA	Prelamin-A/C [Cleaved into: Lamin-A/C		1	4	1		
P02649	APOE	Apolipoprotein E	3	1			1	1
P04921	GYPC	Glycophorin-C	1	1	1	1	1	1
P06576	ATP5B	ATP synthase subunit beta, mitochondrial		1	1	3		1
P09104	ENO2	Gamma-enolase	1	1	1	1		2
P13929	ENO3	Beta-enolase	1	1	1	1		2
P07288	KLK3	Prostate-specific antigen	1	1	1		1	2
P08727	KRT19	Keratin, type I cytoskeletal 19			2	1		3
P08962	CD63	CD63 antigen		2	2			2
P10599	TXN	Thioredoxin	1	1	1	1	1	1
P11166	SLC2A1	Solute carrier family 2, facilitated glucose transporter member 1	2	1	1			2
P11279	LAMP1	Lysosome-associated membrane glycoprotein 1	3	1	1		1	
P14314	PRKCSH	Glucosidase 2 subunit beta		1	2		1	2
P17661	DES	Desmin		1	2	1	2	
P25705	ATP5A1	ATP synthase subunit alpha, mitochondrial		2		1	1	2
P29966	MARCKS	Myristoylated alanine-rich C-kinase substrate	1	1	1	1	1	1
P30040	ERP29	Endoplasmic reticulum resident protein 29	1	1	1	1		2
P32119	PRDX2	Peroxiredoxin-2	2	1	1	1		1
P36269	GGT5	Glutathione hydrolase 5 proenzyme	1	1	1		1	2
P58546	MTPN	Myotrophin	1	1	1	1	1	1
P68104	EEF1A1	Elongation factor 1-alpha 1	1		1	2		2

Appendix Table 3. Proteomic dataset of proteins found in benign prostate hyperplasia prostatic tissue slice cultures (TSCs)

Accn#	Gene name	Protein Name	B1	B2	B3	B4	B5	B6
Q5VTE0	EEF1A1P5	Putative elongation factor 1-alpha-like 3	1		1	2		2
Q04917	YWHAH	14-3-3 protein eta	1	1	1	1	1	1
Q14512	FGFBP1	Fibroblast growth factor-binding protein 1	1	1	1	1	1	1
Q15043	SLC39A14	Zinc transporter ZIP14	1	1	1	1	1	1
Q15746	MYLK	Myosin light chain kinase, smooth muscle	2	1	1		1	1
Q15758	SLC1A5	Neutral amino acid transporter B	1	2	2			1
Q16610	ECM1	Extracellular matrix protein 1	1	1	1	1	1	1
Q6P4E1	CASC4	Protein CASC4	1	1		1	1	2
Q6UX06	OLFM4	Olfactomedin-4	2		1	3		
Q96HE7	ERO1A	ERO1-like protein alpha	1	1	1	1	1	1
Q9HAT2	SIAE	Sialate O-acetyltransferase	1	1		2	1	1
Q9HBR0	SLC38A10	Putative sodium-coupled neutral amino acid transporter 10		2		1	2	1
Q9UHG3	PCYOX1	Prenylcysteine oxidase 1	1		1	1		3
O00391	QSOX1	Sulfhydryl oxidase 1	1			1		3
O14493	CLDN4	Claudin-4	2	1		1		1
O15551	CLDN3	Claudin-3	2	1		1		1
O95484	CLDN9	Claudin-9	2	1		1		1
P56747	CLDN6	Claudin-6	2	1		1		1
O43505	B4GAT1	Beta-1,4-glucuronyltransferase 1	1	1	1		1	1
O60637	TSPAN3	Tetraspanin-3	1	2	1			1
P17693	HLA-G	HLA class I histocompatibility antigen, alpha chain G	1		2	1		1
P02792	FTL	Ferritin light chain	1		2	1		1
P13637	ATP1A3	Sodium/potassium-transporting ATPase subunit alpha-3	1	2	1			1
P50993	ATP1A2	Sodium/potassium-transporting ATPase subunit alpha-2	1	2	1			1
P06731	CEACAM5	Carcinoembryonic antigen-related cell adhesion molecule 5	1		1	1	1	1
P06753	TPM3	Tropomyosin alpha-3 chain	1	2	2			
P07858	CTSB	Cathepsin B	1	1	1	1		1
P07900	HSP90AA1	Heat shock protein HSP 90-alpha	1		1	2		1
P16278	GLB1	Beta-galactosidase	1	1		1		2
P19256	CD58	Lymphocyte function-associated antigen 3	1	1	2			1
P20618	PSMB1	Proteasome subunit beta type-1	2	1	1	1		
P24844	MYL9	Myosin regulatory light polypeptide 9	1	1				3
P26572	MGAT1	Alpha-1,3-mannosyl-glycoprotein 2-beta-N-acetylglucosaminyltransferase	1	1	1	1		1
P27487	DPP4	Dipeptidyl peptidase 4	1	1	1		1	1
P34932	HSPA4	Heat shock 70 kDa protein 4	2	2				1
P36957	DLST	Dihydrolypoyllysine-residue succinyltransferase	1	2				2
P37837	TALDO1	Transaldolase	1	1		1		2
P41732	TSPAN7	Tetraspanin-7	1	1	1	1		1
P51688	SGSH	N-sulphoglucosamine sulphohydrolase		1		2		2
P61981	YWHAG	14-3-3 protein gamma	1	1	1	1		1
P62258	YWHAE	14-3-3 protein epsilon	1	1	1			2
P81605	DCD	Dermcidin		1	1	1	1	1
Q13336	SLC14A1	Urea transporter 1		1	1	1	1	1
Q14CN2	CLCA4	Calcium-activated chloride channel regulator 4	2	2				1
Q15262	PTPRK	Receptor-type tyrosine-protein	2	1	1			1

Appendix Table 3. Proteomic dataset of proteins found in benign prostate hyperplasia prostatic tissue slice cultures (TSCs)

Accn#	Gene name	Protein Name	B1	B2	B3	B4	B5	B6
		phosphatase kappa						
Q6UXS9	CASP12	Inactive caspase-12	2	1	1			1
Q92485	SMPDL3B	Acid sphingomyelinase-like phosphodiesterase 3b	1	1	1		1	1
Q92928	RAB1C	Putative Ras-related protein Rab-1C	1	1	1	1		1
P62820	RAB1A	Ras-related protein Rab-1A	1	1	1	1		1
Q9H0U4	RAB1B	Ras-related protein Rab-1B	1	1	1	1		1
Q96QD8	SLC38A2	Sodium-coupled neutral amino acid transporter 2	1	1	1	1		1
Q9Y3D6	FIS1	Mitochondrial fission 1 protein	1	1		1	1	1
Q9Y4L1	HYOU1	Hypoxia up-regulated protein 1		2		1	1	1
O75874	IDH1	Isocitrate dehydrogenase [NADP] cytoplasmic		2		1		1
O94886	TMEM63A	CSC1-like protein 1	1	1	1		1	
O95292	VAPB	Vesicle-associated membrane protein-associated protein B/C	1	1	1			1
Q9P0L0	VAPA	Vesicle-associated membrane protein-associated protein A	1	1	1			1
O95336	PGLS	6-phosphogluconolactonase		2				2
P07205	PGK2	Phosphoglycerate kinase 2	1		1	1		1
P00750	PLAT	Tissue-type plasminogen activator	1	1	1			1
P20648	ATP4A	Potassium-transporting ATPase alpha chain 1	1	1	1			1
Q12931	TRAP1	Heat shock protein 75 kDa, mitochondrial	1		1	1		1
P08133	ANXA6	Annexin A6		1				3
P12277	CKB	Creatine kinase B-type				4		
P13473	LAMP2	Lysosome-associated membrane glycoprotein 2	1		1			2
P13611	VCAN	Versican core protein	1	1			1	1
P13726	F3	Tissue factor	2				1	1
P13866	SLC5A1	Sodium/glucose cotransporter 1		1	1		1	1
P18564	ITGB6	Integrin beta-6	1	1			1	1
P21291	CSRP1	Cysteine and glycine-rich protein 1	2				1	1
P27824	CANX	Calnexin	1	1	1	1		
P30048	PRDX3	Thioredoxin-dependent peroxide reductase, mitochondrial	1	1		1		1
P31949	S100A11	Protein S100-A11	1		1	1		1
P45880	VDAC2	Voltage-dependent anion-selective channel protein 2	1	1	1			1
P48960	CD97	CD97 antigen		2				2
P49788	RARRES1	Retinoic acid receptor responder protein 1	1	1	1	1		
P52565	ARHGDI1	Rho GDP-dissociation inhibitor 1	1		1	1		1
P60981	DSTN	Destrin	1		1	1		1
P61978	HNRNPK	Heterogeneous nuclear ribonucleoprotein K	1	2		1		
Q02790	FKBP4	Peptidyl-prolyl cis-trans isomerase FKBP4	1	1	1			1
Q03405	PLAUR	Urokinase plasminogen activator surface receptor	1	1	1			1
Q08174	PCDH1	Protocadherin-1		1	2		1	
Q11206	ST3GAL4	CMP-N-acetylneuraminic acid-2,3-sialyltransferase 4	1	1	1			1
Q13308	PTK7	Inactive tyrosine-protein kinase 7	1	1	1			1
Q14118	DAG1	Dystroglycan	1	1			1	1
Q16563	SYPL1	Synaptophysin-like protein 1	1	1	1	1		

Appendix Table 3. Proteomic dataset of proteins found in benign prostate hyperplasia prostatic tissue slice cultures (TSCs)

Accn#	Gene name	Protein Name	B1	B2	B3	B4	B5	B6
Q16790	CA9	Carbonic anhydrase 9	1	1			1	1
Q8N1N4	KRT78	Keratin, type II cytoskeletal 78			1	1	1	1
Q8TDL5	BPIFB1	BPI fold-containing family B member 1	2					2
Q92542	NCSTN	Nicastrin			1		2	1
Q92945	KHSRP	Far upstream element-binding protein 2		1	1	1		1
Q9C0H2	TTYH3	Protein tweety homolog 3	1		1	1		1
Q9HDC9	APMAP	Adipocyte plasma membrane-associated protein		1	1			2
Q9NX62	IMPAD1	Inositol monophosphatase 3	1	1	1			1
Q9NZU0	FLRT3	Leucine-rich repeat transmembrane protein FLRT3	1	1			1	1
Q9UHL4	DPP7	Dipeptidyl peptidase 2	1			2		1
Q13765	NACA	Nascent polypeptide-associated complex subunit alpha		1	1	1		1
E9PAV3	NACA	Nascent polypeptide-associated complex subunit alpha, muscle-specific form		1	1	1		1
Q15293	RCN1	Reticulocalbin-1			1	1	2	
O00264	PGRMC1	Membrane-associated progesterone receptor component 1	1		1	1		
O00462	MANBA	Beta-mannosidase	1	1				1
O00754	MAN2B1	Lysosomal alpha-mannosidase		1	1			1
O14828	SCAMP3	Secretory carrier-associated membrane protein 3		1	1			1
O43396	TXNL1	Thioredoxin-like protein 1		1		1		1
O43688	PLPP2	Phospholipid phosphatase 2	1		1	1		
O60814	HIST1H2B K	Histone H2B type 1-K			3			
P06899	HIST1H2BJ	Histone H2B type 1-J			3			
P23527	HIST1H2B O	Histone H2B type 1-O			3			
P33778	HIST1H2B B	Histone H2B type 1-B			3			
P57053	H2BFS	Histone H2B type F-S			3			
P58876	HIST1H2B D	Histone H2B type 1-D			3			
P62807	HIST1H2B C	Histone H2B type 1-C/E/F/G/I			3			
Q16778	HIST2H2B E	Histone H2B type 2-E			3			
Q5QNW6	HIST2H2BF	Histone H2B type 2-F			3			
Q8N257	HIST3H2B B	Histone H2B type 3-B			3			
Q93079	HIST1H2B H	Histone H2B type 1-H			3			
Q99877	HIST1H2B N	Histone H2B type 1-N			3			
Q99879	HIST1H2B M	Histone H2B type 1-M			3			
Q99880	HIST1H2BL	Histone H2B type 1-L			3			
O60831	PRAF2	PRA1 family protein 2	1	1		1		
O75144	ICOSLG	ICOS ligand	1		1			1
O75223	GGCT	Gamma-glutamylcyclotransferase		1		1		1
O75882	ATRNL1	Attractin	1	1	1			
P35900	KRT20	Keratin, type I cytoskeletal 20			1			2
P02750	LRG1	Leucine-rich alpha-2-glycoprotein			2	1		
P02794	FTH1	Ferritin heavy chain			2			1
P06280	GLA	Alpha-galactosidase A	1	1				1
P48741	HSPA7	Putative heat shock 70 kDa protein 7	1	1	1			

Appendix Table 3. Proteomic dataset of proteins found in benign prostate hyperplasia prostatic tissue slice cultures (TSCs)

Accn#	Gene name	Protein Name	B1	B2	B3	B4	B5	B6
P08571	CD14	Monocyte differentiation antigen CD14	3					
P11047	LAMC1	Laminin subunit gamma-1		1	2			
P11117	ACP2	Lysosomal acid phosphatase	1		1			1
P14406	COX7A2	Cytochrome c oxidase subunit 7A2, mitochondrial	1		1			1
P16144	ITGB4	Integrin beta-4		2	1			
P18084	ITGB5	Integrin beta-5		1			1	1
P19105	MYL12A	Myosin regulatory light chain 12A		1	1			1
O14950	MYL12B	Myosin regulatory light chain 12B		1	1			1
Q9UKY3	CES1P1	Putative inactive carboxylesterase 4		1	1			1
P27797	CALR	Calreticulin	1		1	1		
P29401	TKT	Transketolase		1		1		1
P30041	PRDX6	Peroxiredoxin-6		1		1		1
P31947	SFN	14-3-3 protein sigma		2			1	
P35052	GPC1	Glypican-1 [Cleaved into: Secreted glypican-1]	1	1	1			
P35637	FUS	RNA-binding protein FUS	1	1		1		
Q92804	TAF15	TATA-binding protein-associated factor 2N	1	1		1		
Q01546	KRT76	Keratin, type II cytoskeletal 2 oral			1			2
P40925	MDH1	Malate dehydrogenase, cytoplasmic	1			1		1
P05976	MYL1	Myosin light chain 1/3, skeletal muscle isoform	1	1	1			
P08590	MYL3	Myosin light chain 3	1	1	1			
P63208	SKP1	S-phase kinase-associated protein 1		1			1	1
Q06828	FMOD	Fibromodulin	1			1		1
Q13683	ITGA7	Integrin alpha-7	1	1				1
Q15223	NECTIN1	Nectin-1	1					2
Q8IWA5	SLC44A2	Choline transporter-like protein 2	1	1	1			
Q93052	LPP	Lipoma-preferred partner	1	1	1			
Q9BVC6	TMEM109	Transmembrane protein 109	1		1			1
Q9H0X4	FAM234A	Protein FAM234A	1		1			1
Q9Y277	VDAC3	Voltage-dependent anion-selective channel protein 3	2					1
Q9Y2E5	MAN2B2	Epididymis-specific alpha-mannosidase		1		1		1
Q9Y6M5	SLC30A1	Zinc transporter 1		1	1			1
Q9H3R2	MUC13	Mucin-13	1	2				
P30049	ATP5D	ATP synthase subunit delta, mitochondrial		1		1		1
Q13185	CBX3	Chromobox protein homolog 3		1	1			1
Q15836	VAMP3	Vesicle-associated membrane protein 3		1			1	1
P63027	VAMP2	Vesicle-associated membrane protein 2		1			1	1
Q86XT9	TMEM219	Insulin-like growth factor-binding protein 3 receptor		1	1			1
Q9H4G4	GLIPR2	Golgi-associated plant pathogenesis-related protein 1			1		1	1
Q9HC07	TMEM165	Transmembrane protein 165		1				2
O14672	ADAM10	Disintegrin and metalloproteinase domain-containing protein 10	1	1				
O14818	PSMA7	Proteasome subunit alpha type-7		1	1			
O60635	TSPAN1	Tetraspanin-1	1		1			
O75396	SEC22B	Vesicle-trafficking protein SEC22b		1				1
O75503	CLN5	Ceroid-lipofuscinosis neuronal protein 5					1	1

Appendix Table 3. Proteomic dataset of proteins found in benign prostate hyperplasia prostatic tissue slice cultures (TSCs)

Accn#	Gene name	Protein Name	B1	B2	B3	B4	B5	B6
O95858	TSPAN15	Tetraspanin-15				1		1
P00441	SOD1	Superoxide dismutase [Cu-Zn]	1				1	
P00739	HPR	Haptoglobin-related protein	1	1				
P01906	HLA-DQA2	HLA class II histocompatibility antigen, DQ alpha 2 chain	1					1
P04040	CAT	Catalase				1		1
P04080	CSTB	Cystatin-B		1			1	
P07477	PRSS1	Trypsin-1	1					1
P07478	PRSS2	Trypsin-2	1					1
Q8NHM4	PRSS3P2	Putative trypsin-6	1					1
P08294	SOD3	Extracellular superoxide dismutase [Cu-Zn]			1			1
P09238	MMP10	Stromelysin-2				1		1
P12429	ANXA3	Annexin A3		1				1
P12830	CDH1	Cadherin-1		2				
Q2M2I5	KRT24	Keratin, type I cytoskeletal 24	1	1				
P14384	CPM	Carboxypeptidase M					1	1
P16870	CPE	Carboxypeptidase E	1				1	
Q9Y281	CFL2	Cofilin-2					1	1
P24539	ATP5F1	ATP synthase F	1	1				
P30825	SLC7A1	High affinity cationic amino acid transporter 1			1			1
P52569	SLC7A2	Cationic amino acid transporter 2			1			1
P31946	YWHAB	14-3-3 protein beta/alpha			1	1		
P35580	MYH10	Myosin-10			2			
P39060	COL18A1	Collagen alpha-1	1		1			
P42785	PRCP	Lysosomal Pro-X carboxypeptidase	1					1
P48029	SLC6A8	Sodium- and chloride-dependent creatine transporter 1				1		1
P48739	PITPNB	Phosphatidylinositol transfer protein beta isoform		1				1
P51148	RAB5C	Ras-related protein Rab-5C					1	1
P51571	SSR4	Translocon-associated protein subunit delta				1		1
P55058	PLTP	Phospholipid transfer protein				1		1
P55957	BID	BH3-interacting domain death agonist	1		1			
P60953	CDC42	Cell division control protein 42 homolog	1					1
P61088	UBE2N	Ubiquitin-conjugating enzyme E2 N						2
P61803	DAD1	Dolichyl-diphosphooligosaccharide--protein glycosyltransferase subunit DAD1					1	1
Q05639	EEF1A2	Elongation factor 1-alpha 2	1			1		
P69891	HBG1	Hemoglobin subunit gamma-1					1	1
P69892	HBG2	Hemoglobin subunit gamma-2					1	1
P78324	SIRPA	Tyrosine-protein phosphatase non-receptor type substrate 1	1	1				
Q01105	SET	Protein SET		1				1
Q01844	EWSR1	RNA-binding protein EWS		1			1	
Q02818	NUCB1	Nucleobindin-1			1			1
Q04941	PLP2	Proteolipid protein 2	1				1	
Q07075	ENPEP	Glutamyl aminopeptidase				1		1
Q12805	EFEMP1	EGF-containing fibulin-like extracellular matrix protein 1		1				1
Q13162	PRDX4	Peroxiredoxin-4		1				1
Q14BN4	SLMAP	Sarcolemmal membrane-associated protein	1	1				

Appendix Table 3. Proteomic dataset of proteins found in benign prostate hyperplasia prostatic tissue slice cultures (TSCs)

Accn#	Gene name	Protein Name	B1	B2	B3	B4	B5	B6
Q15365	PCBP1	Poly					1	1
Q15366	PCBP2	Poly			1			1
Q687X5	STEAP4	Metalloreductase STEAP4	1	1				
Q86UP2	KTN1	Kinectin		1	1			
Q8N697	SLC15A4	Solute carrier family 15 member 4		1				1
Q92823	NRCAM	Neuronal cell adhesion molecule	1	1				
Q969P0	IGSF8	Immunoglobulin superfamily member 8			1			1
Q96FN5	KIF12	Kinesin-like protein KIF12		1	1			
Q96KP4	CNDP2	Cytosolic non-specific dipeptidase				1		1
Q99471	PFDN5	Prefoldin subunit 5				1		1
Q99523	SORT1	Sortilin		1			1	
Q9BRX8	FAM213A	Redox-regulatory protein FAM213A		1				1
Q9H330	TMEM245	Transmembrane protein 245		1		1		
Q9NUM4	TMEM106B	Transmembrane protein 106B		1				1
Q9P273	TENM3	Teneurin-3	1					1
Q9UBR2	CTSZ	Cathepsin Z		1				1
Q9UHN6	TMEM2	Cell surface hyaluronidase		1				1
Q9Y333	LSM2	U6 snRNA-associated Sm-like protein LSM2		1		1		
Q9Y394	DHRS7	Dehydrogenase/reductase SDR family member 7				1		1
O43852	CALU	Calumenin				1	1	
Q15800	MSMO1	Methylsterol monooxygenase 1				1		1
Q53GQ0	HSD17B12	Very-long-chain 3-oxoacyl-CoA reductase		1				1
Q9BQE3	TUBA1C	Tubulin alpha-1C chain			1	1		
P68363	TUBA1B	Tubulin alpha-1B chain			1	1		
Q71U36	TUBA1A	Tubulin alpha-1A chain			1	1		